RUSSIAN ACADEMY OF SCIENCES
SCIENTIFIC COUNCIL ON PROBLEMS OF BIOLOGICAL PHYSICS
INSTITUTE OF THEORETICAL AND EXPERIMENTAL BIOPHYSICS
INSTITUTE OF CELL BIOPHYSICS

BIOLOGICAL MOTILITY

Materials of International Symposium

Pushchino • 2016

УДК 577.3
ББК 28.07
В60

Biological Motility. – Pushchino: SYNCHROBOOK – 2016. – 280 p.

This volume contains the presentations that were made during the International Symposium "Biological motility". It took place in Pushchino, Moscow region and was devoted to new ashievements and perspectives in this area of knowledge as: the basics of muscle contraction, muscle plasticity and cytoskeleton, nonmuscle motility, new instrumentation and methodology.
Materials of the Symposium are of interest for biologists, medical and other specialists.

Responsible for the issue S.N. Udaltsov

Support of the Symposium by the following sponsors is gratefully acknowledged:

Russian Academy of Sciences

Russian Foundation for Basic Research, project 16-04-20104

ISBN 978-591874-042-2

BIOLOGICAL ACTIVE SUBSTANCE – MELAFEN, INFLUENCING TO THE CYTOSKELETON OF ERYTHROCYTE'S CELL MEMBRANE

O.M. Alekseeva[1], L.D. Fatkullina[1], Y.A. Kim[2], A.N. Golochshapov[1]

[1]*Emanuel Institute of Biochemical Physics RAS, ul. Kosigina 4, Moscow, 119334, Russia*

[2]*Institute of Cell Biophysics RAS, ul. Institutskaya 3, Pushchino, Moscow Region, 142290, Russia*

Melafen (melamine salt of bis (oximethyl) phosphinic acid) - heterocyclic organic phosphor compound, synthesized at the A.E. Arbuzov Institute of Organic and Physical Chemistry of RAS for the plant growth regulation [1]. There are the great concentration limitations, when Melafen was used. Large concentrations are killer for plants, low – activate seed germination and raise the plant resistance in stress conditions overcooling and drought. Melafen was used as aqua solutions, at wide concentration's region at all our investigations. The main task of this investigation was the clearing of some aspects of Melafen influence on the structural properties of experimental objects of animal's origin.

The primary targets for biological active substances (BAS) at animal's cells are the membranes and their components. When BAS introduced to the blood-vascular system the first targets become the blood cells. This is why for carrying out the tests of Melafen actions as of simple models of primary targets, the erythrocytes were used that were isolated as the whole cells. And then erythrocytes were emancipated from hemoglobin by of hypo osmotic hemolysis [2] under cooling (4°C) for preparing of ghosts. The erythrocyte ghosts are the outer erythrocyte membranes with all elements of cytoskeleton. The main components of ghost are typical for the most of cells of animal body**.** The Melafen interactions with membrane bounded proteins at the erythrocyte's ghost were tested by the differential scanning microcalorymetry (DSC) method. The application of DSC allowed us to receive the structural data of protein microdomains organization at erythrocyte's ghost membranes. Thermograms of erythrocyte ghosts were registered by means of DASM-4. It is known that there are five identified endothermic phase transitions of protein's microdomains (*A*, B_1, B_2, *C*, *D*) at erythrocyte's ghosts when registered by the DSC. The *A*-transition is determined by the microdomains denaturation of cytoskeleton, set up of complex α- and β-spectrin and actin. The denaturation of spectrin-actin complex microdomain results in disappearance of *A*-transition. That is followed by the total loss of erythrocytes and ghost membranes deformability [3]. B_1-transition is linked to denaturation of membranous microdomain, set up of ancyrin and proteins of bands 4.1, 4.2 and demantin. B_2-transition is linked with denaturation of cytoplasm fragment of protein band-3 microdomains. *C*-transition is linked with denaturation of membrane fragment 55 κDa of proteins band-3, which are ion-channels microdomains. *D*-transition is linked with unidentified proteins denaturation and membrane bubbling microdomains. It should be noted

that pathology damaged erythrocytes (for example – oxidized, etc.) in blood stream are lacking, since it were utilized by macrophages. However, we used the native erythrocytes isolated from healthy organism. All treatments were provided without macrophages in experimental test glass. The model of erythrocyte ghosts for DSC studies of cell membranes is quite adequately. Because, the same changes of protein's microdomain organizations are occurred at membranes and cytoskeletons of other cells. The proteins composition of cytoskeletons: spectrin, ancyrin, bands proteins 4, 1 and 4, 2 are developing and band protein 3 is submitted consisting of membranous skeletal in practice all cells of organism. The DSC method allows defining any change in cell membrane and erythrocyte cytoskeleton pathologies when bed environment: oxidative stress, low temperature action, or another [4].

Materials and methods

The materials: Melafen (melamine salt of bis (oximethyl) phosphinic acid) was used as the aqua solutions (10^{-2}, 10^{-3}, 10^{-4}, 10^{-5} M). The erythrocytes and its ghost were prepared by method [5]. The Melafen interactions with membrane bounded proteins at ghost were tested by DSC with aid DASM-4 [4].

Results and discussion

The ghost of rat erythrocytes are the model of fairly simple to be used, and on thermograms are clearly mirrored all peaks of thermo inducted denaturation transitions of cytoskeleton's proteins. The ghost's thermograms in the presence of Melafen aqueous solutions at first and second days following of ghost receiving from rat erythrocytes are submitted. The structure of ghost in keeping of two days (ageing) was changed essentially, but the addition of Melafen solution with large concentrations before DASM-4 scanning was not affecting of curves outlines outwardly. Any dislocations of thermo denaturation peaks and any essential changes of peak amplitudes do not happen under the Melafen action. It indicates that the aqueous solution of Melafen (large concentrations) was not affected directly on the structural organization of protein components of animal's cellular membrane. But the Melafen aqueous solutions caused some restructuring of protein's microdomains, which consist of several proteins as a rule, on freshly-isolated preparations (3–9%), and in the process of ageing of the erythrocytes ghost (table). The small structural changes are representative for biological responses.

As it can be seen from data of table, the Melafen, aqueous solutions when concentrations 10-5 M and 10-3 M, did not cause of important changes in relative

Melafen influence on temperature dependence of relative enthalpy (at thermograms - peak *A*) of membranes suspensions of erythrocyte ghosts at the first day after receiving of erythrocyte ghosts

Erythrocyte ghosts	ΔC_p*	Δ, %**
Without Melafen	17,1±0,01	
10^{-5} M Melafen	17,6±0,01	+3
10^{-3} M Melafen	18,6±0,01	+9

*ΔC_p – change of relative heat capacity (J/K), **Δ (%) – the different quantity, where 100% – the quantity of control answer.

heat capacity (J/K) in peak maximum of heat absorption and (the *A*-transition intensity) (3–9%). *A*-transition is the characteristic of induced endothermic denaturation of two most important protein's cytoskeleton components in practice of all cells of animal origin - spectrin and related actin. Other endothermic transitions, which being the characteristics thermo denaturation properties of cytoskeleton components and channel fragments also, in practice didn't change of its amplitudes. And the same data have been received for thermograms, registered at the second day following the ghost were prepared, i. e. on "aged" ghosts. It is results allude to the fact that micro domain's organization of cytoskeleton proteins and plasma membrane were not undergo of the major changes in the presence of Melafen aqueous solutions of high concentrations.

So that, as this within sensibility of DSC method was occurred, the protein structure of plasma membrane (and channels in its composition) has been identified, and also the cytoskeleton elements in the presence of Melafen aqueous solutions under large concentrations was not suffering some major changes. It indicates that Melafen not made any considerable affects on protein components thermo denaturation properties at cellular membrane and cytoskeleton directly. Melafen not causes a change, leading to proteins loss, or to restructuring of protein's domains at cellular plasmalemma and cytoskeleton. Large concentrations of Melafen are not dangerous for structural properties of microdomains' organization of cellular proteins when temperature was changed. At animal's body the temperature jumps are occurred as normal processes. And it is important to investigate the BAS influence to these processes. But for functional properties of cellular proteins additions of Melafen aqua solutions even under the middle concentration play the role as a strong modificator or inhibitor under the constant temperature [6].

Conclusion

Influence of plant growth regulator Melafen on organisms of animal origin let us mention that as of test object the erythrocytes were chosen. Erythrocytes are the one of the first targets when some material appeared in blood river-bed. This model is very simple for preparation and fairly it is stable for provided somebody measurements. At the same time the erythrocytes have the cytoskeleton protein composition similar of most animal's cells to a considerable extent. By this the investigations that were provided with this experimental object had the essential significance. The obtained data about measurements of proteins thermostability indicated that Melafen didn't exert the great destructive actions to the isolated membranes (with cytoskeleton) under the concentrations that regulate the plant and seeds growth. But Melafen influencing was essential to the functioning of animal's membrane-bounded proteins, when the bigger Melafen concentrations [6].

References

1. Fattachov S.G., Reznik V.S., Konovalov A.I. "Melamine Salt of Bis (hydroxymethyl) phosphinic Acid. (Melaphene) As a New Generation Regulator of Plant growth regulator" // Reports of 13 International Conference on chemistry of phosphorus compounds. S. Petersburg. 2002. S. 80.2.

2. Jackson W.M., Kostyla J., Nordin J.H., Brandts J.F. “Calorimetric study of protein transitions in human erythrocyte ghosts” // Biochemistry. 1973. V.12. P. 3662-3667.
3. Mohandas N., Greenquis, A.C., Shohet S.B. “Effect of heat and metabolic depletion on erythrocyte deformability, spectrin extractability and phosphorilation” // The Red Cell. New York. Alan R. Liss. Inc. 1978. P. 453-472.
4. Akoev V.R., Matveev A.V., Belyaeva T.V., Kim Y.A.” "The effect of oxidative stress on structural transitions of human erythrocyte ghost membranes" // Biochim Biophys Acta. 1998. V. 1371. № 2. P. 284-294.
5. Dodge J.T., Mitchell C., Hanahan D.J. “The preparation and chemical characteristics of hemoglobin-free ghost of human erythrocytes” // Arch. Biochem. Biophys. 1963. V. 100. P. 199-130.
6. Alekseeva O.M. “Melafen - Plant Growth Regulator and Pathways of cells" // Polymers Research Journal, V.7, N 1, 2013 P. 117 - 128.

THE ROLE OF NITRIC OXIDE AND PROSTAGLANDINS IN ENDOTHELIUM-DEPENDENT REGULATION OF THE GROUND SQUIRREL AORTIC TONE DURING HIBERNATION

L.A. Andreeva

Institute of Cell Biophysics, Russian Academy of Sciences, Pushchino, Russia

Mammalian hibernation is a natural adaptation to periods of food scarcity and cold weather. Entrance into hibernation is characterized by a reduction in heart rate to below 3–5 beats/min, respiratory rate of less 2–3 breath/min, metabolism and decrease in systemic blood pressure, followed by decrease in body temperature (T_B) to near 0°C [Lyman, 1965; Nurnberger, 1995]. There is increased vascular resistance in peripheral vessels, maintained by enhanced sympathetic activity, to allow preferential shunting of blood to the heart, lungs and brown adipose tissue. These changes are rapidly reversed (within 2-3 hr) on arousal of animal to euthermy [Lyman & O’Brien, 1988]. It is thought that the enhancement of sympathetic mediation is one of the major contributory factors for regulation of the peripheral vessel tone during hibernation [Ravelic et al., 1997; Karoon et al., 1998]. However endothelial cells play an important role in the control of peripheral circulation under various physiological conditions too [Furchgot & Zawadzki, 1980], but now little has been known about endothelial control vascular tone during hibernation. The goal of the present study was to examine the role of NO and prostaglandins in regulation of the ground squirrel thoracic aorta tone during different phases of hibernation – active state between torpor bouts, torpid state and awakening.

The following groups of ground squirrels (Spermophilus undulates) were studied: animals in torpid state (T_B 2–7°C); in two points during arousals (T_B 10–13°C and 28–32°C) and in active state between torpor bouts. The thoracic aorta was rapidly and carefully excised and placed in bicarbonate-buffering Tyrode solution, which was oxygenated with 95% O_2 and 5% CO_2. The fat and adventitia were dissected and aorta was cut transversely into ~3-

mm-long arterial rings. The vascular ring was mounted onto two tungsten wires. One wire was fixed to the organ bath wall and the other was connected to a force transducer for recording of isometric tension. After an equilibration period of 15 min, resting tension was increased to 2 g and then rings were adapted during 60 min. The temperature of Tyrode solution-circulating tissue bath was 30°C for active and awakening animals with T_B 25–30°C; and 20°C for torpid state and awakening animals with T_B 10–13°C. Rings were pre-contracted with l-phenylephrine (PE, 1–5 μM). Thereafter, rings were exposed to cumulative concentration of acetylcholine (Ach, 10 nM – 50 μM) in the presence or absence of inhibitors of nitric oxide synthase N^{ω}-nitro-L-arginine methyl ester (L-NAME, 100 μM) and cyclooxigenases (COXs) – indomethacin (10 μM). L-NAME was administered 30 min and indomethacin 60 min before application of ACh. In some experiments, the endothelium was removed by moving the aorta ring around two tungsten wires.

In all groups of animals ACh produced two type responses in aortic rings precontracted by phenylephrine: a dose-dependent relaxation (10 nM – 1 μM), which reversed to contraction at the concentrations above 5 μM. The maximum of the concentration-response curves for relaxing effect of ACh was 70–80% at concentration 1 μM. Contraction of aortic rings caused by ACh at the concentrations above 5μM was similar in all groups and the maximum of the concentration-response curves was observed at concentration 50 μM. The relaxant and contractile responses to ACh (0.01 – 50 μM) were abolished by endothelial denudation. The nitric oxide synthase inhibitor L-NAME encreased contractile response of aortic rings pre-contracted by phenylephrine, and was maximal in torpid animals (35% from PE). In the presence of L-NAME acetyl-choline-induced relaxation was abolished in aortic rings in groups of active and arousal squirrels with T_B 28–30°C, but was partly remained in torpid animals (max 30%) and arousal squirrels with T_B 10–13°C (max 40%). The contractile responses to Ach were significantly enhanced in the squirrel aortic rings in the presence of L-NAME. Indomethacin, inhibitor of COXs, had small effect on vasorelaxation, but significantly decreased contractile responces to Ach in the groups active, torpid and awakening animals with T_B 10–13°C. In the groups of awakening animals with T_B 25–30°C indomethacin decreased both relaxant and contractile responses to Ach.

It is known, that Ach evokes the simultaneous release of endothelium-derived relaxing factors (EDRF, in the main nitric oxide) and endothelium-derived contracting factors (EDCF) to control the tone of the underlying vascular smooth muscle [Furchgot & Zawadzki, 1989]. EDCF has been characterized as superoxide and/or TxA_2/PGH_2 generated by COX-mediated metabolism of arachidonic acid [K. Kurahashi et al., 2003]. In animals and human EDCF in peripheral arteries were not observed in control, physiological conditions, and were only observed during vascular disease, for example, hypertension and diabetes. These results demonstrate that ACh initiates two distinct responses in aorta precontracted with phenylephrine: endothelium-dependent relaxation, mediated predominantly by NO,

and endothelium-dependent contraction, which partly mediated by COX metabolism of arachidonic acid. It is obvious, that relaxation, which partly remained in torpid and arousal squirrels with T_B 10–13°C after inhibition of the nitric oxide synthase by L-NAME caused by activation of calcium-activated potassium channels. Thus, hibernating animals have effectively developed mechanisms to preserve vascular function after cooling and rearming.

References

Ravelic V., Hill B., Crowe R., Knight G., Burnstock G. 1997. Effects of hibernation on neural and endothelial control of mesenteric arteries of the golden hamster. Am.J. Physiol. 273, H148-H155.

Karoon P., Knight G., Burnstock G. 1998. Enhanced vasoconstrictor responses in renal and femoral arteries of the golden hamster during hibernation. J. Physiol. 312(3), 927-938.

Furchgott R., Zavadzki F., John V. 1980. The obligatory role of endothelial cells in the relaxation of smooth muscle by acetylcholine. Nature 288, 373-376.

CONTRIBUTION OF THE REVERSE Na^+/Ca^{2+} EXCHANGER TO THE CONTRACTILITY OF THE MYOCARDIUM IN THE GROUND SQUIRREL

A.S. Averin[1], L.S. Kosarsky[1], S.V. Tarlachkov[2], O.V. Nakipova[1]

[1]*Institute of Cell Biophysics, Russian Academy of Sciences, Institutskaya Street 3, 142290 Pushchino (Moscow region);*

[2]*All-Russian Collection of Microorganisms (VKM), G.K. Skryabin Institute of Biochemistry and Physiology of Microorganisms, Russian Academy of Sciences, pr. Nauki 5, Pushchino, Moscow Region 142290, Russia*

Contraction of the heart of hibernators as well as of all other mammals control by the well-coordinated operation of different Ca-transporting systems: 1) potential-dependent plasma membrane Ca-channels (I_{ca}) and sarcoplasmic reticulum Ca-release channels that provide the transient increase in free Ca-concentration in cytoplasm necessary for contraction; 2) Ca-binding and contractile proteins of muscle myofilaments that convert Ca-signals into mechanical response; and 3) Plasma membrane Na^+/Ca^{2+} exchanger (**NCX**) and sarcoplasmic reticulum Ca-ATPase which remove Ca from the cytosol resulting in relaxation.

The role of NCX in maintaining Ca^{2+} homeostasis is complex and poorly studied, which is largely due to its ability to function in two modes – forward and reverse. The direction of NCX operation depends on the gradient of Na^+ and Ca^{2+} ions and the membrane potential. Acting in the forward mode, NCX ($NCX_{forward}$) plays an important role in the process of relaxation by removing calcium from the cytoplasm after contraction. However, under specific conditions, for example, upon artificial depletion of the extracellular concentration of Na^+ or upon increase of intracellular concentration of Na^+ ions, it can pump Ca^{2+} into the cell and act as a trigger for contraction (Bers et al., 2006).

The reverse mode of operation ($NCX_{reverse}$) is more characteristic of the myocardium of rats and mice, which is the closest to the myocardium of the ground squirrel by a number of physiological characteristics, as well as of pathological human myocardium (Neco et al., 2010). Specific blocker KB-R7943 predominantly blocks $NCX_{reverse}$ (Birinyi et al., 2008). It has been shown that this inhibitor has virtually no effect on healthy myocardium; however, it prevents Ca overload under pathological conditions (Satoh et al., 2000; Yoshitomi et al., 2005)

It was shown that the heart of hibernators possesses seasonal variability of the calcium source for initiating contraction: in the periods of summer activity the prominant role belongs to extracellular Ca entering through the potential-dependent channels and partly through the reversible form of Na-Ca-exchanger; during the period of hibernation the prominant role belong to Ca of intracellular depots: I_{Ca} and NCX activity are reduced indicating a shift from transsarcolemmal to intracellular Ca^{2+} cycling.

Suggestions have been made that upon the reduction of activity of Ca-channels during hibernation this mechanism may serve as a supplier of Ca ions from the extracellular space (Willis et al., 1992). However, this hypothesis obtained no confirmation. On the contrary, it has been found that the contribution of Na^{+}/Ca^{2+} exchanger in triggering contraction and in the process of relaxation decreases with temperature reduction, as shown for several species of animals (Mackiewicz, Lewartowski, 2006). Thus, the role of NCX in the seasonal changes of calcium homeostasis of hibernating animals still remains largely unclear. We conducted a study of the role of the reverse form of NCX in the contractility of the ground squirrel myocardium by applying a specific inhibitor KB-R7943 (Sato et al., 2000) in animals of summer and autumn periods.

Ground squirrels, ***Spermophilus undulatus***, of both genders, 500-800 g were recruited to this study. All experiments followed the European Convention for the Protection of Vertebrate Animals used for Experimental and other Scientific Purposes 1986 86/609/EEC. The study was performed on papillary muscles (PM) of the right ventricle from the hearts of ground squirrels during summer (June–July, n=4) and autumn (october-november, n=4) periods. Isolation of PM, stimulation and measurement of the contraction amplitude in an isometric mode were carried out with the methodology described earlier (Nakipova et al. 2007) at 36 ± 0.2°C. The diameter of papillary muscles varied from 0.6 to 1.0 mm, the length – from 1.0 to 3.0 mm.

The effects of KB-R7943 (10 mkM, at IC_{50} – 1.2–2.4 mkM)) on the force-frequency dependence (0.1 to 3.0 Hz), as an indicator of participation of various sources of calcium (external and intracellular) in the activation of contraction, and post-rest potentiation (1–600 s) as an index of the capacity of sarcoplasmic reticulum (intracellular calcium source) to store and release Ca^{2}, are studied in the present work to analyze the role of different calcium-transporting systems in KB-R7943-induced changes in isometric twitch force of ground squirrels papil-

lary muscles. The data are presented as an average value ± SEM ($P < 0.05$ using Student's *t*-test).

The group of summer animals exhibited no significant effect on the dependence of FFR and the pause effect upon long-term application (1 to 1.5 hours) of KB-R7943. The hearts of autumn ground squirrels demonstrated a significant decrease in the force of contraction at low frequencies of stimulation (0.1 – 0.3 Hz) under this blocker. The inhibitory effect of KB-R7943 was 41±4 (n=4, P<0.05) at a frequency of 0.1 Hz, and a statistically significant reduction in the force of contraction was also observed at frequencies of 0.2 and 0.3 Hz, while no significant differences were observed in the area of higher frequencies. At the same time, both groups showed a reduction of pause potentiation at duration of more than 60 s. Kinetic parameters of contraction also remained unchanged. Thus, the obtained data suggest that the contribution of the reverse form of NCX in the regulation of contraction force in the heart of ground squirrels becomes significant only upon reduction of the activity of Ca^{2+} channels in animals during preparatio for hibernation, which is the most important period in the life cycle of hibernators.

This work was partly supported by the Russian Foundation for Basic Research (project 13–04–01234a).

References

1. Bers D.M, Despa S, Bossuyt J.Regulation of Ca^{2+} and Na^{+} in normal and failing cardiac myocytes. Ann N Y Acad Sci. 2006 Oct;1080:165-77
2. Birinyi P, Tóth A, Jóna I, Acsai K, Almássy J, Nagy N, Prorok J, Gherasim I, Papp Z, Hertelendi Z, Szentandrássy N, Bányász T, Fülöp F, Papp JG, Varró A, Nánási PP, Magyar J. The Na^{+}/Ca^{2+} exchange blocker SEA0400 fails to enhance cytosolic Ca^{2+} transient and contractility in canine ventricular cardiomyocytes. Cardiovasc Res. 2008 Jun 1;78(3):476-84. Epub 2008 Feb 5.
3. Mackiewicz U, Lewartowski B.Temperature dependent contribution of Ca^{2+} transporters to relaxation in cardiac myocytes: important role of sarcolemmal Ca^{2+}-ATPase. J Physiol Pharmacol. 2006 Mar;57(1):3-15.
4. Nakipova O.V., Zakharova N.M., Andreeva L.A., Chumaeva N.N., Averin A.S., Kosarskii L.S., Anufriev A.I., Lewinski D.V., Kockskamper J., Pieske B. // Cryobiology 2007. V .55. P. 173-181.
5. Neco P, Rose B, Huynh N, Zhang R, Bridge JH, Philipson KD, Goldhaber JI. Sodium-calcium exchange is essential for effective triggering of calcium release in mouse heart. Biophys J. 2010 Aug 4;99(3):755-64.
6. Satoh H, Ginsburg KS, Qing K, Terada H, Hayashi H, Bers DM.KB-R7943 block of $Ca(^{2+})$ influx via $Na(^{+})/Ca(^{2+})$ exchange does not alter twitches or glycoside inotropy but prevents $Ca(^{2+})$ overload in rat ventricular myocytes. Circulation. 2000 Mar 28;101(12):1441-6.
7. Yoshitomi O, Akiyama D, Hara T, Cho S, Tomiyasu S, Sumikawa K.Cardioprotective effects of KB-R7943, a novel inhibitor of Na^{+}/Ca^{2+} exchanger, on stunned myocardium in anesthetized dogs. J Anesth. 2005; 19(2):124-30.
8. Willis, J. S., Xu, W. and Zhao, Z. Diversities of transport of sodium in rodent red cells. Comp. Biochem. Physiol. 1992. 102,609 -614.

THE EFFECT OF Arg167His, Arg167Gly AND Lys168Glu MUTATIONS IN TPM1 GENE ON POSITION OF TROPOMYOSIN AND SPATIAL ORGANIZATION OF MYOSIN HEADS AND ACTIN DURING THE ATPASE CYCLE

S.V. Avrova[1], N.A. Rysev[1], O.E. Karpicheva[1], D. Borys[2], J. Moraczewska[2], Y.S. Borovikov[1]

[1]*Institute of Cytology, Tikhoretsky Pr., 4, Saint Petersburg, 194064, Russia*

[2]*Kazimierz Wielki University in Bydgoszcz, Department of Biochemistry and Cell Biology, Poland*

Tropomyosin (TM) changes its azimuthal position on F-actin, exposing in the presence of Ca^{2+} (closed position) or blocking in the absence of Ca^{2+} (blocked position) myosin binding sites on actin, thereby controlling myosin interaction with actin and contractility [Lehman et al., 2013, J. Muscle Res. Cell Motil. 34: 155–163]. The positions that TM strands take in both thin filaments and troponin-free actin filaments during the ATPase cycle were found to be correlated with the number of the switched on actin subunits and the amount of the strongly bound myosin heads [Borovikiov et al., 2009, Biochim Biophys Acta, 1794: 985–994]. It was shown that the shift of TM to the inner domain of actin resulted in an increased amount of both switched on F-actin subunits and myosin heads strongly bound to F-actin; the movement of TM to the outer domain of actin led to a decreased proportion of these subunits and the strongly bound myosin heads. This relationship may be uncoupled by point mutations in α- and β-TMs [Rysev et al., 2012, Biochim. Biophys. Acta, 1824: 366–373; Borovikov et al., 2015, Arch. Biochem. Biophys. 577-578: 11–23; Karpicheva et al., 2016, Biochim. Biophys. Acta, 2016, 1864: 260–267].

There is evidence that myopathies in skeletal muscle may be provoked by mutations in the TPM1, TPM2 and TPM3 genes, which may induce contractile dysfunction [Marston et al., 2013, Hum. Mol. Genet. 22: 4978–4987; Marttila et al., 2014, Hum. Mutat. 35: 779–790]. In particular, point mutations in TPM3 gene leading to the Arg167His, Arg167Gly and Lys168Glu replacements have been associated with congenital fiber type disproportion and cap disease. Functional effects of these mutations in TPM1 gene were examined in biochemical assays using recombinant tropomyosin mutants and native proteins isolated from skeletal muscle [Robaszkiewicz et al., 2012, Biochim. Biophys. Acta 1822: 1562–1569]. The work indicated that all these mutations decreased the affinity of tropomyosin for actin, and suppressed the Ca^{2+}-induced activation and the ATPase activity of myosin [Robaszkiewicz et al., 2015, Biochem. Biophys. Acta 1854: 381–390]. However it is unclear how these mutations affect the behaviour of TM strands and the response of actin and myosin during the ATPase cycle when troponin is absent.

To investigate how the Arg167His, Arg167Gly and Lys168Glu mutations in tropomyosin isoform Tpm 1.1 (TM) affect the relocation of TM strands and the conformational state of the myosin heads and actin during the ATPase cycle,

we labelled the recombinant wild-type and mutant TMs with 5-IAF, S1 with 1,5-IAEDANS and F-actin with FITC-phalloidin, incorporated them into the ghost muscle fibres and studied polarized fluorescence. It was shown that the Arg167His mutation shifts TM further to the periphery of the filaments (towards the blocked position) and inhibits the switching on of actin monomers and the strong binding of the myosin heads to actin. On the contrary, the Arg167Gly and Arg168Glu mutations shift TM further to the filament centre (towards the open position) and activate strong binding of the myosin heads throughout the ATPase cycle. The data suggest that the reasons for the defective response of the myosin heads and actin during the ATPase cycle that has been observed in troponin-free filaments containing the Lys168Glu, Arg167Gly and Arg167His mutant TMs are that the Arg167His mutation leads to a shift of TM strands towards the blocked position which inhibits the switching of actin monomers on and the formation of the strong binding of myosin to actin, while Lys168Glu and Arg167Gly mutations facilitate stronger myosin binding to actin. These defects can result in muscle weakness observed at congenital fiber type disproportion and cap disease [Lehtokari et al., 2007, Neuromusc. Disord. 17: 433–442; Clarke et al., 2009, Neuromusc. Disord. 19: 348–351].

This work was supported by the Russian Foundation for Basic Research (№ 14-04-00454) and statutory funds to Kazimierz Wielki University.

ANALYSIS OF ALTERNATING SHUTTLE STREAMING OF ENDOPLASM IN SLIME MOLD PLASMODIUM *PHYSARUM POLYCEPHALUM*

T.I. Avsievich, D.S. Kuzmin, S.V. Frolov, S.G. Proskurin

Biomedical Engineering, Tambov State Technical University, ul. Sovetskaya 106, Tambov, 392000, Russia

Slime mold *Physarum polycephalum* is a classic unicellular organism for amoeboid nonmuscle motility study. Actin-myosin contractile system generates periodic contractile activity causing shuttle endoplasmic motility in *Physarum* strands. However, the nature and number of oscillators that control the contractile activity of plasmodium still remains unclear [1].

In this study velocity time dependencies of alternating shuttle streaming of endoplasm in slime mold plasmodium *Physarum polycephalum* have been investigated. Endoplasm velocity registration was implemented using sign-sensitive laser Doppler microscope. Sign-sensitive mode allows decreasing signal to noise ratio, which is almost equal to one in the case of absolute magnitude registration [2].

Measurements were acquired from horizontally oriented isolated plasmodium strand before and after the treatment of cellular respiration inhibitors [3,4] (KCN and SHAM, 5 and 7 μM, respectively), which cause the complete cessation of endoplasmic motility. After removal of the inhibitors the respiratory system becomes normal, gradually restoring the activity of both harmonic oscillation sources. Power spectra presented in figure: a) – normal conditions, buffer solution,

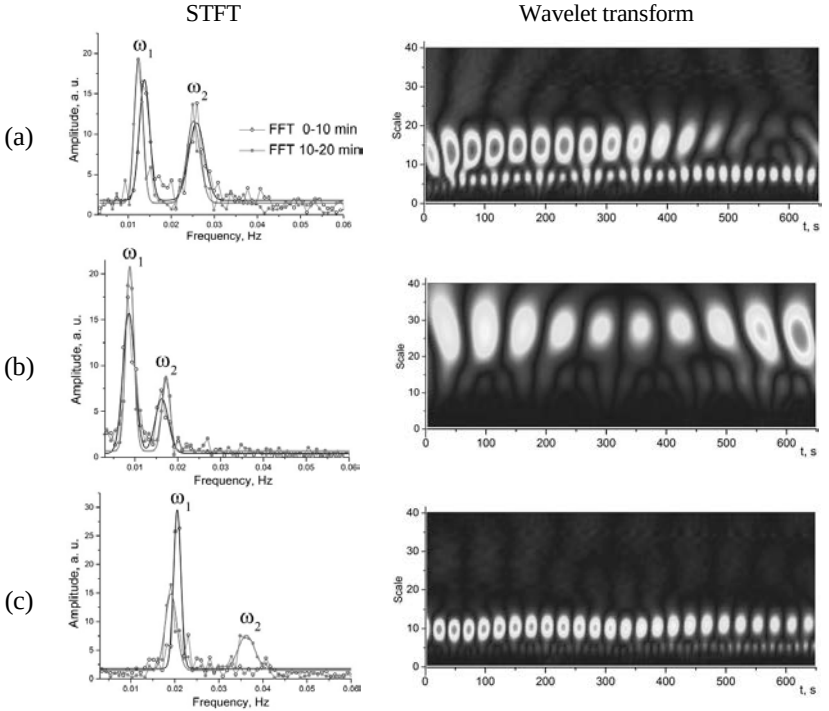

b) – one half treated by KCN and SHAM, c) – 10 min after treatment by KCN and SHAM. The ratio of obtained frequencies with good accuracy equal to two (ω_2/ω_1=1.97±2%) and remains constant in all measurements, regardless the KCN+SHAM treatment. Analyzing the amplitudes of power spectra peaks, their energy interconnection has been reviled. As the amplitude A_1 of the first peak decreases, the amplitude A_2 of the second one increases. The sum of the amplitudes remains constant for each series of experiments. It shows that the frequency of an internal oscillator is doubled and shifted in phase, or alternatively, presence of two types of oscillators which frequencies differ exactly twice [5].

Despite Short Time Fourier Transform (STFT) analysis provides information about the number of oscillators, its time resolution is considerably limited. Wavelet transform allows analyzing signals of a non-stationary nature as well.

The presented results of wavelet transform of obtained velocity time dependencies confirmed the presence of two harmonic components in each of them, and allowed more accurate visualization of the frequency changes in time. Thus, for the velocity dependence with buffer solution (a) the changes of frequency of a harmonic contributions clearly can be seen using wavelet analysis, that is not obvious from the STFT results.

Short Time Fourier Transform and wavelet transform of time velocity dependencies have revealed two harmonic components which differ exactly twice,

independently on the registration conditions. Detected harmonics generated by internal cellular oscillators cause *Physarum* migration. The nature of these oscillators are not clear completely, but it is evident they are dependent on the presence of ATP, needed for the cellular contraction. Further investigations will be focused on more accurate simulation analysis of these oscillations.

References

1. Wohlfarth-Bottermann K. E. Oscillatory contraction activity in Physarum // Journal of Experimental Biology. V. 81. p. 15–32, 1979.
2. Proskurin S.G., Avsievich T.I., Spectral analysis of self-oscillating motility in an isolated plasmodial strand of Physarum polycephalum // Biophysics, 59(6), p. 928–934, 2014.
3. Avsievich T.I., Ghaleb K.E.S., Frolov S.V., Proskurin S.G., Endoplasmic motility spectral characteristics in plasmodium of Physarum Polycephalum // Proc. of SPIE, Vol. 9448, p. 94480H, 2015.
4. Avsievich T.I., Frolov S.V., Proskurin S.G., Spectral characteristics of shuttle self-oscillating endoplasmic motility in slime mold plasmodium // Optics and Spectroscopy. – 2016. – 120(1). – p. 70–75.
5. Avsievich T.I., Frolov S.V., Proskurin S.G., Characterization of endoplasmic streaming in Physarum polycephalum using direction sensitive laser Doppler microscopy // Optical and Quantum Electronics, 48(2), P. 1–10, 2016.

THE SIZE OF MEDIATOR QUANTA AS REGULATED PARAMETER OF SYNAPTIC TRANSMISSION

O.P. Balezina

Lomonosov Moscow State University,
Leninskie Gory, Moscow, 119991, Russia

The quantum of mediator is an elementary unit of synaptic transmissions. It reflects the amount of mediator localized in a single presynaptic vesicle, released into synaptic cleft by exocytosis [Fatt, Katz, 1952]. The parameters of single mediator quantum are usually tested indirectly as amplitude of miniature postsynaptic potentials, generated in response to mediator release from single synaptic vesicles. Variations in quantal size are typically thought to reflect either the postsynaptic modification of receptor density, or the presynaptic changes of mediator content in a vesicle. It is now clear that at certain synapses postsynaptic receptors are not fully saturated during mediator release, and presynaptic change in vesicle filling can effectively modulate quantal size and strenghth of synaptic transmission [Van der Kloot, 1991; Edwards, 2007].

At present time several possibilities to modulate quantal size presynapticaly are postulated. There are: modulations of mediator content in a vesicle or modulation of diameter and kinetic of fusion pore formed during vesicle exocytosis. The most evident and well studied are the probable variations of mediator content in a vesicle [Edwards, 2007].

The list of agents known to modulate the mediator quantal size at presynaptic level in central and peripheral synapses is very poor. So, the question remains

unsolved, what kind of physiologically active biomodulators can specifically promote changes in mediator quantal size via activation of their presynaptic receptors?

To clear this problem we studied the role of three structurally and functionally different peptides:1) *peptide-agonist of thrombin receptors(designate as* ***PARs*** *-Proteinase Activated Receptors*); 2) crustaceans peptide *allatostatin; 3) calcitonin gene related peptide –CGRP*. The peptides were checked as probable presynaptic modulators of ACh quantal size in mice motor synapses.

Objects and methods

Experiments were performed on isolated neuromuscular preparations of the diaphragm-phrenic nerve from adult mice (strain BALB/c) of both sexes (25–30 g body weight).The intracellular recording of miniature endplate potentials (MEPPs) of neuro-muscular end plates was carried out ,using traditional microelectrode method. All drugs were applied to preparations via bath perfusion system (0.5 ml/min). Data were statistically elaborated using the Student's *t*-test.

PAR1-agonist action on ACh quantal size

We used the synthetic penta-peptide (*Ser-Phe-Phe-Leu-Arg-Asn*-NH_2) known as the selective *agonist of thrombine receptors, PARs* (Proteinase Activated Receptors) [Balezina et al., 2004]. PAR agonist peptide (PAR-AP) action on mice diaphragmal muscle in a concentration of 10 mcM, significantly facilitated the frequency of miniature end plate potentials (MEPPs). Simultaneously the changes in the amplitude of MEPPs was found, which reached 25% from the control ($P< 0,05$, $n=34$; $m=10$). PAR-AP did not change the membrane potential of muscle fiber and the time course of MEPPs. PAR-AP induced increase of MEPPs amplitude was blocked by pre-application of ACh-vesicle transporter blocker (-)*vesamicol* (1 μM) or H^+-ATPase blocker *bafilomycine* (2 μM). Further analysis showed that blockade of inositol-1,4,5-trisphosphate receptors (IP_3-R) using 2-aminoethoxydiphenylborate (30 μM) did not prevent the potentiating effects of PAR-AP. But the potentiation of MEPPs amplitude by peptide was fully blocked by protein kinase A inhibitor H89 (1 μM). At the same time, the inhibition of protein kinase C with cheleritrine (1 μM) by itself did not change the MEPPs amplitude but reversed the PARI-AP potentiating effect: instead of potentiation of MEPPs amplitude, the depression on MEPPS amplitude was revealed by preliminary application of PKC inhibitor. The data obtained demonstrate for the first time that the motor nerve terminals of mice can contain the presynaptic PAR1 receptors, which activation by PAR1-agonist can significantly increase the amplitude of MEPPs, due to the activation of PKA and increase of ACh uptake into the synaptic vesicles.

Allatostatin action on ACh quantal size

Allatostatin is a crustaceans peptide consisting of 12 amino acids (*Ala-Pro-Ser-Gly-Ala-Gln-Arg Leu-Tyr-Gly-Phe-Gly-Leu-*NH_2), which is not expressed in mammalian genom (Woodhead et al., 1989; Gaydukov, Balezina 2006). Nevertheless, application of allatostatin (1 nm – 1 μM) on the mouse hemidiaphragm synapses produced a dose-dependent increase of the MEPPs amplitude (that reached 209% of control at 1 μM of peptide), but without affecting statistically significantly

the MEPPs frequency and membrane potential of muscle fibers. Allatostatin (1 μM) caused a twofold rise of EPMC amplitude, but the time parameters of miniature postsynaptic currents did not change statistically significantly. There were revealed no rise of the postsynaptic membrane input resistance by application of alllatostatin. The potentiating allatostatin effect on MEPPs amplitude was prevented by *vesamicol* (1 μM), a blocker of transport of acetylcholine into synaptic vesicles. Preliminary treatment of the nerve-muscle preparation with the inhibitor of protein kinase A (PKA) H-89 (50 nM) prevented the allatostatin-evoked EPMC amplitude increment. The obtained data allow us to suggest that allatostatin in the mouse nerve-muscle synapse acts at the presynaptic level, producing an increase of the ACh quantum size due to an intraterminal cascade of reaction with participation of PKA.

CGRP action on ACh quantal size

Calcitonin gene-related peptide is a 37-amino acid peptide that is formed as a result of alternative processing of calcitonin gene. In motor nerve terminals, endogenous CGRP is localized in large dense-core vesicles [Van der Kloot et al., 1996], which exocytosis from terminals is initiated by calcium release from internal ryanodine sensitive stores [Wong et al., 2009]. So, we activated the presynaptic raynodine receptors (RyRs) of motor nerve terminals to induce CGRP exocytosis into synaptic cleft and to observe its probable presynaptic action on amplitude of MEPPs.

We found that ryanodine application induced significant increase of mean MEPPs amplitude (up to 45%) probably induced by the release of stored calcium. Blockade of RyRs by selective RyRs antagonist (dantrolene, 100 μM) prevented this effect. Preliminary loading of the motor nerve terminals with intracellular calcium buffer EGTA-AM also completely prevented the ryanodine-induced increment of MEPPs amplitude. To test the hypothesis that the Ca^{2+}-dependent ryanodine–induced CGRP release into the cleft caused the increase of the mean MEPP amplitude we used the truncated $CGRP_{8-37}$ molecule known as selective CGRP receptror blocker. $CGRP_{8-37}$ by itself had no significant effect on parame-

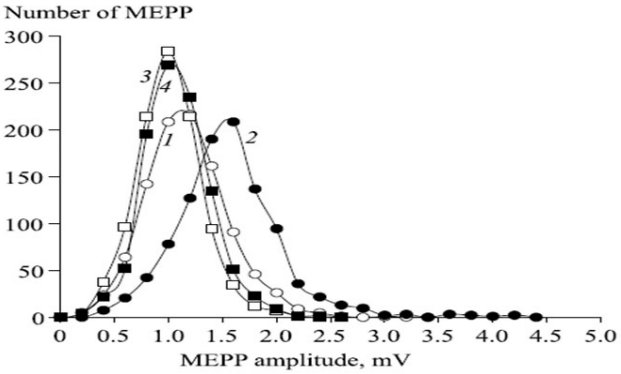

MEPPs amplitude histograms in control (*1*), during ryanodine application (*2*), by pre-application of vesamicol (*3*) and 0,5 μM CGRP8-37 (*4*).

ters of spontaneous ACh release but completely prevented the potentiating effect of ryanodine on the amplitude of MEPPs, respectively ($p<0.05$). We then used vesamicol, a specific blocker of acetylcholine transport into vesicles. In intact nerve-muscle preparation, vesamicol (5 μM) produced no significant changes in the mean amplitude and histogram of MEPPs. However, application of ryanodine (1 μM) to vesamicol-treated preparation produced no significant increase in the mean amplitude of MEPP and no corresponding shift of the MEPPs amplitude histograms (figure).

Taking into account the literature data, demonstrating dependence of CGRP release on activity of CaMKII in nerve terminals and participance of PKA activity in realization of intracellularly CGRP effects, we have tested the effects of CaMKII and PKA blockers on ryanodine-induced MEPPs potentiation. We found, that preliminary treatment of the nerve-muscle preparation with the inhibitor of protein kinase A (H-89, 50 nM) or CaMKII (KN 62 1 μM) prevented the ryanodine-evoked MEPPs amplitude increment. These data suggest, that: 1) the ryanodine induced increase of MEPPs amplitude is due to Ca-CaMKII dependent CGRP release into synaptic cleft and its further presynaptic action 2) that presynaptic CGRP action is aimed to increase of ACh quantal size and is realized with the help of PKA.

General conclusion

On the base of data obtained, we can conclude, that the unkown activity of three different peptides is revealed, which is specifically directed to potentiate the ACh content in synaptic vesicles, i.e., the ACh quantal size, in mice motor synapses. We can suggest the presence of three different types of specific receptors on the membrane of motor nerve terminals, which are selectively sensitive to proteins different in their chemical structure and origin. There are receptors to *peptide-agonist of thrombin (PAR1)*; receptors to crustaceans peptide *allatostatin;* receptors to *calcitonin gene related peptide (CGRP).* The mechanism of ACh quantal size potentiation by three peptides tested provides activation of their special presynaptic G-protein coupled receptors and intracellular cascades, which include activation of presynaptic PKA and increase of ACh content in the vesicles.

The work is supported by RFBR, grant № 16-04-00554.

References

1. Balezina O.P., Gerasimenko N.Yu., Dugina T.N., Strukova S.M., 2004, Usp. Sovr. Physiol., V.35(3), pp. 37-49.
2. Edwards R.H., 2007, Neuron, V.55(20), pp. 836-858.
3. Fatt P., Katz B., 1952, J. Physiol. Lond., V.117, pp. 109-117.
3. Gaydukov A.E., Balezina O.P., 2006. Zhurn. Evol. Biokhim. Fiziol., 2006, V.42(6), pp. 554–558.
4. Van der Kloot W., 1991, Progr. Neurobiol., V.36, pp.90-130.
5. Van der Kloot W., Benjamin W.B., Balezina O.P., 1996, J. Physiol., V.507(3), pp. 689-69.
6. Woodhead A.P., Stay B., Seidel K., Kahn M.A., 1989, PNAS, V.321, pp. 146-51.
7. Wong M., Shakirjanova D., Levitan E.S., 2009, J. Mol. Neurosci., V.37(2), pp. 146–150.

ASSESSMENT OF THE EFFECTS OF METHYLPREDNISOLONUM AND MOTOR TRAINING WITH CONTUSION SPINAL CORD INJURY IN RATS

M.E. Baltin, N.F. Ahmetov, A.D. Militskova

Kazan Federal University, ul. Kremlevskaya 18, Kazan, 420008 Russia

Traumatic injuries to the central nervous system continue to be one of the most difficult problems of modern medicine.

A growing number of treatments for spinal cord injury and out of the laboratories are moving in clinical trials. Many of them are used as soon as possible after the injury with the hope of weakening the secondary damage and maximize the preservation of nerve tissue. The aim of the study was to evaluate the effects methylprednisolonum and motor training at an experimental spinal cord injury in rats. Motor function was assessed in an open field, using BBB screening system. The evaluation was conducted for 24 hours before surgery (day 0) and daily, beginning 24 hours after surgery to the thirtieth day. To investigate the status of the peripheral neuromuscular system registered motor response (M & H) muscles. Reflex excitability of the spinal motor centers tested by H-reflex. Determines the maximum amplitude and the threshold of responses. For a more complete characterization of the reactive motor neuron pool was measured: the ratio of motor and reflex response maximum amplitudes [$(H_{max}/M_{max})\cdot 100\%$)]. In the early period after spinal cord injury was observed a decrease of the maximum amplitude of M-response. With that, in the group of animals with the introduction methylprednisolonum amplitude of M-response was higher than without drug therapy. It is obvious that in acute degenerative changes occurred muscular system, however, as shown by our data administration methylprednisolonum had a positive effect. The amplitude of the H-response in the group with and without methylprednisolonum to 7 days decreased, which indicates a decrease in the excitability of the motor centers of the spinal cord. Also, it decreases the excitability of the centers for 7 days demonstrated a reduction ratio of the maximum amplitude of the M- and H-response. Based on these results, we came to the following conclusions: 1) methylprednisolonum treatment is effective in the acute period, however, can lead to negative consequences in the chronic period after the injury; 2) combination therapy methylprednisolonum and motor training has a positive effect on the recovery of motor function in chronic period after contusion spinal cord injury in rats.

ECG PARAMETERS OF THE HEART MUSCLE REPOLARIZATION: MEASUREMENT AND INTERPRETATION

O.V. Baum[1], L.A. Popov[1], V.I. Voloshin[1], G.A. Muromtseva[2], S.K. Prilutskaya[1]

[1]*Institute of Theoretical and Experimental Biophysics, Russian Academy of Sciences, Pushchino, Russia*

[2]*National Research Center for Preventive Medicine of Russia, Moscow, Russia*

Basic and applied research suggest that one of the reasons for electric instability of myocardium, which in some cases can give rise serious cardiac ar-

rhythmias and even sudden death, is abnormal inhomogeneity of repolarization in the heart ventricles. The occurrence of such a situation is possible, in particular, under development of myocardial ischemia.

Identification of myocardial ischemia by electrocardiographic methods, especially at early stages of the disease, is therefore an important problem of modern electrocardiology. The difficulty is that certain symptoms of ischemia are transient in time, i.e. are observed only in separate cardiac cycles. Besides, on many issues for choice of diagnostically relevant parameters there exist different, sometimes opposite views in this field of knowledge. In addition, the parameters of repolarization used in medicine remain often "one-dimensional" which makes it difficult, in particular, to introduce new results of fundamental development into practice.

The problem asks for development of pattern recognition algorithms [1], new methods for the mathematical description of the measured parameters of the electrocardiosignal (ECS), both in norm and under pathology [2], as well as evolution of biophysical models for electric activity of the heart [3] and specialized archives for parameters and results of modeling [4].

Aim

The purpose of the present study was a search for a set of informative indexes for algorithms of measurement and interpretation of repolarization parameters on ECS under development of n-dimensional methods for estimation of electrophysiological state of myocardium in ventricles of the heart.

Material and Methods

In the study we used material from the Data base (DB) of the real ECSs, which were registered previously in twelve standard and three orthogonal leads with the help of the research system "Uran", developed at the Institute of Theoretical and Experimental Biophysics, Russian Academy of Sciences. Methods of computer modeling, of processing real and model signals, statistical approaches to an estimate of obtained results, as well as methods for formalization of the medical logic were used.

Results and Discussion

A comparative analysis of different classes of algorithms for computer electrocardiodiagnostics, including algorithms for identification of myocardial ischemia, has been carried out. In conformity to tasks of this research, the concepts of an "internal" and "external" image of ischemia have been formulated in [4] and used partially earlier in [5].

Biophysical aspects for the basic indexes of spatial inhomogeneity of the repolarization process in myocardium, as well as problems of measurement of parameters corresponding to them have been considered. It is possible to refer to these indexes such parameters as dispersion of three intervals of the cardiac cycle (QTD, QTaD, and TpTeD), next ventricular electric gradient (G) and the space angle between vectors of de- and repolarization (αQRS-T).

The experimental part of the work was carried out on the basis of two samples of ECGs, "Norm" and "Ischemia" of lateral localization. The samples were formed from material of the DB "Uran" and represent, respectively, 202 and 144

sets of ECGs of real patients in the standard twelve leads. The samples were verified according to criteria of the Minnesota Code.

In accordance with the "internal" image of ischemia and "scenarios" of its development in terms that correspond to characteristic alterations of the transmembrane action potential (TAP) under ischemia, 25 parameters of repolarization part of the cardiac cycle, which could be used, presumably, for identification of ischemia, were selected.

Among the selected parameters we mention just a few: beta – the parameter of asymmetry of the T wave calculated in its limits as the ratio of modules of the maximum values of the derivative of the signal at the left and to the right of the top of the T wave; Asym – analog of the concept of asymmetry in mathematical statistics under formal consideration of the T wave as a distribution of some conditional random variable; GL – the ventricular gradient in lead L; J80 – the shift of the ST segment measured through 80 ms after the generalized J point; JTa/JT and JTa/QT – ratios of durations of the corresponding intervals of the cardiac cycle; ampT1 – the T wave amplitude in lead 1; QTaD – dispersion of the QTa interval; some more parameters characterizing asymmetry of the T wave, and others. A complete list of the parameters, their meaning, and rules for calculating are given in [5]. Tables of measurement results for the selected parameters of all patients in the two samples have been obtained.

For a preliminary comparison of potential diagnostic capabilities of the various parameters obtained, it has been offered to use a corresponding to them number of modified Mahalanobis distances between norm and pathology.

Leaving from "one-dimensionality" in the ECG-image of patients, development and use of the n-dimensional ECG-parameters, rotations of the coordinate system in the n-space, and also other methods of pattern recognition are necessary for increasing the information content of the electrocardiographic measurements.

In diagnostic algorithms several parameters can be used, which are combined by means of Boolean functions "OR" and/or "AND". The Minnesota code (MC code), for example, can be considered as an n-dimensional parameter of ECS in epidemiological studies.

It is possible to design multistage or compound algorithms, using the logical operators **OR** or **AND** to protect the final diagnosis against overdiagnosis (algorithms like "**A** and **B** □**D**") or underdiagnosis (algorithms like "**A** or **B** □D").

There are also algorithms where the diagnosis is defined by the sum of points scored by several independent conditions.

Many algorithms in which there exist attempts to formalize a medical logic, are arranged as multistage algorithms of the tree-type in which the way to the resulting diagnosis depends in each knot of the diagnostic tree on a condition "If **A**, then **B**" where **A** is the condition, and **B** is the chosen tree branch for the further way.

At increase in number of the object parameters considered at a time we are dealing with a multidimensional space. The "external" ECG-image of the patient describing his electrophysiological state is in that case a point in the n-dimensional

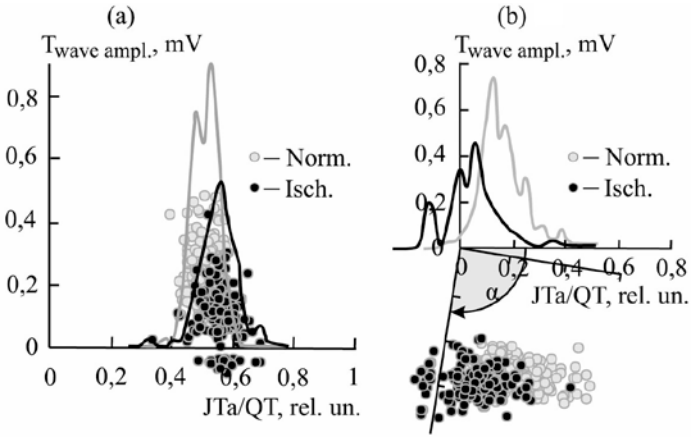

Fig. 1. Transformation of the cloud pattern: (a) – $\alpha = 0°$; (b) – $\alpha = -100°$.

space of electrocardiographic parameters. The simplest case is a two-dimensional space formed, for example, by any pair of the parameters mentioned above.

In the present study, 16 pairs of initially selected parameters were considered. For the samples of "Norm" and "Ischemia" were constructed two-dimensional distributions for all the patients in the form of corresponding points on the plane. In such a way, for each of the considered pairs of parameters, two "clouds" of points, for Norm and Ischemia, have been obtained. As an example, in fig. 1a are shown the clouds of two-dimensional distribution of points for the following pair of parameters: "Ratio of durations of the JTa the QT intervals" and "T wave amplitude in the Lead I". As can be seen from the figure, the two clouds are overlapped markedly. Furthermore, their projections on axes of "JTa/QT" and "ampT1" are that the use of these parameters separately in one-dimensional algorithms of recognition gives relatively low values of ε, i.e. sensitivity of the algorithm. For JTa/QT, for example, $\varepsilon = 34\%$.

The use of the standard procedure of rotating the coordinate system of origins through an angle α changes the index ε, improving it in some cases under the same value of the specificity index with the result of that the efficiency of the algorithm increases.

The effective value of the angle α for rotation is looked for by standard methods of optimization. Fig. 1b shows the transformation of the cloud pattern when α became –100°. The value of ε increased to reach 60%. There were, however, some problems of points in a zone of overlapping of two clouds, and also problems of "foreigner-points"(Norm among Isch. and Isch. among Norm) in zones of "tails" of both clouds. It has been proposed to develop a strategy for working with the 2D-results (as well as with the nD-results), including the separation of patients already at the stage of classification into three samples: "Norm", "Ischemia", "It is very likely that Ischemia".

Conclusions

The results obtained are of interest for the development of new systems for automatic ECS diagnostics operating in the mode of consultation between computer algorithms. In electrocardiology one can conditionally divide diagnostic algorithms into three generations: algorithms for formalization of the medical logic; probabilistic algorithms of decision-making; algorithms for interpreting the state of the cardiac muscle in terms of biophysical models. Such a consultation between algorithms provides for presence in the system of a database for real and model ECSs. Each of algorithms operates with its own set of ECS parameters at the input. Therefore, a search on ECS for new informative parameters of repolarization of the heart muscle, including n-dimensional ones, is an important task in modern electrocardiology.

References

1. Neymark Yu.I. (Ed.). Pattern recognition and medical diagnostics. Moscow: Nauka, 1972 (in Russian).
2. Baum O.V., Voloshin V.I., Popov L.A. Electrocardiographic Image of Myocardial Ischemia: Real Measurements and Biophysical Models. Part II. Biophysics, 2012, 57 (5), 668-675. DOI:10.1134/S0006350912050028
3. Baum O.V., Voloshin V.I., Popov L.A. Biophysical Models of Cardiac Electrical Activity. Biophysics, 2006, 51(6), 940-954. DOI:10.1134/S00063509060601333
4. Baum O.V., Voloshin V.I., Popov L.A. Interactive electronic archive for parameters and results of computer modeling of an electrical state of the heart muscle (in this volume).
5. Baum O.V., Voloshin V.I., Popov L.A. Computer Simulation for Localization and Extensiveness of Myocardial Ischemia. Biophysics, 2014, 59 (5), 814-819. DOI:10.1134/S0006350910050234

INTERACTIVE ELECTRONIC ARCHIVE FOR PARAMETERS AND RESULTS OF COMPUTER MODELING OF AN ELECTRICAL STATE OF THE HEART MUSCLE

O.V. Baum, V.I. Voloshin, L.A. Popov

Institute of Theoretical and Experimental Biophysics, Russian Academy of Sciences, Pushchino, Moscow Region, 142290 Russia

Problems of identifying the electrophysiological state of the heart muscle, including myocardial ischemia, are the main prerequisite for development of new computer technologies of the registration and analysis of electrocardiosignal (ECS). One of the promising methods of research in this field of knowledge is the method of mathematical and computer modeling.

The heart as a complicated biological object requires a systemic approach to study of the relationship between the depolarization and repolarization processes in myocardium, on the one hand, and their manifestation in distribution of electrical potentials on the body surface, on the other hand. Let us consider the set of biophysical parameters and their values that describe processes occurring in the heart muscle as a model of an “internal” state of the heart. The time-dependent distribution of potentials on the body surface which can be recorded, measured,

and represent in terms of the modern electrocardiology, we will then accept as a model of the “external” image of this state.

The problem requires the development of adequate biophysical models of the cardiac electrical activity as well as new methods for mathematical description of external heart parameters. As well as understanding the “scenarios” for development of cardiac pathologies in terms of the appropriate dynamics of their internal parameters. Mainly, it is distribution in the heart ventricles of forms of the transmembrane action potential (TAP) generated by a double electric layer over the surface of electrically active myocardium [1].

Owing to the mentioned complexity of the problem, it is important to keep it all in sight and change "on-the-fly" parameters of the model that is the “internal image” of the electrophysiological state of the modeled heart, during the computer experiment, observing at the same time "on line" the results of modeling. These results are the corresponding changes of the output data of the model, including alterations in the pattern of the model cardiac cycle in different leads. This procedure implies that it is essential to create a joined archive for the model parameters used and for the results of measurement, recognition, and interpretation of parameters of the real and model ECSs.

Aim

The purpose of the present study was to work out an electronic archive for parameters and results of computer modeling of an electrical state of the myocardial muscle in the form of an interactive model, namely, the model with which you can interact, that is, to observe “on line” its reaction and behavior under various external influences.

Methods

The work was carried out on the basis and with the help of the model for the ECS genesis, previously developed at the Institute of Theoretical and Experimental Biophysics RAS [1,2]. The methods used are mathematical and computer modeling and programming.

Results and Discussion

The first version of the interactive electronic archive for input and output data of the biophysical model of electrical activity of the heart has been developed. In the archive, materials necessary for studying the effect of forms of TAPs and their distribution over the ventricles of the cardiac model on the total ECS in standard and orthogonal leads of the electrocardiogram are accumulated. It is also possible to study the partial contributions to the ECS from each model segment or from its single elements.

The archive is intended for the qualitative and quantitative interpretation of results of computer experiments in terms of models of a double electric layer over the surface of electrically active myocardium. The materials of the archive are the source of information for solution of the basic and applied problems of the heart biophysics. In particular, they are used during solution of the problems associated with the development of new methods for identification of an electrical state of the heart [3,4].

The archive contains the description of the model, reference data, tables of parameters, and schemes of conducting computer experiments, "scenarios" of the development of pathologies being simulated, figures, and files of output results, including calculated parameters of the model ECSs.

In the version of the basic biophysical model adapted for the archive, the earlier developed method for segmentation of the model of heart ventricles into separate compartments and the method for calculation of partial curves are used. The second of these methods is based on the principle of superposition, which makes it possible to present ECS in any lead in the form of a weighed sum of the phase-shifted TAPs.

In the test regime of the work with the archive, cases corresponding to the conventionally normal heart and to several hypotheses of "ischemic" changes in TAPs of different localization and extension have been considered. The problem-oriented replenishment of the archive will be performed in the framework of planned tasks.

In the course of work on development of the archive the concepts of "internal" and "external" images of ischemia which were partially used in [3,4] have been specified. Biophysical aspects of the main indexes of spatial inhomogeneity of the repolarization process in myocardium have been considered. These are dispersions of the QT, QTa, and TpTe intervals, as well as the intraventricular electrical gradient G and the spatial angle αQRS-T.

As an example illustrating the work with the archive, fig. 1 shows a section of the model in the frontal plane (a) and specified changes in duration of the TAP on the internal surface of the left ventricle (b) in a computer experiment under simulation of the subendocardial "ischemia". In the same place (b) are given curves of the TAPs on epicardium of the left ventricle and on all surface of the right one; the TAP form on each of these two surfaces is considered, as it seen from the drawing, a constant.

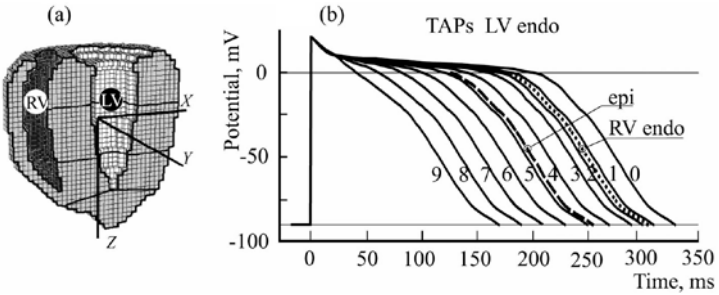

Fig. 1. The cross-section of the model of the heart (a), TAP curves (b) on the epicardial surface of the model (epi), on the endocardium of the right ventricle (RV endo), and on the endocardium of the left ventricle (0, 1,…9).

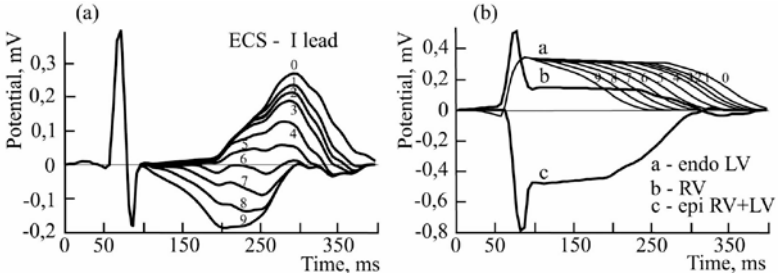

Fig. 2. ECSs (a) and different partial ECSs (b) in lead I corresponding to the experiment.

Fig. 2 shows the resultant changes in the ECS in lead I and partial curves corresponding to contributions from different surfaces of the left and right ventricles into the potential of this lead.

Conclusions

The use of models for the elucidation of the relationship between the systemic parameters of the heart and parameters measured on the ECSs as well as for testing arising hypotheses and for researching diagnostic algorithms, possesses the essential novelty.

Such approach may be virtually the only opportunity of purposeful search of new diagnostic indexes. This can not only improve the efficiency of existing methods for identifying an electrophysiological state of the heart, but also to optimally connect them with other methods of computer diagnosis in cardiology. For a reasonable estimation of the electrophysiological state of myocardium the development of new diagnostic systems should be based on a consultation of three generations of algorithms. It, respectively, the algorithms of formalization of medical logic, probabilistic algorithms of decision-making and algorithms which interpret a condition of the cardiac muscle in terms of biophysical models. An important condition for the effective operation of such systems is the presence in their structure of the database and/or archives of the model and real ECS. In addition, it is necessary to work with cardiosignals of “the model patient” in accordance to algorithms which are created for the real ECS. Therefore, one of the immediate tasks for further progress of this archive is the development and realization of principles for adequate comparison of the model and real ECS.

The illustrated archive of the input parameters of the model and the results of simulation of ECSs is also of interest for development of specialized programs in the field of computer education on the topics “Biophysics and Electrophysiology of the Heart” and “Computer Medicine”.

References

1. Baum O.V., Voloshin V.I., Popov L.A. Biophysical Models of Cardiac Electrical Activity. Biophysics, 2006, 51 (6), 940-954. DOI:10.1134/S0006350906060133

2. Baum O.V., Voloshin V.I., Popov L.A. Realization of Biophysical Models of Cardiac Electrical Activity. Biophysics, 2009, 54 (1), 72-84. DOI:10.1134/S0006350909010138
3. Baum O.V., Voloshin V.I., Popov L.A. Electrocardiographic Image of Myocardial Ischemia: Real Measurements and Biophysical Models. Part II. Biophysics, 2012, 57 (5), 668-675. DOI:10.1134/S0006350912050028
4. Baum O.V., Voloshin V.I., Popov L.A. Computer Simulation for Localization and Extensiveness of Myocardial Ischemia. Biophysics, 2014, 59 (5), 814-819. DOI:10.1134/S0006350910050234

VIOLATION OF ENERGY-DEPENDENT PROCESSES AS ONE OF MOLECULAR MECHANISMS OF STATIN MYOPATHY

E.S. Belousova, Z.I. Mikashinovich, O.G. Sarkisyan
Rostov State Medical University, ul. Nakhichevanskaya 29, Rostov-on-Don, 344022 Russia

Statins, as an HMG-CoA reductase inhibitors may influence the biosynthesis of ubiquinone, which is regarded as one of the possible pathogenic mechanisms of statin myopathy. However, information about changes the level of ubiquinone under the influence of statins remain controversial. I suppose that in the context of inhibiting HMG-CoA reductase violation collector ubiquinone function leads to the disintegration of various metabolic pathways to achieve a stationary intracellular energy capacity required for the proper functioning of muscles [3,4]. It must be said that the publications contain almost no data on the dynamics of energy metabolism and energy-dependent processes in myocytes when using statins.

In this context, the aim is to analyze the dynamics of indicators that reflect the state of the energy metabolism and the ATPase activity of myocytes in laboratory animals during prolonged administration of simvastatin (Zocor).

The study was conducted on 70 mongrel male rats aged 12–14 months (300–350 *g*). Pets correspond to sanitary rules SR 2.2.1.3218-14 “Sanitary requirements to the device, equipment and maintenance of experimental biological clinics (vivariums)” dated 08.29.2014. Animals during 3 months were maintained on a diet enriched with animal fat (melted butter) and easily digestible carbohydrates (sugar cane, semolina). During the experiment, the animals were divided into two groups: a control group – 35 animals fed a diet without addition of drugs; Experimental group – 35 animals treated for 2 months with simvastatin (Zocor, 20 mg) at 0.001 g/100 g of body weight once daily as an aqueous slurry through an esophageal probe. The intact control group of animals was kept on a general vivarium ration. The animals were taken out of the decapitation of the experiment. We collected fragments of skeletal muscle from the back of the animal’s paw for the research. Activity of adenozintriphosphat enzyme complex (Mg^{2+}- and Ca^{2+}-dependent Na^{+}/K^{+}-ATPase) was determined by a method based on splitting under the influence of an enzyme of organic phosphorus compounds to produce an inorganic phosphate, which is recorded by reaction with ammonium molybdate in the presence of ascorbic acid [2].

Mitochondria are isolated by differential centrifugation after homogenization in saline (0.15 M KCl and 10 mM Tris-HCl). Homogenates were centrifuged for 15 min at 640 *g* to remove the nuclear fraction. Mitochondrial fraction was isolated for 25 minutes at 20000 *g* by washing twice with release medium. Active substrate dehydrogenases Krebs cycle: pyruvate dehydrogenase (PDH), α-ketoglutarate dehydrogenase (α-KG-DH), succinate dehydrogenase (SDH) was determined by spectrophotometric method in a model system for the reduction reaction of nitro tetrazolium in the presence of a specific substrate (pyruvate Na, α-ketoglutarate, succinate) [5]. The activity of cytochromeoxydase (CCO) was determined by reaction with paradinitrophenylendiamine [1].

Statistical processing of the experimental data was performed using STATISTICA 6.0 software. Statistically significant difference was considered appropriate assessment of the probability of error $p \leq 0.05$.

Animals on a diet enriched in carbohydrate and fat animals (control group), led to a significant increase in the level of cholesterol in blood serum to 75.38% (p<0,001) relatively to the control group. In determining the activity of enzymes of carbohydrate and energy metabolism showed an increase of PDH activity by 119% (p<0,001), α-KG-DH at 94.12% (p<0,001), CCO activity and SDH did not differ from the control group (table 1).

In the control group animals showed improvement in overall muscle ATPase activity by 28% (p<0.05), ATPase Ca^{2+} 98% (p<0.001) and ATPase in the Mg^{2+} 113.5% (p<0.001) relatively to the control group. Dynamics ATPase activity under conditions of hypercholesterolemia can be considered as a compensatory-adaptive mechanism to preserve the intracellular ion homeostasis (table 2).

Simvastatin (experimental group) helped to reduce the cholesterol levels in blood serum to 1.637 ± 0.136 mmol/l, which was not significantly different from the control group.

Table 1. The concentration of metabolites of glycolysis and energy metabolism enzyme activity in animal muscle tissue treatment groups ($M \pm m$)

Index	Control group, n=35	Comparison group, n=35	Experimental group, n=35
SDH [mkmol/mg of protein]	2.14 ± 0.235	2.44 ± 0.261 p>0.05	0.79 ± 0.066 p_1<0.001 p<0.001
CCO [mkmol/mg of protein]	0.0039 ± 0.00056	0.0036 ± 0.00028 p>0.05	0.0011 ± 0.00011 p_1<0.001 p<0.001
alpha-KG-DH [mkmol/mg of protein]	0.884 ± 0.094	1.716 ± 0.085 p<0.001	0.779 ± 0.089 p_1<0.001 p>0.05
PDH [mkmol/mg of protein]	0.811 ± 0.096	1.774 ± 0.223 p<0.01	1.279 ± 0.137 p_1<0.05 p<0.001

Note: p – significantly relative to the control group; p_1 – significantly relative to the comparison group.

Table 2: ATPase activity in the muscles of animals studied groups ($M \pm m$)

Index	Control group, n=35	Comparison group, n=35	Experimental group, n=35
ATPase total [mkmol/mg of protein]	0.0176 ± 0.0018	0.0225 ±0.0020 p<0.05	0.0072 ± 0.0006 p_1<0.001 p<0.001
Ca^{2+}-ATPase [mkmol/mg of protein]	0.0436 ± 0.0023	0.0865 ± 0.0041 p<0.001	0.0307 ± 0.0018 p_1<0.001 p<0.001
Mg^{2+}-ATPase [mkmol/mg of protein]	0.0577 ± 0.002	0.1232 ± 0.050 p<0.001	0.0676 ± 0.002 p_1<0.001 p<0.001

Note: p – significantly relative to the control group; p_1 – significantly relative to the comparison group.

After injecting the simvastatin in the muscles of animals the decrease in SDH activity at 27.9% (p_1<0.05) and alpha-KG-DH at 54.6% (p_1<0.001) was observed relatively to the comparison group. Regarding the control group, PDH activity remained increased by 57.71 (p_1<0.001). and α-KG-DH did not differ significantly. At the same time, the muscles of animals of the experimental group showed a sharp decrease in SDH activity at 67.62% (p_1<0.001), CCO at 69.44% (p_1<0.001). When comparing the results with a control group. SDH activity and CCO were reduced by 63% (p<0.001) and 71.8% (p<0.001), respectively. Decreased activity of the terminal portion of the respiratory chain may be caused by a deficiency of ubiquinone biosynthesis, which is also performed with HMG Co-A reductase inhibitors.

Injection of simvastatin reduction contributed of the total muscle tissue ATPase activity at 68.00% (p_1<0.001), ATPase Ca^{2+} at 64.1% (p_1<0.001), ATPase Mg^{2+} at 45.13% (p_1 < 0.001) with respect to control group (Table. 2). It should be noted that in comparison with the indices for intact animals total ATPase activity was reduced by 59.1% (p<0.001), ATPase activity of Ca^{2+} at 29.59% (p<0.001), ATPase activity Mg^{2+} it was increased by 17.16% (p<0.001). Reducing the ATPase activity may be due to deficiency of energy phosphates. Violation of the active transport of ions will promote the formation of an ionic imbalance, resulting in a violation of the myocyte excitability, distortion of the regulatory role of Ca^{2+} and Mg^{2+}, and a gradual loss of muscle fiber contraction.

Based on these data it is possible to believe that long-term injection of simvastatin promotes disintegration of energy-production and energy-dependent mechanisms. Since the constant regeneration of ATP maintains the intracellular ion homeostasis, the violation of energy myocytes can be regarded as one of the molecular mechanisms of degenerative changes when taking statins.

References

1. Krivchenkova R.S. Modern methods in biochemistry. M.: Medicine. 1977.
2. Prokhorova M.I. Methods of biochemical research (lipid and carbohydrate metabolism). 1982.

3. Parker B.A., Gregory S.M., Lorson L. et al. A randomized trial of coenzyme Q10 in patients with statin myopathy: rationale and study design. // J. Clin. Lipidol. 2013. Vol. 7(3). P. 187-193.
4. Muraki A., Miyashita K., Mitsuishi M. et al. Coenzyme Q10 reverses mitochondrial dysfunction in atorvastatin-treated mice and increases exercise endurance. // J. Appl. Physiol. 2012. Vol. 113(3). P. 479-486.
5. Nordmann I.N. Determination the activiti dehydrogenasique des mitochondries a 1-acid-dichloride-2.3.5-triphenyl-tetrazolium. // Bull. Sos. Chim. Biol. 1957. Vol. 33. P. 189-197.

INFLUENCE OF NF-*k*B-SIGNALING BLOCKER ON THE E3-LIGASES EXPRESSION IN RAT *soleus* DURING 3 DAY HINDLIMB UNLOADING

S. Belova, T. Nemirovskaya

Faculty of Basic Medicine, Lomonosov Moscow State University, Lomonosovsky prosp. 31/5, Moscow, 117191, Russia

Russian Institute of Biomedical problems RAS, Khoroshevskoe Shosse 76a, Moscow, 123007, Russia

Skeletal muscle atrophy caused by unloading is accompanied by increased proteolysis and decreased protein synthesis. Muscle proteolysis results from the activation of calpain and ubiquitin-proteasome systems. Ubiquitination of myofibrillar and cytoskeletal proteins is carried out by muscle-specific E3 ubiquitin ligases – MuRF-1 and Atrogin1, expression of which is significantly increased on the third day of muscle unloading. But what is the triggering factor of the E3 ligases expression? Until recently FOXO3 was considered to be the only transcription factor that triggers MuRF-1 expression. Recently S. Kandarian and coauthors have shown that NF-kB, but not FOXO3, is required for MuRF-1 transcriptional activation. The aim of present study was to test hypothesis about the key role of NF-kB transcription factors in the initiation of E3 ligases expression and development of skeletal muscle atrophy during unloading.

We have treated rats with IMD-0354 (an inhibitor of IKKβ, blocking the phosphorylation of IκBα) during the 3-day hindlimb suspension. 21 male Wistar rats were randomly divided into 3 groups: intact control (C), rats suspended for 3 days (HS) and rats that were suspended and injected with IMD-0354 (10 mg/kg) (IMD). We did not observe any effect of the IMD on prevention of soleus atrophy at the early stages of unloading. The weight of soleus in HS and IMD groups was significantly decreased compared to control ($p<0.05$). We observed an increased levels of MuRF-1 and Atrogin-1 mRNA expression levels in both suspended groups (HS and IMD) as compared to control group, but, surprisingly, there parameters in IMD group were significantly higher than in the HS group. The similar pattern was obtained on the protein level of MuRF-1 ($p<0.05$). The level of I*k*B*a* was significantly lower in HS group compared to control ($p<0.05$). The level of I*k*B*a* in HS+IMD group was increased compared to control ($p<0.05$). These data confirms that the concentration of IMD-0354 used in our experiments was adequate for the suppression of unloading-induced activation of

NF*k*B pathway. The protein level of transcription factor P105 in the cytoplasm was significantly reduced only in the HS but not in IMD group compared to control ($p<0.05$). Level of NF-κB transcription factors Bcl-3 and p50 in the cytoplasm did not change in HS and IMD groups compared to control. We also investigated the links of Akt-mTOR-S6K and MAPK/Erk anabolic signaling pathways. There was a decrease in p-Akt and p-p90RSK-1 content in both suspended groups compared to control ($p<0.05$).

Our results suggest that at the early stages of unloading (3 days) the main factor inducing the E3 ligases expression could be an alternative pathway, but not NF-κB, which seems to be activated at a later stage.

This work was supported by RFBR grant No. 14-04-01632.

PLASTICITY OF CONTRACTILE SYSTEM IN CULTIVATED RAT NEONATAL CARDIOMYOCYTES AND ITS REGULATION BY EXTRACELLULAR MATRIX

N.B. Bildyug

Institute of Cytology RAS,
Tykhoretski av., 4, St.Petersburg, 194064, Russia

Highly organized myofibrillar apparatus of cardiomyocytes in heart tissue allows for their continuous contractility and is believed to be stable. However, adult and neonatal cardiomyocytes transferred to monolayer culture system undergo rearrangement of their contractile apparatus with the conversion of typical myofibrils into structures of non-muscle type and the loss of contractility. This rearrangement is reversible and is followed by the recovery of initial myofibrillar organization and ability to contract. When transferred to the monolayer culture over extracellular matrix (EMC) substrate, cardiomyocytes restored their myofibrillar apparatus faster than those cultured on pure coverslips. Moreover, upon cultivation of cardiomyocytes in 3D collagen gels, the reorganization of their contractile apparatus did not occur. These data suggested a strong relationship between the dynamics of contractile structures and the presence and organization of extracellular matrix. To reveal this relationship in more detail, the present study was aimed to evaluate expression of actin isoforms and to correlate it with appearance of the main structural ECM components of heart tissue, collagen and laminin, at the successive stages of reversible rearrangement of the cardiomyocyte contractile system in culture.

We show that the reorganization of the contractile system during long-term cultivation of rat neonatal cardiomyocytes is accompanied by the transient replacement of α-cardiac actin by α-smooth-muscle actin isoform and production by cardiomyocytes of their own extracellular matrix proteins and matrix metalloproteinases, which is not typical of these cells in heart tissue. Gradual accumulation of extracellular matrix components correlates with the dynamics of matrix metalloproteinases and is accompanied by reduction of α-smooth muscle actin, which precedes the restoration in cardiomyocytes of myofibrillar apparatus and contractile function.

Our results suggest that synthesis of extracellular matrix by rat neonatal cardiomyocytes in culture and its spatial organization with matrix metalloproteinases is involved in regulation of the dynamics of contractile system and is required for the recovery of myofibrillar apparatus. The inverse correlation between α-smooth muscle actin and extracellular matrix proteins may suggest the negative feedback loop, wherein α-smooth muscle actin modulates synthesis of extracellular matrix, which in turn suppresses α-smooth muscle actin expression and induces expression of α-cardiac isoform.

Supported by the Russian Science Foundation and the Federal Agency for Scientific Organizations (grant 14-50-00068).

IMPACT OF THE PHOSPHATIDYLCHOLINE' MIXTURE INJECTION ON CORTICAL CYTOSKELETON OF RATS *soleus* MUSCLE FIBERS

N.S. Biryukov[1,2], M.V. Maximova[1], I.V. Ogneva[1,3]

[1]*State Scientific Center of Russian Federation Institute of Biomedical Problems of the Russian Academy of Sciences,*
123007, Khoroshevskoe shosse, 76a, Moscow, Russia

[2]*Moscow Institute of Physics and Technology (State University)*

[3]*I.M. Sechenov First Moscow State Medical University*

Exposure to zero gravity may have a negative impact on different organs and tissues in humans and other species (for instance, in rodents). Skeletal muscles (as a specialized organ maintaining posture and providing motor function) are particularly prone to the negative effects of zero gravity. In rodents, antiorthostatic suspension is accompanied by similar effects on a number of systems (for example, on muscle, bone and partially the cardiovascular system) [E. Morey-Holton et al., 2005].

But cell mechanisms of mechanoreception still remain to be unclear. Nevertheless, many of them depend on the state of the cortical cytoskeleton whose integrity structure is affected by content of actin and actin-binding proteins. On the other hand, the state of cortical cytoskeleton strongly depends on cell membrane lipid composition [D.A. Brown, 2006; M. Edidin, 2003; V.I. Chubinskiy-Nadezhdin et al., 2011].

In view of the above, the aim of this study was to test the assumption that the modification of the membrane lipid composition of the soleus muscle fibers by phosphatidylcholine mixture injections may lead to a modification of the cortical cytoskeleton during the hindlimb suspension of the rat.

Materials and Methods

Experiments were performed on the left *soleus* muscle of the Wistar rats (n=14).

There were 7 animals in control group (n = 7), which were housed in the animal breeding facility (vivarium) under the standard conditions .

The experimental group consisted from n=7 animals with the similar masses to the control group animals. Experiment was performed with all conditions of the control: temperature, day/night cycle, standard vivarium feed and water *ad*

libitum. To simulate the microgravity conditions in rodents, antiorthostatic suspension during 6 hours was used according to the Ilyin-Novikov method modified by Morey-Holton et al. (2005).

Dry lecithin was dissolved in 0,9% NaCl + 1% C_2H_5OH in water. The animals were injected 0,5 ml of mixture at a concentration of 200 mg/ml in the right paw everyday (3 days prior to antiorthostatic suspension). The same amount of solution without lecithin was injected into the left paw.

All of the animal experimental procedures were approved by the Commission on Biomedical Ethics of the State Scientific Center of the Russian Federation - Institute for Biomedical Problems, the Russian Academy of Sciences.

Transversal stiffness measurements using atomic force microscopy. The soleus muscle was extirpated from one tendon to another according to the technique which had been previously described by Stevens et al. (1993). Measurements of transversal stiffness were conducted using the Solver-P47-Pro platform (NT-MDT, Russia) in the contact mode with the indentation depth of 150 nm.

Immunohistochemical staining alpha-actinin-4. Samples for immunohistochemical staining were frozen in liquid nitrogen immediately after isolation. Ultrathin sections with thickness of 8 nm were prepared. The staining was performed according to the method based on one described by Goffart et al. (2006). Sections were photographed at the Leica fluorescence microscope (Germany). Pictures were processed by using ImageJ software.

Statistical analysis. The results obtained during the experiments were statistically processed using ANOVA, using the post hoc *t*-test to evaluate the significance of differences between the groups. The data were represented as $M \pm SE$, where M is the mean value and SE is the mean error.

Results and Discusion

According to the mathematical model of the muscle fiber, *soleus* muscle fiber deformation that occurs in antiorthostatic suspension is inversely proportional to the stiffness and thickness of the membrane with the submembrane cytoskeleton [N.S. Biryukov, I.V. Ogneva, 2013]:

$$U_z = \frac{1}{\hat{E}}\left[-\rho g \cos\varphi \cdot \frac{z^3}{6z_1} + z\left(\rho g\left(\cos\varphi \cdot \frac{z_1}{2} + d\sin\varphi \right) - f_0 \frac{l}{T}\cos\left(\frac{2\pi}{T} z_1 \right) + p_{hy} \right) + f_0 \frac{lT}{4\pi^2}\sin\left(\frac{2\pi}{T} z \right) \right],$$

where ρ– density, g – free-fall acceleration, d – diameter of the fiber , φ – the angle between the gravity vector and the fiber longitudinal axis direction, (30° according to the method), f_0– the force generated by the single bridge, l – fiber length, T – the distance between two adjacent myosin heads. With the assumption that the Young's modulus depends on the content of the cytoskeleton submembrane non-muscle isoforms of actin, which filaments form symmetrical links, it can be represented as $\hat{E} = E_\perp \frac{\delta}{l}$, where δ – the thickness of the sarcolemma with submembrane cytoskeleton.

According to the theory of the elasticity [V.Z. Vlasov, 1959] $E_\perp \sim k$, where k – stiffness ratio, in our particular case – a transversal stiffness of the muscle fiber.

To simplify the task, we can assume that $U_z \sim (k\delta)^{-1}$. Thus, reduce of the deformation can be achieved by increasing the stiffness of the fibers and/or thickness of the cortical cytoskeleton. A similar attempt was made in this experiment.

Transversal stiffness of the m. *soleus* fibers remained at the control levels for the respective paws after 6 hours of antiorthostatic suspension: there were no difference between groups without lecithin «C» and «HS», as well as between groups with lecithin «CL» и «HSL». However the transversal stiffness in «CL» group was significantly higher at 22,5% ($p < 0,05$) than in «C» group Therefore, lecithin injections caused the reduce of deformation in rat soleus fibers under antiorthostatic suspension .

One should notice that the direct estimation of the cortical cytoskeleton deformation is an extremely complicated problem. However according to the earlier proposed scheme [I.V. Ogneva, 2011] cortical cytoskeleton deformation can lead to dissociation of different actin-binding proteins. Decrease in deformation at 22.5% caused by lecithin injections results in the fact that alpha - actinin - 4 does not dissociate from the cortical cytoskeleton after 6 hours of hindlimb suspension.

The thickness of the colored layer δ, which is corresponding for the submembrane cytoskeleton, does not change in groups «C», «HS», «CL», but in «HSL» group it is increased by 34%, 30% and 27% ($p <0,05$), respectively. However, increasing of the thickness of the colored layer with increased hardness (in «HSL» group in comparison with groups «C», «HS» and «CL») may indicate the reorganization of the cortical cytoskeleton.

The perimeter of the fiber remains at the same level in all four groups. At the same time, the gap percentage showing the ratio of the gaps in the cortical cytoskeleton fiber to its perimeter length, is higher in suspension groups («HS» and «HSL»), than in the corresponding control groups («C» and «CL»). However, we were unable to detect gaps in the cytoskeleton in the control group after the lecithin mixture injections («CL»).

Thus, the data obtained suggest that lecithin injections result in increase of the transversal stiffness of the m. *soleus* fibers in rat, lead to decrease of the cortical cytoskeleton deformation under the hindlimb suspension, prevent the alpha-actinin-4 migration into cytoplasm and subsequent cortical cytoskeleton reorganization.

Apparently, injections of the phosphatidylcholine could be considered as protection for the cortical cytoskeleton of muscle cells under microgravity conditions, but there is a need to find an optimal mode of delivery of such substances into the muscle cells, as well as to find out the class of phospholipids which is the most suitable for these purposes.

Acknowledgments

This work was supported by program of fundamental research of the SSC RF - IBMP RAS and the RAS Presidium Program "Molecular and cellular biology."

EFFECTIVENESS OF POSTSTROKE REHABILITATION BASED ON THE USE OF HAND EXOSKELETON CONTROLLED BY BRAIN-COMPUTER INTERFACE: A CLINICAL STUDY

E.V. Biryukova[1,2], A.A. Frolov[1,2], P.D. Bobrov[1,2], S.V. Kotov[3], L.G. Turbina[3], A.A. Kondur[3], M.E. Kurganskaya[2], O.G. Pavlova[2], I.Z. Dzhalagonia[2], Y.V. Kerechanin[4]

[1]*Pirogov National Medical Research University, 1 ul. Ostrovitianova, Moscow, 117997, Russia*

[2]*Institute of Higher Nervous Activity and Neurophysiology, Russian Academy of Sciences, 5A ul. Butlerova, 117485, Moscow, Russia*

[3]*Vladimirskii Regional Clinical Research Institute, 61/2 ul. Schepkina, Moscow, 129110, Russia*

[4]*Moscow Institute of Physics and Technology, 9 Institutskii per., Dolgoprudnyi, 141700, Moscow Region, Russia*

The dynamics of motor function recovery in 15 poststroke patients has been investigated during a course of neurorehabilitation assisted by a hand exoskeleton controlled by a brain-computer interface. Biomechanical analysis of the movements of the paretic arm recorded during the rehabilitation course was used for an unbiased assessment of motor function. Ten procedures involving hand exoskeleton control (one procedure per day) yielded the following results: (a) activation of wrist joint immobilized before procedures; (b) increasing and smoothing of joint movement velocity; and (c) inhibition of pathological synergies. These results are interpreted as improvement of the general level of control over the paretic hand.

THE EFFECT OF LYSOPHOSPHATIDIC ACID ON THE COMPOSITION OF MYOSIN-9 AND TROPOMYOSIN CONTAINING CYTOPLASMIC PROTEIN COMPLEXES

D.E. Bobkov, I.V. Kropacheva

Institute of Cytology RAS, Tikhoretsky prosp. 4, Saint-Petersburg, 194064, Russia

Lysophosphatidic acid (LPA) is a bioactive lipid mediator that acts via specific G-protein-coupled receptors and activates Rho/ROCK pathway resulting in actin cytoskeletal rearrangements. LPA stimulation enables fibroblasts to promote tissue remodeling, inflammation, angiogenesis, wound healing and tumor progression. This study is directed to elucidation of mechanisms by which LPA induces modifications of the microfilament system. Myosin-9 is a non-muscle motor protein associated with the wide range of cellular functions, including cell shape and motility. Previously we have demonstrated that myosin-9 forms multimolecular complexes with high molecular weight tropomyosin isoforms and heat shock proteins in cytoplasm of cultured cells. It was found that LPA induced redistribution of tropomyosin between cytosol and cytomatrix in dose-dependent manner. Here we explored the levels of myosin-9 and tropomyosin in cytosol and cytomatrix

extracts at different time points after LPA addition (20 ng/ml) to culture medium. Cytosole extracts from human embryonic lung fibroblasts were subjected to co-immunoprecipitation assay with polyclonal antibodies specific to C-terminal peptide of human myosin-9, or with monoclonal antibodies recognizing high molecular weight tropomyosin isoforms. The cross-immunoprecipitation method revealed changes in the composition of myosin-9/tropomyosin complexes under the action of LPA. We have observed the significant decrease in myosin-9 co-immunoprecipitated tropomyosin level immediately (1 min) after LPA addition. Gel-filtration chromatography confirmed the myosin-9/tropomyosin complex disassemble after LPA treatment. Additionally, we have found that LPA treatment during 1 h induces myosin-9 degradation with accumulation of 130 kDa and 40 kDa fragments in cytomatrix fraction. Further studies are needed to elucidate the molecular mechanisms responsible for these effects of LPA treatment.

This work was supported by a grant (No. 14-50-00068) from the Russian Science Foundation.

ROLE OF ENDOGENOUS AND EXOGENOUS ATP IN FACILITATION OF TRANSMISSION IN MATURE AND REINNERVATED MOUSE NEUROMUSCULAR JUNCTIONS

P.O. Bogacheva, O.P. Balezina

Moscow State University, Biological faculty, Lenin Hill 1/12, Moscow, Russia

ATP is known as a comediator of acetylcholine (ACh) in cholinergic neuromuscular junctions. Being released along with ACh, ATP is able to modulate synaptic transmission and then undergo fast hydrolysis by ectonucleotidases in the synaptic cleft [1]. Modulatory action of ATP is realized via purinergic receptors, which are widely present in motor synapses. The most well-known effect of ATP is the autoregulatory supression of ACh release which is mediated via presynaptic metabotropic P2Y receptors or/and retrograde action of muscle-derived reactive oxygen species, synthesized under influence of postsynaptic ATP action. Whether these complex inhibitory ATP effects stay the same and/or become more pronounced during prolonged ATP presence in the synaptic cleft of mature and newly-formed mouse neuromuscular junctions, remained unknown. In this study ATP effects were examined under conditions of ATP accumulation in the synaptic cleft using ectonucleotidase inhibition, tetanic nerve stimulation or tonic application of exogenous non-hydrolysable ATP.

Methods and materials

Experiments were carried out on an isolated neuromuscular preparation of fast-twitch *extensor digitorum longus muscle* (m. EDL) innervated by *n. peroneus* of adult BALB/C mice.

Mice were anesthetized with diethyl ether and *n. peroneus communis* was aseptically crushed approximately 10 mm from its entrance into the muscle. Animals were allowed to recover for 11 days prior to testing the activity of newly

formed synapses in isolated neuromuscular preparation. Animals were sacrificed by decapitation.

Isolated neuromuscular preparation was pinned on a Sylgard-coated dish, and bathed at room temperature in mammalian Liley solution (pH 7,2–7,4) containing: 135 mM NaCl; mM KCl 4; 0,9 mM NaH_2PO_4; 2 mM $CaCl_2$; 1 mM $MgCl_2$; 16,3 mM $NaHCO_3$; 11 mM glucose. Spontaneous miniature endplate potentials (MEPPs) and evoked endplate potentials (EPPs) were recorded using conventional methods of intracellular microelectrode recording. Glass microelectrodes were filled with 2,5 M KCl (10–15 MΩ resistance).

Transmitter release was evoked by suprathreshold nerve stimulation at 0,3 Hz or 50 Hz. Muscle fibers were cut to prevent muscle contraction in response to nerve stimulation (for details see Barstad, Lilleheil, 1968). Drug solutions were added to the bath solution. Records were rejected when more than a 5 mV change of membrane potential was observed.

EPPs and MEPPs amplitude and time course were analyzed. Quantal content of EPPs (QC) was calculated as a ratio of mean EPP amplitude and mean MEPP amplitude in the same synapse. Correction for nonlinear summation was calculated as $A_{corr}=A/(1–0,8\cdot A/E)$, where A is the recorded EPP amplitude and E is the resting membrane potential. All recordings were performed at room temperature (22–24°C). Data was collected and analyzed using Axoclamp 2B microelectrode amplifier (Molecular Devices, CA, USA) and MiniAnalysis software (Synaptosoft, GA, USA).

Data is presented as mean ± SEM of an indicated number (n) of neuromuscular junctions (NMJs). The Mann-Whitney test was used to evaluate significant difference.

Results and Discussion

We first tested whether endogenous ATP released along with ACh influences synaptic transmission. For that purpose EPPs and s MEPPs were recorded before and after muscle treatment with suramin, a wide range purinergic receptor blocker, which affects both P2X- and P2Y-receptors [1]. Bath application of suramin (10 and 100 microM) did not influence the amplitude or time course of MEPPs, but led to a dose-dependent increase of EPPs QC by 19 and 37% respectively (n=45, p<0,05) during low frequency nerve stimulation (0,3 Hz). It gives evidence to inhibitory effect of synaptic ATP aimed to downregulate ACh release during short term low frequency synaptic activity.

It was interesting to investigate whether this effect will be observed if ATP is accumulated during long time high frequency rhythmic activity of NMJs (50 Hz for 10 s).

In the course of long trains of 500 stimuli, no significant differences in the amplitudes or time courses of MEPPs and EPPs were detected before, during or after nerve stimulation,. This may indicate that even prolonged high frequency activity is not enough to accumulate endogenous ATP to a level that can induce prolongation of cholinergic signals. It was most likely due to high activity of endogenous ectonucleotidases. To increase the presence of synaptic ATP we pre-

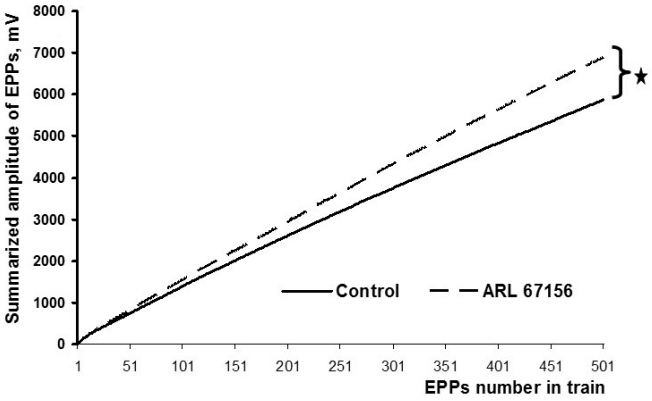

Cumulative histogram of EPPs amplitude during train of 500 stimuli in control and after ARL 67156 application, *p<0,05.

vented its degradation in the cleft, using ARL 67156 – inhibitor of ectonucleotidases. The presence of ARL 67156 during trains of high frequency nerve stimulation caused a significant increase in the time course of MEPPs by 16% (n=35, p<0,05), but did not alter MEPPs frequency or amplitude just after the train.

There was no significant difference in the mean amplitudes of the first EPP in trains in ARL 67156 treated and untreated NMJs. However, beginning from the 10^{th} EPP in the train, mean amplitude of EPPs, recorded in NMJs treated with ARL 67156, began to increase and reached 33% greater level than in untreated NMJs (see figure).

The time course of EPPs slowed down by 20% in the presence of ARL 67156 (n=35, p<0,05), but EPPs QC remained unchanged.

The obtained data shows that during long time high frequency synaptic activity accompanied by simultaneous prevention of ATP breakdown leads to potentiation of synaptic transmission. This potentiation seems to occur at postsynaptic level, as MEPPs amplitude, frequency and EPPs QC were not affected.

Another way to intensify and prolong ATP action in the synaptic cleft is to apply a non-hydrolyzable ATP analogue to the bath. Non-hydrolyzable exogenous ATP analogue γ-S-ATP (10 μM) significantly increased mean MEPPs amplitude 1,3 fold and prolonged their time course almost 1,4 fold. Mean frequency of MEPPs (which reflects spontaneous ACh secretion) remained unchanged.

Mean amplitude and time course of EPPs after treatment of NMJs with γ-S-ATP increased by 25–28% compared to control (n=56, p<0,05), while the QC of EPPs was not altered.

Thus, exogenous non-hydrolyzable ATP analogue did not reveal presynaptic inhibitory effect of ATP in mouse NMJs; on the contrary, the postsynaptic potentiation of transmission was expressed, which was more pronounced than in experiments with ARL 67156 application.

Since γ-S-ATP showed the most potent postsynaptic effect, it was interesting to investigate its possible influence on synaptic transmission in reinnervated NMJs. Bath application of γ-S-ATP (10 μM) led to a 18% increase of MEPPs amplitude and 18–25% progressive increase of EPPs amplitude throughout short rythmic train of stimuli (50 Hz, 1 s), while time course of synaptic potentials slowed down by 15% (n=49, p<0,05. QC of EPPs was not affected). This effect is quite similar to that observed in mature NMJs and is also of postsynaptic nature.

Pronounced postsynaptic potentiation of transmission, induced by ATP, can be due to the recognized ability of exogenous ATP and its analogues, such as γ-S-ATP (10 to 100 μM), to increase the opening frequency of muscle nAChRs [2] and/or to the blockade of chloride leak channels which has been recently found as an ATP effect on muscle fibers. Both effects probably are the result of ATP action on certain subtypes of muscle metabotropic P2Y-receptors [3,5]. Another profound ATP action on skeletal muscle has been recently described under influence of intense muscle contractions [4]. In this case ATP was found to be released from contracting muscle fibers and acting on P2Y1 muscle receptors, which trigger intracellular cascades causing potentiation of contraction [4].

In conclusion it can be suggested that regulatory effects of ATP on neuromuscular transmission strongly depend on its accumulation level in the synaptic cleft which differs along with patterns of synaptic and muscular activity. During low frequency tetanic activity, synaptic ATP decreases mediator secretion, while more significant ATP accumulation and presence around the muscle fibers results in postsynaptic potentiation of transmission, which prevails over or eliminates, presynaptic inhibitory action of ATP on ACh release in neuromuscular junctions .

The work was supported by Russian Foundation for Basic Research grant № 13-04-00413a.

References

1. Burnstock G. // Physiol. Rev. (2007) 87: 659-797.
2. Hoyle C.H. et al. // Br. J. Pharmacol. (1990) 99(3): 617-21.
3. Lu Z., Smith D.O. // J. Physiol. (1991) 436: 45-56.
4. Riquelme M.A. et al. // Neuropharmacology (2013) 75: 594-603.
5. Voss A. // J. Physiol. (2009) 587: 5739–5752.

DYNACTIN IN REGULATION OF ERES MOTILITY

I.B. Brodsky[1], A.V. Burakov[1], E.S. Nadezhdina[1,2]

[1]*A.N. Belozersky Institute of Physico-Chemical Biology, Moscow*

[2]*Institute of Protein Research RAS, Pushchino*

Secretory proteins exit endoplasmic reticulum (ER) in special cites called ERES (endoplasmic reticulum exit sites) and start here their way to Golgi apparatus. Specific proteins called COPII coat form a transport vesicle on ERES membranes. This coat consists of inner layer formed by Sec23-Sec24 heterodimer and outer layer by Sec13-Sec31 proteins. Post ER transport containers move along microtubules to Golgi, which is located in the central area. The direct mechanism how dynein motor protein is attached to the vesicle is currently unknown, although

the Sec23 protein from COPII coat can transitory bind to p150Glued protein from dynactin complex that is a cofactor of dynein motor. The question remains is this interaction sufficient for dynein targeting or whether dynactin presence is always means dynein presence?

To address this question we used chimeric construct that linked Sec23 and p150Glued so the last is constitutively present on ERES membranes. Alternatively we used several mutants of p150Glued for evaluating of its domains functions.

Using immunofluorescent approach we confirmed that this chimeric Sec23-GFP-p150Glued protein was located on ERES. But instead of p150 presence on ERES their motility didn't change in comparison to control (Sec23-GFP production). Deletion of head domain that binds to microtubules in chimeric protein (Sec23-GFP-p150dh) significantly reduced the mobility of ERES. This fact confirms that MT binding domain is important for dynactin function. Another important domain in p150Glued is CC1A domain that act as an internal inhibitor when binds to CC1B domain (Tripathy et al., 2014). The MT binding domain when binds to MT destroy CC1A-CC1B interaction and CC1B can activate dynein motor. To check this mechanism we used another deletion mutant of p150Glued – CC1Bp150Glued where both MT binding and CC1A domains were deleted. In this case ERES showed significant increase in long range motility.

To evaluate the impact of p150Glued attached to ERES on protein secretion from the ER we used the fact that Golgi compact morphology is usually disperses when ER export is inhibited.

In HeLa cells producing Sec23-GFP-p150dh chimeric protein Golgi shows disperse morphology in compare to WT p150Glued. In Vero cells instead both constructs lead to Golgi dispersion, and also to MT system disruption. Only production of Sec23-GFP-CC1Bp150 didn't induce that changes.

This work is supported by RFBR grants 14-04-31496 mol-a, 14-04-01729-a и 15-04-02609-a.

CERAMIDE IN THE MECHANISMS OF INTRACELLULAR SIGNALING IN SKELETAL MUSCLE DURING HINDLIMB UNLOADING

I.G. Bryndina, M.A. Shalagina, A.A. Yakovlev, S.V. Ovechkin

Izhevsk State Medical Academy,

Kommunarov St., 281, Izhevsk, 426034, Russia

The growing mass of data received by nowadays evidences that sphingolipids including ceramide play a pivotal role in the regulation of skeletal muscle function. In muscle, ceramide is involved in development of force depression, weakness, fatigue, enhances prooxidant activity, inhibits proteins synthesis and increases their degradation; negatively affects mitochondrial function, promotes induction of apoptosis [M. Nikolova-Karakashian et al., 2011]. Ceramide also is known to induce insulin resistance [R. Mahfouz, 2014].

In our previous experiments in mice subjected to antiorthostatic suspension (AOS) the levels of ceramide and sphingomyelin in skeletal muscles (un-

loaded and not unloaded ones) were studied [I.G. Bryndina et al., 2014]. It is shown that ceramide accumulates in unloaded skeletal muscle (m. soleus) at both 4 and 30-day AOS. Increased amounts of ceramide were also found in m. biceps brachii at 4-day AOS.

In the present work we studied the mechanisms of ceramide accumulation in skeletal muscle during hindlimb unloading (HU) and the effects of drugs inhibiting its generation on phosphorylated mTOR protein level in conditions of HU.

To elucidate the mechanism of ceramide increase in muscle we investigated the expression of some enzymes involved in sphingolipid metabolism (at protein levels), such as: sphingomiyelin synthase, acid sphingomyelinase, serine palmitoyltransferase, neutral ceramidase, sphingosine kinase (ELISA).

The following changes were observed in m. soleus during AOS: acid sphingomyelinase, which takes part in sphingomyelin degradation, was increases by 4^{th} and 14^{th} days. The level of neutral ceramidase was increased as well, whereas the amount of serine palmitoyltransferase was not changed or decreased in dynamics of AOS. No significant changes of sphingomyelin synthase and sphingosine kinase were found out.

Thus, we have identified sphingomyelinase hydrolysis as a main mechanism for ceramide accumulation in m. soleus during unloading. *De novo* synthesis is not involved in enhanced ceramide formation: it is confirmed by low level of serine palmitoyltransferase (a key enzyme for sphingoid bases synthesis, including ceramide).

It is interesting to notice that ceramide accumulates not only in unloaded hindlimb muscle (*m. soleus*) but in non-unloaded forelimb muscle (*m. biceps* brachii) as well. As we had previously speculated [I.G. Bryndina et al., 2014], the accumulation of ceramide in loaded muscle is not associated with either sphingomyelinase hydrolysis or de novo synthesis. The main mechanism involved is a limitation of ceramide degradation – the level of neutral ceramidase was lower than in control group of animals. It should be noted that, in contrast to this, a neutral ceramidase amount in m. soleus was increased, which can be regarded as a compensatory mechanism in the conditions of intensive ceramide formation by sphingomyelinase hydrolysis.

In order to determine which of the intracellular ceramide targets may be associated with the development of skeletal muscle disorders (atrophy, dysfunction) during simulated weightlessness, we estimated the amount of phosphorylated mTOR protein (p-mTOR) by ELISA. mTOR is known to be one of the key factors in cellular protein synthesis regulation. P-mTOR was determined in m. soleus and m. biceps brachii during AOS and AOS on the background of ceramide formation inhibitors treatment. Two inhibitors were used: the first one was myriocin, which blocks serine palmitoyltransferase activity and thereby de novo synthesis of ceramide; the second one was clomipramine as an acid sphingomyelinase inhibitor.

We have shown that p-mTOR level in m. soleus decreased during 4-day unloading. Both clomipramine and myriocin inhibited mTOR dephosphorylation in m. soleus, but more pronounced effect was demonstrated after clomipramine pre-

treatment, which is consistent with our data mentioned above and concerning the mechanisms of ceramide accumulation in unloaded soleus muscle. Taking into account that muscle atrophy in AOS depends on the enhancing of protein degradation or limitation of protein synthesis, and based on the fact that mTOR system is one of the key regulators of intracellular protein synthesis we can assume that ceramide might be involved in the development of muscle disuse atrophy in weightlessness.

References

1. Bryndina I.G., Shalagina M.N., Ovechkin S.V., Ovchinina N.G. [Sphingolipids in skeletal muscles of C57B1/6 mice after short-term simulated microgravity]. Ross. Fiziol. Zh. Im. I.M. Sechenova. 2014.100(11):1280-6. Russian.
2. Mahfouz R., Khoury R., Blachnio-Zabielska A., Turban S. et al. Characterising the inhibitory actions of ceramide upon insulin signaling in different skeletal muscle cell models: a mechanistic insight. PLoS One. 2014. 9 (7):e101865.
3. Nikolova-Karakashian M. (2011) Sphingolipid metabolism, oxidant signaling, and contractile function of skeletal muscle. Antioxidants & Redox Signaling. 15, 2501-2517.

THE INFLUENCE OF 2-BENZAMIDO-2-(2-OXOINDOLIN-3-ILIDEN) ACETIC ACID DERIVATIVE ON RATS' INTEGRATIVE MOTILITY AFTER TRAUMATIC BRAIN INJURY

Yu.S. Bukataru[1], I.I. Zamorskii[1], S.V. Kolesnik[2]

[1]*Bukovinian State Medical University,*
Theatre Square, 2, Chernivtsi, 58002, Ukraine

[2]*National University of Pharmacy,*
Pushkinska str. 53, Kharkiv, 61002, Ukraine

Traumatic brain injury (TBI) is the most difficult and dangerous pathological condition in the structure of injuries. TBI continues to be the main cause of death (up to 60% among injured) and disability of population (25% of survived patients) in the age group of 20–40 years. As a rule main symptoms of closed TBI include the formation of muscle-tonic disorders resulting in disturbances of muscular tone, reflexes and coordination of complex motor acts. Among the neurogenic consequences blood circulatory and respiration disorders usually develop.

During the screening studies of the 24 2-benzamido-2-(2-oxoindolin-3-iliden) acetic acid derivatives an antihypoxic activity of certain compounds under the conditions of acute hypobaric hypoxia was established [3]. Among the studied derivatives the most significant antihypoxic activity was observed when using compound number 15 (ZNM), which suggests the neuroprotective properties of this substance.

The aim of the study was to establish the impact of 2-benzamido-2-(2-oxoindolin-3-iliden) acetic acid derivative ZNM on the course of experimental acute traumatic brain injury by the criteria of motor and exploratory activity, the state of muscle tone and coordination, physical endurance.

The research was conducted on 32 white nonlinear mature male rats weighting 180–200 g, divided into 4 groups (n = 8): the first group was injected

intraperitoneally the substance ZNM at a dose of 15 mg/kg in the form of an aqueous suspension stabilized by polysorbate 80 (Tween 80) prior the TBI of moderate severity modeling; the second group was administered prior the TBI the reference drug mexidol at a dose of 100 mg/kg; the third (control) group was administered an equivalent amount of solvent; the fourth group - intact control (ether anesthesia without TBI). TBI of moderate severity was modeled under the ether anesthesia with a standardized weight-drop device (49.5 g, 0.315 J) inducing a focal blunt injury over the unprotected parietal-occipital head area [2]. Drugs were administered during 3 days before (last injection – 30 min before TBI) and 2 days after TBI. With the help of an open-field test during the acute phase of injury (48 h after TBI modeling) the behavioral and neurological disorders in animals were evaluated by determination of the locomotor activity (number of crossed squares and reaching the central area of the open field), orienteering and exploratory activity (number of stands and examined holes), emotional reactions (number of grooming, defecation and urination acts). Physical endurance was determined in a swimming test with a 10% of body weight load, coordination of movements and muscle tone – by the rod test, rotating at 10 rev/min [1].

Statistical analysis of the results was performed using Statistica 10.0 and Microsoft Excel 2013. Statistical significance was evaluated using parametric Student's t-test (for normal distribution), Mann-Whitney U-test (for non-normal distribution) and angular Fisher transformation. The critical level of significance was accepted with $p \leq 0.05$.

As a result of the research was noted that in the first group of animals (use of substance ZNM on the background TBI) the number of crossed squares decreased by 38.3%, the number of reaching the central area of the open field increased by 11.3%, the number of stands increased by 6.8 % and examined holes – by 9.3%. Indicators of the emotional reactions and their vegetative maintenance decreased by the number of bowel movements and urination by 3.2 times compared to the control pathology group ($r \leq 0.05$). These data suggest the changing of locomotor activity profile of animals with increase of an orienteering and exploratory activity and reduction of emotionality after TBI on the background of treatment with substance ZNM.

In the rotating rod test indicators of muscle tone and coordination in the substance ZNM group and in the group of reference drug mexidol were the same: the number of animals fallen within period of 30 seconds – 2 (25%), 30 s – 1 min – 3 (37.5%), after 1 minute – 3 (37.5%), which is significantly higher than the intact control parameters ($p \leq 0.05$).

Physical endurance by the time of forced swimming with a load in the control pathology group significantly decreased by 30% ($p \leq 0.05$). ZNM drug and mexidol restored this index up to the level of intact animals.

Thus, according to the study results, the 2-benzamido-2-(2-oxoindolin-3-iliden) acetic acid derivative ZNM changes profile of the locomotor activity of animals with increase of an orienteering and exploratory activity and reduction of an emotionality of animals on the model of a closed craniocerebral injury of

moderate severity in the open-field test, increases physical endurance by swimming with the load test and improves coordination in the rotating rod test. The research results indicate a close profile in pharmacological activity of the substance ZNM and reference drug mexidol - specifically cerebroprotective, anxiolytic and sedative action.

References

1. Bures J., Buresova O., Huston J. P. Techniques and basic experiments for the study of brain and behaviour. Amsterdam, N.Y., Elsevier, 1983, 2nd ed. 326 pp.
2. El'skij V. N., Zyablicev S. V. Modelirovanie cherepno-mozgovoj travmy. Donetsk, Novyj mir, 2008. 139 pp.
3. Zamorskii I. I., Bukataru Yu. S., Kolesnik S. V. Activity definizione antihypoxants in derivati del 2-benzammide-2-(2-oksoindolin-3-ilidene)-vinegary acido in acuta ipossia iperbarica. Ital. Sci. Rev. 2016, Vol. 1, N 34, P. 79–83.

AMPK DOES NOT PLAY KEY ROLE IN REGULATION OF THE PPARGC1A GENE EXPRESSION IN HUMAN SKELETAL MUSCLE

A.D. Butkov, E.A. Lysenko, T.F. Vepkhvadze, D.V. Perfilov, D.V. Popov

Laboratory of Exercise Physiology, Institute of Biomedical Problems of Russian Academy of Sciences, 76A Khoroshevskoe Shosse, Moscow, 123007, Russia

The PPARGC1A (PGC-1α) is a principal regulator of mitochondrial biogenesis in skeletal muscle. The expression of *PGC-1α-b* mRNA via the alternative promoter plays a significant part in exercise-dependent expression of *PGC-1α* gene; probably the expression of *PGC-1α-b* mRNA is regulated by CREB1. Acute endurance exercise activates AMPK in skeletal muscle in intensity dependent manner. It is possible to suggest, that AMPK might be involved in mediating stimulus-induced phosphorylation of $CREB1^{Ser133}$ in human skeletal muscle. The purpose of the study was to evaluate a role of AMPK in regulation of *PGC-1α* gene expression via the alternative promoter.

For this goal, we analysed activation of AMPK and *PGC-1α* gene expression in skeletal muscle of amateur endurance-trained athletes (n=9) before and after exercise (45 min, 38% of $\dot{V}O_{2\,max}$), with or without administration of a single dose of acute metformin administration (2 g), well known AMPK activator. Biopsies from the vastus lateralis muscle were taken at baseline and at 2 min, 4 h, and 8 h after exercise in both control and metformin trials.

The phosphorylation level of $AMPK^{Thr172}$ did not change at 2 min after the exercise in either the metformin or placebo trials. However, $ACC^{Ser79/222}$ (the substrate of AMPK, i.e. a endogenous marker of AMPK activity) showed a 2.6-fold ($P < 0.01$) increase in phosphorylation level immediately after exercise in the metformin trial only. But post-exercise expression of *PGC-1α* gene via both the alternative and canonical promoters did not vary between trials. This study does not confirm a role of AMPK in regulation of *PGC-1α* gene expression in endurance-trained human skeletal muscle.

This work was supported by the Russian Science Foundation (grant № 14-15-00768).

MESENCHYMAL-TO-AMOEBOID TRANSITION OF TUMOR CELLS AS MANIFESTATION OF THEIR MIGRATION PLASTICITY AND REORGANIZATIONS OF CYTOSKELETON UNDERLYING THIS PROCESS

A.S. Chikina[1,2], T.M. Svitkina[2], A.Y. Alexandrova[1]

[1]N.N. *Blokhin Russian Cancer Research Center, 24 Kashirskoe shosse, Moscow 115478, Russia*

[2]*Department of Biology, University of Pennsylvania, Philadelphia, PA, USA*

One of the hallmarks of tumor progression is activation of invasion and metastasis that involves alterations of the cell characteristics leading to enhanced cell motility and thus increased tumor dissemination [Hanahan and Weinberg, 2011]. Cells can change the mode of their motility, what includes not only alterations of the quantitative characteristics, such as the migration rate, but also transitions between basic molecular mechanisms regulated cell motility. The two main modes of cell motility are collective migration which is typical for epithelial cells, when cells migrate as a group and maintain cell-cell contacts; and individual cell motility, when cells separate from each other and migrate individually. Individually migrating cells most frequently use the mesenchymal motility mode, which is best characterized for fibroblasts (mesenchymal cells). Transition from epithelial to mesenchymal motility modes (epithelio-mesenchymal transition, EMT) is associated with tumor progression. Alternatively motility mode is amoeboid one, which normally used by free living amoebae, such as Dictyostellium [Friedl and Wolf, 2008, 2010, Sabeh et al., 2009, Madsen and Sahai, 2010]. In multicellular organisms, the amoeboid motility is usually used by cells of leukocyte lineages. Molecular mechanisms underlying each mode of cell migration are different. During mesenchymal motility actin polymerization drives leading edge protrusion in the form of filopodia and lamellipodia what depend on Arp2/3 and Rac activity. In contrast, amoeboid motility involves formation of blebs - hollow membrane protrusions extruded from the cell surface by actin-myosin contraction and regulated by Rho [Wolf et al, 2003, Charras and Paluch, 2008, Weiser et al, 2009]. Mesenchymal-to-amoeboid transition (MAT) of tumor cells is believed to be associated with an increased metastatic potential and a poor cancer prognosis. However, mechanistic connections between amoeboid motility and metastasis are not fully understood. Here, we show that experimental conditions limiting mesenchymal cell motility induce MAT in fibrosarcoma HT1080 cells, but not in non-transformed subcutaneous fibroblasts. Surprisingly, only up to 30% of fibrosarcoma cells undergo MAT independent of the type of MAT-inducing stimulus, and this population can show back amoeboid-to-mesenhymal transi-

tion when stimulus removed. These data suggest an existence of plasticity-competent subpopulation of fibrosarcoma cells. Indeed, the subpopulation of fibrosarcoma cells expressing the stem marker CD133 is significantly enriched in cells undergoing MAT upon stimulation, suggesting that MAT is preferentially expressed by cells with stem-like properties. We show that amoeboid cell motility is more efficient than mesenchymal one in the constrained 3D environment mimicking solid tissues, but not in 2D culture conditions. The transition from mesenchymal (lamellipodial) to amoeboid (blebbing) mode of protrusion occurs through an intermediate stage of filopodia formation with early blebs emerging at the base of filopodia. Electron microscopy analysis of the cortical cytoskeleton of mesenchymal and amoeboid cells correlated with dynamics of individual blebs revealed regions of sparse actin cytoskeleton at filopodial bases, thus explaining preferential bleb formation at these sites. Using correlative video and EM microscopy we show bleb architecture on different stages of blebbing. Fist of all we show that although actin mostly accumulates in the cortical region of the bleb, as expected from light microscopy studies, some actin filaments also extend from the cortical network into the bleb interior, where they are organized into 3D structures inside blebs. We characterize actin cytoskeleton on different stages of bleb cycle. Existance of complicate cytoskeleton organization and clear dynamics of cytoskeleton during blebbing as well as numerous data showed that there should be special machinery for bleb formation [Paluch and Raz, 2013] and the advantages which this motility gives to cells in special condition serve as additional confirmation that blebbing should be considered as specific mechanism of cell motility. The fact that amoeboid motility give advantages in some conditions, and in others is not so effective as mesenchymal one suggests that important adaptation for cell dissemination is plasticity of motility mechanisms. Our data suggest that plasticity of cell motility is an additional characteristic feature of cancer stem cells. This idea parallels the now well established correlation between EMT and acquisition of stemness features in multiple cancer models [Mani et al., 2008; Polyak and Weinberg, 2009; Giannoni et al., 2010] and extends this concept by showing that MAT capability also correlates with stem-like features of cancer cells. The migration plasticity of cancer stem cells complements their resistance to apoptosis and a self-renewal potential, which enables MAT-competent cancer stem cells not only to disseminate effectively, but also survive and colonize new niches.

Work was supported by RFBR, grant # 14-04-01228a (to AYA) and NIH grant R01 GM095977 (to TMS).

References

1. Charras G, Paluch E (2008). Nat Rev Mol Cell Biol. 9(9), 730-736.
2. Friedl P, Wolf K (2008). Cancer Res. 68(18), 7247-7249.
3. Friedl P, Wolf K (2010). J Cell Biol. 188(1), 11-19.
4. Giannoni E, Bianchini F, Masieri L, Serni S, Torre E, Calorini L, Chiarugi P (2010). Cancer Res. 70(17), 6945-6956.

5. Hanahan D, Weinberg RA (2011). Cell 144(5), 646-74.
6. Madsen CD, Sahai E (2010). Dev Cell. 19(1), 13-26.
7. Mani SA, Guo W, Liao MJ, Eaton EN, Ayyanan A, Zhou AY, Brooks M, Reinhard F, Zhang CC, Shipitsin M, Campbell LL, Polyak K, Brisken C, Yang J, Weinberg RA (2008). Cell 133(4), 704-715;
8. Paluch EK, Raz E. Curr Opin Cell Biol. 2013 Oct;25(5):582-90
9. Polyak K, Weinberg RA (2009). Nat Rev Cancer 9(4), 265-273;
10. Sabeh F, Shimizu-Hirota R, Weiss SJ (2009). J Cell Biol. 185(1), 11-9
11. Weiser DC, Row RH, Kimelman D. (2009) Development, 136:2375-2384
12. Wolf K, Müller R, Borgmann S, Bröcker EB, Friedl P (2003). Blood 102(9), 3262-3269

INCOMPLETE CARDIAC RECOVERY FROM ACUTE MENTAL STRESS IS ASSOCIATED WITH HIGHER VITAL EXHAUSTION IN HEALTHY MIDDLE-AGED ADULTS: THE YOUNG FINNS STUDY

N. Chumaeva[1], L. Pulkki-Råback[2,1], M. Hintsanen[3], M. Elovainio[1,4], N. Hutri-Kähönen[5], O.T. Raitakari[6,7], L. Keltikangas-Järvinen[1]

[1]*Institute of Behavioural Sciences, University of Helsinki, Helsinki, Finland*

[2]*Helsinki Collegium for Advanced Studies, Helsinki, Finland*

[3]*Unit of Psychology, University of Oulu, Oulu, Finland*

[4]*National Institute for Health and Welfare, Helsinki, Finland*

[5]*Department of Pediatrics, University of Tampere and Tampere University Hospital, Tampere, Finland*

[6]*Research Centre of Applied and Preventive Cardiovascular Medicine, University of Turku, Turku, Finland*

[7]*Department of Clinical Physiology and Nuclear Medicine, Turku University Hospital, Turku, Finland*

Incomplete recovery from acute mental stress is an independent predictor for cardiovascular events. Background chronic or prolonged psychological stress may exaggerate these relations decreasing individual's coping abilities to acute stress. Recent evidences suggest that psychological stress influences diseases processes that ultimately can lead to cardiovascular diseases (CVD) [Portais, Pyke, 2013; von Känel, 2012]. A state of prolonged psychological stress – vital exhaustion (VE) - contributes to cardiovascular events in healthy individuals [Williams et al., 2010] and to poor prognosis in patients with established CVD [Smith et al., 2011]. VE is defined as a state of excessive mental and physical fatigue with increasing irritability and demoralization feelings [Appels, 2004]. The state of VE was originally described in patients with heart diseases [Appels, 2004]. Later, VE has been reported in medically healthy subjects without established diseases [Williams et al., 2010]. VE has been considered one of the key harmful factors impairing quality of life and rehabilitation in CVD patients [Appels, 2004; Appels et al., 2006; Smith et al., 2011]. More than 50% of patients with heart

diseases have demonstrated high level of VE after 18 months of investigations (Appels et al. 2006). Patients with myocardial infarction and heart failure, who reported high VE over a 1 year period, had an increased risk of future adverse CVD events [Smith et al., 2011]. Behavioral and neurohormonal alterations may account for poor prognosis for cardiac rehabilitation [Appels et al., 2006]. The suggested mechanism operates through dysregulation in hypothalamic-pituitary-adrenal axis function and autonomic nervous system (ANS) sympathetic-parasympathetic balance [Harris, Matthews, 2004; von Känel, 2012], which impact both to VE symptomatology and to the link between VE and CVD.

The relations between acute mental stress response, which reflects ANS sympathetic and parasympathetic function alterations and chronic stress have not been examined in detail. So far, stress studies have mainly concentrated on stress reactivity; however, impaired recovery after acute mental stress has been related to CVD risk independently of stress reactivity [Chida, Steptoe, 2010]. Post-stress recovery has been considered an important contributor to CVD outcomes because it reflects cardiovascular situation after exposure to acute stress. Experiencing background chronic stress leads to incomplete cardiac recovery after acute mental stress and, on the other hand, impaired acute stress reactions, which reflect autonomic imbalance, may influence chronic stress level. The role of neurogenic origin (sympathetic or parasympathetic), which has been proposed to be responsible for the relations between acute stress reactiveness and chronic stress is unclear.

Heart rate (HR) is the main physiological parameter reflecting sympathetic-parasympathetic balance [Berntson et al., 1997; Cacioppo et al., 1994]. More specific parameters indicate sympathetic (PEP: pre-ejection period) or parasympathetic control of HR (RSA: respiratory sinus arrhythmia) [Berntson et al., 1997; Cacioppo et al., 1994]. The present study examines associations between indicators of sympathetic and parasympathetic activity/balance such as HR, RSA and PEP during recovery after active and passive brief laboratory tasks and chronic stress assessed by VE in 47 medically healthy adults aged 24-39 years. The aim of the study is to explore whether impaired post-stress recovery is associated with VE. We suggest associations between impaired cardiac post-stress recovery and higher VE.

Methods and Participants

Participants were enrolled from the Young Finns study, which has been developed to investigate risk factors for CVD from childhood to adulthood in Finnish children, adolescents and young adults at intervals of 3 or 5 years [Raitakari et al., 2008]. Originally, 3596 participants from different geographical parts of Finland participated in the first baseline study in 1980. Several follow-up studies have been conducted between 1980 and 2012. In the 21-year follow-up, clinical and life-style risk factors measurements were performed in 2001 for 2109 participants aged 24 to 39 years. Standard methods were used for determining plasma insulin level, triglycerides, low-density lipoprotein and high-density lipoprotein cholesterol concentrations, body-mass index (BMI), systolic blood

pressure and diastolic blood pressure [Raitakari et al., 2003]. We also measured life-style characteristics: smoking status (daily smoking/non-smokers), alcohol intake (how often beer, wine, or spirits was used at least 6 portions or more at a time ranging from 1 – once a year or never to 6 – at least twice a week) and physical activity [Hintsanen et al., 2005]. VE was assessed in 2001 from 2080 subjects by the Maastricht Questionnaire. Psychophysiological experiment data were collected in 1999 and are available from 95 participants. Heart rate, RSA and PEP during recovery after mixed active and passive brief psychological stress tasks (acoustic startle, mental arithmetic, reaction time and public speaking) were determined by impedance electrocardiography [Sherwood et al., 1990]. Nineteen subjects were excluded due to diabetes and arrhythmias. In the current study, 47 healthy individuals had complete psychophysiological and VE measurements data. The Young Finns study was approved by the local ethics committees in Helsinki, Turku, Tampere, Kuopio and Oulu. The study was conducted in accordance with the Declaration of Helsinki. All invited participants gave their written informed consent in 1999 and in 2001.

Results

In the present study, 36.2% of participants showed incomplete HR recovery, 46.8% had incomplete RSA recovery, and 31.9% of participants had incomplete PEP recovery. No correlations were found between baselines HR, RSA or PEP measurements and VE as well as between RSA or PEP recovery and VE. Bivariate (Pearson's) correlations between HR recovery and VE were found *(r* = 0.30; p = 0.038). Incomplete HR recovery was associated with higher VE in unadjusted model (p = 0.038), after controlling for age/gender and after additionally controlling for life-style (smoking, alcohol intake and physical activity) (p = 0.005–0.011) and clinical (lipoproteins, blood pressure, BMI and plasma insulin) risk factors (p = 0.035–0.044) as well as in the fully-adjusted model (p = 0.042). Increased HR was associated with lower RSA during recovery.

Discussion

In the present study, almost half of the participants demonstrated incomplete RSA recovery after brief laboratory stress and more than 35% of participants had incomplete HR recovery. We found that poorer HR recovery from acute mental stress was associated with higher level of VE in unadjusted and in risk factors adjusted models. Our main findings are in accordance with our hypothesis, which suggests the associations between delayed cardiac recovery from acute mental stress and higher VE. The results support our previous findings demonstrating detrimental interrelations between chronic and acute psychological stress [Chumaeva et al., 2009]. Accordingly, higher VE has been associated with reduced HR recovery after exercise in patients with chronic heart failure [von Känel et al., 2009]. However, no studies have examined the influence of impaired acute stress recovery on VE level in medically healthy individuals. Acute stress response is characterized by increasing of sympathetic activity and elevating HR, however, rapid restoring of HR during recovery period mainly depends on vagal function [von Känel et al., 2009]. Associations between lower

RSA and higher HR during recovery were found in the present study showing that HR recovery is driven by vagal tone during rest. We can suggest that acute mental stress elicits prolonged vagal withdrawal (reflected by low RSA during the last rest) that continues for some time after the stressful situation is over. HR variability analyses have shown that VE has been related to supressed vagal function but not to changes of sympathetic activity during rest after overwork in healthy but exhausted workers [Watanabe et al., 2002]. Incomplete HR recovery found in our study reflects inability to recover quickly, possibly, as a result of autonomic alterations that has prognostic significance. Delayed HR recovery has been related to increased CVD risk and associations with chronic stress may intensify these relations. Mechanism of the relationships is unclear. Participation of acute and chronic stress in autonomic imbalance leading to endothelial dysfunction [Harris, Matthews, 2004; Poitras, Pyke, 2013] includes neuroendocrine, metabolic, inflammatory, hemodynamic and haemostatic pathways [von Känel, 2012]. Indirect pathways can also participate in stress and CVD relations suggesting individual's health behaviour (smoking, exercise, diet, life style) influence.

Conclusions

We found associations between impaired HR recovery after acute mental stress and higher chronic stress level in the small sample of exhausted participants. Our results suggest that autonomic imbalance resulted predominantly from vagal withdrawal may link incomplete HR recovery after acute mental stress and higher VE. Improving vagal control can reduce VE level; reducing VE is critically important for rehabilitation from cardiac events. The results of the study may be useful for cardiac rehabilitation programs.

The study was supported by the Academy of Finland (grant 258711 (L.K.-J.), 258578 (M.H.), and 265977 (M.E.)) and by Jenny and Antti Wihuri Foundation (for N. Chumaeva).

References

1. Appels A. Exhaustion and coronary heart disease: the history of a scientific quest. Patient Educ Counsel 2004;55:223-229.
2. Appels A. et al. Effects of a behavioural intervention on quality of life and related variables in angioplasty patients: results of the exhaustion intervention trial. J Psychosom Research 2006;61:1-7.
3. Berntson GG. et al. Heart rate variability: origins, methods, and interpretive caveats. Psychophysiology 1997;34:623-648.
4. Cacioppo JT. et al. Individual differences in the autonomic origins of heart rate reactivity: The psychometrics of respiratory sinus arrhythmia and pre-ejection period. Psychophysiology 1994;31: 412-419.
5. Chida Y, Steptoe A. Greater cardiovascular responses to laboratory mental stress are associated with poor subsequent cardiovascular risk status: a meta-analysis of prospective evidence. Hypertension 2010;55:1026-1032.
6. Chumaeva N. et al. Interactive effect of long-term mental stress and cardiac stress reactivity on carotid intima-media thickness: The Cardiovascular Risk in Young Finns study. Stress 2009;12:283-293.

7. Harris KF, Matthews KA. Interactions between autonomic nervous system activity and endothelial function: a model for the development of cardiovascular disease. Psychosom Med 2004;66:153-164.
8. Hintsanen M. et al. Job strain and early atherosclerosis: the Cardiovascular Risk in Young Finns study. Psychosom Med 2005;67:740-747.
9. Poitras VJ, Pyke KE. The impact of acute mental stress on vascular endothelial function: evidence, mechanisms and importance. Int J Psychophysiology 2013;88:124-135.
10. Raitakari O. et al. Cohort profile: The Cardiovascular Risk in Young Finns study. Int J Epidemiol 2008;37:1220-1226.
11. Raitakari O. et al. Cardiovascular risk factors in childhood and carotid artery intima-media thickness in adulthood: the Cardiovascular Risk in Young Finns study. JAMA 2003;290:2277-2283.
12. Sherwood A. et al. Methodological guidelines for impedance cardiography. Psychophysiology 1990;27:1-23.
13. Smith OR. et al. Vital exhaustion and cardiovascular prognosis in myocardial infarction and heart failure: predictive power of different trajectories. Psychol Med 2011;41:731-738.
14. Von Känel R. et al. Heart rate recovery after exercise in chronic heart failure: role of vital exhaustion and type D personality. J Cardiol 2009;53:248-256.
15. Von Känel R. Psychosocial stress and cardiovascular risk - current opinion. Swiss Med Weekly 2012;20:142.
16. Watanabe T. et al. Effects of vital exhaustion on cardiac autonomic nervous functions assessed by heart rate variability at rest in middle-aged male workers. Int J Behav Med 2002;9:68-75.
17. Williams JE. et al. Vital exhaustion as a risk factor for adverse cardiac events (from the Atherosclerosis Risk In Communities [ARIC] study). Am J Cardiol 2010;105:1661-1665.

CARDIOMYOPATHY-ASSOCIATED MUTATION K15N IN TROPOMYOSIN AFFECTS INTERACTIONS WITH ITS BINDING PARTNERS

M. Colpan, D. Tolkatchev, T. Ly, S. Grover, A. S. Kostyukova

Voiland School of Chemical Engineering and Bioengineering, Washington State University, Pullman, WA 99164, USA

The development of some familial dilated cardiomyopathies (DCM) correlates with the presence of mutations in proteins that regulate the organization and function of thin filaments in cardiac muscle cells. The K15N mutation in striated muscle α-tropomyosin was shown to be associated with familial DCM. The mutation is located next to Glu16, which is known to interact with actin, and within the newly identified leiomodin-binding site of tropomyosin. We have demonstrated that the mutation destabilized coiled-coil in this region and decreased actin-binding affinity by two-fold. Using circular dichroism we studied the effect of this mutation on tropomyosin's binding to leiomodin and tropomodulin. The mutation reduced binding affinity for both leiomodin and tropomodulin. Effect of the mutation on ability of tropomodulin to bind tropomyosin-coated actin filaments has been

studied by a co-sedimentation assay followed by Western blot. We have found that tropomodulin binding was decreased two-fold in the presence of mutated tropomyosin. The effect of the K15N mutation on tropomyosin interactions provides a molecular rationale for the development of familial DCM. Tropomodulin and leiomodin are responsible for correct lengths of thin filaments by regulating actin dynamics at the pointed end. Tropomyosin is an important regulator of the actin-nucleating ability of leiomodin and recruits tropomodulin and leiomodin to the pointed end. The K15N mutation reduces the localization of leiomodin and tropomodulin to the pointed end of thin filaments due to the decreased binding affinity. This alone may lead to formation of thin filaments with improper lengths and result in cardiomyopathies since reduced levels of Lmod2 and Tmod1 in cardiomyocytes disrupts myofibril formation.

Physarum polycephalum FORAGING AND NETWORK TOPOLOGY

H.G. Döbereiner, A. Fessel, J. Lee, C. Oettmeier

Institut für Biophysik, Universität Bremen, Bremen, Germany

The slime mold *Physarum polycephalum* is a unicellular but multinucleated organism, which amazingly can grow up to square meters. It forms extended vein networks in order to search for food. The structure and dynamics of the foraging units is dependent on environmental conditions and life stage. We find oscillating microplasmodia [1], which percolate into a network directly or fuse into compact satellites before transforming into networks as well. We model the percolations transition, which occurs in well-fed conditions, analytically within the configuration model of graph theory utilizing all partaking types of nodes. [2] Quite generally, we find that at the percolation transition the formation of a small link degree network is topologically highly constrained and only weakly dependent on environmental factors. Structuring of the network as characterized by global efficiency and centrality measures precedes area search in order to forage. [3] In contrast, satellites are found to be predominant after prolonged starvation of microplasmodia. The number and size of satellites forming out of a spherical patch of single microplasmodia shows characteristic scaling behavior with coverage [4]. After radially swarming away from the patch, satellites develop holes and transform into networks. We have obtained flow patterns within external (network) and internal (satellite) veins and gained ultra-structural insights into their morphology and topology [5]. On a more coarse-grained level, network topology can be modeled with a Master equation of the link degree distribution [6].

References

1. E. Bernitt, C. Oettmeier, and H.-G. Döbereiner, Microplasmodium Dynamics of *Physarum Polycephalum*, Springer IFMBE proceedings 31 1133 (2010).
2. A. Fessel, C. Oettmeier, E. Bernitt, N.C.L. Gauthier, and H.-G. Döbereiner, *Physarum polycephalum* percolation as a paradigm for topological phase transitions in transportation networks, Phys. Rev. Lett. 109 078103 (2012).

3. A. Fessel, C. Oettmeier, C., and H.-G Döbereiner, Structuring precedes extension in percolating *Physarum polycephalum* networks, Nano Communication Networks 6 87 (2015).
4. J. Lee, C. Oettmeier, and H-G Döbereiner, Growth pattern of *Physarum polycephalum* during starvation, PhysNet 2015 (in press)
5. C.Oettmeier, and H-G Döbereiner, A close look at amoeboid locomotion: An integrated picture of a migrating, starvation-induced foraging unit of *Physarum polycephalum*, PhysNet 2015 (in press)
6. A. Fessel, and H-G Döbereiner, Motifs of Growth and Fusion Govern *Physarum polycephalum* Network Formation, PhysNet 2015 (in press)

USE OF TAURINE FOR TREATMENT OF THE MYOGLOBINURIC ACUTE RENAL INJURY CAUSED BY RHABDOMYOLYSIS

V.M. Drashuk, I.I. Zamorskii
Bukovinian State Medical University,
Teatralna Sq., 2, Chernovtsy, 58002, Ukraine

Acute kidney injury (AKI) is a syndrome that results in a sudden decrease in kidney function or kidney damage within a few hours or few days. Clinically AKI is characterized by a rapid reduction in kidney function resulting in a failure to maintain fluid, electrolyte and acid-base homoeostasis. AKI occurs in 33–50% of patients with rhabdomyolysis.

Rhabdomyolysis is a clinical and biochemical syndrome that occurs when skeletal muscle cells disrupt and release creatine phosphokinase, lactate dehydrogenase, and myoglobin into the interstitial space and plasma. The main causes of rhabdomyolysis include direct muscular injury, strenuous exercise, drugs, toxins, infections, hyperthermia, seizures, metabolic and/or electrolyte abnormalities. The main pathophysiological mechanisms of renal injury are renal vasoconstriction, intraluminal cast formation and direct myoglobin toxicity. The pathophysiological hallmark of the syndrome is an increase in intracellular free ionized calcium due to either cellular energy depletion, or direct plasma membrane rupture. The increased intracellular calcium activates several proteases, intensifies skeletal muscle cell contractility, induces mitochondrial dysfunction and increases the production of reactive oxygen species, ultimately resulting in skeletal muscle cell death. Clinically, the syndrome presents with severe muscular pain, weakness and myoglobinuria. Increased myoglobin and creatine phosphokinase as a consequence of muscular cell death are the major laboratory findings, which, in combination with the clinical presentation, lead the clinician to the final diagnosis of the syndrome.

Rhabdomyolysis-induced myoglobinuric AKI accounts for about 10% to 40% of all cases of AKI. Early recognition of rhabdomyolysis and prompt management of complications are crucial to a successful outcome. Myoglobin is an important myocyte compound released into plasma. After muscle injury, massive plasma myoglobin levels exceed protein binding (of haptoglobin) and can precipitate in glomerular filtrate. Excess myoglobin may thus cause renal tubular obstruction, direct nephrotoxicity (ischemia and tubular injury), intrarenal vasoconstriction, and AKI [3–5].

Our research study was targeted at the examination of the influence of sulphur-containing amino acid taurine (2-aminoethanesulphonic acid), exhibiting diverse biological actions including antioxidant effect [1], on rhabdomyolytic AKI in rats.

Taurine is an ubiquitous sulfur-containing amino acid which is normally present in high concentrations in mammalian plasma and cells. It plays various important physiological functions including in osmoregulation and bile acid conjugation, pharmacological actions, pathological states and prevention of oxidant-induced injury in many tissues. The useful effects of taurine as an antioxidant in biological systems have been attributed to its ability to stabilize biomembranes, to scavenge reactive oxygen species, and to decrease the peroxidation of unsaturated membrane lipids and thus act as an indirect antioxidant [2].

Twenty-one non-linear adult white rats were divided into three equal groups: I group – control, II group – modeling of rhabdomyolytic AKI by intramuscular injection of 50% glycerol (10 ml/kg), III group – glycerol (10 ml/kg) and taurine (100 μg/kg). After 24 h of glycerol administration urine, blood and kidney samples were collected. Data were compared by Statistica 10.0 software and Mann-Witney test at $p \leq 0.05$.

As has been found in our experiments, glycerol administration induced severe loss in renal function, to illustrate: glomerular filtration rate (GFR) decreased by 2.8 times ($p \leq 0.01$), diuresis decreased by 1.8 times, plasma creatinine concentration increased by 2.2 times and proteinuria increased by 2.7 times ($p \leq 0.01$).

Under the conditions of AKF taurine-treated rats featured improvements in the excretory functions of kidneys. When using taurine GFR increased by 1.7 times ($p \leq 0.01$), diuresis increased by 1.3 times ($p \leq 0.05$), plasma creatinine concentration decreased by 1.6 times ($p \leq 0.05$) and proteinuria decreased by 2.1 times ($p \leq 0.01$) in comparison with the group of untreated animals.

Development of myoglobinuric AKF was accompanied with an increase in the malondialdehyde (MDA) content in the kidney tissue of untreated animals by 1.6 times ($p \leq 0.05$), oxidative modification of proteins (OMP) – by 1.3 times along with the decrease in glutathione-peroxidase (GPx) activity in the kidney tissue by 1.6 times ($p \leq 0.05$) and a tendency to compensatory increase in catalase (CAT) activity comparing to the intact animals.

The use of a powerful antioxidant taurine resulted in normalization of prooxidant-antioxidant balance in rat kidney, confirmed by the reduction of MDA content in the kidney tissue by 1.3 times, OMP content – by 1.4 times ($p \leq 0.01$), along with an increase in GPx activity in the kidney tissue by 1.4 times ($p \leq 0.05$) and normalization of the CAT activity as compared with a group of untreated rats.

The obtained results suggest the renoprotective action of taurine under the conditions of rhabdomyolysis-induced kidney injury.

References

1. Bidri M., Choay P. Taurine: a particular aminoacid with multiple functions. Ann. Pharm. Fr. 2003. Vol. 61, N 6. P. 385–391.

2. Nandhini A., Thirunavukkarasu V., Ravichandran M. K. et al. Effect of taurine on biomarkers of oxidative stress in tissues of fructose-fed insulin-resistant rats. Singapore Med J. 2005. N. 46. P. 82–87.
3. Chatzizisis Y. S., Misirli G., Hatzitolios A. I. The syndrome of rhabdomyolysis: Complications and treatment. Eur J. Int. Med. 2008. N 19. P. 568–574.
4. Khan F. Y. Rhabdomyolysis: a review of the literature. Neth. J. Med. 2009. Vol. 67, N 9. P. 272–283.
5. Korrapati M. C., Shaner B. E., Schnellmann R. G. Recovery from glycerol-induced acute kidney injury is accelerated by suramin. J. Pharm. Exp. Ther. 2012. Vol. 341. P. 126–136.

PRODUCTS OF FATTY ACIDS ω-OXIDATION AS INDUCERS OF Ca^{2+}-DEPENDENT AGGREGATION AND PERMEABILIZATION OF RED BLOOD CELLS

M.V. Dubinin[1], K.A. Scherbakov [1], A.E. Stepanova[1], K.N. Belosludtsev[1,2], M.S. Kondratyev [3], V.N. Samartsev[1]

[1]*Mari State University, pl. Lenina 1, Yoshkar-Ola, 424038, Russia*

[2]*Institute of Theoretical and Experimental Biophysics RAS, Institutskaya 3, Pushchino, 142290, Russia*

[3]*Institute of Cell Biophysics RAS, Institutskaya 3, Pushchino, 142290, Russia*

It is known that free fatty acids may have different effects on biological membranes depending on their concentration and structure. Today, it is considered that free fatty acids can exhibit detergent-like action as well as perturbing and protonophoric effects. In addition, recently it has been extensively studied the effect of free fatty acids as an inducers of the nonspecific permeability of the biological and artificial membranes, which is greatly enhanced in the presence of Ca^{2+}. It is known that the saturated monocarboxylic fatty acids (among them palmitic acid is the most effective) can effectively induce Ca^{2+} -dependent permeability of both artificial (liposomes, BLM) and natural phospholipid membranes, in particular, mitochondrial inner membrane [1] and the plasma membrane of erythrocytes [2].

One of the pathways of monocarboxylic fatty acid metabolism in mammals and humans is their ω-oxidation, which occurs mainly in liver and kidney cells and leads to the formation of the corresponding α,ω-dicarboxylic acids (α,ω-dioic acids) [3]. In some cases, ω-oxidation can be enhanced and accompanied by accumulation of the end products of this process – α,ω-dicarboxylic acids and intermediates – ω-hydroxyl monocarboxylic acids in the blood and cells [3].

We have previously demonstrated that long chain α,ω-dioic acids are able to induce Ca^{2+}-dependent nonspecific permeability in both mitochondrial and artificial (liposome) lipid membranes, which suggests a lipid nature of this phenomenon as in the case of monocarboxylic fatty acids. It is assumed that the mechanism of Ca^{2+}-dependent nonspecific permeability induced by α,ω-dioic acids is associated with processes of fusion and/or aggregation of lipid membranes [4].

As mentioned above, in some cases there may be an increase in the content of ω-oxidation products in the blood serum, so it can be assumed that first of all, the

cytoplasmic membrane of the cells, rather than the mitochondrial membrane, will be exposed to their influence. The aim of this work was to study the effects of products of palmitic acid ω-oxidation as inducers of Ca^{2+}-dependent nonspecific permeability of the erythrocyte membrane.

Materials and methods

Erythrocytes from adult male mongrel albino rats were collected as previously described [2]. Erythrocytes were counted under a light microscope using a Goryaev's cell-counting chamber. The permeability of the erythrocyte membrane was evaluated by the degree of hemolysis. In this case, erythrocytes (~$8–10 \cdot 10^6$ cells/ml) were incubated in the PBS–glucose buffer for 20 min at 25°C in the absence or presence of permeability inducers. After incubation, the erythrocytes were precipitated by centrifugation (500*g* × 10 min). The optical density of the supernatant was measured at 540 nm using a KFK-3-01 spectrometer (ZOMZ, Russia).

Results and discussion

In the experiments, we used palmitic acid as one of the most abundant natural fatty acid, and the intermediate and final products of its ω-oxidation – 16 hydroxypalmitic acid (HPA) and α,ω-hexadecanedioic acid (HDA) acid, respectively. Previously, it was shown that palmitic acid in the presence of Ca^{2+} was able to induce the lysis of erythrocytes by inducing nonspecific permeability of the cytoplasmic membrane [2]. In this work we have shown that the addition of HDA and Ca^{2+} to a suspension of erythrocytes as in the case of palmitic acid, leads to a decrease in number of living cells (fig. 1). A similar effect is observed in the case of the addition of the HPA and Ca^{2+} (fig. 1). As shown in fig. 2, the effect of HDA in the presence of Ca^{2+} is accompanied by hemolysis of red blood cells, so we can assume that in this case there is induction of nonspecific permeability of the cytoplasmic membrane of cells. However, the HDA as an inducer of Ca^{2+}-dependent permeability of erythrocytes is significantly inferior to palmitic acid in its effectiveness (fig. 2). At the same time HPA in the presence of Ca^{2+} has almost no effect on the permeability of red blood cells.

Results of experiments with erythrocytes are consistent with the data obtained on liposomes [4], suggesting that Ca^{2+}-dependent permeabilization of these membranes induced by products of palmitic acid ω-oxidation, caused by universal mechanism associated with their fusion and/or aggregation. Indeed, microscopic studies have shown that reducing the number of living cells in the case of the addition of HDA or HPA and Ca^{2+} to a suspension of erythrocytes caused by the aggregation of cells.

Therefore, it can be assumed that in the case of increasing the level of metabolites of fatty acids ω-oxidation in the serum, which occurs in a number of pathologies, it can be observed processes of aggregation of blood cells, particularly erythrocytes due to changes in their surface properties that leads to disruption of the microcirculation processes, and ultimately to their destruction.

In this work we also studied the effect of bovine serum albumin (BSA) on the induction of erythrocyte permeability by palmitic acid, HPA and HDA. It is known that albumin, which found in blood plasma and serum, is able to bind fatty

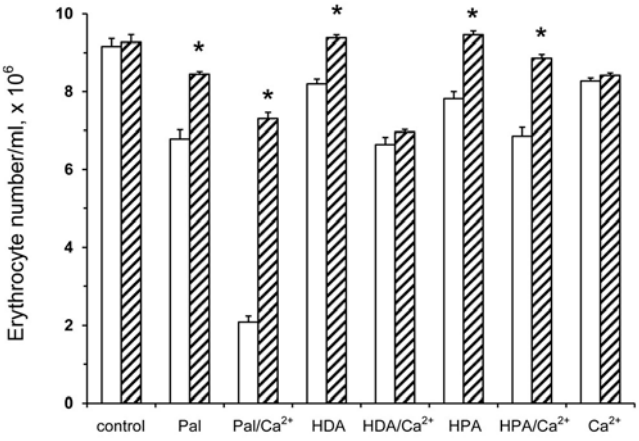

Fig. 1. Changes in the number of erythrocytes upon the addition of fatty acids and Ca^{2+} in the absence (unshaded columns) and presence (shaded columns) of 10 mg/ml BSA. Additions: 30 μM Pal, 30 μM HDA, 30 μM HPA and 100 μM Ca^{2+}. Medium composition: 138 mM NaCl, 2.7 mM KCl, 10 mM Na_2HPO_4, 5 mM glucose, pH 7.4. Mean values ± SEM are presented (n = 6–7). *p<0.05

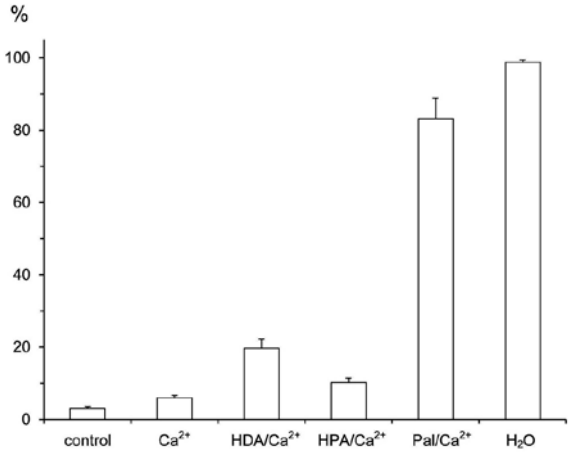

Fig. 2. Hemolytic activity of fatty acids and Ca^{2+} in rat erythrocyte suspension. Medium composition and additions as in fig. 1. Mean values ± SEM are presented (n = 4).

acids quickly and with high affinity. As shown in fig. 1, in the presence of BSA effect of palmitic acid as inductor of the Ca^{2+}-dependent permeability was significantly lower. At the same time BSA completely prevented HPA/Ca^{2+}-induced decrease in the number of erythrocytes, but did not affect the effect of HDA/Ca^{2+} (fig. 1). It is well known that BSA binds α,ω-dioic acids weaker than their mono-

carboxylic analogues [5]. Therefore, the observed difference in the inhibitory effect of BSA may be due to the fact that BSA has a lower affinity for HDA than for palmitic acid and HPA.

References

1. Belosludtsev K.N., Belosludtseva N.V., Agafonov A.V., Astashev M.E., Kazakov A.S., Saris N.-E.L., Mironova G.D. (2014) Biochim. Biophys. Acta, 1838, 2600-2606.
2. Belosludtsev K. N., Trudovishnikov A.S., Belosludtseva N.V., Agafonov A.V., Mironova G.D. (2010) J. Membr. Biol., 237, 9-13.
3. Wanders R.J., Komen J., Kemp S. (2011) FEBS J., 278, 182–194.
4. Dubinin M.V. Samartsev V.N., Astashev M.E., Kazakov A.S., Belosludtsev K.N. (2014) Eur. Biophys. J., 43, 565-572.
5. Tonsgard J.H., Meredith S.C. (1991) Biochem. J., 276, 569–575.

NEW APPROACH TO THE STUDY OF GOLGI AS A MICROTUBULE ORGANIZING CENTER

A.D. Fedorova[1], A.A. Penin[1], E.S. Nadezhdina[1,2], A.V. Burakov[1]

[1]*A.N. Belozersky Institute of Physico-Chemical Biology, 119992, Moscow, Leninskye Gory, 1-40*

[2]*Institute of Protein Research, Russian Academy of Sciences, 117988, Moscow, Vavilova str, 34*

Microtubules in mammalian cultured cells are usually arranged as a star-like structure, presumably it facilitates intracellular transport by means of motor proteins. Such radial array is organized around the microtubule-organizing center (MTOC) which includes the centrosome and sometimes Golgi. We reported previously about different contribution of Golgi as a MTOS in cognate cell lines with the equal centrosomal activity. Subsequently we carried out a series of experiments on expression of various exogenous proteins presumably affecting the activity of Golgi as a MTOC. Since such a method could not guarantee the complete coverage of all potential participants in the process of microtubule organization, we decided to use a fundamentally different approach. Specifically, we conducted the transcriptome analysis of two cognate cell lines differing by activity of Golgi as a MTOC. Analysing the obtained total data array, we compared the amount of RNAs encoding all the proteins which could potentially take part in microtubules organization at the centrosome and at the Golgi membranes. Such analysis allowed us to identify several promising candidates for the role of the main actor in this process.

FUNCTIONAL CONDITION OF EFFERENT PATHWAYS IN SPINAL CORD AT GRAVITY DISCHARGE

A.O. Fedyanin, A.A. Eremeev, T.V. Baltina, M.E. Baltin, A.M. Eremeev

Institute of Fundamental Medicine and Biology, Kazan Federal Universiry, Kremlevskaya 18, Kazan, 420008, Russia

Gravity discharge that occurs during space flights significantly modifies the integral properties of the musculoskeletal system and individual muscle

groups, as well as basic characteristics of muscles (Kozlovsky 2004;. Gustafsson et al, 2010; Ogneva et al, 2011, etc...). For a long time this phenomenon is associated with a decline in physical activity and weightlessness, respectively, atrophic processes. However it is known that the characteristics of the muscle fibers is largely determined by the influence motor neuron (Pette, Vrbova, 1985; Gabriel et al, 2006;. Eremeev et al, 2011.). About reflex nature of the formation of "hypogravitation musculoskeletal syndrome" also shows a high rate of development recorded changes.

In this regard, it is important to obtain direct information about the functional state of the central structures of the neuro-motor system in a gravity discharge. The aim of this work was to study the functional condition of efferent pathways in spinal cord at conditions of simulated gravity discharge.

The study was conducted on laboratory nonlinear rats. Experimental conditions are created for the animals hanging tail antiorthostatic (head down) position (Ilyin, Novikov, 1980; Morey-Holton, Globus, 2002). After 7 days of exposure to the experimental conditions, motor potentials recorded gastrocnemius muscle (myocardial infarction) caused by magnetic stimulation of the cervical-thoracic and lumbosacral spinal cord. The stimulus intencity reaching 4 T, 0.5 ms duration, frequency of 0.5 pulses / min. Determines the threshold of occurrence, latency, maximum amplitude and duration of the evoked motor potentials (GWP). Also, the difference in propagation time evaluated magnetic pulse from the time, the stimulation of the spinal cord cervical-thoracic prior to registration VMP and the propagation time of the magnetic pulse from the time, the stimulation of the spinal cord of the lumbosacral prior to registration VMP - central motor conduction time (TSVMP). As controls, we used data obtained during the study of intact animals.

It is shown that in 7 days after exposure to experimental conditions parameters VMP MI differ from those recorded in the control. Thus, the threshold HMP when stimulated cervical-thoracic spinal cord decreased to 77.14 ± 12.1% (p> 0.05), the amplitude was 65.5 ± 9.3% (p <0.05), the latency period-68.7 ± 11.3% (p <0.05), duration VMP - 81.6 ± 5.8% (p> 0.05). Upon stimulation of the lumbosacral spinal cord threshold VMP MI was 65.0 ± 8.4% (p <0.05), the amplitude decreased to 28.3 ± 5.1% (p <0.05), the latency period - 64.06 ± 7.7% (p <0.05), duration increased to 126.9 ± 7.9% (p <0.05). Central motor conduction time in 7 days. antiorthostatic hanging decreased to 69.3 ± 7.5% (p <0.05) compared with the data obtained in the study of intact animals

Changes in the amplitude and duration of the VMP in your opinion may be associated with incomplete number of motor units, generating an action potential, and/or desynchronization on intraspinal efferent tract level. At the same time, reducing the latency threshold and VMP probably indicates an increase in transmission efficiency of excitation in locomotor system following structures: movement path of the spinal cord motor neurons, motor roots, peripheral axons. It is known that WCMC reflects the functional state of intraspinal structures providing afferent conduction of excitation. Reduction index determined at refer-

ence unloading may be associated with activation processes in these conditions facilitate the transmission of excitation and CNS level, which generally also indicates an increase in the effectiveness of the spinal cord wires.

Probably discovered in the experiments change VMP IM parameters are the result of restrictions afferent input, including the support, as well as the central nervous system adaptation to the new conditions of motor activity.

The study was financially supported by RFBR (project № 15-04-05951.).

CERTAIN TITIN AND MYOMESIN DOMAINS STIMULATE MYOBLAST PROLIFERATION

V.A. Furalyov, I.V. Kravchenko, V.O.Popov

Bach Institute of Biochemistry, Research Center of Biotechnology of the Russian Academy of Sciences, 33, bld. 2 Leninsky Ave., Moscow 119071, Russia

Investigation of the mechanisms of skeletal muscle hypertrophy development as well as its regeneration after injury is of great interest from the point of view both fundamental biochemical science and possible medical applications. Earlier we have shown that myofibrillar proteins titin and myomesin releasing from damaged muscle stimulate the expression of both IGF-1 splice forms. Certain Fn type III and Ig-like domains included in the structure of titin and myomesin were found to be responsible for this effect. Domains of each type were established to bind with their own receptor and to have different mechanism of action. The effect of Fn type III domains was more sensitive to inhibition of Ca^{2+}/calmodulin dependent protein kinase activity, whereas the effect of Ig-like domains showed greater sensitivity to the inhibition of cAMP – PKA pathway. The aim of this work was to study the ability of titin and myomesin as well as their distinct domains to stimulate myoblast proliferation and to investigate the signalling pathways providing this effect.

The ability of titin and myomesin isolated from mouse skeletal muscle to stimulate murine myoblast proliferation was investigated. It was found that both myofibrillar proteins at 5 a-g/ml conc
tistically reliably. So the treatment of cells by myomesin enhanced MTT reduction by 89% relative to control whereas the treatment by titin increased this value by 67% (fig. 1A). As this takes place, the treatment of myoblasts by BSA, mouse transferrin and mouse actomyosin had no statistically significant influence on cell proliferation.

A similar picture was observed in the experiment with labelled thymidine incorporation in DNA (fig. 1B). Myomesin treatment increased [^{3}H]-thymidine incorporation 2.56 times, and titin treatment enhanced it 2.14 times, the differences from control were statistically reliable in both cases. In analogous manner with MTT assay experiments, albumin, transferrin and actomyosin did not stimulate myoblast proliferation.

Then the ability of distinct domains or group of domains of titin and myomesin to stimulate human myoblast proliferation was studied. Among protein

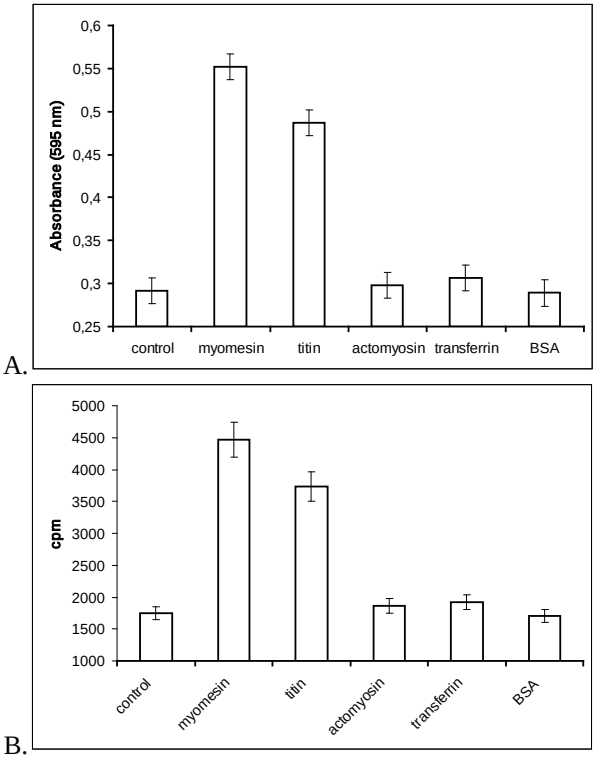

Fig. 1. Induction of the proliferation of murine myoblasts by titin and myomesin measured by MTT-test (A) and by [3H]-thymidine incorporation (B).

samples tested myomesin domains My5 and My11-13 and titin domains TM4 and TA170 were shown to have mitogenic effect on myoblasts. So the treatment of cells by these domains at 5 μg/ml enhanced MTT reduction statistically reliable by 45% - 56% relative to control (fig. 2A). My2, My3, My4, My7-9 and TA166-167 domains demonstrated no ability to stimulate myoblast proliferation.

A similar picture was observed in the experiment with [^{3}H]-thymidine incorporation in DNA (fig. 2B). Domains activating MTT reduction stimulated this incorporation also the range of effect was 2.08 – 2.37 times. At the same time domains that were inactive in experiments with MTT did not show mitogenic activity in experiments with labelled thymidine.

Domains stimulating myoblast proliferation belong to two different types: My5 and TA170 are Fn type III domains whereas My11-13 and TM4 – Ig-like domains. Next the sensitivity of mitogenic effect of different domains to the inhibitors of several signalling pathways was investigated. All studied inhibitors in used concentrations were not cytotoxic for human myoblast and did not lower MTT reduction and [^{3}H]-thymidine incorporation in DNA.

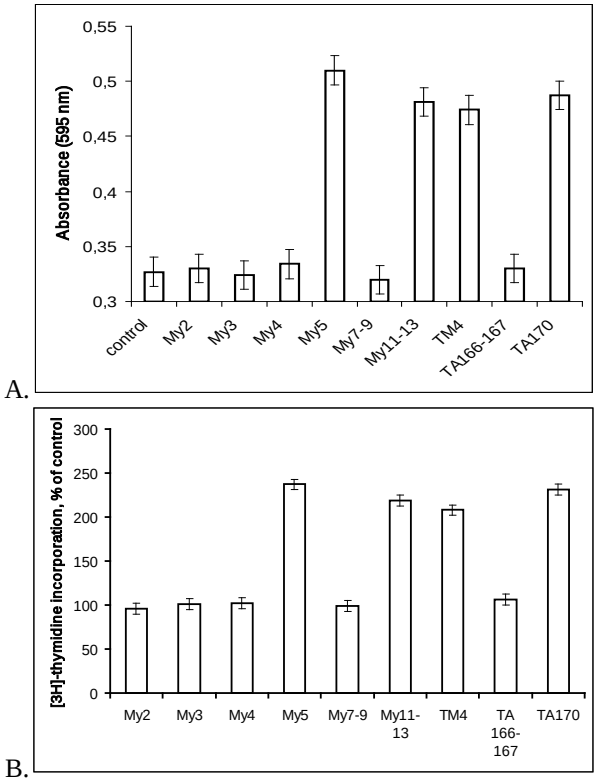

Fig. 2. Induction of the proliferation of human myoblasts by certain titin and myomesin domains measured by MTT-test (A) and by [3H]-thymidine incorporation (B).

The effects of Fn type III domains and Ig-like domains appeared to differ in their sensitivity to the action of inhibitors of diverse signalling cascades. Proliferative effect of Fn type III domains My5 and TA170 was strongly inhibited by Ca^{2+}/calmodulin dependent protein kinase inhibitor. Thus KN93 decreased MTT reduction by myoblast cultures to 72–75% of the level observed without inhibitor (fig. 3A). In the experiments with [^{3}H]-thymidine incorporation inhibitory action was pronounced even stronger: mitogenic effect of Fn type III domains decreased to 59–61% of the level observed without inhibitor (fig. 3B). In all cases the inhibition of domain mitogenic effects was statistically reliable.

At the same time proliferative effect of Fn type III domains was of little sensitivity to the inhibitors of adenylyl cyclase and protein kinase A. DDA and Rp-cAMPS impaired MTT reduction by myoblast cultures as little as to 93–95% of the level observed without inhibitor. These effects were manifested as a trend only and were statistically unreliable. Inhibition of [^{3}H]-thymidine incorporation in DNA

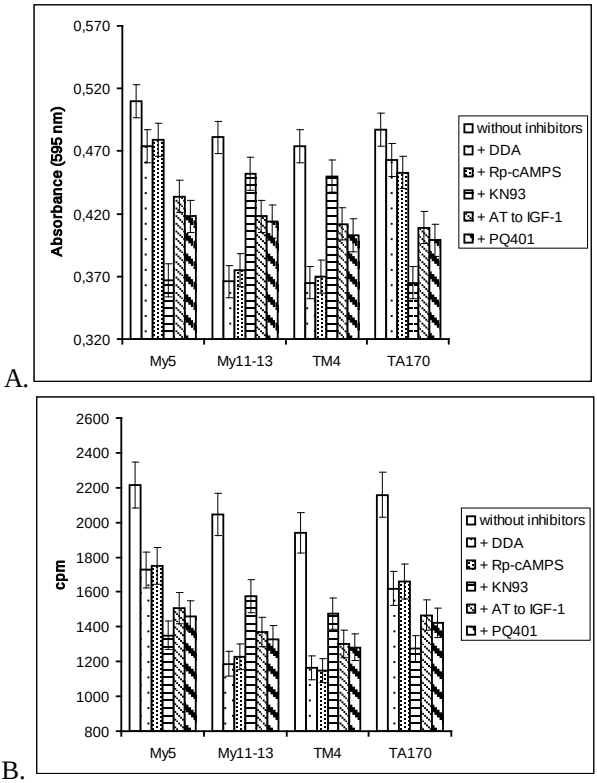

Fig. 3. Titin and myomesin domains mitogenic effect decrease of by the inhibitors of different signalling pathways measured by MTT-test (A) and by [3H]-thymidine incorporation (B).

was also slightly pronounced though statistically reliable: its including was decreased to 75–79% of the level observed without inhibitor.

The character of inhibition of Ig-like domain mitogenic effects was quite a different. Proliferative action of My11-13 and TM4 domains was strongly depressed by inhibitors of adenylyl cyclase and protein kinase A. DDA and Rp-cAMPS lowered MTT reduction to 76–78% of the level observed without inhibitor. Inhibitory action of these compounds was even more pronounced in the experiments with [^{3}H]-thymidine incorporation: mitogenic effect of Ig-like domains was lowered to 58–60% of the level observed without inhibitor. In all cases the inhibition of domain mitogenic effects was statistically reliable.

At the same time proliferative effect of Ig-like domains was of little sensitivity to the inhibitor of Ca^{2+}/calmodulin dependent protein kinase. KN93 decreased MTT reduction to 94–95% of the level observed without inhibitor. These effects were manifested as a trend only and were statistically unreliable. Inhibition

of [^{3}H]-thymidine incorporation in DNA was also slightly pronounced though statistically reliable: its including was decreased to 76–77% of the level observed without inhibitor.

Inhibition of IGF-1 signaling lead to statistically reliable decrease of mitogenic effects of both type domains. Neutralizing antibodies to this growth factor as well as its receptor inhibitor PQ401 lowered MTT reduction by myoblast cultures treated with domains of both types to 82–87% of the level observed without inhibitor. These inhibitors decrease labelled thymidine incorporation in DNA also: mitogenic effect of domains was decreased to 65–68%. In all cases the inhibition of domain mitogenic effects was statistically reliable.

In previous works we showed that myofibrillar proteins titin and myomesin stimulate expression of IGF-1 splice forms. However, it remains uninvestigated whether these stimulators activate myoblast proliferation. Here the ability of titin and myomesin as well as their certain domains to stimulate MTT reduction and [^{3}H]-thymidine incorporation in DNA by myoblast cultures was shown. Mitogenic properties were exhibited by both Fn type III and Ig-like domains. It should be stressed that from all studied domains only those who activated IGF-1 splice form expression stimulate myoblast proliferation also.

Earlier we have shown that stimulation of MGF and IGF-1Ea synthesis induced by Fn type III domains was more sensitive to inhibition of Ca^{2+}/calmodulin dependent protein kinase activity, whereas the effect of Ig-like domains showed greater sensitivity to the inhibition of adenylyl cyclase–cAMP–PKA pathway. In present work we have described that stimulation of proliferation induced by domains of these two types demonstrate the same pattern of sensitivity to signaling pathway inhibitors.

Since certain domains stimulate both myoblast proliferation and IGF-1 production, it was of special interest to investigate the role of IGF-1 in manifestation of mitogenicity of all domains. All domains appear to have pronounced proliferative effect in the conditions of IGF-1 signaling suppression. At the same time this suppression leads to significant decrease of mitogenic action of both type domains, so it may be declared that IGF-1 signaling is partially involved in proliferative effects of titin and myomesin.

A possible application of different IGF-1 splice forms for the treatment of sarcopenia and different myodistrophies is widely discussed. Earlier we had proposed the possibility to use the low molecular weight inductors of growth factor expression binding with receptors of titin and myomesin domains instead of usage of growth factors by themselves. In present work we describe the mitogenic effects of several domains of titin and myomesin that makes this approach even more perspective.

These studies were supported by the grants from the Russian Foundation for Basic Research (15-04-06229a) and the Molecular and Cell Biology Program of the Russian Academy of Sciences, grant 6P.

BRANCHED ACTIN NETWORKS IN CELL MIGRATION AND PROLIFERATION

A. Gautreau

CNRS, Ecole Polytechnique, University Paris-Saclay, France

Branched actin networks are the product of the Arp2/3 molecular machine. In vitro branched actin networks have been shown to generate a pushing force. In vivo these networks have been identified at different subcellular locations to drive membrane protrusion and remodeling during intracellular traffic. Here we will discuss the integration of positive and negative regulation of membrane protrusions and how it impacts the essential parameters of cell migration. Surprisingly we found that the signaling pathway that generates branched actin at membrane protrusions, Rac-WAVE-Arpin, also controls cell cycle progression. In fact, this signaling pathway has all the expected properties of a cell cycle checkpoint: signaling is required in normal cells but this requirement is lost in cancer cells. The branched actin network of membrane protrusions integrates growth factor stimulation with mechanotransduction of cell adhesion to instruct the cell that its environment is permissive for migration and cell cycle progression.

INCREASE OF ACETYLCHOLINE QUANTAL SIZE PROVOKED BY ACTION OF CALCITONIN GENE-RELATED PEPTIDE IN NEUROMUSCULAR JUNCTIONS OF MICE

A.E. Gaydukov, O.P. Balezina

Department of Human and Animal Physiology, Biological Faculty, Lomonosov Moscow State University, Leninskie Gory 1/12, Moscow 119234, Russia

Calcitonin gene-related peptide is a 37-amino acid peptide that is formed as a result of alternative processing of calcitonin gene. In spite of difference in 4 amino acids in the peptide molecules of human and rodent CGRP, both isoforms have been used extensively in studies of CGRP physiological activities. The peptide is widely distributed both in CNS and peripheral synapses. In motor nerve terminals, endogenous CGRP is localized in large dense-core vesicles and may be released as a co-transmitter in synaptic cleft. Possible acute presynaptic effects of CGRP in vertebrate motor synapses are poorly investigated. Here we compared the action of exogenously applied human and rat isoforms of CGRP on evoked and spontaneous quantal ACh release in mouse motor synapses in order to determine possible targets and mechanisms of the peptides effects. Second task was to release the endogenous CGRP from the motor terminals and to analyze if endogenous peptide may regulate synaptic transmission in motor synapses as exogenous one.

Experiments were performed at 20–22ºC on isolated neuromuscular preparations of the diaphragm-phrenic nerve from adult mice (strain BALB/c) of both sexes (25–30 g body weight). Left hemidiaphragm with the phrenic nerve was excised and mounted to a 3-ml recording chamber and perfused with oxygenated (95% O_2, 5% CO_2) Liley solution (pH 7.2–7.4). Studies on ACh secretion

evoked by stimulation of phrenic nerve with suprathreshold stimuli (0.3 Hz, 0.1 ms) were performed with cut neuromuscular preparations. At least 30 multiquantal evoked endplate potentials (EPPs) were recorded in each synapse studied, and spontaneous (miniature) endplate potentials (MEPPs) were recorded for 60 s immediately before the nerve stimulation (mean value of the MEPP amplitudes recorded within this period was used for the calculation of the quantal content of the EPP). MEPPs were recorded for 180 s using intact (uncut) preparations when only spontaneous activity was studied. Synaptic responses were acquired using amplifiers Axoclamp 2B or Axoclamp 900A (Molecular Devices) and digitized using a E-154 interface with PowerGraph 3.3 software (L-Card, Russia) or a Digidata 1440A interface with pCLAMP 10 software (Molecular Devices), then stored and analyzed using MiniAnalysis software (Synaptosoft). As a control, MEPPs only or EPPs with MEPPs from 5 or more different synapses were recorded; after that, the drugs were added into the perfusion solution in the desired order and the activity of various synapses was recorded for 0.5–1.5 hour. In each experimental series, at least three neuromuscular preparations were used. We estimated membrane potential of muscle fibers, as well as the MEPP and EPP amplitude and time course and the MEPP frequency. The MEPP and EPP amplitudes were standardized to the membrane potential of –50 mV when evoked synaptic activity was analyzed. Quantal content of EPP was calculated as a ratio between the mean standardized EPP amplitude corrected to nonlinear summation and the mean standardized MEPP amplitude. The MEPP amplitudes were standardized to the membrane potential of –70 mV when only spontaneous ACh release was studied. Data are presented as the mean ± SEM (n is a number of the synapses studied). Statistical significance between sample means was assessed using the Student's t-test (in the case of normal distribution) or one-way analysis of variance ANOVA. The difference was considered significant at $p < 0.05$.

In the first series of experiments, we compare the action of human CGRP (hCGRP) and rat CGRP (rCGRP) (both – 100 nM) on parameters of EPPs and MEPPs. In the presence of hCGRP the amplitude of MEPPs increased significantly by 32% from 1.32 ± 0.06 mV (n=21) in the control to 1.74 ± 0.09 mV (n=20, p<0.05). The amplitude of single evoked EPPs also increased from 27.71 ± 1.67 mV under control conditions to 38.67±2.06 mV in the presence of CGRP (p<0.05). This effect was not accompanied by a relative increase in quantal content of EPPs (control – 21.06 ± 0.86; hCGRP – 22.61 ± 1.09 (p>0.05)). Application of rCGRP caused the same effect as the hCGRP did. Both MEPP and EPP amplitudes were increased to 131.83 ± 7.38 % and 140.04 ± 9.96 % (n = 15, p<0.05) of control (n = 19), respectively. No changes were observed in the quantal content of EPPs in the presence of rCGRP. Thus, both peptide isoforms enhance evoked ACh release (augment the EPP amplitude) due to the increase in the amplitude of each ACh quantum (MEPP) within multiquantal EPP instead of upregulating EPP quantal content. We test the dose-dependence (1 nM – 1 μM) of hCGRP and rCGRP effects on the MEPP parameters. A concentration-dependent increase of MEPP amplitude was revealed after application of hCGRP. In the presence of 1 nM of the

peptide, the amplitude of MEPPs increased by 32%, from 1.21 ± 0.07 mV in control (n=24) to 1.56 ± 0.08 mV (n=25, p<0.05). An increase in the peptide concentration to 100 nM induced more pronounced increment of MEPP amplitude – up to 151% of the control (n=25, p<0.05). This effect seemed to reach maximum because no further increase in MEPPs amplitude was observed in the presence of 1 μM hCGRP. In the presence of 1 or 10 nM of rCGRP the amplitude of MEPPs increased by 30%. Higher concentrations of the rat peptide isoform (0.1 and 1 μM) caused a greater increase in MEPP amplitude – up to 150–160% of control. Both human and rat truncated peptides – CGRP8-37, known as blockers of CGRP-receptors – by itself had no significant effect on parameters of spontaneous ACh release but completely prevented the potentiating effect of human or rat CGRP on the amplitude of MEPPs, respectively (p<0.05). The obtained results suggest that the effect of human or rat CGRP isoforms on MEPP amplitude is mediated by peptide action on their specific receptor. Taking into account the similarities in qualitative and quantitative strength of the effect between hCGRP and rCGRP further analysis was made using just one peptide isoform. We examined the input resistance of diaphragm muscle fiber using two-electrode recordings –during rCGRP (1 μM) application it remained at the same level (0.66 ± 0.06 MΩ (n=15, p>0.05) as under control conditions(0.67 ± 0.06 MΩ (n=15)). The obtained results together with unchanged membrane potential and MEPP time parameters argue against any acute postsynaptic actions of CGRP in the mouse NMJs. CGRP-induced augmentation of postsynaptic potentials amplitude may be the consequence of the presynaptic increment of quantal size due to increased ACh loading into the synaptic vesicles. Vesamicol (1 μM), which directly inhibits vesicular ACh transporter, alone had no significant effect on MEPP amplitude (1.72 ± 0.09 mV (n = 24) in control versus 1.62 ± 0.07 mV (n = 31, p>0.05) under vesamicol). Further application of CGRP (1 μM) under these conditions did not change the MEPP amplitude significantly (1.65 ± 0.06 mV (n = 26, p>0.05) (Fig. 3A,B). The obtained data provide strong argument in favor of our suggestion that the effect of CGRP on transmitter release in mouse NMJs is presynaptic and results from an increase in quantal size due to upregulation of ACh transport into vesicles.

Next we studied the presynaptic effect of CGRP in the presence of PKA inhibitor, H-89. The preliminary application of H-89 (1 μM) for 50 min by itself provided no significant changes in MEPP characteristics, however, under these conditions CGRP (1 μM) lost its ability to increase the amplitude of MEPPs (p>0.05)). Overall, the obtained data indicate that exogenously CGRP acts on its presynaptic receptors and triggers an intracellular signaling cascade that involves PKA and leads to increased loading of ACh in synaptic vesicles and upregulation of ACh quantal size in mouse motor nerve endings.

Next we tried to test if the endogenous CGRP being released from nerve terminal may produce the same effect as exogenouse one – increase in MEPP amplitude. According to our previous results, activation of ryanodine receptors in nerve terminals induced an increase in MEPP amplitude, which could be prevented by vesamicol and H-89. An assumption was made that intraterminal release of

stored calcium can upregulate the release of endogenous CGRP which in turn increases the quantal size. Indeed, application of ryanodine (0.1 μM) showed an increase in MEPP amplitude – from 1.34 ± 0.11 mV (n=18) in control to 2.07 ± 0.13 mV (n=15, p<0.05). Such potentiating effect of ryanodine was prevented by preliminary blockage of CGRP receptors with 0.5 μM of CGRP8-37 (p>0.05). Previously it was shown that activation of CaMKII triggered by release of stored calcium is necessary for exocytosis of peptide-containing dense core vesicles in neuromuscular junctions of Drosophila. To test the role of CaMKII in ryanodine effects in mammalian motor synapses the inhibitors of CaMKII KN-62 (3 μM) or KN-93 (3 μM) were applied. Both CAMKII inhibitors by themselves had no significant effects on MEPPs amplitude, but further application of ryanodine (0.1 μM) did not potentiate the amplitude of MEPPs. Moreover, inactive analog of KN-93 – KN-92 (3 μM) – failed to prevent the increase of MEPPs caused by subsequent ryanodine application. The obtained data indicate that the effect of calcium released from intraterminal stores on MEPPs amplitude is mediated by activation of CaMKII and the initiation of endogenous CGRP secretion which is responsible for the increase of quantal size in mouse motor synapses.

In summary, it was revealed for the first time that in mouse NMJ two exogenous isoforms of CGRP facilitate the neurotransmitter release by increasing presynaptically the quantal size of ACh which leads to the enlargement of both MEPP and EPP amplitudes. Thus exogenous CGRP has replenished the poor choice of known effective regulators of neurotransmitter quantal size which may potentiate cholinergic transmission in motor synapses of mammals. We also identified particular conditions (activation of presynaptic ryanodine receptors followed by release of stored calcium with subsequent activation of CaMKII) when endogenous CGRP may release from motor nerve terminals and exert similar specific presynaptic regulatory role in cholinergic synaptic transmission. The ability of CGRP to potentiate presynaptically the size of uniquantal miniature signals declares a rather new effective way of enhancement of synaptic transmission via presynaptic modulation of mediator quantal size - alongside with traditionally accepted changes in the number of quanta released.

This work was supported by Russian Foundation for Basic Research, grant 16-04-00554a.

VASCULAR SMOOTH MUSCLE POTASSIUM CHANNELS IN EARLY POSTNATAL ONTOGENESIS

D.K. Gaynullina, A.A. Shvetsova, D.S. Kostyunina, R. Schubert, O.S. Tarasova

Faculty of Biology, Lomonosov Moscow State University and SRC RF Institute for Biomedical Problems RAS, Moscow, Russia; Heidelberg University, Medical Faculty Mannheim, Germany

Potassium channels play an important role in the regulation of vascular tone. Their activation leads to hyperpolarization and relaxation of arterial smooth

muscle. There are four types of potassium channels in arterial smooth muscle: voltage-dependent K^+ channels (K_v, the most functionally relevant subtype in arterial smooth muscle is K_v7), Ca^{2+}-activated K^+ channels (BK_{Ca}), inward rectifier K^+ channels (K_{IR}), ATP-sensitive K^+ channels (K_{ATP}). We hypothesized that the role of K^+ channels in the regulation of vasocontractile responses changes during postnatal maturation.

Saphenous arteries were isolated from young (10-15-days old) and adult (2–3-month old) male rats, endothelium was denuded and arterial contractile responses were studied using wire myography. Blockers of K_{ATP} (glibenclamide, 3 μM), K_v7 (XE991, 3 μM), BK_{Ca} (iberiotoxin, 0.1 μM) and K_{IR} ($BaCl_2$, 30 μM) channels were used in order to evaluate the role of different K^+ channels in the regulation of basal tone and contractile responses to $alpha_1$-adrenoceptor agonist methoxamine. mRNA expression levels were determined by qPCR.

K_{ATP} blocker had no effect on basal tone and contractile responses to methoxamine in arteries in both groups. Blockade of K_v7 caused a significant increase of basal tone and contractile responses in young, but not adult rats; this was consistent with higher expression levels of $K_v7.1$ and $K_v7.5$ in arteries of young rat. The effects of BK_{Ca} blocker iberiotoxin were more prominent in arteries of adult animals. This was accompanied by higher expression level of beta-subunit of BK_{Ca} channel in their arteries, while the expression level of alpha-subunit was similar in saphenous arteries of young and adult rats. K_{IR} blockade augmented contractile responses in both age groups, however the effects were more prominent in arteries of young animals.

In conclusion, our results show that in saphenous arteries (i) K_{ATP} channels have no impact on contractile responses to alpha1-adrenoceptor agonist in both age groups; (ii) the influence of K_v7 and K_{IR} channels on the regulation of contractile responses decreases, while (iii) the contribution of BK_{Ca} increases during early postnatal ontogenesis.

This study was supported by the RFBR (grant № 16-04-01395-a).

EFFECTS OF ELEVATED HOMOCYSTEINE LEVEL ON THE RATE OF MATURATION OF RAT SENSORY-MOTOR REFLEXES

A.I. Gilmutdinov*, E.V. Gerasimova, *G.K. Ziyatdinova, N.N. Khaertdinov*, E.R. Ziganshina**, O.V. Yakovleva*, G.F. Sitdikova***

**Institute of Fundamental Medicine and Biology, Kazan Federal University, Kremlevskaya st.18, Kazan, 420008, Russia*

***Institute of Chemistry, Kazan Federal University, Kremlevskaya st.18, Kazan, 420008, Russia*

Homocysteine is a sulpho-containing endogenous amino acid, which is produced in the methylation cycle of protein metabolism and involved in maintaining the cells redox balance. Inherited deficiency of the enzyme methylenetetrahydrofolate reductase (MTHFR), transforming Homocysteine into methionine through remethylation, is associated with severe muscular hypotonia. The reduction in activity of this enzyme is one of the main reasons for homocysteine accumulation in the

body – hyperhomocysteinemia [1]. Extremely high homocysteine levels (up to 200 μM) has been found in some patients with disrupted homocysteine metabolism, and is believed to be at the root of certain vascular disorders including stroke and coronary occlusions [2]. Increased homocysteine concentrations lead to cardiovascular disease, renal dysfunction, associated with a number of neurodegenerative diseases, contributes to the pathologies of nervous system development, leading to disruption of cognitive functions, which one way or another will occur in roughly-motor activity and fine motor skills of the animal [3]. Significantly elevated plasma homocystein levels were detected in mothers of affected children and in maternal plasma and amniotic fluid in neural tube defects pregnancies [4]. The aim in our study was to reveal the rate of maturation of sensory-motor systems in rat's pups born from the rat females with elevated concentration of homocysteine in blood during pregnancy.

The work was carried out on Wistar rats, grown in vivarium of KFU. 88 pups between the ages of 0 and 16 days of life were used. Rats were obtained from 12 female's rat, divided into control and experimental groups. The females of the experimental group (n = 6) for 3 weeks prior to pregnancy, during and after delivery, while feeding have got methionine in the dose of 7.7 g/kg per day with food. The females of the control group (n = 6) were on a standard diet.

The homocysteine quantification is based on its 1,4-Michael addition reaction with *o*-quinone. The product formed undergoes electrochemical reduction at -0.16 V on glassy carbon electrode modified with multi-walled carbon nanotubes (MWNT/GCE) under conditions of square-wave voltammetry [5]. Voltammetric measurements were performed on potentiostat/galvanostat μAutolab type III with the software GPES, version 4.9.005 (Eco Chemie B.V., The Netherlands). Phosphate buffer solution pH 7.0 was used as supporting electrolyte. The electrochemical cell consisted of working MWNT/GCE, silver-silver chloride saturated KCl reference electrode and counter electrode (platinum wire). 3.66 mL of supporting electrolyte, 40 μL of catechol and 300 μL of plasma were added in electrochemical cell and square-wave voltammograms were registered within the potential range from 0.5 to –0.4 V using the frequency of 25 Hz, amplitude 50 mV, step potential 8.0 mV and scan rate 200 mV s^{-1}. Baseline correction by moving average algorithm included in GPES software has been applied for the better peaks identification. Homocysteine concentration was calculated using calibration graph.

Concentration of the homocystein on blood in the control group was 7±1 μM, in the experimental group was 124±23 μM.

The physical development of the animals of the experimental and control groups was assessed: the weight, the detachment of the ear, the appearance of hair and eye opening. To study somatosensory maturation in rat pups a standard battery of tests assessing the developing behavioral phenotype of rats (P2-P16) during the feeding was used [6].

In the experimental group the physical development of rat pups (the detachment of the ear, the appearance of hair and eye opening) did not significantly differ from the control animals. The most important indicator of somatic development of animals is the dynamic of the body weight. The analysis of the weight

Table 1. Dynamics of weight of newborn rat pups

Group/ Age	2 days	8 days	16 days
Control group	7.9± 0.6g	17.3± 0.5g	35.3± 0.2g
Homocysteine group	6.5± 0.2g	13.7± 0.5g	28.6± 1.6g

dynamics of rat pups has shown the lower body weight of experimental animals compare to control animals (table 1).

The prenatal damaging neurotoxic effects of homocysteine have been studied using sensorimotor reactions in the postnatal period. In tests conducted in early developmental stages of animals (P2-P9), there was a significant impairment in the formation of a number of reflexes (table 2).

In the test "rolling on a horizontal plane" no significant differences were observed in the day of the reflex formation (day 8 after birth), but the reliably faster reflex fulfillment was established in animals of the control group ($p<0.05$). "Pendulum" reflex in rat pups of both groups were formed by 8 days after birth, but the number of head rotations per minute was significantly lower in experimental group compare to the controls (table 2).

In the test, "avoiding the cliff" with a fixed time (10 sec), we observed a significant slowdown in the formation of the reflex in the experimental group. So in rat pups of the control group, the reflex was formed by day 6 after birth, and in the experimental group only by day 7 (table 2). The muscle strength in rat pups of the control group during the specified observation period was greater than in the experiment (table 2).

Table 2. The speed of sensory-motor reflexes maturation in rat pups

Index	Control group	Experimental group
Rolling on a horizontal plane (mean time in sec.) *P*=8	1.62±0.18	2.03±0.21*
Avoiding the cliff (mean day of formation of the reflex)	5.90±0.18	7.11±0.29*
"Pendulum" reflex (mean number of movements) *P*=8	6.52±0.68	2.31±0.30*
Muscle strength (sec)		
P=4	1.44±0.97	0.32±0.24*
P=10	5.06±1.16	1.31±0.32*
P=16	14.97±3.84	2.38±0.83*

* $P_u \leq 0{,}05$ – U-criterion Mann-Whitney

Thus, the obtained data suggest that in rat's pups born from the rat females with elevated concentration of homocysteine the lower weight and the delay of maturation of several sensory-motor reflexes were observed.

This work was supported by Russian Science Foundation №14-15-00618.

References

1 Skvortsov, I. Y. Homocysteine as a risk factor for coronary artery disease / Y. I. Skvortsov, A. S. Korolkova // Saratov scientific medical journal. 2011. Vol. 7, No. 3. P. 619-624.

2 Bukharaeva, E. Homocysteine aggravates ROS-induced depression of transmitter release from motor nerve terminals: potential mechanism of peripheral impairment in motor neuron diseases associated with hyperhomocysteinemia / Bukharaeva, E. A. Shakirzyanova, Khuzakhmetova V., Sitdikova G., Giniatullin R // Frontiers in Cellular Neuroscience – 2015 – Vol. 9 Article 391 – P. 1-8.

3 West, R. K. Homocysteine and cognitive function in very elderly nondemented subjects / R. K. West, M. S. Beeri, J. Schmeidler // Am. J. Geriatr. Psychiatry. – 2011. – Vol. 19 (7). – P. 673-677.

4 Greene N.D.E., Dunlevy L.P.E., Copp A.J. homocysteine is embryonic but does not cause neural tube defects in mouse embryos // Anat Embryol. – 2003 – Vol. 206 - P. 185-191.

5 Lee P. T., Lowinsohn D., Compton R. G. Simultaneous detection of homocysteine and cysteine in the presence of ascorbic acid and glutathione using a nanocarbon modified electrode // Electroanalysis - 2014. – V. 26. – P. 1488-1496

6 Guidance on experimental (preclinical) study of new pharmacological substances. Ed. by R. U. Habrieva. – 2-ed., revised and enlarged. – Medicine, 2005 – 832p.

COMPARISON OF THE PROPERTIES OF "NATURAL" MOLLUSCAN ACTIN WITH STRAUB-TYPE RABBIT ACTIN

U.V. Girich, N.S. Shelud'ko

A.V. Zhirmunsky Institute of Marine Biology,
Far Eastern Branch of the Russian Academy of Sciences,
Palchevsky str. 17, Vladivostok, 690041, Russia

Recently, we have proposed our method for isolation of "natural" actin from the molluscan catch muscle. The need for such a method is determined by the fact that the current method for isolation, designed for the skeletal muscles of vertebrates, is not valid for smooth muscles of invertebrates. Therefore, studies of the muscle contractile apparatus of invertebrates often use the Straub-type rabbit actin combined with muscle proteins of invertebrates. Although actin is a highly conservative protein, we have no full confidence in the correctness of this combination.

In this study, we compared the properties of the Straub-type actin from rabbit skeletal muscles and "natural" mussel actin isolated by us from the catch muscle of *Crenomytilus grayanus.*

We have obtained the following results:

1. Slight differences were detected in the degree of activation of MgATPase activity of the rabbit skeletal muscle myosin in solutions with a low ionic strength (30 mM KCl), while no difference between actins were observed

in the degree of activation in a medium with the physiological ionic strength (75 mM KCl).

2. Electron microscopy did not reveal any difference between the polymer forms of these actins.
3. Actin of the mussel was virtually identical to rabbit actin in the speed and extent of polymerization.
4. Substantial differences were detected in viscosity. The value of the characteristic viscosity of the rabbit actin 4–5 times exceeded viscosity of the mussel actin. The difference in the viscosity increased with an increase in concentration.
5. In combination with tropomyosin, the actin viscosity increased both for the mussel and for the rabbit. The rabbit tropomyosin increased the viscosity more strongly than mussel tropomyosin did.
6. The viscosity of an actin-tropomyosin complex increased with addition of tropomyosin to achieve a molar ratio of 1:1. Further addition of tropomyosin lead, on the contrary, to a lower viscosity. This pattern was observed only at the use of the low shear (falling-ball viscometry). At higher shear forces (capillary- and vibro-viscometers), this effect was not observed.
7. Purification of actins by the depolymerization-polymerization procedure did not appreciably affect the viscosity of both actins. However, the actin viscosity was strongly affected by actin purification through gel-filtration: the viscosity of both actins increased; the difference between the actins maintained.
8. Interestingly, various chromatographic fractions of actin have different properties. Fractions of the right edge of the peak showed a 30-fold viscosity increase compared to that of the crude actin before chromatography. On the other hand, fractions of the left edge of the peak had lower viscosities than that of the crude actin. This is also characteristic of mussel and rabbit actins and might indicate the presence of some factor in both actins, and that affects the length of actin polymers. These factors are present only in very low concentrations; and SDS-electrophoresis showed no impurity in the chromatographic preparations.
9. The fractions with a low viscosity are polymerized very rapidly and do not possess thixotropy, while the fractions of a high viscosity are polymerized slower and are thixotropic. That, all taken together, suggests that an impurity contained in the “natural” mussel actin is a barbed end capping protein like CapZ that was previously found in the Straub-type actin preparations from skeletal muscles of vertebrates.

STUDY OF THE INFLUENCE OF FLOCALIN ON THE ENERGY AND ION EXCHANGES IN RAT LIVER MITOCHONDRIA

O.S. Gorbacheva[1,2], R.B. Strutynskyi[3], N.V. Khmil[1,4], N.V. Belosludtseva[1,2], S.V. Murzaeva[2], M.O. Korobeynikova[1,2], G.A. Alilova[1,2], E.I. Lezhnev[1,2], G.D. Mironova[1,2]

[1]*Institute of Theoretical and Experimental Biophysics RAS, Pushchino, Russia,*

[2]*Pushchino State Institute of Natural Sciences, Pushchino, Russia*

[3]*Bogomoletz Institute of Physiology NASU, Kyiv, Ukraine*

[4]*V.N. Karazin Kharkiv National University, Kharkiv, Ukraine*

It is known that cardiovascular diseases are the main problem of present medicine. Recently, for the treatment of these diseases have been widely used various modulators of calcium and potassium channels, as well as inhibitors of the renin-angiotensin system [1].

With the collaboration of laboratories O.O.Moibenko and L.M. Yagupolskii developed technological scheme of synthesis of a new cardioprotective fluorine-containing pinacidil derivative preparation flocalin [2]. It was shown that this preparation at experimental acute ischemia/reperfusion has pronounced cardioprotective properties in animals and reduces myocardial infarct size relative to control without treatment by 42% [3]. It is assumed that one of the mechanisms cardioprotection in this case may be to increase the proportion cNOS/iNOS activity. In addition, it is shown that flocalin promotes normalization of bioenergetic metabolism in the ischemic brain, restoring the content of adenine nucleotides and creatine phosphate against decrease metabolic acidosis and growth of glucose [4].

Since flocalin is a fluorine-containing analog of pinacidil - known opener of ATP-sensitive potassium channel both cytoplasmic (sarcK_{ATP}) and mitochondrial (mitoK_{ATP}) membranes [5], the aim of work was to investigate the effect of this preparation on the functioning of mitochondria, and in particular, on work of mitoK_{ATP} channel.

Materials and Methods

Mitochondria were isolated from the liver of Wistar rats weighing 220–250 g using a standard differential centrifugation technique. The isolation medium contained 210 mM mannitol, 70 mM sucrose, 0.1% BSA, 0.5 mM EGTA, 30 mM Hepes-KOH, (pH 7.4).

Respiration of mitochondria was measured by the polarographic method using polarograph OROBOROS Oxygraph-2k (Oroboros Instruments, Austria). The incubation medium contained: 100 mM sucrose, 50 mM mannitol, 60 mM KCl, 10 mM Hepes, pH 7.4, 0.5 mM EGTA-K, 5 mM KH_2PO_4, 2.5 mM $MgCl_2$. The concentration of mitochondrial protein was ~ 0.5–1.0 mg/ml.

The kinetics of swelling was recorded using a spectrophotometer UV2450 (PC) (Shimadzu, Japan) by following the change in the optical density of the suspension of mitochondria at the wavelength of 520 nm. The swelling of mitochondria was triggered by the addition of substrate (5 mM succinate/2 μM rotenone).

The incubation medium contained 120 mM KCl, mM Tris, 5 mM K_2HPO_4, 0.1 mM EDTA (pH 7.4). The concentration of mitochondrial protein in cuvette was 0.2 mg/ml.

DNP-induced output of K^+ from mitochondria was studied by K^+-selective electrode [7]. The incubation medium contained: 170 mM sucrose, 80 mM D-mannit, 5 мМ Na_2HPO_4, 10 mM Tris-HCl (pH 7.4). The output of K^+ from mitochondria was initiated by the addition of 50 μM 2,4-dinitrophenol in incubation medium. The concentration of mitochondrial protein in cuvette was 1-1,5 mg/ml.

The rate of H_2O_2 production was detected using the system of the fluorescent dye Amplex red (AR) with horseradish peroxidase (HRP) [8]. The incubation medium contained 120 mM KCl, 5 mM KH_2PO_4, 10 mM Hepes/KOH (pH 7.4), 1 mM EGTA, 2 mM $MgCl_2$, 2 μM oligomycin and respiration substrate, than were added 1U/ml HRP, 10 μM AR and mitochondria (0.09–0.1 mg/ml of protein). The measurements were carried out using a CARY spectrofluorimeter (Varian Inc., USA).

Results

The influence of flocalin on the energy, ion and oxidative exchange in rat liver mitochondria was investigated. Energy metabolism had been studied by measuring mitochondrial respiration. As seen in fig. 1, flocalin activated uncoupled respiration (V_2 and V_4) and inhibited the respiration rate in the presence of ADP (V_3) when using succinate as respiratory substrate. The uncoupled respiration in the presence of DNP was not changed by flocalin. In this case, flocalin reduced an efficiency of phosphorylation and increased the time phosphorylation of added ADP, ie reduced the rate of formation of ATP.

When used α-ketoglutarate as a substrate (fig. 2), the action of flocalin was slightly different. It also activated the uncoupled respiration, but did not affect the coupled respiration. Substitution of potassium in the incubation medium on sodium ions did not eliminate the effect of flocalin on mitochondrial respiration when both succinate and NAD-dependent substrates were used.

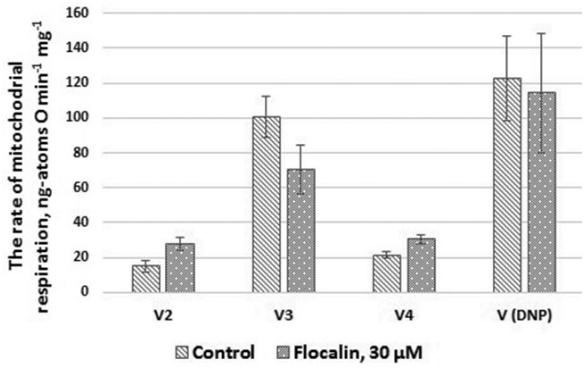

Fig. 1. Effect flocalin on respiration of liver rat mitochondria in the presence of potassium succinate as respiratory substrate.

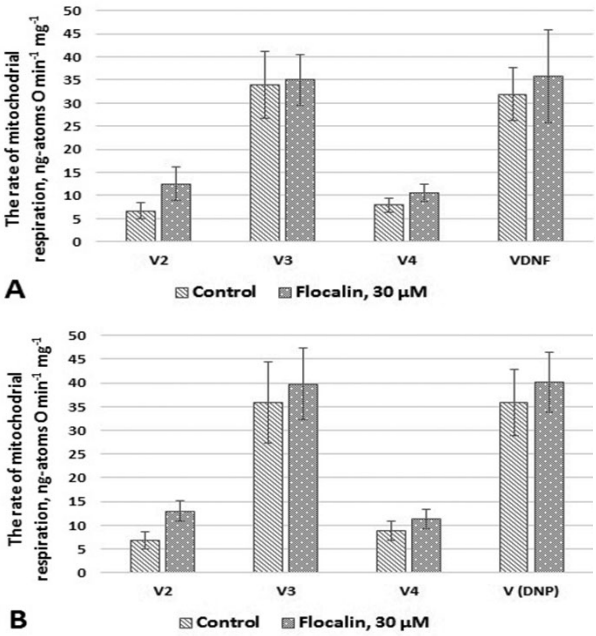

Fig. 2. Effect flocalin on respiration of liver rat mitochondria in presence of α-ketoglutarate as respiratory substrate. A – the incubation medium contained NaCl, B – the incubation medium contained KCl.

The action of flocalin on ion exchange is estimated by its influence on the rate of formation of hydrogen peroxide in the mitochondria. It was found that this rate did not significantly change when both substrates were used. Preliminary data showed that incubation of mitochondria with flocalin for 3 min did not lead to the accumulation of lipid peroxides in the organelles that was determined by accumulation of MDA products.

The effect of flocalin on mitoK_{ATP} channel functioning was evaluated by two methodological approaches: energy-dependent swelling of mitochondria and DNP-induced efflux of potassium ions of mitochondria. As can be seen from table, flocalin inhibited the mitochondrial swelling rate in a dose-dependent manner.

Influence of flocalin on the energy-dependent swelling rate of rat liver mitochondria defined mitoKATP channel functioning

Concentration of flocalin, µM	Inhibition of mitochondrial swelling rate, % of control
30	58.0
15	38.0
7,5	13.0
3,75	24.5
1,88	5.0

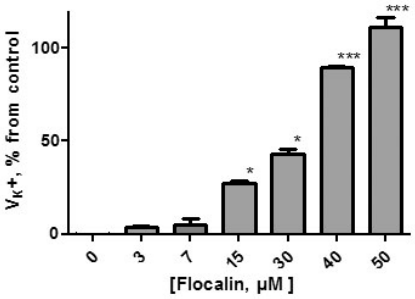

Fig. 3. Flocalin activates DNP-induced efflux of K^+ ions from rat liver mitochondria in a dose-dependent manner. Means ± standard deviations are presented (n=3). *P<0.05, ***P<0.001, the differences are statistically significant compared with the control (0 μM flocalin).

Probably, the effect of flocalin is associated with its influence on mitochondrial respiration and, consequently, with energy component of mitochondrial transport required for efflux of potassium ions into the mitochondria.

Therefore, we investigated the functioning of mitoKATP channel using the method for determination of the rate of DNP-induced efflux of potassium ions from rat liver mitochondria. It should be emphasized that this method allows you to register a reversible functioning of ATP-dependent potassium channel, occurring as a result of a sharp decline in mitochondrial membrane potential under the addition of an uncoupling agent. So, it makes possible to determine the channel activity independently of the energy state of the mitochondria [7]. Thus, the efflux of potassium ions in this case occurs on the concentration gradient of ions (the incubation medium lacks potassium ions), and does not depend on the presence of respiratory substrates. Previously, we have shown that the incubation of mitochondria with flocalin at concentrations up to 60 μM did not affect the amount of potassium ions in these organelles.

As can be seen from fig. 3, flocalin at concentrations of 15–50 μM increased the rate of DNP-induced efflux of potassium ions from rat liver mitochondria in a dose-dependent manner.

Discussion

The results show that flocalin affects the parameters of mitochondrial functioning. Its effects on mitochondrial respiration consist in an increasing of V_2 and V_4 rates when α-ketoglutarate is used as substrate, and this occurs in the presence of both potassium and sodium ions in the incubation medium. At the same time, it does not affect V_3 (in the presence of ADP) and the rate of uncoupled respiration (V_{DNF}). When succinate (with rotenone) was used as substrate, flocalin inhibits V_3 respiration rate, which can be typical if mitoK_{ATP} channel is in the open state [9]. The fact that flocalin may facilitate to open mitoK_{ATP} channels in mitochondria is also confirmed by our experiments on the study of DNP-induced efflux potassium

ions from mitochondria, which reflects the reversible activity of this channel. It has been established that flocalin substantially activates DNF-induced potassium transport in the mitochondria. On the other hand, the fact that the effect of the drug is saved under a substitution of potassium ions in the incubation medium mitochondria on sodium ions, can indicate a complex effect of flocalin in the mitochondria. Finally, in this work, it has been also established that flocalin does not significantly affect oxidative exchange of mitochondria.

Conclusion

Thus, the investigation of the molecular mechanism of action of new cardioprotective preparation - flocalin on mitochondrial functions showed that, on the one hand, it possess uncoupled action, and, on the other hand, activates potassium transport in mitochondria through the opening of the ATP-sensetive potassium channel. Both of these properties of the preparation, according to the literature, may be important for the manifestation of its cardioprotective properties when administered to organism [10,11].

This work was supported by grants from the Government of the Russian Federation №14.Z50.31.0028, the Russian Science Foundation №16-15-00157, and from the Russian Foundation for Basic Research №16-04-00692a.

References

1. Burbello A.T., Shabrov A.V., Denisenko P.P. (2006), Modern drugs. ***C***linical and pharmacological directory practitioners. Saint Petersburg, Moscow: Neva, 896 c.
2. Moibenko O.O., Strutynskyi R.B., Yagupolskii L.M. et al. (2009), Sci Innov 1, 80-84.
3. Strutyns'kyĭ R.B., Rovenets' R.A., Neshcheret O.P. et al. (2011), Fiziol Zh. 57(1), 55-65.
4. Denysiuk O.M. (2011), Buk. Med. Herald. 1 (57), 131-134.
5. Mironova G.D. et al. (2007),Vesnik Ross. AMN, 2, 34-43.
6. Jaburek M., Yarov-Yarovoy V., Paucek P., Garlid K. (1998), J. Biol.Chem. 273, 13578.
7. Baranova O. V., Skarga Y. Y., Negoda A. E., Mironova G. D. (2000), Biochem. 65, 218.
8. Ferranti R., Silva M.M., Kowaltowski A.J. (2003), FEBS Letters. 536, 51-55.
9. Akopova O. et al. (2016), Bioenerg. Biomembr., 48, 67-75.
10. Bakeeva L.E. et al. (2008), Biochemistry (Mosc):1288-1299.
11. Garlid et al. (2003), BBA,1606, 1-21.

SPREADING AND PHAGOCYTE MOTILITY IN SPECIES OF DICTYOPTERA

E.A. Grebtsova

Belgorod State University, Pobedy str., 85, Belgorod, 308015, Russia

Cell adhesion to substrate, spreading, taking the specific for this type of cell shape and locomotion may be determined by several elementary cell responses: pseudopodial attachment reactions, contact inhibition of locomotion and reaction of stabilization of surface. Objects that due to the large size can not be phagocytosed, surrounded plasmocytes and / or granulocytes and encapsulated. Reactions

encapsulation and phagocytosis fundamentally similar: cell spreading in the encapsulation can be viewed as an attempt to absorption is too large object [2].

Earlier petaloid (with petal formations), lamellar and filopodia form regarded as different cell types, but after Edds research [3], it's became known that the morphological transformation of one form into another cell due to rearrangements of the cytoskeleton (contact-dependent filopodium transformation after attachment to the substrate).

Insects hemocytes compose the cellular army of their innate immune system. Plasmocytes, putative homologues to mammalian macrophages, and granulocytes in cockroaches, represent, 70% of the migratory hemocyte population in circulation and are responsible for the phagocytosis of bacteria and apoptotic tissues that arise during metamorphosis [1]. It is not known as to how hemocytes become activated from a sessile state in response to such infectious and developmental cues. Hemolymph samples from 7 insect species (Nauphoeta. cinerea, Blaberus craniifer, Gromphadorhina portentosa, Shelfordella tartara, Periplaneta americana, Blatta orientalis, Blatella germanica) were studied within one technique. Hemolymph of adult insects was collected using standard methods. The collected hemolymph incubated in physiological solution, in hypo- and hyper medium, and with cells of Saccharomyces cerevisiae. Hemocytes are motile, phagocytic cells that are present at all stages of the life cycle and represent the cellular component of the animal's innate immune system at postembryonic life stages [5]. The most common cell types are plasmocytes and granulocytes. Accordingly, the main function of post-embryonic hemocytes is to clear infection from invading microorganisms as well as debris from apoptotic cells by performing phagocytosis [4,5]. As a brief description, the most common morphology of untreated hemocytes (incubated in physiological solution for insects) – "normal spread" represented a fully adhered cell with a uniformly protruding and retracting cell membrane (at all angles surrounding the central region). Normal spread represented the quiescent sessile behavior of these hemocytes. The two active morphological classes, "non-polarized" and "polarized", are predominant at medium with S. cerevisiae. Both of "nonpolarized" and "polarized" morphology are typical for granulocytes, and only "non-polarized" characteristic for plasmocytes. Both classes represent a fully adhered cell that exhibits an extremely active cell membrane that protrudes and retracts at varied angles to the cell central region producing multiple membrane ruffles. The essential difference between these two classes is that polarized cells produce a visual lamellopodium and trailing edge during random migration *Ex vivo* hemocytes exhibited 100% normal membrane spread. Rizopodium are uniformly distributed over the surface of the membrane, and their length was no higher 1,5 μm. Both of granulocytes and plasmocytes activity rapidly decreased in hypotonic medium. Over a period of time rizopodium length shorten to 0,6 μm in hypertonic medium. The rate of spreading was decreased considerably. S. cerevisiae addition to hemocytes in physiological solution led to appearance 28% of normal spread granulocytes, 44% – "polarized" and 28% "non-polarized". Among the plasmocytes no some

of polarized, 84% nonpolarized and 16% normal spread cells. Beyond the rhizopodium (which ramification was at the elongation of 1 μm), has came up long filopodium about 3,5 μm in length. Both of pseudopodia types located irregularly on the membrane surface leading in the direction of the yeast cells.

During the spreading fagocytes acquire filo–lamellipodia form. Incubation in a hypertonic medium led to the appearance on the periphery of the cells long thin branching filopodia. With such transformation hemocytes, attached to the substrate, acquire the ring of a circular flattened rim (lamellae), which is 10–15 min up to a maximum diameter. By this time almost all of the cytoplasm with its granules appear in the lamellae. The nucleus hidden in the intact cell by cytoplasmatic inclusions, becomes visible. Cytoplasmic strands of hemocytes are combined in the total net. Aggregation and hemocytes spreading on the substrate can be regarded as the activation of the contact with the predominance of cell-cell contact or cell-substrate and expression *in vitro* protective cellular responses in conditions simulating damage to the body.

References

1. Гребцова Е.А., Присный А.А. Определение мембранного резерва гемоцитов Periplaneta americana и Blaberus craniifer и изучение влияния гипоосмотической нагрузки на объем клеток // «Научные достижения биологии, химии, физики»: материалы международной заочной научно-практической конференции. – Новосибирск: Изд. «Сибирская ассоциация консультантов». – 2012. – 114 с.
2. Dybas L, Fankboner PV. Holothurian survival strategies: Mechanisms for the maintenance of a bacteriostatic environment in the coelomic cavity of the sea cucumber. – Dev. Comp. Immunol. – 1986 – V.10 – P.311-330,
3. Edds, K.T. Dynamic aspects of filopodial formation by reorganization of microfilaments. – J. Cell Biol. – V. 73 – P.479-491
4. Holz A., Bossinger B., Strasser T., Janning W., Klapper R. The two origins of hemocytes in Drosophila. – Development. – 2003– V.130. – P.4955– 4962. 3
5. Lanot R., Zachary D., Holder F., Meister M. Postembryonic hematopoesis in Drosophila. – Dev. Biol. – 2001 – V. 230. – P.243–257.

THE ROLE OF CALPAIN SYSTEM IN ATROPHY OF SKELETAL MUSCLES OF ALCOHOL-FED RATS

Y.V. Gritsyna[1], I.M. Vikhlyantsev[1], N.N. Salmov[1], A.G. Bobylev[1], N.I. Kukushkin[2], Z.A. Podlubnaya[1,3]

[1]Institute of Theoretical and Experimental Biophysics, Russian Academy of Sciences, Pushchino, Moscow region, Russia

[2]Institute of Cell Biophysics, Russian Academy of Science, Pushchino, Moscow region, Russia

[3]Pushchino State Institute of Natural Science, Pushchino, Moscow region, Russia

Chronic ethanol intoxication is known to lead to the development of a symptom complex of alcohol-induced damage in both skeletal (alcoholic myopathy) and cardiac (alcoholic cardiomyopathy) muscles [1]. The development of alcoholic myo-

pathy/cardiomyopathy was shown to be accompanied by the atrophy and weakness of skeletal muscles and deterioration of heart function in humans and animals [2,3]. Reduced total content of RNA, DNA, and proteins (e.g., myosin heavy chains, actin, desmin, and throponin I) [4], as well as decrease in myofibrillar ATPase activity [5] contribute to development of the contractile defects. Molecular mechanisms of the development of alcohol-induced damage in muscles are not completely clear; nevertheless, ethanol and mainly its oxidation product acetaldehyde were shown to be involved in the suppression of protein synthesis via the toxic damage of a number of key components in signal systems, controlling synthesis of protein, in particular, mTOR complexes [6–8].

The calpain system includes 14 different members, plus calpastatin, in those mammals that have been studied carefully [9]. Striated muscle contains significant amounts of the 2 ubiquitous wellcharacterized calpains, the micromolar Ca^{2+}, requiring Ca^{2+}-dependent protease (μ-calpain), and the millimolar Ca^{2+}, requiring Ca^{2+}-dependent protease (m-calpain), and their specific inhibitor, calpastatin. It is suggested that these 2 calpains and calpastatin are involved in turnover of myofibrillar proteins. Apparently, μ- or m-calpains are the main proteases for cleaving a great variety of substrates, including titin, nebulin, troponin, tropomyosin, M-line proteins and other [9], which then are degraded to amino acids by ubiquitin-proteasome pathway [9]. It was shown that acute alcohol intoxication increases mRNA of atrogin-1 and MuRF1 (the muscle-specific E3 ubiquitin ligases) in m. gastrocnemius of rats [10]. The increased level of gene expression of atrogin-1 in plantaris muscle of alcohol-fed rats was observed [11]. In recently conducted research [3] increase of mRNA of MuRF1 and MAFbx/atrogin-1 in m. vastus lateralis of patients in early stages of development of alcohol-induced lesions of skeletal muscles was also detected. Taking into account these data, we hypothesized that prolonged chronic alcohol consumption will increase calpain activity.

In this research changes of expression and proteolitic activity of μ-calpain, as well as calpastatin expression in heart and skeletal (m. soleus, m. gastrocnemius, m. longissimus dorsi) muscles of rats after 3 and 6 mouths of chronic alcoholization were studied. A separate task was a study of changes in content and gene expression of giant sarcomeric proteins titin and nebulin – substrates of calpain proteases.

Materials and methods

Male Wistar rats (150 g ± 5 g) were divided in two groups: “Control” (n = 14) and “Alcohol” (n=14). Animals of alcohol group were alcoholized by method [12] with use of agar blocks during 3 (n=5) and 6 (n=5) months and by method with use of Lieber-DeCarli regular control rat diet during 3 months (n=4). After ending the experiment, *m. soleus*, *m. gastrocnemius*, *m. longissimus dorsi* and cardiac muscle (left ventricles) were used for analysis. Muscle tissue samples were immediately frozen in the liquid nitrogen and subsequently stored at –70°C. Extraction of μ-calpain from muscle tissues was carried out by method [13]. Extraction of calpastatin and GAPDH (reference protein) from muscles was carried out using lysis buffer (12 mM Tris-HCl, 1.2% SDS, 5 mM EGTA, 10% glycerol, 2%

β-mercaptoethanol, 5 μg/mL leupeptin, and E64, pH 6.8–7.0). Protein samples were analyzed in 6.5% (for μ-calpain) and 9.5% (for calpastatin and for GAPDH) polyacrylamide slab gels [14]. Measurements of protein concentration were made by using NanoDrop 1000 (Thermo Scientific, USA), then equal amount of protein (30–45 μg/line) was applied. Transfer of proteins to the PVDF membrane was carried out by the method [15]. Membranes were incubated for 2 h at room temperature with the primary rabbit monoclonal antibodies against μ-calpain (Abcam, 1:4000), calpastatin (Abcam, 1:3000) and GAPDH (Abcam, 1:2000). Secondary antibodies conjugated to alkaline phosphatase (goat antirabbit Ig, Abcam, 1:3000) were used. Substrate solution NBT/BCIP (Roche, Germany) was used to visualize the complex. To detect changes in the isoform composition and the content of titin (2000–3700 kDa) and nebulin (700 kDa), agarose-strengthened 2.2% SDS-polyacrylamide gels [16] were used. In order to prevent destruction of titin at high temperatures [17], the electrophoretic samples were not boiled but incubated at 40°C for 30–40 min [18]. The content of titin and nebulin (relative to the content of myosin heavy chains) as well as μ-calpain, calpastatin, GAPDH was determined by densitometry method (Total Lab v.1.11). Real time PCR was carried out using DT-322 amplifier (DNA-Technology, Russia) with Taq-DNA polymerase (Evrogen, Russia) and SYBR Green I fluorescent dye (Invitrogen). The changes in μ-calpain, calpastatin, titin and nebulin gene expression was determined according to the method $2^{-\Delta\Delta Ct}$ [19]. Housekeeping gene (GAPDH) was used for normalization of all quantitative PCR analysis experiments in the current study. Determination of titin phosphorylation level in muscles of alcohol-fed rats was carried out by the method described in [20]. The results obtained during the experiments were statistically processed using the Mann-Whitney *U*-test with the confidence levels $P \leq 0.01$ and $P \leq 0.05$. The data were represented as $M \pm SD$, where M is the mean value and SD is the standard deviation.

Results and discussion

Our study was to test the assumption about increase of μ-calpain proteolytic activity in rat striated muscles after chronic alcohol consumption. It is known that Western blot analysis of μ-calpain content is one of the methods for assessment of calpain activity. In particular, it was shown, that activation of full-length μ-calpain (80 kDa) involves autolysis to a 78-kDa and then to a 76-kDa protein, with both of these autolysed isoforms being proteolytically active [21]. The results of our Western blot analysis revealed significant increase relative content of autolysed isoform (78 kDa) of μ-calpain in two of the four studied muscles: in *m. gastrocnemius* (by 3,5 times, $P \leq 0.01$) and in *m. soleus* (by 1,47 times, $P \leq 0.05$) of rats fed alcohol for 6 months, but not for 3 months. The obtained results point out an increase of proteolytic activity of μ-calpain in leg muscles of rats after 6-months chronic alcohol consumption and explain the development of atrophy in *m. soleus* (significant decrease of relative weight of the muscle, $P \leq 0.05$). However, similar atrophic changes were not observed in *gastrocnemius* muscle of rats fed alcohol for 6 months. In order to identify this discrepancy, Western blot analysis of calpastatin content in these muscles was conducted. Significant changes of calpastatin

content in *m. soleus* were not revealed, while increase (by 26%, $P \leq 0.01$) of calpastatin content in m. gastrocnemius of alcohol-fed rats was found. These data may explain the absence of atrophy in the *gastrocnemius* muscle of alcohol-fed rats.

It is known that disuse atrophy leads to increased proteolysis of titin and nebulin in m. soleus of human and animals [18]. To find out whether there are similar changes in m. soleus of alcohol-fed rats, SDS-PAGE analysis of titin and nebulin content was conducted. A decrease (by ~10%, $P \leq 0.01$) in the content of intact titin-1 (T1) was detected in this muscle of alcohol-fed rats. These changes were accompanied by increase (by ~48%, $P \leq 0.01$) in the content of proteolytic T2-fragments. Undoubtedly, these changes were consequence of increased proteolytic activity of calpains, in particular, μ-calpain. It should be noted, that decrease in the content of T1 was observed on the background of increased (by ~50%, $P \leq 0.01$) level of its mRNA. The results indicate the predominance of degradation processes in titin over processes of its synthesis in m. soleus of alcohol-fed rats. These data are consistent with our earlier results about the decrease of T1 content in rat soleus after 6-months alcoholization with ethanol-containing (20%) drinking water [22]. No decrease of nebulin content in m. soleus of alcohol-fed rats was revealed. Possibly, it is associated with significant increase (by ~123%, $P \leq 0.01$) of nebulin mRNA level. It may compensate for decrease in nebulin content due to its increased proteolysis. Despite a significant decrease of mRNA levels of titin and nebulin in m. longissimus dorsi and m. gastrocnemius of rats fed alcohol for 6 months, decrease in the content of these proteins was not detected. These data are consistent with results, obtained for gastrocnemius and plantaris muscles of Wistar rats fed ethanol-containing diet for 10 wk [23]. However, in our study a significant increase (by ~45%, $P \leq 0.01$) of T2 content in m. gastrocnemius of alcohol-fed rats was found. The decrease (by ~15%) in nebulin content was also found in some cases, which were accompanied by an appearance on the gel of a duplet band of the protein. The results indicate the predominance of degradation processes in giant proteins over processes of their synthesis in m. gastrocnemius of alcohol-fed rats, although higher calpastatin content probably resulted in a significant reduction of μ-calpain proteolytic activity in this muscle. In heart of control animals and rats fed alcohol for 6 months significant changes neither in titin content, nor in its gene expression were not revealed. Taking into account our data about absence of changes in parameter “heart weight/weight of animal” in alcohol group, we can assume that rat heart is resistant to long-term alcohol intoxication.

Discussing obtained data, it is necessary to pay attention to the fact that increased proteolysis of giant sarcomeric proteins in hind limb muscles of alcohol-fed rats was accompanied by increase of titin phosphorylation level, especially T2-fragments. Similar changes in T1 and T2-phosphorylation levels, accompanied by decrease in T1 content and increase in T2 content were found in mice *gastrocnemius*, atrophied in conditions of real microgravity [24]. It is known, that sensitivity of proteins to proteolysis by μ-calpain is changed depending on level of their phosphorylation [25]. We did not find evidence of changes in sensitivity of titin to proteolysis depending on its level of phosphorylation. However, using monoclonal antibodies to phosphoserine pS26 it was shown that a threefold increase in the de-

gree of phosphorylation of titin PEVK region in quadriceps of patients with the Ehlers–Danlos syndrome was accompanied by insignificant decrease in the content of this protein [26]. Taking into account these data and our obtained results, we assumed that hyperphosphorylation of titin leads to increase its proteolytic degradation by calpains. Undoubtedly, decrease in the content of the giant protein, which maintains highly ordered sarcomeric structure [27], regulates muscle contraction [28], as well as plays an important role in regulation of intracellular signaling processes [29], will cause disturbances in the contractility of atrophied muscles. A negative contribution to decrease of contractility in hind limb muscles of alcohol-fed rats may also be made by increased titin phosphorylation level. This conclusion is based on our *in vitro* studies pointing that an increase of T2 phosphorylation decreases activating effect of this protein on the actin-activating ATPase activity of reconstructed filaments of myosin [30].

As for rats fed alcohol for 3 months (short-term alcohol consumption), we did not reveal significant changes in μ-calpain, calpastatin, titin and nebulin content as well as in expression of genes of these proteins in striated muscles. Significant changes in titin phosphorylation level also were not observed in these muscles. So, we conclude that prolonged chronic alcohol consumption (6 months) resulted in increase in the content of autolysed isoforms of μ-calpain in rat hand limb muscles, to hyperphosphorilation of titin, increase its proteolytic degradation and development of atrophy in *m. soleus*. This is the first results confirming a significant role of μ-calpain in development of negative alcohol-induced changes in muscles.

This work was supported by the Russian Foundation for Basic Research (grants nos. 14-04-00112, 14-04-32240 and 14-04-32171).

References

1. Preedy V.R., Adachi J., Ueno Y., Ahmed S., Mantle D., Mullatti N., Rajendram R., Peters T.J. 2001. Alcoholic skeletal muscle myopathy: definitions, features, contribution of neuropathy, impact and diagnosis. Eur. J. Neurol. 8(6):677–687.
2. Lang C.H., Frost R.A., Summer A.D., Vary T.C. (2005). Molecular mechanisms responsible for alcohol-induced myopathy in skeletal muscle and heart. Int. J. Biochem. Cell. Biol. 37(10):2180–2195.
3. Shenkman B.S., Lomonosova Iu.N., Lysenko E.A., Kazantseva Iu.V., Zinov'eva O.E., Iakhno N.N. (2013). Proteolytic signaling mechanisms in skeletal muscles in patients with alcohol-induced muscle disease. Fiziol. Cheloveka 39(5):112–118.
4. Vary T.C., Deiter G. (2005). Long-term alcohol administration inhibits synthesis of both myofibrillar and sarcoplasmic proteins in heart. Metabolism 54(2):212–219.
5. Reddy Y.S., Beesley R.C. (1990). Effects of acute and chronic ethanol on cardiac contractile protein ATPase activity of Syrian hamsters. Biochem. Med. Metab. Biol. 44(3):259–265.
6. Lang C.H., Frost R.A., Deshpande N., Kumar V., Vary T.C., Jefferson L.S., Kimball S.R. (2003). Alcohol impairs leucine-mediated phosphorylation of 4E-BP1, S6K1, eIF4G, and mTOR in skeletal muscle. Am. J. Physiol. Endocrinol. Metab. 285(6):E1205–1215.
7. Hong-Brown L.Q., Kazi A.A., Lang C.H. (2012). Mechanisms mediating the effects of alcohol and HIV anti-retroviral agents on mTORC1, mTORC2 and protein synthesis in myocytes. World J. Biol. Chem. 3(6):110–120. doi: 10.4331/wjbc.v3.i6.110.

8. Steiner J.L., Lang C.H. (2015). Dysregulation of skeletal muscle protein metabolism by alcohol. Am. J. Physiol. Endocrinol. Metab. 308(9):E699-712. doi: 10.1152/ajpendo.00006.2015. Epub 2015 Mar 10.
9. Goll D.E., Neti G., Mares S.W., Thompson V.F. (2008) Myofibrillar protein turnover: the proteasome and the calpains. J. Anim. Sci. 86(14 Suppl):E19–35. Epub 2007 Aug 20.
10. Vary T.C., Frost R.A., Lang C.H. (2008). Acute alcohol intoxication increases atrogin-1 and MuRF1 mRNA without increasing proteolysis in skeletal muscle. Am. J. Physiol. Regul. Integr. Comp. Physiol. 294(6):R1777–1789. doi: 10.1152/ajpregu.00056.2008. Epub 2008 Apr 9.
11. Otis J.S., Brown L.A., Guidot D.M. (2007). Oxidant-induced atrogin-1 and transforming growth factor-beta1 precede alcohol-related myopathy in rats. Muscle Nerve 36(6):842–848.
12. Lang C.H., Wu D., Frost R.A., Jefferson L.S., Kimball S.R., Vary T.C. (1999). Inhibition of muscle protein synthesis by alcohol is associated with modulation of eIF2B and eIF4E. Am. J. Physiol. 277(2 Pt 1):E268–276.
13. Murphy R.M., Snow R.J., Lamb G.D. (2006). mu-Calpain and calpain-3 are not autolyzed with exhaustive exercise in humans. Am. J. Physiol. Cell. Physiol. 290(1):C116–122. Epub 2005 Aug 17.
14. Laemmli U.K. (1970). Cleavage of structural proteins during the assembly of the head of bacteriophage T4. Nature 227(5259):680–685.
15. Towbin H., Staehelin T., Gordon J. (1979). Electrophoretic transfer of proteins from polyacrylamide gels to nitrocellulose sheets: procedure and some applications. Proc. Natl. Acad. Sci. U S A 76(9):4350–4354.
16. Tatsumi R., Hattori A. (1995). Detection of giant myofibrillar proteins connectin and nebulin by electrophoresis in 2% polyacrylamide slab gels strengthened with agarose. Anal. Biochem. 224(1):28–31.
17. Granzier H.L., Wang K. (1993). Gel electrophoresis of giant proteins: solubilization and silverstaining of titin and nebulin from single muscle fiber segments. Electrophoresis 14(1-2):56–64.
18. Vikhlyantsev I.M., Podlubnaya Z.A. (2012). New titin (connectin) isoforms and their functional role in striated muscles of mammals: facts and supposi-
tions. Biochemistry (Mosc) 77(13):1515–1535.
doi: 10.1134/S0006297912130093.
19. Livak K.J., Schmittgen T.D. (2001). Analysis of relative gene expression data using real-time quantitative PCR and the 2(-Delta Delta C(T)) Method. Methods 25(4):402–408.
20. Borbély A., Falcao-Pires I., van Heerebeek L., Hamdani N., Edes I., Gavina C., Leite-Moreira A.F., Bronzwaer J.G., Papp Z., van der Velden J., Stienen G.J., Paulus W.J. (2009). Hypophosphorylation of the Stiff N2B titin isoform raises cardiomyocyte resting tension in failing human myocardium. Circ. Res. 104(6):780–786. doi: 10.1161/CIRCRESAHA.108.193326. Epub 2009 Jan 29.
21. Murphy R.M., Verburg E., Lamb G.D. (2006) Ca2+ activation of diffusible and bound pools of mucalpain in rat skeletal muscle. J. Physiol. 576(Pt 2):595–612. Epub 2006 Jul 20.
22. Gritsyna Iu.V., Salmov N.N., Vikhliantsev I.M., Ulanova A.D., Sharapov M.G., Teplova V.V., Podlubnaia Z.A. (2013). Changes in gene expression and content of titin (connectin) in striated muscles of chronically ethanol-fed rats. Mol. Biol. (Mosk). 47(6):996–1003.

23. Hunter R.J., Neagoe C., Järveläinen H.A., Martin C.R., Lindros K.O., Linke W.A., Preedy V.R. (2003). Alcohol affects the skeletal muscle proteins, titin and nebulin in male and female rats. J. Nutr. 133(4):1154–1157.
24. Ulanova A., Gritsyna Y., Vikhlyantsev I., Salmov N., Bobylev A., Abdusalamova Z., Rogachevsky V., Shenkman B., Podlubnaya Z. (2015). Isoform composition and gene expression of thick and thin filament proteins in striated muscles of mice after 30-day space flight. Biomed. Res. Int. 2015:104735. doi: 10.1155/2015/104735. Epub 2015 Jan 18.
25. Di Lisa F., De Tullio R., Salamino F., Barbato R., Melloni E., Siliprandi N., Schiaffino S., Pontremoli S. (1995). Specific degradation of troponin T and I by mucalpain and its modulation by substrate phosphorylation. Biochem. J. 308 (Pt 1): 57–61.
26. Ottenheijm C.A., Voermans N.C., Hudson B.D., Irving T., Stienen G.J., van Engelen B.G., Granzier H. (2012). Titin-based stiffening of muscle fibers in Ehlers-Danlos Syndrome. J. Appl. Physiol. (1985). 112(7):1157–1165. doi: 10.1152/japplphysiol.01166.2011. Epub 2012 Jan 5.
27. Udaka J., Ohmori S., Terui T., Ohtsuki I., Ishiwata S., Kurihara S., Fukuda N. (2008). Disuse-induced preferential loss of the giant protein titin depresses muscle performance via abnormal sarcomeric organization. J. Gen. Physiol. 131(1):33–41. doi: 10.1085/jgp.200709888.
28. Niederländer N., Raynaud F., Astier C., Chaussepied P. (2004). Regulation of the actin-myosin interaction by titin. Eur. J. Biochem. 271(22):4572–4581.
29. Voelkel T., Linke W.A. (2011). Conformation-regulated mechanosensory control via titin domains in cardiac muscle. Pflugers Arch. 462(1):143–154. doi: 10.1007/s00424-011-0938-1. Epub 2011 Feb 25.
30. Vikhlyantsev I.M., Podlubnaya Z.A. (2003). Phosphorylation of sarcomere cytoskeletal proteins as an adaptive factor of inhibiting the contractile activity of muscle in hibernation. Biophysics 48(3):471–476.

ISULIN ADMINISTRATION AFFECTS THE RATE OF AROUSAL OF HIBERNATING GROUND SQUIRRELS *Spermophilus undulatus*

D.A. Ignat'ev[1], L.A. Andreeva[1], Z.G. Amerchanov[1], A.I. Anufriev[2], A.E. Alekseev[3,4], O.V. Nakipova[1]

[1]Institute of Cell Biophysics, Russian Academy of Sciences, Institutskaya str. 3, 142292 Pushchino, Moscow region, Russia, 142290

[2]Institute of Biology, Yakutsk Branch, Siberian Division, Russian Academy of Sciences, Yakutsk, Russia, 677891

[3]Institute of Theoretical and Experimental Biophysics, Russian Academy of Science, Institutskaya 3, Pushchino, Moscow Region, Russia,142290

[4]Division of Cardiovascular Diseases, Department of Molecular Pharmacology and Experimental Therapeutics, Stabile 5, Mayo Clinic, 200 1st Street SW, Rochester, MN 55905, USA

Induction of hypometabolic states aimed at reducing the risk of ischemic injuries is considered to be promising in treatments of various metabolic disorders associated with the development of infarction or stroke [Malatesta et al.,

2007; Bouma et al., 2012]. At present, nevertheless, the ability of humans to withstand the hypometabolic traits typical for hibernating animals seems unimaginable [Lee, 2008]. Indeed, during winter hibernating animals are capable of enduring a deep hypothermia with an extremely diminished metabolic activity, which however can be safely recovered to normal levels after arousal [Carey et al., 2003; Andrew et al., 2009; Heinis et al., 2015]. Prototypical hibernating species, ground squirrels *Spermophilus undulates*, at the body temperature close to 0^{o}C survive through the prolong periods of lowered hemodynamics, and following rewarming can restore normal circulation throughout the body without detrimental consequences even for the brain cell functions [Solomonov et al., 1987; Ignat'ev et. al, 1992; Popov, Bocharova, 1992; Drew et al 2001; Drew, 2013]. During arousal the heart rate of hibernating ground squirrels increases from 2–3 to 350–600 beats/min during rising thermogenesis and decreases to 130–160 beats/min at the normal active state. Although the overall mechanism of hibernation remains unresolved, these animals represent a suitable model for studying and development of hypometabolic approaches intended for the recruitment of native protective mechanisms [Carey et al., 2012; Drew, 2013; Quinones et al., 2014; Geiser et al., 2014]. While targeted temperature management is deemed to provide beneficial clinical outcomes [Peberdy et al., 2010], drug-induced deep hypothermia implementing available pharmacological agents in non-hibernating animal species is usually associated with the risk of cardiac arrest. Therefore, further exploring the mechanisms governing induction of native hypometabolic states appears to be urgent to propel novel effective clinical strategies against metabolic disorders, stress and traumas [Boum et al., 2012].

Our previous studies [Nakipova et al., 1997; 2000] in line with data available from literature (i.e. [Wu et al., 2013] for review) suggest the involvement of insulin in regulation of reversible transitions between the metabolic states of hibernators. Plasma insulin levels in hibernating species has been found significantly elevated during fat accumulation in the fall season, before entering deep torpor, and dropped down during December to January [Boswell et al, 1994]. In fact, insulin, accumulated during hibernation states in pancreatic β-cells, can be timely released to secure temporal awakening between bouts of torpor. It has been demonstrated that during these arousals the tissue insulin sensitivity is recovered, and plasma insulin levels can considerably exceeds its levels in blood of active summer animals [Laurila and Soomalainen, 1984; Hoo-Paris et al., 1978, Caster et al., 1984; Florant 1985; Nakipova et al., 2000]. Of note, such reversed type 2 diabetes mellitus-like dysregulation in hibernators reveals that an inherited adaptive mechanism governing their transitions between the metabolic states can rely on the capability to actively tune endocrine system, and thereby lipid and glucose homeostasis [Castex & Hoo-Paris, 1987; Wu et al., 2013].

Suggesting the pivotal role of such homeostatic processes in setting metabolic states we proposed herein to assess the insulin-dependent transition of hibernating ground squirrels from deep torpor to active metabolic state. In this study we have tracked changes in core bogy temperature and heart rates, as

awaking parameters, in response to administration of insulin versus a vehicle in hibernating groups of ground squirrels. Obtained data indicate that in general exogenous insulin slows down the rate of arousal, yet can accelerate exiting from hibernation during later stage of arousal.

Material and Methods

Ground squirrels *Spermophilus undulatus*, of both genders, 500–800 g were recruited to this study. All experiments followed the European Convention for the Protection of Vertebrate Animals used for Experimental and other Scientific Purposes 1986 86/609/EEC. Measurements were performed during the hibernation season from end of December to beginning of January. Arousal were induced on the 4th day of hibernation bouts in a warm room (18–20°C) by I.P. injection of 3U of insulin diluted in 0.7 ml of normal saline. The control group was injected with the same volume of normal saline. Changes in body temperature (T_b) were monitored in the middle intestine using a RST 1Q307 thermometer (Switzerland) that provides ±0.1°C measurement accuracy. Cardiac rhythms were recorded using ЭЭГП4-02 with two electrodes placed percutaneously in near fore leg and above scapula. Heart rate and T_b were estimated each 4 min following the injections. Some animals were decapitated during different arousing stages to directly measure temperature in the heart region (T_h). Blood samples were collected during torpor at T_b = 3–5°C, as well as during arousal at T_h = 20–22°C and 28–32°C that corresponded T_b 10–12°C и 18–20°C [Ignat'ev et. al, 2001] and in active state between bouts under fasting conditions. Statistical analysis was performed using the Microcal Original 5.0 software. Results are expressed as mean ± SEM. Student's *t*-test was used to define *P* values, which at $P < 0.05$ was considered statistically significant.

Results and Discussion

Administration of external insulin or saline in hibernating ground squirrels resulted in arousal of animals in both experimental groups. Following injections, during the first stage (T_b < 10–12°C) the measured parameters were not differ in both animal groups. During the second stage, that is characterized by rising thermogenesis (T_b >13°C), in insulin-treated animals the elevation of heart rates and T_b was significantly delayed and the duration of this stage was estimated at ~ 110 min compared to 80 min in control group (n = 5). However, at T_b >20°C insulin-treated ground squirrels exhibited the elevated rates of changes in heat rate and Tb compared to control. The duration of this stage was reduced to 40 min compared to 60 min of the control value (n = 5).

It has been demonstrated that during periods of hibernation blood glucose was not regulated by insulin, but pharmacological doses of glucagon could increase blood glucose concentrations [Castex & Hoo-Paris, 1987]. Our measurements in hibernating ground squirrels reviled nominal levels of blood glucose at 5.6 ± 0.7 mmol/L (n = 10), typical for fasting conditions, while during arousal it drastically increased up to 10.5 ± 1.4 mmol/L (n = 6) at the T_b > 13–15°C (T_h > 28–30°C), which appears to be critical in supporting the active tissue rewarming by carbohydrate substrates. Concomitantly, insulin levels increased from 11.7 ± 1.8 μU/ml, n = 8 under hibernation state to 21.4 ± 1.2 μU/ml, n = 2 during the

initial stage of rewarming (T_b 10–12°C, T_h 18–20°C; $P<0.05$) that was followed by a gradually decrease of glucose levels with the T_b approaching euthermic values [Castex & Hoo-Paris, 1987]. Of note, the respiratory ratio (RER) in arousing ground squirrels at the initial stage of rewarming was found around 0.7 pointing towards fat as the major energy metabolite, which, following increase of T_b, yielded a mixture of fat and carbohydrates fuel. The critical demand of blood glucose appears to be occurred at T_b > 25–30°C, when blood insulin levels in natively arousing ground squirrels reached maximal values at 34.5 μU/ml, n = 7, and RER approached 1, indicating that carbohydrate became the predominant fuel source.

According to these findings, the administration of external insulin in this study may decelerate the awakening progression by stabilizing blood glucose at lower levels. It is feasible to suggest that the insulin-induced hypoglycemia would limit the glucose availability necessary for the rewarming organism program in line with the special role of glucose signaling and anaerobic energetic during the stages of arousal [Andrew at al., 2009]. The excess of insulin, among other mechanisms, can trigger UDP glucosyltransferase-dependent glycogen synthesis in liver that would counteract the glucagon-dependent mobilization of the glycogen stores and, thereby, glucose production. However, on the latest stage the remaining external insulin would promote blood glucose utilization as has been seen with the acceleration of changes of heart rates and T_b beyond 25°C at the maximal RER values. Furthermore, while insulin had no effect on contractility of papillary muscles of ground squirrels at low T_h during arousals, it induced a significant inotropic effect at T_h around 33–35°C (Nakipova et al., 2000).

Hence, this study demonstrates that the remarkable plasticity of the endocrine system of hibernators ensures the timing regulation of glucose homeostasis in adaptive metabolic program governing the transitions of hibernating animals between the metabolic states.

This study was partly supported by the Russian Foundation for Basic Research (project №13–04–01234а).

The work is dedicated to the memory of Stella Germanovna Kolaeva, an inspired researcher into the phenomena of winter hibernation.

References

Andrews, M., Russeth, K., Drewes, L., & Henry, P. Adaptive mechanisms regulate preferred utilization of ketones in the heart and brain of a hibernating mammal during arousal from torpor. American Journal of Physiology. 2009;296,R383–R393.

Boswell T, Woods SC, Kenagy GJ. Seasonal changes in body mass, insulin, and glucocorticoids of free-living golden-mantled ground squirrels. Gen. Comp. Endocrinol. 1994 Dec;96(3):339-46.

Bouma HR, Verhaag EM, Otis JP, Heldmaier G, Swoap SJ, Strijkstra AM, Henning RH, Carey HV. Induction of torpor: mimicking natural metabolic suppression for biomedical applications. J Cell Physiol. 2012 Apr;227(4):1285-90.

Carey HV, Andrews MT, Martin SL. Mammalian hibernation: cellular and molecular responses to depressed metabolism and low temperature. Physiol Rev. 2003 Oct;83(4):1153-81.

Carrey HV, Martin SL, Horwitz BA, Yan L, Bailey SM, Podrabsky J, Storz JF, Ortiz RM, Wong RP, Lathrop DA. Elucidating nature's solutions to heart, lung, and blood diseases and sleep disorders. Circ Res. 2012 Mar 30;110(7):915-21.

Castex C, Hoo-Paris R. Regulation of endocrine pancreas secretions (insulin and glucagon) during the periodic lethargy-waking cycle of the hibernating mammal. Diabete Metab. 1987, 13:176-81.

Castex C, Tahri A, Hoo-Paris R, Sutter BC. Glucose oxidation by adipose tissue of the edible dormouse (Glis glis) during hibernation and arousal: effect of insulin. Comp Biochem Physiol A Comp Physiol. 1987, 88:33-6.

Drew K. Raising the 'dead' - reperfusion from Torpor. J Exp Biol. 2013 Mar 15;216(Pt 6):927-9.

Drew K.L., Rise M.T, Kuhn T.B., Smith M.A. Neuroprotective adaptations in hibernation: therapeutic implication for ischemia-reperfusion, traumatic brain injury and neurodegenerative diseases. Free Radic. Biol. Med. 2001; 31:563-573

Florant GL, Lawrence AK, Williams K, Bauman WA. Seasonal changes in pancreatic β-cell function in euthermic yellow-bellied marmots. Am J Physiol. 1985;249:R159–R165.

Geiser F, Currie SE, O'Shea KA, Hiebert SM. Torpor and hypothermia: reversed hysteresis of metabolic rate and body temperature. Am J Physiol Regul Integr Comp Physiol. 2014 Dec 1;307(11):R1324-9.

Heinis FI, Vermillion KL, Andrews MT, Metzger JM. Myocardial performance and adaptive energy pathways in a torpid mammalian hibernator. Am J Physiol Regul Integr Comp Physiol. 2015 Aug 15;309(4):R368-77.

Hoo-Paris R, Castex Ch, Sutter BC. Plasma glucose and insulin in the hibernating hedgehog. Diabete Metab. 1978, 4:13-8.

Ignat'ev DA; Sukhova GS, Sukhov VP The dependence of the heart rate of the Yakutian long-tailed ground squirrel Citellus undulatus from the ambient temperature. J Evol Biochem Phys. 1992; 28(5):582-90.

Ignat'ev DA; Sukhova GS, Sukhov VP Analysis of changes in the heart rate and body temperature of the ground squirrel Citellus Undulatus in different physiological states. Zh Obshch Biol. 2001; 62(1):66–67.

Laurila M, Soomalainen P. Studies in the physiology of the hibernating hedgehog. The changes in the insulin level induced by seasons and hibernation cycle. Ann Acad Sci Fenn Biol. 1974, 0:1-40.

Lee CC. Is human hibernation possible? Annu Rev Med. 2008;59:177-86.

Malatesta M, Biggiogera M, Zancanaro C. Hypometabolic induced state: a potential tool in biomedicine and space exploration. Rev Environ Sci Biotechnol 2007, 6: 47–60.

Nakipova OV, R Z Gaĭnullin, V G Safronova, L S Kosarskiĭ, B F Bakaneva, D A Ignat'ev, Z G Amerkhanov, S G Kolaeva, N I Kukushkin, N G Solomonov The action of insulin on cardiac contractility in active, hibernating and arousing susliks Citellus undulatus. Biofizika 01/1997; 42(6):1297-300.

Nakipova OV., Gainullin RZ., Andreeva LA., Safronova VG., Kosarski LS., Kolaeva SG., Solomonov NG., Kukushkin NI. Effect of insulin on the myocardium of the active, hibernating and awakening Ground squirrels Citellus undulatus. Biophysics, 2000, 45(2): 335-342.

Peberdy MA, Callaway CW, Neumar RW, Geocadin RG, Zimmerman JL, Donnino M, Gabrielli A, Silvers SM, Zaritsky AL, Merchant R, Vanden Hoek TL, Kronick SL. Part 9: post-cardiac arrest care: 2010 American Heart Association Guidelines for

Cardiopulmonary Resuscitation and Emergency Cardiovascular Care. Circulation. 2010, 122(18 Suppl 3):S768-86.
Popov V.I., Bocharova L.S. Hibernation-induced structural changes in synaptic contacts between mossy fibers and hippocampal pyramidal neurons // Neuroscience. 1992. V. 48. № 1. P. 53-60.
Quinones QJ, Ma Q, Zhang Z, Barnes BM, Podgoreanu MV. Organ protective mechanisms common to extremes of physiology: a window through hibernation biology. Integr Comp Biol. 2014 Sep;54(3):497-515.
Solomonov NG, Ahremenko AK, Anoufriev AI. The dynamics of the energy substrates in the tissues of awakening ground squirrels. Mechanisms of hibernation. Pushchino: ONTI PSC. 1987, pp 48-56.
Wu C-W, Biggar KK, Storey KB. Biochemical adaptations of mammalian hibernation: exploring squirrels as a perspective model for naturally induced reversible insulin resistance. Braz J Med Biol Res. 2013, 46:1-13.

THE MOLECULAR MECHANISMS OF REGULATION OF ACTIN-MYOSIN INTERACTION BY TROPONIN-TROPOMYOSIN COMPLEX DURING THE ATPASE CYCLE. POLARIZED FLUORESCENCE STUDY

O.E. Karpicheva[1], S.V. Avrova[1], N.A. Rysev[1], N.V. Kuleva[2], C.S. Redwood[3], Y.S. Borovikov[1]

[1]*Laboratory of Mechanisms of Cell Motility, Institute of Cytology RAS, Tikhoretsky Av., 4, St. Petersburg,194064, Russia*
[2]*Saint Petersburg State University, Universitetskaya nab., 7-9, Saint Petersburg, 199034, Russia*
[3]*University of Oxford, John Radcliffe Hospital, Oxford OX3 9DU, United Kingdom*

It is known that contraction of striated muscles is initiated by the increase in calcium concentration within the muscle cell. The sensor of calcium concentration is a component of thin filaments, troponin, which undergoes conformational rearrangements resulting in a shift of the position of tropomyosin on F-actin. Depending on its location TM prevents or allows strong interaction of the myosin heads with actin. We have studied the molecular mechanisms by which troponin–tropomyosin regulates actin-myosin interaction in the ATPase cycle using fluorescent probes specifically bound to Cys36 or Cys190 of α- or β-tropomyosin, Cys707 of myosin subfragment-1 (S1) and Cys374 of actin or in the groove, in the region of the contacts between adjacent actin subunits. The fluorescently labeled proteins were incorporated into a single ghost muscle fiber to measure the polarized fluorescence in the absence or presence of Ca^{2+}, nucleotides and analogs of ATP. Analysis of the data allows us to determine the angles of orientation of emission (Φ_E) and absorption (Φ_A) dipoles, the mobility of the fluorescent probes (N) and the flexibility of the thin filaments ($\theta_{1/2}$) in each simulated state of the ATPase cycle.

It was observed that during the simulation of transition from the weak- to strong-binding stages of the ATPase hydrolysis cycle in the absence of troponin the value of Φ_E (or Φ_A) increases for 1,5-IAEDANS-labeled actin and for 5-IAF-

labeled tropomyosin, and decreases for FITC-phalloidin-labeled actin and for 1,5-IAEDANS-labeled S1. These changes in the parameters were interpreted as showing, respectively, the rotation of actin subdomain 1 from the filament axis to the periphery, the shifting of the tropomyosin strands towards the inner domain of actin (to the open position), and the tilt of actin monomers and the myosin motor domain towards the filament axis.

Troponin modulates these spatial rearrangements in a Ca^{2+}-dependent manner. At high Ca^{2+}, troponin–tropomyosin causes the additional rotation of actin subdomain 1 to the periphery of the thin filaments switching some extra actin monomers on, and increases the area of stereospecific interactions between actin and myosin. This favors the formation of the strong-binding states of actin–S1 and thus increases the efficiency of the actomyosin motor. At low Ca^{2+}, troponin–tropomyosin complex, on the contrary, inhibits the work of actomyosin motor, restricting the myosin-induced movement of tropomyosin and switching a part of the actin monomers off.

The application of the mutant tropomyosins in polarized fluorescence study provides new data about the molecular mechanisms of muscle contraction. It appeared that local changes in the surface charge of tropomyosin or altered bending of tropomyosin coiled coil can disorder the concordant conformational changes of actomyosin system. The different point mutations in tropomyosin associated with inherited forms of myopathies are able to decrease or increase the amount of the strongly bound myosin heads and switched on actin monomers by shifting the tropomyosin strands towards the open or closed position. The abnormal behavior of tropomyosin and the defective response of actomyosin system during the ATPase hydrolysis cycle is likely to underlie the muscle dysfunction in inherited skeletal and cardiac myopathies.

This work was supported by the Russian Foundation for Basic Research (grants No. 14-04-00454, 16-34-00865).

A NOVEL MODEL OF CONCERTED REGULATION OF MYOSIN II ACTIVITY IN ENDOTHELIAL CELLS

O.A. Kazakova, A.Y. Khapchaev, M.V. Samsonov, V.P. Shirinsky
Institute of Experimental Cardiology, Russian Cardiology Research and Production Center, Moscow, 121552, Russia

Regulation of endothelial cell barrier function is an important fundamental and therapeutic task. Actomyosin activity contributes to an increase in endothelial monolayer permeability. Myosin light chain kinase (MLCK), Rho-kinase (ROCK), and myosin light chain phosphatase (MLCP) are believed to be the main regulators of myosin II in endothelial cells. However, there is a controversy concerning time- and / or stimulator-specific contribution of these enzymes in the development of endothelial monolayer permeability. In this study, we utilized an inhibitor analysis approach to quantify the contribution of MLCK and ROCK in thrombin-dependent myosin II phosphorylation in EA.hy926 human endothelial cell line.

In EA.hy926 cells, thrombin elicited a biphasic permeability of FITC-dextran: during the first 20 min, we observed a rapid increase in permeability followed by a reversal to the basal permeability values. ROCK inhibitor Y27632 or MLCK peptide inhibitor PIK2 attenuated the response to thrombin indicating pivotal roles of both ROCK and MLCK in the development of endothelial monolayer permeability.

For quantitative analysis of myosin II regulatory light chain (RLC) phosphorylation dynamics in cells, we used in-vitro phosphorylated purified RLC as a reference standard to obtain calibration curves for RLC phosphorylation measurements by the Western blot technique with phosphospecific antibodies that discriminate between monophosphorylated at Ser 19 RLC and diphosphorylated at Thr 18 and Ser 19 RLC (P-RLC and PP-RLC). The quantitative analysis demonstrated that in EA.hy926 cells, basal P-RLC is 29± 4%, basal PP-RLC level is 30±3%. In 20 min after treatment with thrombin, we observe a minimum in P-RLC (17±2 %), and a maximum in PP-RLC (65±7 %). Within the following hour, the level of P-RLC slowly decreases to 25±3 % and the level of PP-RLC decreased to 53±6 %.

Under resting conditions, MLCK inhibitors, ML-7 or PIK2, decreased the portion of P-RLC and PP-RLC to 15±3 % and 30±4 %, respectively, indicating a role for alternative myosin kinases, e.g. ROCK. In the presence of Y27632, an inhibitor of ROCK, the basal P-RLC content dropped to 11±1.5 %; PP-RLC were undetectable under these conditions. These data suggest that in EA.hy926 cells, ROCK is exclusively involved in PP-RLC production and appears more readily generate PP-RLC using P-RLC as a substrate.

Microcystin, an inhibitor of type 1 and 2A phosphatases, was applied to evaluate the contribution of MLCP in thrombin-induced myosin phosphorylation. While P-RLC were undetectable in the presence of microcystin, PP-RLC rised to 60±5 % as soon as 10 min after thrombin administration and proceeded to increase further up to 97±4.5 %. Simultaneous treatment of EA.hy926 cells with MLCK inhibitor ML-7 and microcystin attenuated the rate of thrombin-induced PP-RLC accumulation but did not affect maximum PP-RLC level attained (99±4.8 %).

Collectively, our data allow suggesting a novel model of the thrombin-induced myosin II activity regulation by a concerted action of MLCK, ROCK, and MLCP in EA.hy926 cells. In this cell line, both MLCK and ROCK produce P-RLC, however, ROCK is the primary protein kinase to generate PP-RLC. After stimulation with thrombin, MLCK converts RLC into P-RLC, which further serves as a substrate for ROCK to yield PP-RLC. As a result, in this collaborative manner, within 20 min after thrombin stimulation, higher levels of PP-RLC are achieved. By this time-point, MLCP activity starts to prevail. It results in slow RLC dephosphorylation that correlates with the recovery in FITC-dextran basal permeability levels.

Supported by RFBR grant 14-04-32039 to OAK.

FROM POLYMORPHISM OF CONTRACTILE SYSTEMS TO THE ROLE OF CYTOSKELETON IN SIGNAL TRANSDUCTION (IN MEMORY OF PROFESSOR G.P. PINAEV)

S.Yu. Khaitlina

Institute of Cytology RAS,
Tykhoretski av., 4, St.Petersburg, 194064, Russia

Nowadays studies on muscle and cytoskeleton proteins are not separated as different fields of science but are closely interrelated in the field of Biological Motility. This integration had been accepted, however, only about 20–25 years ago, and professor G.P. Pinaev was one of a few "muscle people" of that time who promoted this process. Already the first G.P. Pinaev's works revealed essential difference in the physical-chemical properties of actomyosin and actin isolated at successive stages of rabbit skeletal muscle myogenesis [Pinaev, 1965; Pinaev, Khaitlina, 1972; Khaitlina, Pinaev, 1976], probably due to replacement of cell-specific proteins of actomyosin complex by the muscle-specific isoforms. Indeed, with appearance of isoelectric focusing, multiple isoforms of actin had been found in a variety of mammalian cell lines and tissues, with four "muscle isoforms" distinguished from the two "nonmuscle" actins (reviewed in [Rubenstein, 1990]). Further development of these studies showed that synthesis of specific actin isoforms is accompanied by their subcellular compartmentalization, with both processes being regulated by factors of cell proliferation and differentiation. Actin isoforms cannot substitute for each other, and the high-level synthesis of exogenous actins leads to alterations in cell organization and morphology. This indicates that the highly conserved actins are functionally specialized for the tissues in which they predominate, and the difference in their properties correlates with the dynamics of actin microfilaments versus the stability of myofibrillar systems (reviewed in [Khaitlina, 2001; 2007]). Actin isoforms differ in the rate of polymerization [Prochniewicz, Yanagida, 1993; Khaitlina, 1986; Khaitlina et al., 1999; Rubenstein et al., 2010] and their efficiency to stimulate ATPase activity of non-sarcomeric myosins [Muller et al., 2013]. Furthermore, development of specific antibodies against cellular actin isoforms revealed different functional activity of β- and γ-cytoplasmic actins in tumur cells, including the most recent data demonstrating tumor promotion by γ-actin and suppression by β-actin isoforms [Dugina et al., 2015].

Two other directions of G.P. Pinaev's studies on polymorphism and dynamics of the contractile system involve specificity of the contractile systems in different muscles and reorganization of the contractile system during cardiac myogenesis. The presence of numerous minor proteins in muscle tissues of bivalve mollusks was documented [Margulis, Pinaev, 1977], and specificity of some molluscan proteins was shown [Shelud'ko et al., 1978; Tskhovrebova et al., 1981; Khaitlina et al., 1982]. With time, these initial studies led to a systematic investigation of the mechanisms underlying catch-type contraction of molluscan smooth muscles. To start with, the ability of twitchin, a titin-like giant protein of molluscan catch muscles, to interact with F-actin was found. The twitchin-actin interaction

was shown to be regulated by twitchin phosphorylation. These data suggested that the catch muscle twitchin might provide a mechanical link between thin and thick filaments, which contributes to catch contraction [Shelud'ko et al., 2004]. Phosphorilation was found to regulate interactions with actin and myosin of other molluscan catch muscle protein, myorode, localized on the surface of thick filaments together with twitchin and myosin [Matusovsky et al., 2011]. These findings, together with the new data on the properties of molluscan snooth muscle calponin-like [Dobrzhanskaya et al., 2013] and troponin-like (Vyatchin et al., 2015] proteins, not only unveil mechanisms of catch contraction, but also raise important questions of whether contractile proteins isolated from different muscle tissues are compatible in the model experiments [Shelud'ko et al., 2015].

Another attractive model to elucidate the mechanisms regulating assembly and function of contractile systems turned out to be reorganization of myofirbrillar apparatus during cardiac myogenesis. During long-term cultivation of rat neonatal cardiomyocytes, their contractile system undergoes a reversible conversion of typical myofibrils into stress-fiber-like structures leading to the loss of contractility [Borisov et al., 1989]. This conversion is accompanied by production of extracellular matrix (ECM) which typically is not produced by cardiomyocytes [Bildyug, Pinaev, 2013, Bildyug et al., 2016] as well as by switching of actin isoforms. Thereby the appearance of α-smooth muscle actin precedes the conversion of myofibrils into structures of non-muscle type, while a gradual accumulation of ECM proteins corresponds to the α-smooth muscle actin disappearance. These results indicate that the enhanced expression of α-smooth muscle actin may be induced by the lack of extracellular matrix, whereas the accumulation of the appropriate matrix may be a signal for cardiac isoform re-expression [Bildyug et al., 2016].

Further studies on cultivated cells confirmed a strong effect of extracellular matrix proteins on rearrangements of actin cytoskeleton also in non-muscle cells suggesting relationship between specific ligand-receptor interactions and cytoskeleton organization [Are et al., 1999]. The following experiments showed that RelA/p65 subunit of transcription factor NF-kappaB, an inductor of a variety of cellular genes, interacts with actin-containing structures. Moreover, a direct binding of p65 to F-actin was demonstrated by affinity chromatography [Are et al., 2000]. Re-distribution of RelA/p65 was shown to follow the stress-fibers restoration upon cell adhesion to fibronectin or their disassembly in response to cytochalasin D treatment, when a part of RelA/p65 pool was preserved in a very tight association with actin-rich structures, while the other part of RelA/p65 pool was simultaneously translocated into nucleus [Bolshakova et al., 2013; 2015]. In addition, alpha-actinin-4 was shown to enhance RelA/p65-dependant expression of several genes, although actin-binding domains of alpha-actinin-4 were not critical for the RelA/p65 nuclear translocation and co-activation of RelA/p65-dependent transcription [Aksenova et al., 2013]. These studies are in progress now to clarify a special regulatory role of the cytoskeleton in NF-kB stimulation.

It is tempting to complete this overview of the G.P. Pinaev's scientific activity with a short description of the experiments that would lead us back to the

mechanisms of actin assembly and its regulation. It was found that, in non-muscle cells, tropomyosin, albeit mostly connected with stress-fibers and bundles of actin filaments, is also present in specific particles ('dots') (Hilbert et al., 2006). Stimulation of cells with growth factors induces a rapid, actin polymerization-dependent outgrowth of lamellipodia and filopodia, which is accompanied by a decrease in the number of tropomyosin-containing particles, suggesting their possible involvement in actin filament formation [Grenklo et al., 2008]. Along with actin and tropomyosin, the isolated particles contain myosin-9 [Bobkov et al., 2012] that seems to co-precipitate in the complex with tropomyosin [Bobkov et al., submitted]. These studies are also in progress.

Supported by RFBR grant 14-04-00316.

NOVEL INSIGHTS INTO MOLECULAR ANATOMY OF LONG MYOSIN LIGHT CHAIN KINASE

A.Y. Khapchaev, V.P. Shirinsky

Institute of Experimental Cardiology, Russian Cardiology Research and Production Center, Moscow, 121552, Russia

High and low molecular weight myosin light chain kinases (long MLCK and short MLCK, respectively) are highly specialized enzymes to phosphorylate Ser^{19}/Ser^{19}, Thr^{18} of myosin II regulatory light chain (RLC). MLCK isoforms are involved in a large variety of cellular motile events and show different developmental and tissue distribution as well as localization in cells. Both MLCKs are believed to reside on actin-containing filaments, however localization in different cell types may be dependent on the relative abundance of actin-containing stress fibers. In short MLCK, three DFRxxL motifs at the very N-terminus of the enzyme are responsible for its binding to actin. Long MLCK shows higher affinity to actin-containing filaments both *in vitro* and in cells due to two additional DF/VRxxL motifs and additional amino acid sequence(s) present in the unique N-terminal extension of long MLCK. Recent studies have confined the N-terminal actin-binding site to two IgG-like domains while the first IgG-like domain retained a reduced ability to bind actin. Moreover, for long MLCK, there is a growing list of protein partners, which may serve to target long MLCK to specific areas in non-muscle cells. Still, there are large gaps in our understanding of the long MLCK domain structure and molecular mechanisms that are involved in regulation of MLCK-partner interactions in cells and direct MLCK to subcellular compartments where MLCK enzymatic and/or scaffolding activity is needed.

In this study, we attempted to gain further insights into molecular anatomy of long MLCK by using long MLCK truncation mutants to investigate their contribution in MLCK subcellular localization. In CV-1 cells, full-length EGFP-tagged long MLCK localized to stress fibers. However, truncated EGFP-tagged ΔN245-long MLCK, which lacks two N-terminal IgG-domains involved in actin binding, showed a significant reduction in its actin-binding properties. Instead, ΔN245-long MLCK readily redistributed to a submembrane compartment and accumulated in focal adhe-

sions. Moreover, as revealed by imaging of living transfected CV-1 cells, ΔN245-long MLCK induced multiple podosomes. Interestingly, a FLAG-tagged MLCK fragment consisting of two IgG-like domains also demonstrated a reduced binding to stress fibers and redistributed to the submembrane compartment. However, in this case, no active podosome formation was evident. Collectively, our findings demonstrate that several distinct MLCK actin-binding domains should play in concert to provide for a stress-fiber residence of long MLCK and override the effects of distinct active sequences that target MLCK to other partners / localization. These findings are inconsistent with the widely accepted model, which assumes that long MLCK is tightly bound to actin through its DFRxxL-domains, while its N-terminal domain may search for transient interactions with other actin filaments or microtubules. The relative affinities of actin-binding regions of long MLCK to microfilaments may vary within the context of full-length MLCK and, perhaps, depend on type of cells, in which long MLCK is expressed.

Our results provide a rationale for further elucidation of mechanisms of fine-tuning MLCK transient localization (and activity) in cells through regulation of MLCK affinity to actin and/or other protein partners. For a cell, one possible way of such regulation is by means of posttranslational modifications. Indeed, recently we demonstrated that long MLCK N-terminal actin-binding site might be a subject for Ser / Thr phosphorylation-dependent regulation. Additionally, in this study, we found that upon in-vitro phosphorylation at Ser^{25} and Thr^{56}, recombinant human short MLCK DFRxxL-domain demonstrated reduced ability to bind and bundle filamentous actin *in vitro*.

Thus, it is tempting to hypothesize that phosphorylation might represent a "switching mechanism" to regulate long MLCK partnership in cells. We suggest that in attempts to identify regulatory sites, it is reasonable to rely on MLCK phosphorylation discovered *in vivo* by mass-spectrometry techniques.

Supported by RFBR grant 16-04-01742 to AYK.

INFLUENCE OF ORGANOSELENIUM COMPOUNDS ON FUNCTIONING OF RAT LIVER MITOCHONDRIA

N.V. Khmil[1,2], A.A. Mosencov[2], T.N. Ovsyannikova[2], V.D. Dyachenko[3], M.S. Goncharenko[2], O.V. Kolomytkin[1], G.D. Mironova[1]

[1]*Institute of Theoretical and Experimental Biophysics RAS, Pushchino, Russia*

[2]*Vasyl Karazin Kharkiv National University, Kharkiv (Ukraine)*

[3]*Taras Shevchenko Lugansk National University, Lugansk (Ukraine)*

It has been determined that 80% of population in Russia lack selenium [1,2]. At the same time, the problem of diseases caused by deficit of selenium, and as a result the development of oxidative stress in patients, has been left unsettled. The data shows that various organoselenium compounds are able to demonstrate antitoxic, antibacterial, antioxidant, anantiviral, antiarrhythmic and fungicidal ac-

tivity. During the past few years, a number of laboratories have synthesized the organic forms of selenium with the purpose of preventing deficit of selenium and other diseases. In the recent decade, several selenium-containing compounds have been synthesized at the Taras Shevchenko Luhansk National University [3–5]. It has been shown that some of them can be of strong antioxidant effect [6,7]. It is known that the positive effect of antioxidants is achieved through their ability to remove excessive peroxide: up to 85–90% of peroxide are formed in the electron transport chain of mitochondrion. Thereby, the relationship study between the structure and biological activity of these compounds and their influence on energy and oxidative metabolism in the mitochondria undoubtedly is of interest.

Thus, the aim of this work was to study and compare the influence of six different selenium-containing newly synthesized compounds on respiratory and phosphorylation parameters, as well as on the concentration of peroxide lipids in liver mitochondria of rats.

Materials and Methods

In this work, we have compared the activity of six different selenium-containing compounds, which have been coded as DVD 14, DVD 13, DVD 12, DVD 11, DVD 10, DVD 7. The following two parameters have been used to study the influence of organoselenium compounds on mitochondria functioning: the respiration rates and the amount of peroxide lipids produced in mitochondria after addition of these compounds. Respiration of mitochondria was measured by the polarographic method using polarograph OROBOROS Oxygraph-2k, Austria. The succinate+glutamate were used as the respiration substrates. The amount of peroxide lipids was measured by the production of malondialdehyde (MDA) after addition of thiobarbituric acid. The molar extinction coefficient of MDA/thiobarbituric acid complexis is $\varepsilon = 1{,}56 \cdot см^{-1} \cdot мМ^{-1}$ [Stalnaya, Garishvili, 1977].

The study of oxidative phosphorylation parameters of rat liver mitochondria after addition of organoselenium compounds revealed that 6 of used compounds only DVD 10 and DVD 7 provided uncoupling action, at the same time, DVD 10 was of strongest effect (see table 1 and fig. 1).

Results

It has been found that two drugs: DVD 10 and DVD 7 have an uncoupling effect, as they increase V2 and V4. However, DVD 7 has a much smaller effect than DVD 10. Other four drugs have no effects on the coupled respiration of rat liver mitochondria.

The rates of V_2; V_3; V_4; VDP were measured in ng-atom O/min·mg; ΔT was measured in sec.; ADP/O was measured in micmol/ng-atom O. The substrates of mitochondrial respiration – 5 mM succinate + 2.5 mM glutamate. Incubation medium of mitochondria contains: 110 mM sucrose, 60 mM KCl, 20 mM Hepes, 3 mM KH_2PO_4, 3 mM $MgCl_2$, 0.5 mM EGTA, 0.5 mM DTT, pH 7.1. The concentration of mitochondrial protein was 1 mg/ml. Selenium derivatives were administered at a concentration of 28.6 μM during determination of respiration rate. This rate was designated as $V_{2Se.}$ Other respiratory rates, besides control experiments, were determined on a background of entered selenium derivatives.

Table 1. Effect of selenium derivatives (SP) on the respiration of rat liver mitochondria

№	SP	V_2	V_{2Se}	V_3	V_4	V_{DNP}	ΔT	ADP/O
1	Control	10,83	10,72	49,48	13,08	78,75	157,23	1,74
2	DVD 7	11,38	20,78	47,84	24,87	64,25	206,00	1,30
3	DVD 10	10,09	27,40	48,91	26,50	59,48	250,67	1,09
4	DVD 11	11,03	11.07	44,06	15,04	76,29	188,00	1,61
5	DVD 12	11,50	11.42	49,01	14,02	78,70	157,00	1,70
6	DVD 13	11,50	11.47	41,67	15,13	70,40	171,00	1,83
7	DVD 14	11,21	11,25	49,44	14,17	71,46	151,00	1,78

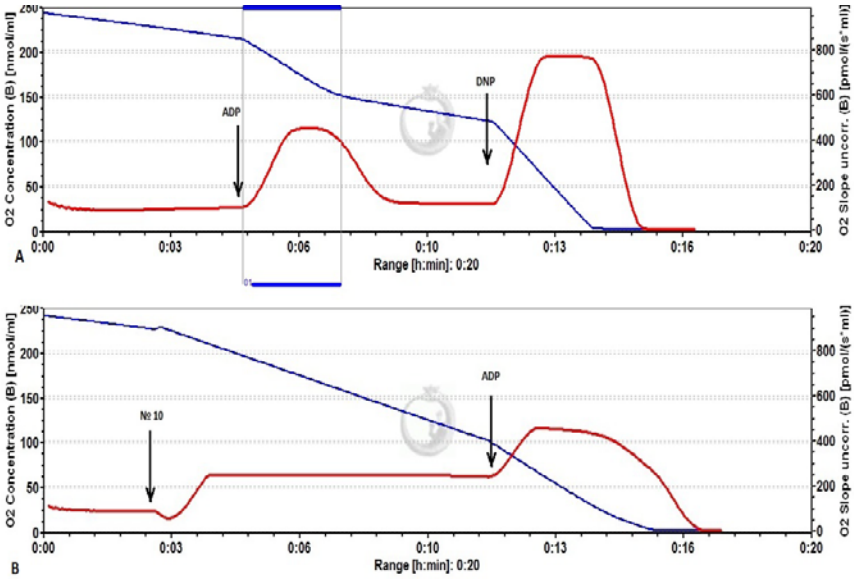

Fig. 1. A typical curve of oxygen consumption by rat liver mitochondria with 5 mM succinate + 2.5 mM glutamate as the substrates. The conditions were as in table 1. A-controle rats, B-with addition 28.6 μM DVD 10.

As shown in table 1, preparations of DVD 10 and DVD 7 do not affect the rate of respiration in the presence of ADP (V_3), but slightly decrease the rate of uncoupled respiration (V_{DNP}). These drugs also decrease the parameters of phosphorylation by dose-dependent decrease in the ADP/O (fig. 2) and an increase in time of ADP phosphorylation, ie, decrease rate of formation of ATP.

Effect DVD 10 depends on the used concentration (fig. 2).

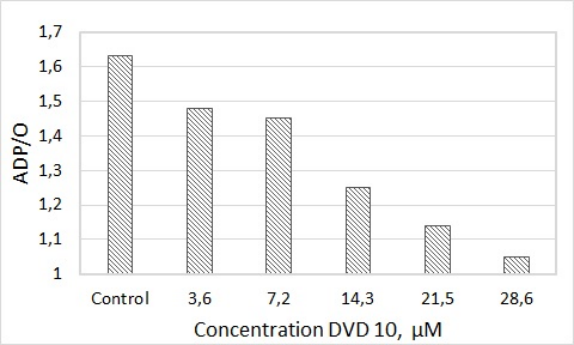

Fig. 2. The effect of different concentrations of DVD 10 on the ADP/O ratio.

Table 2. The changes in amount (% of control) of malondialdehyde after addition of various organoselenium drugs

№	SP	Decrease of MDA concentration,%
1	DVD 7	28
2	DVD 10	10
3	DVD 11	–
4	DVD 12	–
5	DVD 13	–
6	DVD 14	15

Experiments on measuring the product of lipid peroxidation (MDA) showed a marked reduction of its content in mitochondria under the influence of DVD 7, and a small reduction under the influence of DVD 10 and DVD 14 (table 2). Other selenium derivatives have no such properties.

Conclusion

Thus, DVD 7 may be used as an antioxidant, reducing the rate of formation of reactive oxygen species in electron transport chain of mitochondria. DVD 10 having the properties of a weak respiratory chain uncoupler, may act as a cardioprotector, as it is known that the weak uncouplers have a cardioprotective effect [8].

This work was supported by a grant from the Government of the Russian Federation № 14.Z50.31.0028, grant of the Russian Science Foundation № 16-15-00157 and grant RFBR № 16-04-00692A.

References

1. Senkevich O.A., Golubkina N.A., Kowalski Y.G. (2011), Far Eastern Medical Journal, 4, 78-80.
2. Shirshova T.I., Golubkina N.A., Besley I.V., Matistov N.V. (2011), Izvestiya of Komi Scientific Center Ural Branch of Russian Academy of Sciences, 3 (7), 48-54.
3. Litvinov V.P., Dyachenko V.D. (1997), Russian chemical Reviews, 66(11), 1025–1053.

4. Dyachenko I. V., Dyachenko V. D. (2015), Russian Journal of General Chemistry, 85(7), 1673–1676.
5. Dyachenko V.D., Bityukova O.S., Dyachenko A.D. (2010), Chemistry of Heterocyclic Compounds, 8 (518), 1162-1164.
6. Ovchinnikova T.N., Dyachenko V.D., Kovalenko A.A., Biryukov D.Y. (2014), Ukrainian biochem. Journal, 86 (5), 209.
7. Ovsyannikov S.E., Dyachenko V.D., Tkachev R.P., Nikishin A.A., Krasnikov D.A., Ovsyannikova T.N. (2008), Bulletin of Taras Shevchenko Luhansk National University. Biological Sciences, 2(141), 61- 71.
8. Bakeeva L.E. et al. (2008), Biochemistry, 1288-1299.

THE MECHANISM TO REVERSIBLY STOP THE MOLECULAR MOTORS DURING THE CELL TRANSITION INTO ANABIOSIS STATE

A.T. Khodko, Yu.S. Lysak

Institute for Problems of Cryobiology and Cryomedicine,
23, Pereyaslavskaya str., 61015 Kharkov, Ukraine

Physical and chemical processes of the vital activity of biological systems at any organization level are inextricably linked to intracellular and intercellular substance transport meeting macronutrient requirements of the organism.

This function is carried out by various mechanisms activating simple diffusion, facilitated diffusion, osmosis, and active transport.

The latter function is executed by certain specialized molecular motors with different structures and functional concepts. Molecular propulsion systems are remaining continuously active during almost the entire period of life process, ending with the onset of cell death. There are some mechanisms to regulate this process.

All intracellular molecular motors operate in the cytoplasm, which is a concentrated solution of complex composition, containing some low- and high-molecular-weight electrolytes and non-electrolytes. The rheological properties of such solution are gel-like, i.e. such solution has a critical shear stress. According to the classification of aggregate and phase state, which is common in the domestic literature on polymers and polymer systems, such systems are specified as jelly [1].

The jelly-like structure, being an intermediate between solid and liquid state, is the only one structure which allows to combine the function of cell shape retention, diffusing capacity, and active intracellular transport. An additional useful feature of such a system is the rapid decrease of convective flows arising from the biological object moving therein. Failing this, a severe disruption of intracellular substance flows would occur [1].

Two types of systems can basically have gel-like properties. Namely: two- (and more) -phase low-molecular colloids and true solutions of single-phase polymers. The latter systems are called jellies. Having similar rheological properties, gels and jellies differ however in the structure of their spatial framing grid [2].

The energy of any real motor is used to perform some useful activity, to overcome frictional forces of its own structure and environmental resistance.

Proceeding from the general theory of control, it can be concluded that the activity of molecular motors can be adjusted by some specific regulators to selectively affect certain motor type. The functioning of molecular motors can be as well adjusted non-specifically, by changing the mechanical resistance of the operational environment of molecular motors.

Two traditionally prevailing trends in the cell biophysics are the membranology and the biophysics of macromolecules. At that, the environment, in which these systems operate, will not even be per se taken in consideration.

Meanwhile, the physical and chemical factors of external environment can dramatically affect the state of the cytoplasm, causing phase changes therein. This will result in an abrupt change in the phase and in the aggregation state thereof. As a consequence, the viscosity of cytoplasm, which is initially a non-Newtonian fluid, increases dramatically. This will inevitably affect the operation of biological motors, up to the full stop of their functioning.

By recording critical opalescence phenomena and by evaluating garlic cellular fluid consistency during cooling, Khodko and Lysak [3] have shown the liquid-liquid phase transition (FTL-L) in this system.

To this phase change pertains a critical state, i. e. a limiting condition during the transition of a single-phase system into two-phase system, and *vice versa*, depending on the direction of the phase transition. This condition is characterized by a number of so-called critical phenomena and, in particular, by abnormal light scattering caused by the strong concentration fluctuations in the particles of liquid dispersed phase. The phenomenon of critical opalescence is easily detected by optical methods reliably stating the fact that the liquid-liquid phase transition is occurring in the system. Phase transformation of such type is very typical for solutions in general, taking place each time as the variables of state in the polymer-solvent systems, to which cytoplasm pertains, undergo a change [1].

Khodko and Lysak [4] came to the conclusion that the transition of a biological system into anabiosis state (suspended animation) is primarily caused namely by the FTL-L. Said transition occurs due to the sharp deceleration of diffusion processes immediately prior to the critical state. Subsequently, a disperse system will be formed, namely a highly concentrated emulsion having a much higher plastic viscosity, than the initial viscosity of the cytoplasm. The anabiosis state being inseparably associated with the cessation of activity of the biological motors differs from the state of death in that the above activity can be revived if the FTL-L is directed to the mixing and to the renewal of the single-phase structure of the cytoplasm.

The components of the cytoskeleton and of the biological motors, such as microtubules, are dynamic structures capable to assemble, dissemble, and reassemble themselves. This property allows partially understanding and explaining the renewed vitality upon exiting the state of suspended animation. The existing significant changes in volume during the FTL-L being generally specific for the phase transitions of the first order and the destruction of intramolecular structures caused thereby are likely to be partially repaired due to their dynamic nature.

The FTL-L, which takes place both due to the temperature variations change and due to the concentration (the state of cryoanabiosis and xeroanabiosis respectively), is a non-specific shutoff of life beyond physiological parameters of functional state of cells. Taking into account the cooperative nature of the FTL-L, the state of suspended animation must be itself regarded as an instantaneous, although reversible full stop of functioning of biological motors due to an abrupt increase in viscosity and, accordingly, in mechanical resistance of the operational environment of intracellular motors and due to the termination of diffusional supply with energy substrate i.e. with ATP.

The cooling of cells and tissues to the temperatures causing the phase transition and hence being capable to change the original cytoplasm structure is also used in order to produce samples for electron microscopy. This should be necessarily taken into account when analyzing the electron diffraction patterns.

References

1. Papkov S. P. Ravnovesie faz v sisteme polimer-rastvoritel' / S. P. Papkov. – M.: Himiya, 1981. – 272s.
2. Papkov S. P. Studneobraznoe sostoyanie polimerov / S. P. Papkov. – M.: Himiya, 1974. – 256s.
3. Hodko A.T., Ly'sak YU.S. Priroda i dinamika fazovy'h prevrasch'eniy pri ohlajdenii-otogreve kletochnogo soka chesnoka // Bi'ofi'zichniy vi'snik. - 2014. - Vip. 32 (2). - S. 48-60.
4. Hodko A.T., Ly'sak YU.S. Fazovy'e perehody' tipa jidkost'-jidkost' v citoplazme pri ohlajdenii kak prichina perehoda biologicheskoy sistemy' v sostoyanie anabioza // Kriokonservaciya geneticheskih resursov, sovremennoe sostoyanie, problemy' i perspektivy'. Sbornik materialov mejdunarodnoy konferencii. Pusch'ino, 2014. S. 206-208. // Biofizika jivoy kletki. 2014. T. 10. S. 206-208.

ENTOSIS AND CELL CYCLE IN TUMOR CELL CULTURE

O.P. Kisurina-Evgenieva, L. A. Khashba, and G. E. Onishchenko

Lomonosov Moscow State University, Biological Faculty, 119991 Moscow, Russia

Entosis is a type of cell cannibalism during which one tumor cell invades the other tumor cell.

It was shown that invasion occurs with participation of acto-myosin complex and formation of adhesive junctions between outer and inner cells. The fate of inner cell can be different: it can leave the entotic vacuole, divide within it, or be subjected to lysosome-mediated degradation. Entosis is now shown to perturb cytokinesis of outer cell and induce the formation of aneuploid cells. The aim of our work was to determine whether the cells can pass cell cycle phases during entosis. A431 (human epidermoid carcinoma cell line) and MCF7 (human breast adenocarcinoma cell line) cell culture lines were used in this work. The frequency of entotic cells was 0,42 ± 027% in A431 culture and 1,01 ±0,37 % in MCF7 culture. It was shown that cells after detachment from substrate can penetrate the neighboring cell (it took up to 2h). Some cells penetrated at the late telophase. Inner cell could be

inside the vacuoles during more than 72 h. Lysosome-mediated degradation is a slow process and takes about 48 hours. Frequently inner cell could leave entotic vacuole and this exit lasted from 30 to 100 min. Inner cells as well as outer cells could synthesize DNA and enter mitosis. S-phase index and mitotic index of the outer cells coincided with corresponding indexes of the whole cell population. Mitotic index of the inner cells was higher, than of the cell population. Probably it was a result of mitosis delay in the inner cells. At the same time the S-phase index of the inner cells was lower that of the cell population. So the entering DNA replication seemed to be disturbed at the entosis. Block of the cell cycle at G1/S and S-phase by hydroxyurea treatment did not affect the entosis frequency. Thus, the data obtained showed that the outer and inner cells could pass different phases of the cell cycle including S-phase and mitosis.

This work was financially supported by the Russian Science Foundation (project No. 14-50-00029).

COMPARISON OF Ca^{2+}-REGULATION OF ACTO-MYOSIN INTERACTION IN ATRIAL AND VENTRICLE MYOCARDIUM

G.V. Kopylova[1], S.R. Nabiev[1], M.E. Filippova[1, 2], L.V. Nikitina[1] D.V. Shchepkin[1], S.Y. Bershitsky[1]

[1]*Institute of Immunology and Physiology, Russian Academy of Sciences, Yekaterinburg, Russia*

[2]*Ural Federal University, Institute of Physics and Technology, Yekaterinburg, Russia*

Contractile function of the heart depends on the isoform pattern of sarcomere proteins in cardiomyocytes. In mammals myocardium there are two isofoms of myosin heavy chain (MHC), α and β. In ventricle together with ventricular isoforms of light chains they form two isomyosins: V1 and V3, homodimers of α- and β-MHC, respectively. In atria α- and β-MHC together with atrial light chains form A1 (αα) and A2 (ββ) isomyosins. In myocardium two isoforms of α-actin, skeletal (*sk*A) and cardiac (*ca*A), and two isoforms of tropomyosin chains (α- and β-chains) are also expressed. Expression of cardiac protein isoforms is switched in ontogenesis and at change of the conditions of heart functioning. For example, at pressure overload of the heart the expression of certain proteins (β-chain of tropomyosin, *sk*A, β-MHC) is increased [1]. We studied the role of sarcomere protein isoforms for functioning of atrial and ventricle myocardium. Characteristics of unitary interactions of myosin molecule with α-actin isoforms were measured with an optical trap. The role of α-actin isoforms and tropomyosin (Tpm) with different ratio of α- and β-chains in Ca^{2+}-regulation of myosin interaction with regulated thin filaments was studied in an *in vitro* motility assay. For this a dependence of the sliding velocity of the reconstructed thin filaments on Ca^{2+} concentration was obtained and parameters of the Hill equation of '*p*Ca-velocity' relationship were analyzed.

αβ-Tpm and *sk*A were prepared from *m. psoas* of the euthyroid rabbits. Troponin, *ca*A, αα-Tpm and atrial myosin (A1) were extracted from the hearts of

the euthyroid rabbits. αβ-Tpm from rabbit skeletal muscle contained 40% β-chain. Myosin from atria had α-MHC and atrial light chains. V1 and V3 isoforms were obtained from left ventricles of hyper- and hypothyroid rabbits, and contained 90% α- and 90% β-MHC, respectively. The regulated thin filaments were reconstructed from F-actin, troponin and Tpm in the flow cell [2].

Experiments in optical trap were done as early described [3]. Step size (*d*), duration of actin-myosin interaction (*t*) and average force (*F*) sustained by single molecule of cardiac isomyosins were measured. The *in vitro* motility assay was performed as described previously [4]. The dependence of sliding velocity of the reconstructed thin filaments over myosin on Ca^{2+} concentration were fitted to the Hill equation: $V = V_{max}(1+10^{h(pCa - pCa50)})^{-1}$, where V and V_{max} are velocity and maximal velocity at saturating calcium concentration, respectively, pCa_{50} (i.e. calcium sensitivity) is pCa at which half maximal velocity is achieved, and h is the Hill coefficient.

We found that cardiac myosin isoforms have no differences in *d* and *F* with both α-actin isoforms (table 1). The event (i.e. interaction of myosin with F-actin) duration of every cardiac isomyosins did not depend on α-actin isoform. Step size duration of A1 isomyosin with both α-actin isoforms is shorter as compare to V1

Table 1. Parameters of single molecule interaction of cardiac isomyosins with α-actin isoforms

Isoforms		Step size		Force	
myosin	α-actin	*d* (nm)	duration (ms)	*F* (pN)	duration (ms)
V1	skeletal	11.2±2.0 (1723)	54.2±1.3	1.8±0.6 (835)	55.5±5.0
	cardiac	9.5±2.0 (835)	55.8±1.9	1.8±0.7 (382)	58.2±2.9
V3	skeletal	12.5±2.7 (773)	62.1±2.7	2.1±0.5 (614)	72.1±4.5
	cardiac	12.5±2.5 (699)	66.8±2.9	2.0±0.5 (373)	68.7±1.8
A1	skeletal	9.8±2.4 (462)	51.9±1.0	2.6±1.0 (547)	46.8±2.0
	cardiac	10.8±2.6 (276)	47.7±2.9	2.5±0.9 (206)	43.3±4.2

Values d and F are represented as mean ± S.D. Durations of the events are mean ± S.E.M. Figures in brackets are numbers of the events analyzed.

Table 2. Parameters of the Hill equation of "pCa–velocity" relation of atrial myosin

Isoforms		Parameters of Hill equation		
α-Actin	Tpm	V_{max} (μm/s)	pCa_{50}	*h*
*sk*A	ααTpm	4,8 ± 0.2	6.83	3.8
	αβTpm	4.4 ± 0.3	6.80	3.8
*ca*A	ααTpm	4.9 ± 0.6	**7.35**	**1.9**
	αβTpm	4.4 ± 0.7	6.76	3.5

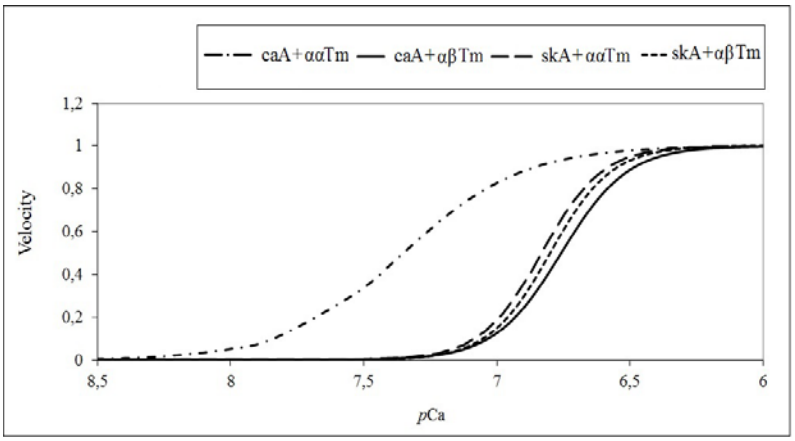

Fig. 1. The 'pCa–velocity' relation for A1 isomyosin. To not overload drawing the experimental data are omitted.

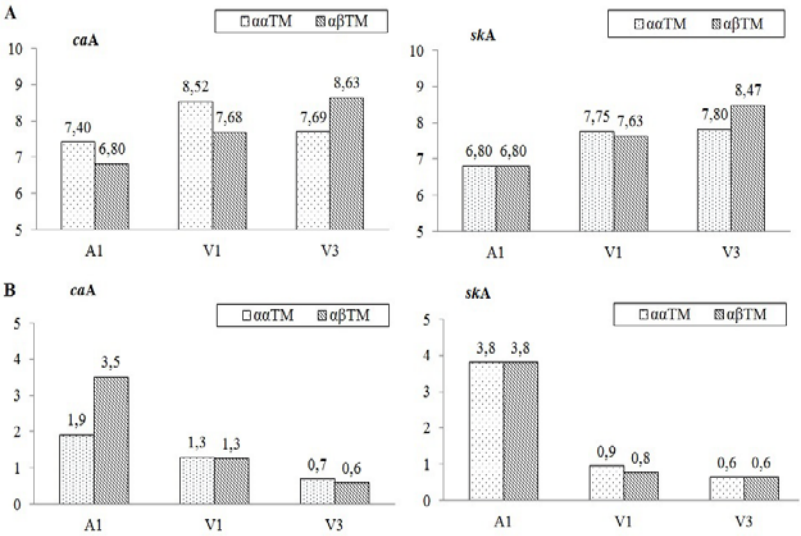

Fig. 2. Comparison of the effect of the α/β-chains Tpm ratio on the Ca^{2+}-regulation of actin-myosin interaction in atrium and ventricle. (A) Calcium sensitivity of "pCa–velocity" relation of atrial myosin and V1 and V3 isomyosins. (B) Hill coefficient of "pCa–velocity" relation of atrial myosin and V1 and V3 isomyosins.

isomyosin. Step size duration of V3 isomyosin with both α-actin isoforms is longer than V1. Therefore the sliding velocity of F-actin over A1 myosin in the *in vitro* motility assay is fastest but over V3 is slowest. The duration of force produced by single molecule of V3 was longer than that of V1 and A1 irrespective of the type

of α-actin. The duration of force event of A1 myosin was shortest. Thus, V3 isomyosin is the strongest and A1 myosin is the weakest with both α-actin isoforms. Atrial myosin is weakest and faster as compare to both ventricular isomyosins.

Using the *in vitro* motility assay with A1 we found that: a) α/β-chains ratio of Tpm did not affect V_{max} of the regulated thin filaments over A1 (table 2); b) pCa_{50} and *h* of "*p*Ca–velocity" relation did not depend on the α/β-chains ratio of Tpm with *sk*A (table 2, fig. 1); c) pCa_{50} of "*p*Ca–velocity" relation with *ca*A was higher for αα-Tpm as compare to αβ-Tpm (table 2, fig. 1); d) *h* of "pCa–velocity" relation with *ca*A was higher for αβ-Tpm as compare to αα-Tpm (table 1, fig. 2).

We compared of the effect of the α/β-chains Tpm ratio on Ca^{2+} -regulation of actin-myosin interaction in atrium and ventricle. It was found that: a) pCa_{50} of "pCa–velocity" relation of atrial myosin was lower than that of V1 and V3 (Fig. 2A); b) *h* of "*p*Ca–velocity" relation of A1 was higher than that of V1 and V3 (Fig. 2B); c) β-chain of Tpm decreased calcium sensitivity of "pCa–velocity" relation of isomyosins containing α-MHC A1 and V1 and increased pCa_{50} velocity of thin filament over isomyosins containing β-MHC (V3; fig. 2A).

Thus, isoforms of α-actin, tropomyosin and myosin affect calcium regulation of actin-myosin interaction in myocardium. Differences in calcium regulation in atrium and ventricle underlie their functional specificity. Switching of the expression of sarcomere proteins isoforms can be one of the mechanisms of adaptation of the working heart to changing conditions of functioning.

Supported by RAS (0401-2014-0002), RFBR (grants 15-34-20136 and 15-04-01558).

References

1. Izumo S et al. (1988) Proc Natl Acad Sci USA 85: 339-343.
2. Köhler J et al. (2003) Physiol Genomics 14(2):117-28.
3. Nabiev et al. (2015) Biophys J. 80 (13):1748-1763
4. Shchepkin et al. (2010) Biocheml and Biophys Res Com. 401:159-16.

FUNCTIONAL STUDIES OF TROPOMYOSIN WITH DILATED AND HYPERTROPHIC CARDIOMYOPATHY MUTATIONS

G.V. Kopylova[1], D.V. Shchepkin[1], S.R. Nabiev[1], D.I. Borovkov[1,2], A.M. Matyushenko[3,4], D.I. Levitsky[3,5]

[1]*Institute of Immunology and Physiology, Russian Academy of Sciences, Yekaterinburg, Russia*

[2]*Ural Federal University, Department of Immunochemistry, Yekaterinburg, Russia*

[3]*A.N. Bach Institute of Biochemistry, Russian Academy of Sciences, Moscow, Russia*

[4]*Department of Biochemistry, School of Biology, Moscow State University, Moscow, Russia*

[5]*A.N. Belozersky Institute of Physico-Chemical Biology, Moscow State University, Moscow, Russia*

The inherited hypertrophic cardiomyopathy (HCM) and dilated cardiomyopathy (DCM) can be caused by missense mutations in the TPM1 gene encoding α-

tropomyosin (Tpm). To date about thirty mutations in human TPM1 are identified [1]. Four of them (D175N, E180G, E40K, E54K) were well characterized structurally and functionally [2–14]. Functional properties of DCM and HCM Tpms are different. The HCM mutations, D175N, E180G, increase the cross-bridge cycling rate, the sliding velocity of thin filaments in an *in vitro* motility assay and its calcium sensitivity, they also impair relaxation [5–11]. On the contrary, DCM mutations, E40K and E54K, decrease calcium sensitivity of the velocity and besides E40K leads to a decrease in the cross-bridge cycling rate [12–14]. To study molecular base of the effect of these mutations on calcium regulation of acto-myosin interaction in myocardium we used the *in vitro* motility assay and an optical trap.

The human α-Tpm mutants were expressed and purified as described previously [15]. Tpm C190A was used as a control. Actin and myosin were obtained from the ventricle of rabbit hearts and troponin was extracted from the ventricle

Table 1. Parameters of Hill equation of pCa-velocity relationship

	V_{max} (μm/s)	h	pCa_{50}
D175N/ C190A	3.9 ± 0.5*	1.9 ± 0.3	6.65 ± 0.10*
E180G/ C190A	3.8 ± 0.2*	2.4 ± 1.2	6.85 ± 0.14*
E54K/ C190A	2.7 ± 0.2	3.4 ± 0.4	6.36 ± 0.01
E40K/ C190A	1.9 ± 0.03*	2.9 ± 0.9	6.10 ± 0.14*
C190A	3.0 ± 0.05	2.7 ± 0.8	6.36 ± 0.01

Symbol * is significance of differences of Hill equation parameters of pCa-velocity relationship for the regulated thin filaments with Tpm mutants from that with Tpm C190A.

Table 2. Parameters of unitary myosin interactions with F-actin and the regulated thin filaments containing Tpm with HCM and DCM mutations

	Step size		Average force	
	d (nm)	*t* (ms)	*F* (pN)	*t* (ms)
F-actin	13 ± 6.8 (1079)	28 ± 1.4	3.3 ± 1.4 (651)	25.0 ± 2.0
Reconstructed thin filament				
E54K	13.4 ± 6.9 (415)	23.0 ± 6.0	3.1 ± 1.3 (417)	32.2 ± 2.9*
E40K	12.7 ± 7.5 (450)	23.1 ± 1.8	2.4 ± 0.7 (586)	24.3 ± 1.3
D175N	7.54 ± 3.1 (845)	36.3 ± 1.2*	2.4 ± 1.5 (691)	42.4 ± 1.6*
E180G	12.2 ± 4.3 (490)	51.3 ± 5.4*	2.7 ± 1.7 (504)	20.5 ± 1.0
C190A	15.8 ± 3.3 (153)	15.2 ± 1.3*	2.7 ± 1.6 (996)	24.3 ± 0.6

Step size (*d*) and average force (*F*) are shown as mean ± S.D. Durations (*t*) of the interactions are shown as mean ± S.E.M. Figures in the brackets are number of the events analyzed. Symbol * denotes statistical significance of differences in the duration of the myosin interactions with thin filament containing Tpm mutant with respect to that with F-actin.

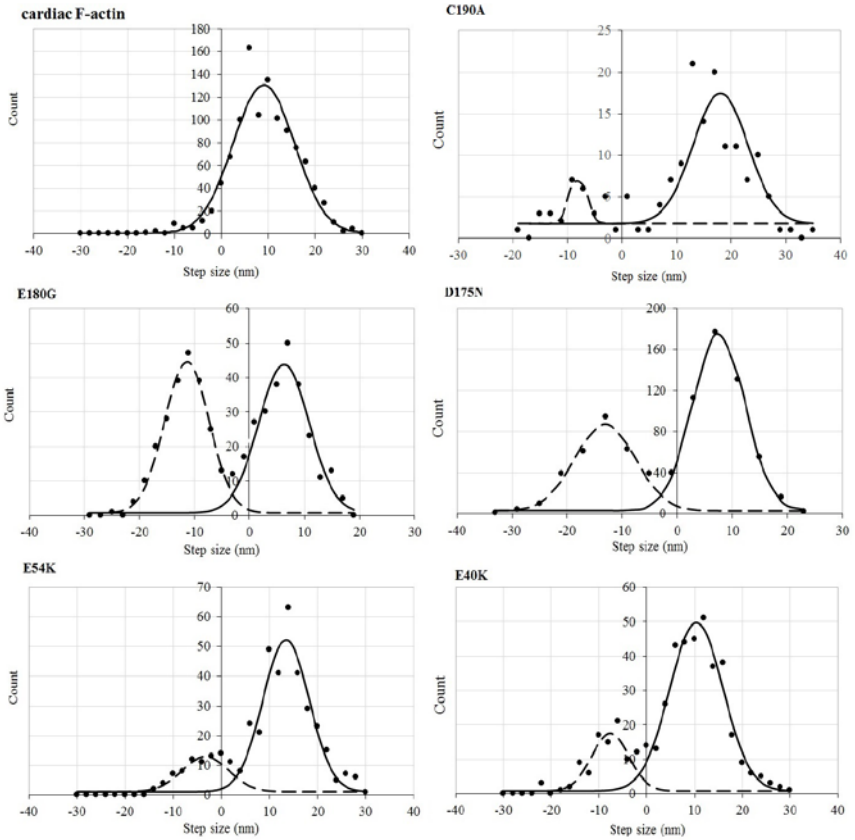

Frequency histogram of the step size distribution of myosin head during its interaction with the regulated thin filament containing Tpm with HCM and DCM mutations.

of bovine heart. Thin filaments were reconstructed from F-actin, troponin and Tpm.

We have analyzed the dependence of the sliding velocity of reconstructed thin filaments on calcium concentration over myosin coated surface in the *in vitro* motility assay using the Hill equation: $V_{max}(1+10^{h(pCa-pCa50)})^{-1}$, where V and V_{max} are the velocity and the maximal velocity at saturating calcium concentration, respectively, pCa_{50} (i.e. calcium sensitivity) is pCa at which half maximal velocity is achieved, and h is the Hill coefficient. Tpm mutation E40K decreased the maximal sliding velocity of thin filaments over myosin and its calcium sensitivity while both of HCM mutations increased both the velocity and the calcium sensitivity (table 1). Mutation E54K did not affect the characteristics of pCa-velocity relation in the *in vitro* motility assay (table 1).

Using the optical trap we measured step size, average unitary force developed by myosin head and the duration of its interaction with the reconstructed thin filament at saturating calcium concentration. The results of measurements of step size in displacement mode (i.e. with no load), unitary force using isometric clamp [16], and duration of the events in these both modes are shown in table 2. Both the HCM and DCM mutation affected the characteristics of the single myosin interaction with thin filament (table 2). Interestingly, during its interaction with thin filament containing HCM or DCM Tpm mutant besides forward steps of myosin there was a substantial amount of backward steps while with F-actin the backward steps did not present (figure). Proportion of the backward steps was higher with thin filaments containing HCM Tpms as compared to DCM Tpms.

Thus both HCM and DCM mutations of Tpm molecule affect the single interaction of myosin molecule with the regulated thin filament. The data obtained may contribute to understanding the molecular mechanisms of the HCM and DCM genesis.

Supported by RFBR grants 15-34-20136, 15-04-01558.

References

1. Gupte et al. (2015) J Biol Chem. 290(11):7003-15.
2. Olson et al (2001) J Mol Cell Cardiol. 33: 723-732.
3. Kremneva et al. (2004) Biophys J. 87(6):3922-33.
4. Mirza et al. (2007) J Biol Chem. 282(18):13487-97.
5. Bing et al. (1997) Biochem. Biophys. Res. Commun. 236:760-764.
6. Evans et al. (1998) Biophys J. 74(2):A346.
7. Muthuchamy et al. (1999) Circ Res. 85:47-56.
8. Bing et al. (2000) J Mol Cell Cardiol .32, 1489-1498.
9. Jagatheesan et al. (2007) Am J Physiol Heart Circ Physiol 293: H949-H958.
10. Bai et al. (2011) Biophys J. 100(4):1014-1023.
11. Alves et al. (2014) Circ Cardiovasc Genet. 7(2):132-4.
12. Rajan et al. (2007) Circ Res. 101(2):205-14.
13. Bai et al. (2012) PLoS ONE 7(10):e47471.
14. Memo et al. (2013) Cardiovasc Res. 99(1):65-73.
15. Matyushenko et al. (2014) FEBS J. 281(8):2004-16.
16. Takagi et al. (2006) Biophys. J. 90:1295-1307.

STABILIZING OF THE CENTRAL PART OF α-TROPOMYOSIN AFFECTS ACTO-MYOSIN INTERACTION

G.V. Kopylova[1], D.V. Shchepkin[1], S.R. Nabiev[1], A.M. Matyushenko[2], D.I. Levitsky[2], N.A. Koubassova[3], A.K. Tsaturyan[3], S.Y. Bershitsky[1]

[1]*Institute of Immunology and Physiology, Russian Academy of Sciences, Yekaterinburg, Russia*

[2]*A.N. Bach Institute of Biochemistry, Russian Academy of Sciences, Moscow, Russia;*

[3]*Institute of Mechanics, Moscow State University, Moscow, Russia*

Replacement of non-canonical aminoacid residues Gly126 and Asp137 in the central part of α-tropomyosin (Tpm) molecule by canonical Arg126 and

Leu137 appreciably affects its structure and properties as revealed by increased thermal stability, tolerance to tryptic cleavage, Ca^{2+}-dependent ATPase of myosin S1 interaction with thin filaments containing these mutants, and sliding velocity in the *in vitro* motility assay (Matyushenko et al., FEBS J., 2014). Here we studied how Tpm mutants G126R/C190A, D137L/C190A and G126R/D137L/C190A affect the properties of thin filaments and characteristics of actomyosin interaction. With an optical trap we have measured parameters of single interactions of skeletal myosin molecules with reconstructed thin filaments containing each of these Tpm mutants and troponin (Tn) at pCa 4: step size in displacement mode, unitary force in isometric clamp [Takagi et al., Biophys. J., 2006], and duration of the events in both these modes. The results are shown in tables 1 and 2.

The extent of activation of reconstructed thin filaments containing the listed Tpm mutants was evaluated by dependence of their sliding velocity along the surface of immobilized myosin at pCa 4 and in the presence of Tn on the myosin concentration infused into the flow cell. It was found that the maximal velocity of the filaments containing Tpm with stabilizing mutations by 20–50% higher than that with the control Tpm C190A. Myosin concentration required to achieve half-maximal velocity (p_{50}) for thin filaments with Tpms with single mutations was half, and with double mutation more than 20-fold less than that for the control Tpm C190A (figure, table 3).

We can conclude that there is a certain link between the data presented here and the results of the bending stiffness measurements of these Tpm mutants [Nabiev et al., Biophys. J., 2015] which showed a rise of the thin filament stiffness with the degree of the Tpm molecule stabilization.

Table 1. Duration of unitary events of myosin with thin filament containing Tpm mutants

Tpm mutant	Step duration, ms	Unitary force duration, ms
C190A	39±4.0 (1723)	13.9±0.8 (835)
G126R/C190A	28±2.0 (835)	11.1±0.4 (382)
D137L/C190A	29±3.0 (773)	21.3±1.4 (614)
D137L/G126R/C190A	21±1.0 (699)	21.3±2.3 (373)

Number of analyzed events shown in brackets

Table 2. Probability of distribution of step size and unitary force

Specimen	Step size median, nm	Unitary force median, pN
C190A	14.3	8.3
G126R/C190A	9.9	6.8
D137L/C190A	9.5	5.8
D137L/G126R/C190A	7.4	7.3
F-actin	4.8	4.8

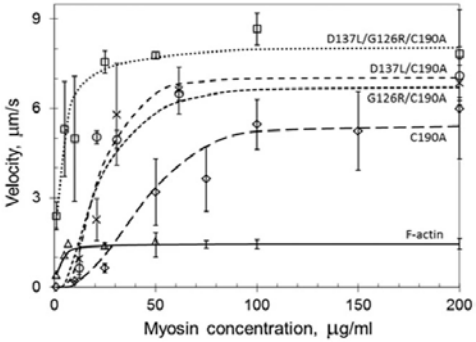

Dependence of the of thin filament sliding velocity on myosin concentration in flow cell.

Table 3. Characteristics of dependence of the thin filament sliding on myosin concentration

Specimen	V_{max}, μm/s	p_{50}, μg/ml
C190A	5.6 ± 0.4	28.1 ± 2.1
G126R/C190A	6.8 ± 0.4*	15.7 ± 1.3*
D137L/C190A	7.1 ± 0.5*	15.7 ± 1.5*
D137L/G126R/C190A	8.3 ± 0.5*	1.2 ± 0.2*
F-actin	1.8 ± 0.2	3.2 ± 0.2

Supported by RFBR grants 15-34-20136, 15-04-01558 and program 15-9-4-18 UB RAS.

THE STUDY OF BLOCKING EFFECTS OF Pr^{3+} AND La^{3+} ON CALCIUM-DEPENDENT PROCESSES IN RAT HEART MITOCHONDRIA AND FROG CARDIAC MUSCLE

S.M. Korotkov, C.V. Sobol, I.V. Shemarova, A.R. Shumakov, V.V. Furaev, V.P. Nesterov

Sechenov Institute of Evolutionary Physiology and Biochemistry, Russian Academy of Sciences, Thorez prosp. 44, St. Petersburg, 194223, Russia

It is known that Ca^{2+} [Zoratti, Szabò, 1995; Gunter, Sheu, 2009] but not Ni^{2+} [Bragadin, Viola, 1997] or La^{3+} [Lehninger, Carafoli, 1971; Reed, Bygrave, 1974] are transported in the matrix by the mitochondrial calcium uniporter (MCU). The influence of these cations on mitochondrial Ca^{2+} uptake depends on their ionic crystal radii [Reed, Bygrave, 1974; Tedeschi, 1981]. Therewith Ni^{2+} [Bragadin, Viola, 1997], Y^{3+} [Harris, Zaba, 1977], La^{3+} [Lehninger, Carafoli, 1971; Reed, Bygrave, 1974], Nd^{3+} [Reed, Bygrave, 1974], and Pr^{3+} and Ga^{3+} [Harris, Zaba,

1977; Gunter, Sheu, 2009] are competitive inhibitors of the Ca^{2+} uptake, which occurs with the participation of low-affinity sites, facing the cytoplasmic side of the inner mitochondrial membrane (IMM). Maximal inhibition of the uptake was shown in experiments with La^{3+} which resulted in their interaction with these sites [Reed, Bygrave, 1974]. The mild calcium load of mitochondria following membrane depolarization causes the interaction of Ca^{2+} with high affinity sites, directed to the matrix side, and results in the mitochondrial permeability transition pore (MPTP) opening in the low conduction state [Zoratti, Szabò, 1995; Ichas, Mazat, 1998]. In this case, the IMM becomes easily permeable to inorganic cations (H^+, K^+, and Ca^{2+}). This MPTP opening leads to a swelling, oxidative stress, inner membrane potential ($\Delta\Psi_{mito}$) dissipation, as well as release of Ca^{2+} from calcium-preloaded mitochondria.

It was earlier shown that La^{3+} and Y^{3+} showed negative inotropic effect and 2 mM of these metals visibly reduced excitation-contraction amplitude of *Rana ridibunda* frog myocardium preparations under electric stimulation [Shemarova et al., 2013; Shemarova et al., 2014; Korotkov et al., 2016]. On the other hand, La^{3+} [Shemarova et al., 2013], Y^{3+} [Shemarova et al., 2014; Korotkov et al., 2016], and Ni^{2+} [Shemarova et al., 2010] induced transport of K^+ in the matrix of energized rat heart mitochondria (RHM). La^{3+} and Y^{3+} increased transport of K^+ surrogate Tl^+ in the matrix of isolated rat liver mitochondria [Korotkov et al., 2014]. Y^{3+} and La^{3+} slightly increased basal respiration of isolated RHM and did not affect state 3 or 2,4-dinitrophenol (DNP)-uncoupled respiration of these organelles [Shemarova et al., 2013; Korotkov et al., 2016]. Y^{3+} inhibited Ca^{2+}-induced increase in the basal state of RHM, energized by glutamate and malate [Korotkov et al., 2016]. Therewith, this metal prevented Ca^{2+}-induced diminution both in state 3 or DNP-uncoupled respiration of these mitochondria and dissipation in $\Delta\Psi_{mito}$ [Korotkov et al., 2016]. Considering literature data on blocking effects of lanthanides on both potential-gated Ca^{2+} channels [Campbell et al., 1988; Mlinar, Enyeart, 1993; Triggle, 1996] and transport of Ca^{2+} into the matrix [Reed, Bygrave, 1974; Harris, Zaba, 1977], it was shown that Y^{3+} and La^{3+} like Ni^{2+} [Shemarova et al., 2010] can markedly affect calcium-dependent mitochondrial processes and, in particular, inhibit mitochondrial Ca^{2+}-uniporter and influence on the respiration of mitochondria being in different energetic states [Korotkov et al., 2016]. Thus this research tests effects of Pr^{3+} and La^{3+} being analogue of Y^{3+} on both electro-stimulated excitation-contraction of *Rana ridibunda* frog myocardium preparations and Ca^{2+}-loaded RHM, energized by glutamate with malate or succinate in the presence of rotenone which are correspondingly substrates of I- and II-complexes of the respiratory chain. In this regard, proton and potassium transport via IMM was accordingly tested by swelling of RHM in media containing 125 mM NH_4NO_3 or 25 mM potassium acetate and 100 mM sucrose. In addition, effects of Pr^{3+} and Ca^{2+} were studied on both respiration of RHM being different energetic states (the basal, 3, and DNP-stimulated) and $\Delta\Psi_{mito}$ dissipation.

This study found that 1-3 mM Pr^{3+}, injected into Ringer, decreased electro-stimulated excitation-contraction of *Rana ridibunda* frog myocardium preparations.

Pr^{3+} prevented the increase in Ca^{2+}-induced basal state of RHM, energized by both glutamate with malate and succinate. Both Pr^{3+} and La^{3+} did not affect state 3 and DNP-uncoupled respiration mitochondria energized by these substrates. Pr^{3+} inhibited the Ca^{2+}-induced decrease in state 3 and DNP-uncoupled respiration and prevented by Ca^{2+}-induced decline in $\Delta\Psi_{mito}$. La^{3+} less than Pr^{3+} affected these effects of Ca^{2+} on the respiration and the IMM potential in experiments with RHM, energized by glutamate with malate. Swelling of non-energized RHM in the NH_4NO_3 medium was stimulated by Pr^{3+}. This suggests that Pr^{3+} like La^{3+} and Y^{3+} possesses mild protonophoric effect on proton permeability of the IMM. Ca^{2+}-induced swelling of RHM, energized by these above substrates and injected in NH_4NO_3 medium, was potently inhibited by Pr^{3+}. Therewith, Pr^{3+} potently decreased Ca^{2+}-induced swelling of energized RHM, added in medium containing above substrates, potassium acetate and sucrose. The Ca^{2+}-induced dissipation of $\Delta\Psi_{mito}$ in experiments with RHM, energized by both glutamate with malate and succinate, was visibly decreased by Pr^{3+}. Influence of La^{3+} on the Ca^{2+}-induced increase in both swelling and $\Delta\Psi_{mito}$ dissipation was not as marked as the first effects of Pr^{3+}. The retard by Pr^{3+} of these Ca^{2+}-induced processes (increased swelling, decreased respiration, dissipated potential) suggests that this metal inhibits MPTP opening in Ca^{2+}-loaded RHM. This manuscript data are important to better understand mechanisms in affecting Pr^{3+} on myocardial calcium-dependent processes. Thus, this research showed that Pr^{3+} possesses negative inotropic effect on the myocardium and inhibits the Ca^{2+}-dependent processes in rat heart mitochondria. On the other hand, Pr^{3+} as La^{3+} and Y^{3+} did not affect respiratory enzymes of isolated rat heart mitochondria. The combination in these effects of Pr^{3+} on cardiomyocytes' functions may cause in a decrease in cardiac muscle contractility at the contact between an organism and praseodymium salts.

Safranin fluorescence was measured using of Research Resource Center equipment for the physiological, biochemical and molecular-biological studies (Sechenov Institute of Evolutionary Physiology and Biochemistry of the Russian Academy of Sciences).

References

Bragadin M., Viola E.R. Ni^{2+} as a competitive inhibitor of calcium transport in mitochondria. J. Inorg. Biochem. 1997. 66(4):227-229.

Campbell D.L., Giles W.R., Hume J.R., Shibata E.F. Inactivation of calcium current in bull-frog atrial myocytes. J. Physiol. 1988. 403: 287-315.

Gunter T.E., Sheu S.S. Characteristics and possible functions of mitochondrial Ca^{2+} transport mechanisms. Biochim. Biophys. Acta. 2009. 1787(11): 1291-1308.

Harris E.J., Zaba B. The phosphate requirement for Ca^{2+}-uptake by heart and liver mitochondria. FEBS Lett. 1977. 79(2): 284-290.

Ichas F., Mazat J.P. From calcium signaling to cell death: two conformations for the mitochondrial permeability transition pore. Switching from low- to high-conductance state. Biochim. Biophys. Acta 1998. 1366(1-2): 33-50.

Korotkov S., Konovalova S., Emelyanova L., Brailovskaya I. Y^{3+}, La^{3+}, and some bivalent metals inhibited the opening of the Tl^{+}-induced permeability transition pore in Ca^{2+}-loaded rat liver mitochondria. J. Inorg. Biochem. 2014. 141: 1-9.

Korotkov S.M., Sobol C.V., Shemarova I.V., Furaev V.V., Nesterov V.P. The comparative study of Y^{3+} effects on calcium-dependent processes in frog cardiac muscle and mitochondria of rat cardiomyocytes. 2016. In press.
Lehninger A.L., Carafoli E. The interaction of La^{3+} with mitochondria in relation to respiration-coupled Ca^{2+} transport. Arch. Biochem. Biophys. 1971. 143(2): 506-515.
Mlinar B., Enyeart J.J. Block of current through T-type calcium channels by trivalent metal cations and nickel in neural rat and human cells. J. Physiol. 1993. 469: 639-652.
Reed K.C., Bygrave F.L. Accumulation of lanthanum by rat liver mitochondria. Biochem. J. 1974. 138(2) 239-252.
Reed K.C., Bygrave F.L. The inhibition of mitochondrial calcium transport by lanthanides and ruthenium red. Biochem. J. 1974. 140(2): 143-155.
Shemarova I.V., Korotkov S.M., Demina I.N., Nesterov V.P. Influence of mitochondrial oxidative reactions on myocardial contractility. Effects of Ni2+. Zh. Evol. Biokhim. Fiziol. 2010. 46(2): 138-142.
Shemarova I.V., Korotkov S.M., Nesterov V.P. Action of La^{3+} on the systems providing contractility of vertebrate myocardium. Zh. Evol. Biokhim. Fiziol. 2013. 49(4): 285-289.
Shemarova I.V., Sobol C.V., Korotkov S.M., Nesterov V.P. Action of yttrium on calcium-dependent processes in myocardium of vertebrates. Zh. Evol. Biokhim. Fiziol. 2014. 50(3): 196-200.
Tedeschi H. The transport of cations in mitochondria. Biochim. Biophys. Acta 1981. 639(3-4): 157-196.
Triggle D.J. The classification of calcium antagonists. J. Cardiovasc. Pharmacol. 1996. 27: S14.
Zoratti M., Szabò I. The mitochondrial permeability transition. Biochim. Biophys. Acta 1995. 1241(2): 139-176.

EFFECT OF DIET-INDUCED OBESITY ON INCREASED INTRAMYOCELLULAR LIPID ACCUMULATION AND CHANGES IN GENE EXPRESSION IN SKELETAL MUSCLES OF OSSABAW SWINE

T.Y. Kostrominova

Department of Anatomy and Cell Biology, Indiana University School of Medicine-Northwest, 3400 Broadway, Gary, IN 46408.

Skeletal muscle is the second largest organ in the human body. It makes ~40% of body mass and is a major organ for insulin-dependent glucose uptake. Expectedly, skeletal muscle plays a key role in the regulation of glucose metabolism and in the development of diabetes in the setting of obesity. However, the specific mechanisms by which obesity affects muscle metabolism and its contribution to diabetes are incompletely understood. Moreover, this is a barrier to the development of therapeutic options for obese pre-diabetic and diabetic individuals

Obesity-related abnormalities lead to excessive accumulation of triglycerides and fatty acids in skeletal muscle fibers in the form of intramyocellular lipids (IMCL). IMCL accumulation is strongly associated with the impairment of glucose metabolism, oxidative stress, deficiency in energy production, insulin resistance and eventually the development of type 2 diabetes. Interestingly, endurance-trained

athletes also have increased accumulation of IMCL droplets in skeletal muscles with improved glucose metabolism and insulin sensitivity. The main difference between individuals with metabolic syndrome and highly trained athletes could be in the increased production of reactive oxygen species (ROS) by impaired mitochondria incapable of efficient utilization of IMCL droplets in patients with metabolic syndrome. Moreover, accumulation of palmitate-rich IMCL droplets leads to the increase in intracellular lipid metabolites (diacylglycerol, ceramide, and triacylglycerol) suppressing insulin-stimulated signaling. On the contrary, mitochondria in muscles of endurance-trained athletes are highly adapted to the utilization of IMCL as fuel during regular bounds of exercise followed by IMCL replenishment. Understanding of the mechanisms regulating mitochondrial interaction with IMCL droplets under normal and pathological conditions could be a key for the development of therapeutic options for obese pre-diabetic and diabetic individuals.

Ossabaw swine is an excellent model to study the effects of diet-induced obesity on skeletal muscles and might provide data closely related to the regulatory mechanisms found in humans. Although mice provide cost-effective models with diverse genetic modifications for many studies, glucose metabolism in rodents is mostly regulated by liver. In both humans and swine skeletal muscle weight relative to total body weight as well as significance of skeletal muscle in regulation of whole body glucose metabolism is much higher than in rodents. Ossabaw swine fed excess kcal and atherogenic diets develop metabolic syndrome characterized by obesity, dyslipidemia, hypertension, insulin resistance, and glucose intolerance. The purpose of this study was to test the hypothesis that obesity and metabolic syndrome would cause changes in skeletal muscle structure, promote intramyocellular lipid accumulation and alter expression of genes involved in lipid and glucose metabolism.

Methods

Adult male Ossabaw swine were fed for 24 weeks high-fat/cholesterol/fructose diet that induces dyslipidemic metabolic syndrome (DMetS). Obese DMetS swine were compared to the lean swine on control (C) diet. Control diet contains 16% kcal from protein, 72% kcal from carbohydrates, and 12% kcal from fat (Purina Test Diet, Richmond, Indiana, USA). DMetS diet contains 8% kcal from protein, 46% kcal from carbohydrates (20% kcal from fructose), 46% kcal from fat (hydrogenated soybean oil; 56% trans fatty acid), and supplemented with 2% cholesterol by weight.

Results

Total and LDL cholesterol were both highly up-regulated in DMetS swine. There was ~1.2-fold increase in the cross sectional area of muscle fibers in DMetS group compared with C for biceps femoris and plantaris muscles. In plantaris muscles DMetS diet caused ~2-fold decrease in slow MHC mRNA and protein expression and ~1.2–1.8-fold increase in the number of IMCL droplets without large changes in the size of the droplets. These data correlate well with the data on total plasma cholesterol (C=60 mg/dL and DMetS =298 mg/dL) and LDL (C=29 mg/dL and DMetS =232 mg/dL). There were ~7-fold and ~6-fold increases in UCP3 and SCD1 mRNA expression, respectively, in plantaris muscles of DMetS swine. There

was ~4-fold increase in adiponectin mRNA expression and ~2-fold increase in adiponectin receptor 2 mRNA expression. There was also ~2.5-fold increase in fibroblast growth factor mRNA expression. While mRNA expression of GLUT4, CD36/FAT, FATP 1, SCD5 and UCP2 was not changed.

Conclusion

Major changes observed in skeletal muscle of obese Ossabaw swine correlate with those previously reported for obese humans. These observations and the ability to perform serial skeletal muscle biopsies in Ossabaw swine will enable precise studies of the time course of gene expression, IMCL accumulation, and time-dependent metabolic changes during development of metabolic syndrome in large animal model highly comparable to humans.

The work was supported by IUSM-Northwest.

THE ROLE OF INWARDLY RECTIFYING POTASSIUM CHANNELS IN THE REGULATION OF RAT ARTERIES CONTRACTILE RESPONSES

D.S. Kostyunina, A.A. Shvetsova, D.K. Gaynullina, O.S. Tarasova

Faculty of Biology, Lomonosov Moscow State University

SRC RF Institute for Biomedical Problems RAS, Moscow, Russia

Potassium channels play an important role in the regulation of vascular tone. There are four types of potassium channels in vascular smooth muscle cells: voltage-dependent (K_v), Ca-activated (K_{Ca}), ATP-sensitive (K_{ATP}) and inward rectifier potassium channels (K_{IR}). K_{IR} play an important role in forming of membrane potential in vascular smooth muscle cells. Furthermore, their hyperpolarizing influence increases at moderate elevation of extracellular K^+ ($[K^+]_{out}$). Increase of $[K^+]_{out}$ in a blood flow can happen during active organ metabolism and be one of the mechanisms of functional hyperemia. Besides, K_{IR}activation my be induced by endothelial-derived hyperpolarizing factor (EDHF), which can be provided, in particular, by a local elevation of $[K^+]_{out}$ between vascular endothelial and smooth muscle cells. Potassium ions are not metabolites and local blood flow regulators in every body organ. In this regard, our aim was to define K_{IR} contribution in vascular tone regulation in two functionally different vascular regions of rat distal hindlimb. We hypothesized that K_{IR} contribution in vascular tone regulation may vary in arteries of skeletal muscles, and in skin supplying arteries.

In the study we used Wistar rats (males), body weight of rats was 277–440 g. Two arteries of skin region were isolated: saphenous artery (inner diameter 598±9 mcm) and ventral branch of saphenous artery (247±15 mcm). Also, we used arteries of lateral and medial heads of gastrocnemius muscle (309±9 mcm). Two-millimeter artery segments were placed in isometric myograph (wire myograph, DMT A/S). During a preconstriction induced by methoxamine (agonist of α_1-adrenoreceptors) we registered relaxation induced by two factors: (1) elevation of $[K^+]_{out}$ (from 4,5 mM to 15 mM), (2) increase of acetylcholine from 10^{-8} to10^{-5}M. In order to identify EDHF acetylcholine-induced relaxation was studied during

inhibiting of NO-synthase (L-NNA, 10^{-4}M) and cyclooxygenase (indomethacin, 10^{-5} M). Contribution of K_{IR} in relaxation mechanisms was defined by K_{IR}-blocker (Ba^{2+}, $3 \cdot 10^{-5}$ M).

Saphenous artery demonstrated small relaxation induced by increase of $[K^+]_{out}$ (only 20% of initial constriction), its branch did not relax almost at all. Meanwhile, arteries of gastrocnemius muscle produced almost complete relaxation (80–100%) at elevation of $[K^+]_{out}$ from 4,5 mM to 15 mM. K_{IR} blockade led to a decrease of gastrocnemius arteries relaxation, especially at high $[K^+]_{out}$ concentrations (from 9 mM to 15 mM). Combined inhibition of K_{IR} and Na^+/K^+-ATPase (ouabain, 10^{-3} M) completely suppressed relaxation induced by $[K^+]_{out}$ increase.

Endothelium activation induced 80–90% relaxation of each studied artery. After inhibiting of NO-synthase and cyclooxygenase acetylcholine did not induce dilation in saphenous artery and its branch, meanwhile, arteries of gastrocnemius muscle produced 80-100% relaxation. In a presence of Ba^{2+} EDHF-induced relaxation was significantly decreased, especially at high $[K^+]_{out}$ concentrations (from 9 mM to 15 mM). Combined inhibition of K_{IR} and Na^+/K^+-ATPase completely suppressed EDHF-induced relaxation.

Our results propose that arteries of skeletal muscles are more likely to relax at elevating of $[K^+]_{out}$, than skin supplying arteries. Skeletal muscle supplying arteries relax at general $[K^+]_{out}$ increase (like as during active muscle metabolism) and at local $[K^+]_{out}$ increase (induced by endothelium activation). In both cases studied reactions decreased while K_{IR} were blocked. All in all, K_{IR} are more important for regulating vascular tone of skeletal muscle arteries, than of skin arteries, as it correlates with the functions of these arteries in the organism.

Study was supported by RFBR (grant № 16-04-01395-a).

SOLVING THE STRUCTURE OF MYOSIN FILAMENT IN THE RELAXED MUSCLE OF TARANTULA

N.A. Koubassova[1], L. Alamo[2], A.K. Tsaturyan[1], R. Padrón[2]

[1]*Institute of Mechanics, Moscow State University, Mitchurinsky prosp. 1, Moscow, 119992, Russia*

[2]*Centro de Biología Estructural, Instituto Venezolano de Investigaciones Científicas (IVIC), Caracas, Venezuela*

Tarantula striated muscle is an outstanding system for understanding the molecular organization of the myosin filaments. 3D reconstruction of tarantula filaments based on cryo-EM images and single particle image processing revealed that in the relaxed state, myosin molecules undergo intra-molecular head-head interactions, explaining how head activity is switched off [1–4]. A new model (PDB code 3JBH) explains the structural origin of the low ATP turnover rate detected in relaxed tarantula muscle by ascribing the very slow rate to docked unphosphorylated heads, the slow rate to phosphorylated docked heads, and the fast rate to phosphorylated undocked heads.

We used direct modeling approach developed for the analysis of X-ray diffraction data from contracting rabbit muscle fibres [5] to verify the 3D reconstruction against the low angle diffraction patterns obtained from live relaxed muscle of

tarantula (data obtained at DESY synchrotron radiation source were provided by J. Wray and R. Padrón). We considered one myosin filament with 4-stranded helix of myosin molecules, axial distances between the crowns of myosin heads were taken as 14.5 nm, single unit cell contained 6 crowns or 48 heads.

Equator and first six myosin layer lines were calculated and compared with the low angle x-ray diffraction pattern. To understand the nature of the equatorial reflections at high reciprocal radii the contributions of myosin heads [residues 1–859 of 3JBH] and coiled-coil tail of LMM [residues 860–1920 3JBH] to these reflections were calculated separately. The calculations showed good correspondence between experimental and calculated layer lines. Equatorial peak at ~4.3 nm is well reproduced by the model, while the calculated reflections at ~2 nm have spacings slightly different from those observed experimentally. To complete the model of the thick filament in relaxed muscle we plan to include 12 paramyosin rods to the myosin backbone.

Supported by RFBR grant No. 15-04-02174 A to N.A.K. and 16-04-00693 A to A.K.T.

References

1. Woodhead J. L., Zhao F. Q., Craig R., Egelman E. H., Alamo L., Padrón, R. (2005). Atomic model of a myosin filament in the relaxed state. Nature 436, 1195-1199.
2. Alamo L., Wriggers W., Pinto A., Bartoli F., Salazar L., Zhao F. Q., Craig R., Padrón, R. (2008). Three-dimensional reconstruction of tarantula myosin filaments suggests how phosphorylation may regulate myosin activity. J. Mol. Biol. 384, 780-797.
3. Alamo, L., Qi, D., Wriggers, W., Antonio, Zhu, J., Bilbao, A., Gillilan, R.E., Hu, S. & Padrón, R. (2016) Conserved intramolecular interactions maintain myosin interacting-heads motifs explaining tarantula muscle super-relaxed state structural basis. J. Mol. Biol. In Press. doi: 10.1016/j.jmb.2016.01.027
4. Stewart M.A., Franks-Skiba K., Chen S., Cooke R. Myosin ATP turnover rate is a mechanism involved in thermogenesis in resting skeletal muscle fibers. (2010) Proc. Natl. Acad. Sci. U S A. 107: 430–435.
5. Koubassova N.A., Bershitsky S.Y., Ferenczi M.A., Tsaturyan A.K. (2008) Direct modeling of X-ray diffraction pattern from contracting skeletal muscle. Biophys J. 95, 2880–2894.

REDUCTION IN THE NUMBER OF ACTIN-BOUND MYOSIN HEADS IN FULLY ACTIVATED MUSCLE FIBRES DOES NOT INDUCE AN "OPEN" TO "CLOSED" TRANSITION IN THE THIN FILAMENTS

N.A. Koubassova[1], S.Y. Bershitsky[2], G.V. Kopylova[2], M.A. Ferenczi[3], T. Narayanan[4], A.K. Tsaturyan[1]

[1]*Institute of Mechanics, Moscow State University, Moscow, Russia*
[2]*Institute of Immunology and Physiology, Russian Academy of Sciences, Yekaterinburg, Russia*
[3]*Lee Kong Chian School of Medicine, Nanyang Technological University, Singapore*
[4]*European Synchrotron Radiation Source, Grenoble, France*

The three-state model of Ca^{2+} regulation of thin filaments [McKillop, Geeves, *Biophys. J.*, 1993] suggests that Ca^{2+} binding to troponin (Tn) shifts the

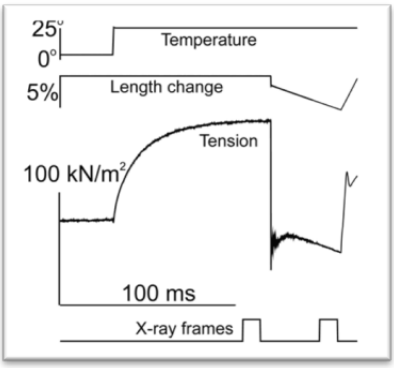

Fig. 1. A typical record of the experimental protocol. Bundles of three permeabilized fibers from fast rabbit muscle were activated at low temperature and then heated up from ~5°C to 25–27°C with a joule temperature jump [Tsaturyan et al., Biophys. J. 2011]. Diffraction patterns were taken at the steady level of isometric tension at the elevated temperature and after shortening when tension decreased to about a third of its isometric value.

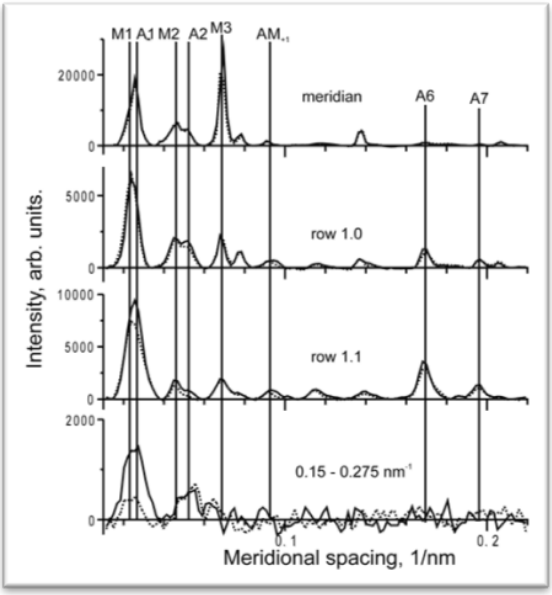

Fig. 2. X-ray intensity profiles at different reciprocal radii. Continuous lines: isometric contraction; dotted lines: shortening. Reflections of interest are labelled.

tropomyosin (Tpm) distribution from the "blocked" state (where myosin heads cannot bind actin) to the 'closed' state where they are able to bind actin weakly. In the subsequent shift to the "open" state, the heads bind actin strongly. As the model

was based on *in vitro* experiments, a question remains: whether reduction in the number of strongly bound myosin heads during shortening of contracting muscle can induce a return of Tpm distribution towards the 'closed' state.

We used x-ray diffraction at ID02 beamline at ESRF (Grenoble, France) to monitor changes in intensities of the actin layer lines upon transition from isometric contraction to steady shortening under low load which is known to decrease substantially the fraction of attached heads (see fig. 1 for details). X-ray diffraction pattern at the end of the shortening was compared to the isometric one (fig. 2).

During shortening the intensity of the myosin meridional M3 x-ray reflection decreased as well as the intensities of the A1 and A2 layer line within the 1.0 and 1.1 row lines and of the A6, A7 layer lines indicating a decrease in the number of myosin heads stereo-specifically bound to actin (fig. 2). However no decrease in the A2 intensity at reciprocal radii 0.15–0.275 nm^{-1} expected to accompany an "open" to "closed" transition was observed. The data suggest that myosin heads, which remain strongly bound to actin during shortening (about a half of their number during isometric contraction), are sufficient for keeping Tpm in the "open" state.

Supported by the Russian Foundation for Basic Research and ESRF.

THE INFLUENCE OF MYOFIBRILS ON MYOBLASTS IN CO-CULTURE WITH MACROPHAGES

I.V. Kravchenko, V.A. Furalyov, V.O. Popov

Bach Institute of Biochemistry, Research Center of Biotechnology of the Russian Academy of Sciences, 33, bld. 2 Leninsky Ave., Moscow 119071, Russia

There are many cell types participating in the processes of skeletal muscle regeneration and development of functional hypertrophy. Macrophages are one of the most important among them. Macrophages are able to secrete different compounds with opposite effects on myoblasts, cytotoxic on the one hand and mitogenic on the other hand. In our earlier works we have shown that myofibrils released from damaged muscle can take part in the process of muscle regeneration because they can stimulate the expression of growth factors in muscle cells. However the possible effects of myofibrils on macrophages present in muscle remain unexplored. The aim of this work was to investigate the influence of myofibrils on proliferation and differentiation of myoblasts in co-culture with macrophages.

No cytotoxic effects were observed in co-culture experiments as well as in experiments with incubation of cells with media conditioned by macrophages. Cell viability measured with trypan blue was more than 98%.

The influence of macrophages on myoblast proliferation was studied. In experiments with co-cultures of myoblasts and macrophages it was shown that macrophages significantly stimulated myoblast proliferation increasing the value of MTT reduction by 73% (fig. 1). In the presence of myofibrils the stimulating

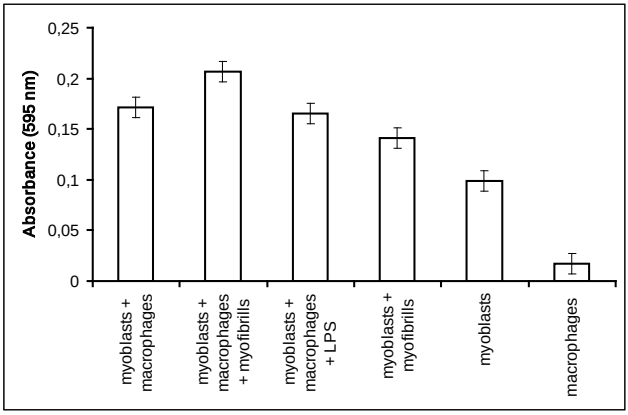

Fig. 1. Effect of co-culturing with macrophages on myoblast proliferation under exposure with myofibrils and LPS (measured by MTT-test).

effect was even stronger and achieved 109%. Both effects were statistically reliable. At the same time in the presence of lipopolysaccharide (LPS), a compound known as classical pathway macrophage activator, there were no stimulation of myoblast proliferation. Instead of it some tendency to inhibition of proliferation was shown: MTT reduction was decreased by 4% but the effect was statistically unreliable. It should be noted that macrophages by themselves made a very minor contribution to the total value of reduced MTT: the rate of MTT reduction in macrophage monoculture accounted for 17% of the value of this parameter in myoblast monoculture.

As we have shown previously myofibrils by themselves stimulate myoblast proliferation in culture, and under conditions of this experiment the stimulating effect achieved 42%. In this regard it was of great interest to investigate whether myofibrils activate the secretion of mitogenic for myoblasts compounds by macrophages or their mitogenic effect is caused by direct binding with myoblast receptors only. For this purpose we have studied the influence of culture media conditioned by macrophages under exposure with different compounds on myoblast proliferation, and we have compared the values stimulating effects of myofibrils and culture media conditioned by macrophages. It was established that culture medium conditioned by macrophages has statistically reliable stimulating effect on myoblast proliferation by itself: treatment with it increases the value of MTT reduction by 49% (fig. 2). Incubation of macrophages with myofibrils enhanced the mitogenic action of conditioned medium: the value of MTT reduction increased by 84%. At the same time the incubation of macrophages with LPS lead to the fact that they begin to secrete compounds inhibiting myoblast proliferation: MTT reduction was decreased by 21%. As we have mentioned above myofibril treatment of myoblasts by itself stimulate MTT reduction by 42%. All described effects were statistically reliable.

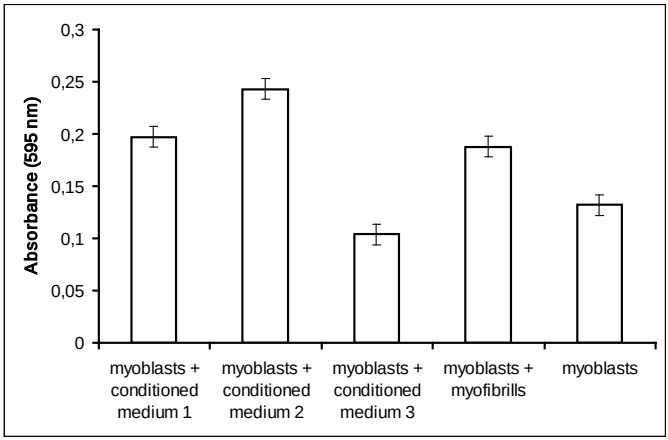

Fig. 2. Effect of media conditioned by macrophages treated with different compounds on myoblast proliferation (measured by MTT-test). 1 - medium conditioned by untreated macrophages, 2 - medium conditioned by macrophages treated with myofibrils, 3 - medium conditioned by macrophages treated with LPS.

For characterization of spectrum of secreted by macrophages proteins stimulating myoblast proliferation the fractioning of media conditioned by macrophages treated with different compounds by gel-filtration on Superdex 75 10/300 GL column was performed. It was shown that medium conditioned by untreated macrophages contained spectrum of activeting myoblast proliferation proteins different from medium conditioned by macrophages treated with myofibrils. Thus, medium conditioned by untreated macrophages contained myoblast proliferation activators in fraction including proteins with molecular mass 40–60 kDa, whereas the same fraction of medium conditioned by macrophages treated with myofibrils had no mitogenic activity. At the same time medium conditioned by macrophages treated with myofibrils contained myoblast proliferation activators in fraction including proteins with molecular mass 8–20 kDa, whereas the same fraction of medium conditioned by untreated macrophages had no mitogenic activity. Medium conditioned by macrophages treated with LPS did not contain fractions stimulating myoblast proliferation.

Then we have studied the influence of macrophages on myoblast differentiation. In experiments with co-cultures of myoblasts and macrophages it was shown that macrophages significantly inhibited myoblast differentiation: myogenic index decreased by half (fig. 3). In the presence of myofibrils the inhibitory effect was even stronger: myogenic index decreased 1.8-fold. Myofibrils by themselves demonstrated strong inhibitory effect and lowered myogenic index 2.7-fold.

Also we have studied the influence of culture medium conditioned by macrophages under exposure with myofibrils as well as conditioned by untreated macrophages on myoblast differentiation. To our surprise culture

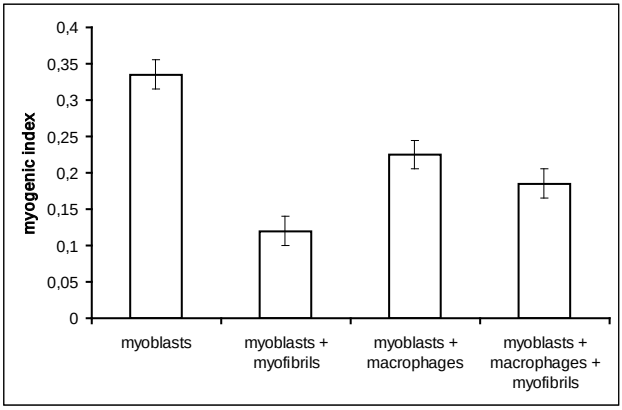

Fig. 3. Effect of co-culturing with macrophages on myoblast differentiation under exposure with myofibrils.

medium conditioned by untreated macrophages has no statistically reliable effect on the differentiation of murine macrophages (fig. 4). At the same time culture medium conditioned by macrophages under exposure withmyofibrils significantly inhibited myoblast differentiation: myogenic index decreased to 69% of the value observed in the culture of control myoblasts. The effect was statistically significant. The difference of effects of macrophages in co-culture and medium conditioned by untreated macrophages can be explained by secretion by macrophages of

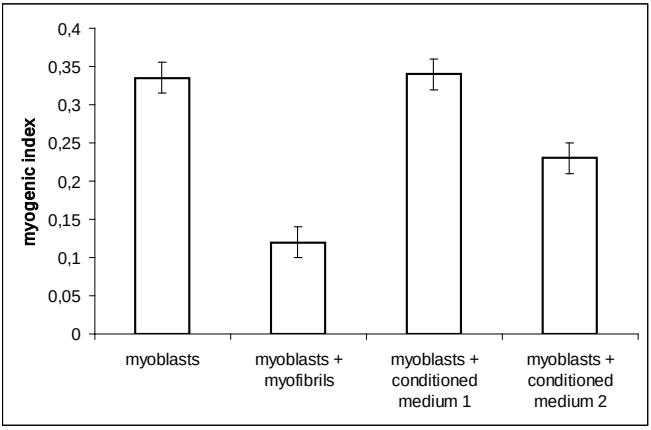

Fig. 4. Effect of media conditioned by macrophages treated with myofibrils or untreated macrophages on myoblast differentiation (measured by MTT-test): 1 – medium conditioned by untreated macrophages, 2 – medium conditioned by macrophages treated with myofibrils.

short-lived compounds inhibiting myoblast differentiation or by the influence on myoblast differentiation of direct cell-to-cell contacts.

The effects of myofibrils on myoblast proliferation and differentiation in co-culture with macrophages were studied. It was shown that macrophages by themselves stimulate myoblast proliferation and inhibit differentiation, and myofibrils enhance both effects.

These studies were supported by the grants from the Russian Foundation for Basic Research (15-04-06229a) and the Molecular and Cell Biology Program of the Russian Academy of Sciences, grant 6P.

INNERVATION OF PLANARIAN MUSCLATURE BY NEUROPEPTIDES OF NPFs AND FMRFs FAMILIES: POSSIBLE ROLE IN MUSCULAR FUNCTION?

N.D. Kreshchenko[1], A.V. Kuchin[1], O.O. Tolstenkov[2]

[1]*Institute of Cell Biophysics, Pushchino, Moscow region, Russia*

[2]*Severtsov Institute of Ecology and Evolution, Center of Parasitology, Moscow, Russia*

Free-living freshwater flatworms, planarians, (Tuirbellria, Platyhelminthes) are used as a biological model to study the processes of morphogenesis, regeneration and development. Planarians musculature serves for the locomotion, capturing and holding their food, feeding and reproductive behaviour. In several planarian species the morphological structure of their muscular system was investigated using electronic and fluorescent microscopy [McRae 1963; Bueno et al., 1997; Kreshchenko et al., 1999; Orii et al., 2002; Kreshchenko, 2010; Kreshchenko, 2012]. A little is known about the muscle function in these simple organisms. In present study the muscle structure has been visualized using histohemical staining of filametous actin by the fluorescently-labelled phalloidin. For the identification of nervous system elements in present study the immunostainings to neuropeptides NPF [Maule et al., 1991] and FMRF [Price, Greenberg, 1977; Johnston et al., 1996] have been applied with the special attention to its relationship with the muscle filaments in planarian body.

Methods

Planarians *Girardia tigrina* (Turbellaria, Dugesiidae) were kept hungry for one week before the experiment. Animals of 9-10 mm in length were flat fixed in 4% paraformaldehyde in phosphate-buffered saline (PBS). The whole-mount preparations were processed for histo- and immunostainings as follow: the incubation with primary antibody to neuropeptide NPF (kindly donated by prof. A.G. Maule, Belfast Queens University) or FMRF (Sigma), the washing in PBS-T (PBS with Triton X-100) and the incubation with secondary fluorescently labelled immunoglobulines (Daco). The samples then were washed in PBS and stained with TTRITC-labelled phalloidin (Sigma). After final wash they were mounted in 75% glycerol under the cover slips and examined with the confocal laser scanning microscope Leica TCS SP5 (Germany).

Results and discussion

The muscular system of planarian *G. tigrina* comprised of body wall musculature and somatic musculature, and was partly described previously [Kreshchenko et al., 1999; 2010]. The body wall musculature (fig. 1A,B) contains three

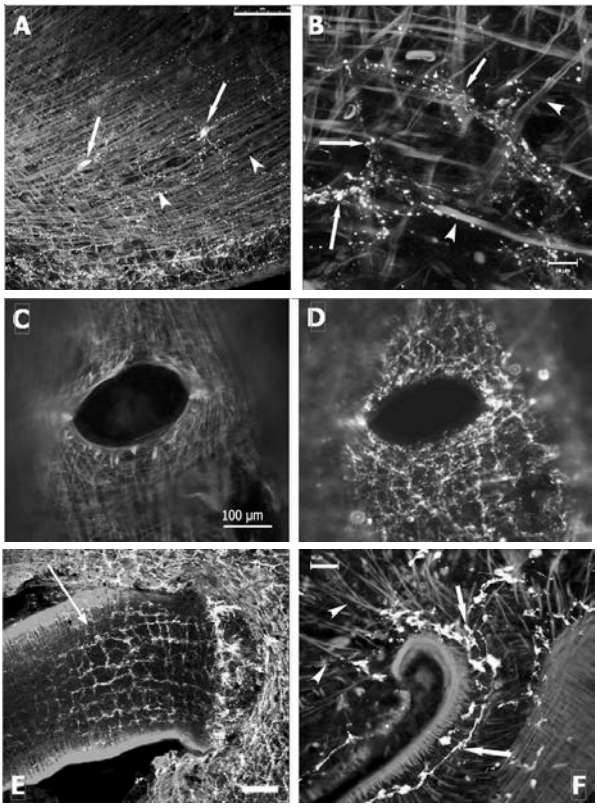

Fig. 1. Histohemical staining of the musculature with TRITC-labelled phalloidin (red) and immune positive staining to neuropeptides NPF (B, E) and FMRF (A, D, F) in the nerve cells and fibres of *G. tigrina* nervous system (green) are presented. Long arrows point the nervous element, arrowheads – the muscle elements. Scale bars: on A – 10 µm, B – 75 µm, F – 50µm, on C, E – 100µm.

A – a row of FMRF-IP multipolar neurons (arrows) situated in the depth of the muscles (arrowheads) with thin numerous nerve fibres running in different directions towards the muscle filaments comprising longitudinal muscle layer of the body wall musculature.

B – the longitudinal, circular and diagonal muscle fibres in body wall musculature surrounding by thin NPF-IP nerve fibres (arrows) with varicosities situated on/or nearby of the muscle filaments.

C – the sphincter muscles of the mouth opening which situate on the ventral side of the body, are comprising of circular, longitudinal and radial muscle fibres, rich-

ly innervating by FMRF-IP nerve fibres (D, green); several small neurons are visible in the vicinity of the mouth opening.

E – the tubular pharynx is situated in the pharyngeal cavity of planarian body with its densely packed muscle fibres, comprising the pharyngeal tube (arrow); a ladder-like net of NPF-IP elements innervating the pharyngeal muscle system and the anchoring muscles.

E – the anchoring muscles (arrowheads) innervated by FMRF-IP nerve fibres (green), connecting the pharynx with the body wall; the FMRF-IP neurons and its fibres observed inside of the muscular pharynx (arrows).

muscle layers: outer circular, inner longitudinal and diagonal muscles situated in between. Staining to phalloidin is found in muscle fibres connecting the dorsal and ventral body sides and in the transversal muscle filaments running from one to other lateral sides of the body.

Somatic musculature of *G. tigrina* comprises of the pharyngeal musculature, musculature of digestive tract, mouth opening and the anchoring muscles. Pharyngeal musculature is represented by inner circular, outer longitudinal and the radial muscle fibres (fig. 1E,F). The anchoring muscles (fig. 1E) connect the cylindrical muscular pharynx to the body wall musculature. The mouth opening situated on the ventral surface of the body is surrounded by the circular, diagonal and radial muscle fibres forming the muscular sphincter which serve for the pharynx movement out of the body during its pumping the food (fig. 1C,D).

The study revealed a close spatial relationship of peptidergic nerves and the musculature. The results show that the NPF- and FMRF-immunopositive (-IP) nerve elements takes part in the innervations of the body wall muscles and specific musculature in planarians (fig. 1A,B,D,E,F). FMRF–IP neurons with cell bodies (sizing from about 7 to 17μm) and numerous nerve fibres were found in pharyngeal musculature, in the anchoring muscles, mouth opening, in the body wall muscle layers (fig. 1A,E) and in the tail part of the body. NPF-IP nerve elements were identified in submuscular nerve net and in the pharyngeal tube (fig. 1B,D,F). Beside of that, the FMRF-like-immunoreactivity was well pronounced in planarian central nervous system [Kreshchenko, 2013].

Thus, histo- and immunocytochemical methods applied allowed characterizing the morphology of the musculature in the model flatworm *Girardia tigrina* and in conjunction with confocal laser scanning microscopy to disclose the details of its innervations by peptidergic elements of the planarian nervous system. The results indicate that the all muscular structures of the planarian body were richly supplied by FMRF-IR and NPF-IR nerve elements (pharynx, mouse opening, body wall musculature, tail region). Such identification of the NPF- and FMRF-IP neurons and its fibres close to the body wall and somatic muscles may indicate an important role of these neuropeptides in planarian muscle function.

The study is supported by RFBR grant № 15-04-05948a.

References

1. Bueno D., Baguna J., Romero R. 1997. Histochem. Cell. Biol., 107(2): 139-149.
2. Kreshchenko N., Reuter M., et al. 1999. Invert. Rep. Dev., 35(2): 109-125.

3. Kreshchenko N.D. 2010. Biological motility: from fundamental achievements to nanotechnologies, Pushchino, P. 142-145.
4. Kreshchenko N.D. 2012. Biological Motility: Fundamental and Applied Science, Pushchino, Moscow region, P. 93-96.
5. MacRae E.K. 1963. J. Cell Biol. 18: 651-662.
6. Orii H., Ito H., Watanabe K. 2002. Zool. Sci. 19(10): 1123-1131.
7. Maule A.G., Shaw C., et al. 1991.Parasitology. 12: 309–316.
8. Price D.A., Greenberg M.J. 1977. Science. 197: 670-671.
9. Johnston R.N., Shaw C., et al. 1996. J. Neurochem. 67: 814–821.
10. Kreshchenko N.D. 2013. Biologicheskie membrany. 30 (5-6): 430-437.

Na,K-ATPase AND SKELETAL MUSCLE MOTOR ACTIVITY

I.I. Krivoi

St. Petersburg State University, St. Petersburg, Russia

Investigations into the early molecular events which precede muscle atrophy are important for understanding the pathways involved in this disorder [Baldwin et al., 2013]. Mechanical unloading of skeletal muscle under conditions of bed rest, joint immobilization, spinal cord injury, weightlessness during space flight, simulated microgravity and other forms of disuse leads to loss of muscle mass, wasting and functional decline. While the Na,K-ATPase is critically important for excitability, electrogenesis, and contractility of skeletal muscle [Clausen, 2013], its possible role in disuse-induced muscle atrophy is not known.

The Na,K-ATPase is an ubiquitous plasma membrane integral protein detected in all types of animal cells. The Na,K-ATPase maintains the steep Na^+ and K^+ gradients across the cell plasma membrane that generate the resting membrane potential, provide electrical excitability and furnish the driving force for numerous other transport mechanisms. The Na,K-ATPase composed of α and β subunits as well as regulatory FXYD subunit. The α subunit is responsible for the catalytic and transport properties of the Na,K-ATPase. Four isoforms of the α subunit are known to exist in tissues of vertebrates. It is generally accepted that the ubiquitous $\alpha1$ isoform plays the main "house-keeping" role while the other isoforms expressing in a cell- and tissue-specific manner possess additional regulatory functions that are still poorly understood. The largest pool of Na,K-ATPase in a vertebrate's body is contained in the skeletal muscles where the $\alpha1$ and $\alpha2$ isoforms of α subunit are expressed as well as a muscle-specific auxiliary FXYD1 subunit (phospholemman). In cardiac and skeletal muscle, phospholemman associates with both Na,K-ATPase $\alpha1$ and $\alpha2$ isoforms. Some studies have shown that phospholemman acts as a brake on the Na,K-ATPase, while phosphorylation removes this brake and increases pump activity [Pavlovic et al., 2013].

The Na,K-ATPase is critically important for electrogenesis, excitability and contractility of skeletal muscle. Although the $\alpha2$ isoform is expressed in high abundance in skeletal muscle, the functional role and mechanisms of regulation of this isoform remain unclear and are now being intensively investigated [DiFranco et al., 2015].

Skeletal muscle functioning is essential for health and survival and it is well known that content of Na,K-ATPase strong depends on skeletal muscle motor activity: muscle activity increases Na,K-pump abundance while inactivity decreases it [Clausen, 2013]. Some data indicates that increased motor activity differently regulates α1 and α2 isoforms of the Na,K-ATPase. Whether skeletal muscle disuse induces isoform-specific changes in Na,K-ATPase functioning remains unclear.

Among animal models, hindlimb suspension (HS) of rodents by the tail is a well validated model that mimics many of the important effects of microgravity on the skeletal musculature and has provided insight into the underlying molecular and cellular mechanisms. HS induces progressive and marked atrophy of the postural skeletal muscles. EMG activity of the soleus muscle disappears immediately after the onset of HS, and reduced motor nerve activity is evident on neurogram [De-Doncker et al., 2005]. The animals show an initial, transient stress response during the first few days of adaptation to HS [Thomason, Booth, 1990]. Atrophy is evident after 3–7 and more days of HS, in association with dramatic phenotypic changes that include a slow-to-fast shift in myosin heavy chain expression and genetic re-programming. While these later events are well characterized, much less is known about the early molecular events which precede overt muscle atrophy. A number of results show that pre-mRNA and mature mRNA expression of muscle proteins and muscle-specific signaling factors are significantly reduced even after only 1 day of HS, suggesting that the protein imbalance is initiated rapidly [Baldwin et al., 2013]. Knowledge of the early molecular events induced by HS is needed to identify the important signaling pathways that lead to this disorder.

Latest data [Kravtsova et al., 2016] indicates that even acute disuse (6–12 h of HS) dynamically and isoform-specifically regulates the electrogenic activity, protein, and mRNA content of the Na,K-ATPase α2 isozyme in rat soleus muscle. The loss of α2 Na,K-ATPase activity results in reduced electrogenic pump transport and depolarized resting membrane potential. The decreased α2 Na,K-ATPase activity is caused by a decrease in enzyme activity rather than by altered protein and mRNA content, localization in the sarcolemma, or functional interaction with the nicotinic acetylcholine receptors. The loss of extrajunctional α2 Na,K-ATPase activity depends strongly on muscle use, and even the increased protein and mRNA content as well as enhanced α2 Na,K-ATPase abundance at this membrane region after 12 h of HS cannot counteract this sustained inhibition. In contrast, additional factors may regulate the subset of junctional α2 Na,K-ATPase pool that is able to recover during HS. Notably, acute, low-intensity muscle workload restores functioning of both α2 Na,K-ATPase pools. Multiple earlier disuse-induced remodeling events also include phospholemman phosphorylation (which is expected to stimulate the Na,K-ATPase) as well as its increased abundance and association with α2 Na,K-ATPase (which is expected to inhibit this isoform) (Kravtsova et al., 2016). In sum, these results demonstrate that the α2 Na,K-ATPase in rat skeletal muscle is regulated by motor activity and provide the

first evidence that acute disuse specifically alters the α2 Na,K-ATPase of rat soleus muscle with involvement of phospholemman-dependent regulatory mechanism.

Supported by RFBR #16-04-00562 and St. Petersburg State University research grant #1.38.231.2014.

References

Baldwin K.M., Haddad F., Pandorf C.E., Roy R.R., Edgerton V.R. (2013). Alterations in muscle mass and contractile phenotype in response to unloading models: role of transcriptional/ pretranslational mechanisms. Front Physiol 4: 284. doi: 10.3389/fphys.2013.00284.

Clausen T. (2013). Quantification of Na^+,K^+ pumps and their transport rate in skeletal muscle: Functional significance. J. Gen. Physiol. 142: 327–345.

De-Doncker L., Kasri M., Picquet F., Falempin M. (2005). Physiologically adaptive changes of the L5 afferent neurogram and of the rat soleus EMG activity during 14 days of hindlimb unloading and recovery. J. Exp. Biol. 208: 4585–4592.

DiFranco M., Hakimjavadi H., Lingrel J.B., Heiny J.A. (2015). Na,K-ATPase α2 activity in mammalian skeletal muscle T-tubules is acutely stimulated by extracellular K+. J. Gen. Physiol. 146: 281–294.

Kravtsova V.V., Petrov A.M., Matchkov V.V., Bouzinova E.V., Vasiliev A.N., Benziane B., Zefirov A.L., Chibalin A.V., Heiny J.A., Krivoi I.I. (2016). Distinct α2 Na,K-ATPase membrane pools are differently involved in early skeletal muscle remodeling during disuse. J. Gen. Physiol. 147: 175–188.

Pavlovic D., Fuller W., Shattock M.J. (2013). Novel regulation of cardiac Na pump via phospholemman. J. Mol. Cell. Cardiol. 61: 83–93.

Thomason, D.B., Booth F.W. (1990). Atrophy of the soleus muscle by hindlimb unweighting. J. Appl. Physiol. 68: 1–12.

ROLE OF Ca^{2+}-INDUCED Ca^{2+} RELEASE IN MAINTAINANCE OF CONTRACTILE FORCE IN SLOW *M. soleus* DURING TETANIC ACTIVITY

I.V. Kubasov, R. S. Arutyunyan, E.V. Matrosova, I.I. Kubasov

I.M. Sechenov Institute of Evolutionary Physiology and Biochemistry RAS, St.Petersburg, Russia

During direct stimulation of m. Soleus by train of 5, 10 and 50 stimuli with a frequency of 20 Hz in the control (n = 16) was observed a biphasic change in the amplitude of the last contractile responses (LCR_N) depending on N, where N is number of individual contractile responses within the tetanus. Thus, an initial decrease of LCR_N amplitude (up to 54±8% for LCR_5) was replaced by their subsequent growth (up to 218 ± 14% for LCR_{50}) associated with a significant shortening of the half-relaxation time in relation to the initial response (to 44±8% for LCR_{50}). Caffeine at concentrations of 5 mM (n = 6) and 10 mM (n = 4), while preserving the overall two phase character of the responses exacerbated LCR_5 depression during the initial inhibitory phase (31±8% and 15 ± 4%, respectively). The subsequent growth of LCR_N amplitude in the presence of caffeine was significantly lower than in the control (114 ± 18% and 46 ± 9% for LCR_{50} at 5 and 10 mM caffeine, respectively). LCR_{50} half-relaxation time during the action of both caffeine concentrations remained still con-

siderably shorter than the individual responses recorded either in the presence of caffeine or in control. In contrast to the control and caffeine effects, LCR_5 and LCR_{10} amplitude during the action of 10 μM of dantrolene (n = 5) remained at the level close to the value of the first response (102±7% and 106 ± 8%, respectively), and LCR_{50} amplitude demonstrated a significantly smaller increase (to 143 ± 14%) than was observed in the control muscle. Additionally, dantrolene enhanced muscle relaxation at rest. Caffeine (10 mM) restored the dynamics of changes of amplitude-time characteristics of the last contractile responses caused by dantrolene to values close to the control. The amplitude-time characteristics of the extracellular AP registered in individual muscle fibers in *m. soleus* did not significantly changed during the transition from single to the tetanic stimulation using a protocol similar to that used for mehanografical experiments. These data can be interpreted to support the previously suggested theory about the participation of "Ca^{2+}-dependent Ca^{2+} release" as an additional mechanism of excitation–contraction coupling in skeletal muscle under conditions of tetanic stimulation.

This work was supported by grant Russian Science Foundation N15-15-20008.

THE ROLE OF MYOGLOBIN NITRITE-REDUCTASE ACTIVITY IN MAMMALIAN ADAPTATION TO HYPOXIA

N.V. Kuleva, I.E. Krasovskaya, T.E. Shumilova

St.-Petersburg State University,
Universitetskaya nab.7/9, St.-Petersburg, 199034

Myoglobin (Mb) is one of the most investigated cytosolic proteins of muscle tissue. It is expressed in muscle organs of terrestrial animals (3-10 mg for 1 mg of wet weight) and much more in ones of marine diving mammals (10–95 mg for 1 g of wet weight).. This protein is considered as the representative of globin protein family specific especially for muscle. The only polypeptide chain of Mb consists of 146–153 amino acid residues and has folded structure typical for globin proteins. Its most known functions are the oxygen storage and transport from sarcolemma to mitochondria of skeletal and cardiac muscle cells in nearly all vertebrates. Sperm whale myoglobin was the first protein whose structure had been investigated with X-ray analysis and since 1959 year it had used as the best model for studying structure-function relations in proteins.

During 15 passed years of this century our knowledge of functional role of myoglobin has substantially expanded. Myoglobin has appeared to fulfil functions different from oxygen storage and facilitated diffusion, including the removal and production *in vivo* of nitric oxide (NO), one of the main signaling molecules which plays a critical role in the control of oxygen consumption, vasodilatation and protection against reactive oxygen species (ROS). It has been shown that myoglobin could be expressed in non-muscle cells: blood vessel endothelium, brain and liver and may have different isoforms in the same species. Furthermore, myoglobin functional properties (O_2 affinity and nitrite-reductase enzymatic activity) appeared

to correlate with the species physiology and metabolic demands, including the tolerance to hypoxia-for fish and diving mammals [Helbo et al., 2013].

So, in our days the event analogous to discovery of myosin in non-muscle cells has happened with myoglobin. Therefore this report is devoted to new-discovered properties of myoglobin and new-discovered mechanisms of myoglobin participation in mammalian adaptation to hypoxia.

Under hypoxia cells produce NO without participation of oxygen-dependent NO-synthases (as under normoxia), but from endogenic NO_2^- due to nitrite-reductase enzymatic activity. The main nitrite-reductases are heme-containing globin proteins of vertebrates: hemoglobin, myoglobin, cytoglobin, neuroglobin and others, in which at the beginning of our century nitrite-reductase activities had been discovered [Shiva et al., 2007]:

$$NO_2^- + \text{deoxyMb}(Fe^{2+}) + H^+ \rightarrow \text{MetMb}(Fe^{3+}) + NO,$$

where deoxyMb(Fe^{2+}) – deoxymyoglobin and MetMb (Fe^{3+}) –metmyoglobin

Nitrite-reductase activity was revealed only at hypoxia, when globins are in deoxygenated form. In conditions of normoxia globins could act as dioxygenases by transforming NO into NO_3:

$$\text{oxyMb}(Fe^{2+}) + NO \rightarrow \text{MetMb}(Fe^{3+}) + NO_3$$

It was stated that at normoxia dioxygenase activity of myoglobin played an important role by supporting functions of mitochondrial electron-transporting chain (ETC) as this reaction removes NO excess which could bind to cytochrome c oxidase and to inhibit it. Finally, it could result in decrease of ATP production what decreases of heart and muscle contractility.

At acute hypoxia O_2 diffuses from myoglobin (which became deoxygenated) and Mb transforms into chemical reactor: it reduces nitrite to NO 60 times faster than deoxyhemoglobin. Special experiments evidenced that in myocardium during hypoxia or ischemia Mb really revealed nitrite-reductase properties. Knocking out of this function in knock-out for Mb mice has appeared more dangerous than knocking out of O_2 binding.

At moderate hypoxia NO produced by myoglobin regulates energetics and functioning of muscle by means of decrease of O_2 consumption at hibernation of terrestrial animals in response to deficit of food and temperature decrease and during diving of marine mammals.

During reperfusion of myocardium after ischemia (or reoxygenation after diving) nitric oxide produced by myoglobin nitrite-reductase interacts with complex 1 of mitochondrial ETC and could nitrosylate its sulfhydryl groups. This results in decreasing of the functional activity and limits ROS generation by ETC, increasing in such way viability of myocardial cells [Shiva, 2010].

Plausibility for Mb to function as a nitrite reductase and to fight against ROS is supported by the data about the absence of oxidative modifications in water soluble proteins of rat heart after moderate nitrite hypoxia [Kuleva et al., 2014].

At modeling of myocardial infarction the injection of small concentration of nitrite into rat (that increase myoglobin nitrite-reductase activity) resulted in de-

creasing of infarction size and improvement of myocardial function [Hendgen-Cotta et al., 2008].

Nitrite-reductase activity was demonstrated *in vivo* in endothelial myoglobin of blood vessels .Produced NO activates canonical soluble guanylate cyclase/cGMP signaling pathways. It plays key role in regulation of hypoxic vasodilatation of vessels and explains about 50% of vasodilatation [Totsek et al., 2012]. In a mice having deficit for Mb nitrite- induced effects (vasodilatation and decreasing of blood pressure) were decreased or absent.

More detailed description of enzymatic properties of Mb and other heme-containing globin proteins is presented in review [Kuleva, Krasovskaya, 2015, Tsitologia v.57, №8, p.563-571].

These enzymatic properties of Mb could contribute into extreme tolerance to internal hypoxia in whales during long-term diving. When 5 species of whales with different diving time were studied and the data were compared with similar data for other species of cetaceans studied before [Helbo, Fago, 2012] it was shown that some difference between myoglobin of different species was really exists on O_2-binding , nitrite-reductase and peroxidase activities, but these variations did not correlated to average time of diving. Rather, they may reflect phylogeny and the difference in foraging behavior of cetaceans as the most significant difference was revealed between toothe and baleen whales, toothed whales having higher O_2 affinity and nitrite reductase activity. .

Average time and depth of diving strongly correlates to myoglobin concentration in muscle tissue of whales and this correlation results in high increase of total activity of myoglobin in organism *in vivo* (including capability to store O_2 and reduce NO_2 into NO). This may increase in high degree the time of diving of long-time diving animals. Therefore. diving duration is rather determined by myoglobin content in organism than myoglobin specific functional reactivity as nitrate-reductase.

It is interesting that terrestrial mammals living in high-land (for example, camelides) and adapted to chronic hypoxia have increased level of myoglobin in their skeletal muscle as compared with their relatives living in low-land (cited according to [Helbo et al, 2013]).

Thus, total nitrite-reductase activity of myoglobin in whole organism may be one of factors determining hypoxia tolerance in mammals.

H_2S INHIBITED HIPPOCAMPAL NETWORK ACTIVITY IN NEWBORN

E.D. Kurmasheva, A.V. Yakovlev, G. F. Sitdikova

Department of Human and Animal Physiology, Institute of Fundamental Medicine and Biology, Kazan Federal University, Kremlevskaya str. 18, Kazan , 420008, Russia

Hydrogen sulfide (H_2S), produced by the desulfuration of cysteine or homocysteine, functions as a signaling molecule in an array of physiological processes. In the nervous system H2S induces long-term potentiation in the hippocampus modulates neuronal excitability of subfornical organ, the nucleus of the solitary

tract and trigeminal neurons, modulates transmitter release as well as exo- and endocytosis of synaptic vesicles in motor nerve endings [Abe and Kimura, 1996, Malik and Ferguson, 2015, Chen et al., 2013; Gerasimova et al., 2015]. H_2S action is critically dependent from its concentration and cellular location: high H_2S concentrations may lead to a complete inhibition of cell respiration, mitochondrial depolarization and superoxide generation, whereas low physiological concentration exerts antioxidative effects [Wedmann et al., 2014]. It was shown that H_2S can change neuronal excitability through modulation of Na^+ channels [Kuksis and Ferguson, 2015] and different types of K^+ channels [Pan et al., 2010; Mustafina et al., 2015], Cl^- channels [Tang et al., 2010] and Ca^{2+} channels [Kukis and Ferguson, 2015]. In spite of the increasing acceptance of hydrogen sulfide as a neuromodulator and of the reported alterations of neuronal excitability, there is no report on the putative alterations of in hippocampi neurons. The aim of our research to examine the influence of H_2S on the voltage-dependent Na^+ currents and K^+ currents, since such currents are an important factor in the regulation of excitability.

Experiments were performed on neonatal Wistar rats (postnatal days P3–P7). The work has been carried out in accordance with EU Directive 2010/63/EU for animal experiments and all animal-use protocols were approved and Kazan Federal University on the use of laboratory animals (ethical approval by the Institutional Animal Care and Use Committee of Kazan State Medical University N9-2013). After isolation, the rat brains were placed into a cooled oxygenated artificial cerebrospinal fluid (ACSF) of the following composition (in mM): NaCl 126; KCl 3.5; $CaCl_2$ 2.0, $MgCl_2$ 1.3, $NaHCO_3$ 25, NaH_2PO_4 1.25 and glucose 10, (pH 7.4). Horizontal slices (400 μm thick) were cut using a HM 650 V vibratome (Microm International, Germany). All recordings were made from the CA3 pyramidal cell layer under visual control by means of an Axio Examiner A1 microscope (400×, Carl Zeiss, Germany) using differential interference contrast and patch-clamp amplifier Axopatch 200B (Axon Instruments, USA). For whole-cell recordings electrodes filled with either 135 mM potassium gluconate solution contained (mM): $CaCl_2$ – 0.1, EGTA – 1, HEPES – 10, NaATP – 2 and NaGTP – 0.4 (pH 7.25), osmolarity 290 mOsm, with the pH adjusted to 7.3 with CsOH or KOH. To study Na^+ currents a voltage clamp protocol was used with depolarizing test pulses of 250 ms duration which were applied at 10 mV increments from −70 to +40 mV from a holding potential of –75 mV using cesium methylsulphate based pipette solution and TEA 2 mM in external solutions. Current–Voltage (*I–V*) relationships were constructed from measurements of peak inward currents. To estimate an inactivation profile of Na^+ currents we used an inactivation step protocol by holding neurons at -75 mV, inducing 100 ms voltage steps from –110 to –20 mV at 10 mV increments and then finally stepping the voltage to the test potential of –10 mV for 500 ms where the measurement was taken. To study K^+ currents a voltage clamp protocol was used with depolarizing test pulses of 250 ms duration which were applied at 10 mV increments from −130 to +40 mV from a holding potential of –75 mV using potassium gluconate based pipette solution and TTX (1 μM) in external solutions. Current–voltage (*I–V*) relationships were constructed from measure-

ments of current amplitudes at the end of the 250 ms test pulses. The signals were digitized using an analog-to-digital converter (Digidata 1440A, Axon Instruments, Molecular Devices, USA). PClamp10.3n (Axon Instruments, USA), and Origin 8.5 (OriginLab Corporation, USA) programs were used for acquisition and analysis of electrophysiological data. Group measurements are expressed as mean ± SEM; error bars through data points indicate SEM. The statistical significance of differences was assessed with Student's *t*-test. The level of significance was set at $p < 0.05$. For a source of H_2S was used sodium hydrosulfide (NaHS, Sigma-Aldrich, USA) and in solution this compound dissociates to give HS^- which associates with H^+ to produce H_2S. Our previous experiments indicate that from base concentration of NaHS, only 11–13% is effective as H_2S in solution when taking pH, temperature, salinity of the perfusate and evaporation of H_2S into account [Sitdikova et al., 2014]. Stock solutions of NaHS were prepared immediately before each experiment and kept hermetically sealed in a dark place. In control conditions a current peak of I_{Na} activation was observed at –30 mV with amplitudes of 1.4 nA and the voltage of half-maximal activation were –35 mV mV ($n = 8$). Bath application of 100 μM NaHS induced a rightward shift of I_{Na} activation current peaks at –10 mV without changing the amplitude of inward currents. The voltage of half-maximal activation also shifted to close 0 mV and were –11 mV ($n = 7$). Application of an inactivation step protocol revealed a rightward shift of the inactivation curve in response to 100 μM NaHS. It was shown that half-maximal inactivation shifted in average from –47 mV ($n = 8$) compared to control conditions with –29 ($n = 7$, $p<0.05$) after NaHS application. Thus NaHS did not influence the I_{Na} amplitude but induced a rightward shift of the activation curve which in turn increases the threshold of action potentials and decreases excitability. Bath application of TTX (1 μM) did not prevent NaHS-induced depolarization of the membrane potential of CA3 pyramidal neurons.

Also NaHS had effects on the K^+ channels of hippocampal neurons. So, bath application of NaHS induced the reduction of outward K^+ currents at voltages from +5 to + 40 mV ($n=3$, $p<0.05$) and these effects were prevented by preliminary application of TEA (5 mM).

So in hippocampal CA3 neurons NaHS reduced outward potassium currents which may underlie the neuron's depolarization. Also H_2S induced rightward shift of activation and inactivation of Na^+ current thus decreasing neuronal excitability and preventing network activity. In conclusion, our experiments reveal a potential neuromodulatory role of H_2S in the nervous system by direct regulation of ion channels.

The work was supported by Russian Science Foundation, grant 14-15-00618.

References

Abe K, Kimura H (1996) The possible role of hydrogen sulfide as an endogenous neuromodulator. J Neurosci 16:1066–1071.

Chen L, Zhang J, Ding Y, Li H, Nie L, Yan X, Zhou H, Zheng Y (2013) KATP channels of parafacial respiratory group (pFRG) neurons are involved in H2S-mediated central inhibition of respiratory rhythm in medullary slices of neonatal rats. Brain Res 1527: 141-148.

Gerasimova E, Lebedeva J, Yakovlev A, Zefirov A, Giniatullin R, Sitdikova G (2015) Mechanisms of hydrogen sulfide (H2S) action on synaptic transmission at the mouse neuromuscular junction. Neurosci 303:577-585.

Kuksis M, Ferguson AV (2015) Actions of a hydrogen sulfide donor (NaHS) on transient sodium, persistent sodium, and voltage-gated calcium currents in neurons of the subfornical organ. J Neurophysiol 114:1641–1651.

Malik R, Ferguson AV (2015) Hydrogen sulfide depolarizes neurons in the nucleus of the solitary tract of the rat. Brain Res pii: S0006-8993(15)00968-3.

Mustafina AN, Yakovlev AV, Gaifullina ASh, Weiger TM, Hermann A, Sitdikova GF (2015) Hydrogen sulfide induces hyperpolarization and decreases the exocytosis of secretory granules of rat GH3 pituitary tumor cells. Biochem Biophys Res Commun 465(4):825-31

Pan JG, Hu HY, Zhang J, Zhou H, Chen L, Tang YH, Zheng Y (2010) Protective effect of hydrogen sulfide on hypoxic respiratory suppression in medullary slice of neonatal rats. Respir Physiol Neurobio 171:181-186.

Sitdikova GF, Fuchs R, Kainz V, Weiger TM, Hermann A (2014) Phosphorylation of BK channels modulates the sensitivity to hydrogen sulfide (H2S). Front Physiol 12:431.

Tang G, Wu L, Wang R (2010) Interaction of hydrogen sulfide with ion channels. Clin Exp Pharmacol Physiol 37(7):753–763.

Wedmann R, Bertlein S Macinkovic I, Böltz S, Miljkovic JL, Muñoz LE, Herrmann M, Filipovic MR (2014) Working with "H2S": facts and apparent artifacts. Nitric Oxide 41:85-96.

INTERDOMAIN INTERACTIONS THAT MAY OCCUR IN THE MYOSIN HEAD DURING ATPase CYCLE

D.I. Levitsky[1,2], D. Logvinova[1,3], D. Markov1, O. Nikolaeva[2]

[1]*A.N. Bach Institute of Biochemistry, Research Center of Biotechnology of the Russian Academy of Sciences, Moscow, Russia*

[2]*A.N. Belozersky Institute of Physico-Chemical Biology, Moscow State University, Russia*

[3]*Department of Biochemistry, School of Biology, Moscow State University, Moscow, Russia;*

Myosin head (myosin subfragment 1, S1) consists of two major structural domains, the motor (or catalytic) domain and the regulatory domain, and functioning of the myosin head as a molecular motor is believed to involve a rotation of the regulatory domain (lever arm) relative to the motor domain during the ATPase cycle. According to predictions, this rotation can be accompanied by an interaction between the motor domain and the C-terminus of the essential light chain (ELC) associated with the regulatory domain [1,2]. To check this assumption, we applied differential scanning calorimetry (DSC) combined with temperature dependences of fluorescence to study the changes in the thermal unfolding and the domain structure of S1, which occur upon formation of the ternary complexes S1-ADP-AlF_4^- and S1-ADP-BeF_x that mimic the S1 ATPase intermediate states $S1^{**}$-ADP-P_i and $S1^{*}$-ATP, respectively. To identify the thermal transitions on the DSC profiles (i.e. to assign them to the structural domains of S1), we

compared the DSC data with temperature-induced changes in fluorescence of either tryptophan residues, located only in the motor domain, or recombinant ELC mutants (light chain 1 isoform), which were first fluorescently labeled at different positions in their C-terminal half and then introduced into the S1 regulatory domain. We showed that formation of the ternary complexes S1-ADP-AlF_4^- and S1-ADP-BeF_x significantly stabilize not only the motor domain, but also the regulatory domain of the S1 molecule implying interdomain interaction via ELC [3]. These results indicate that in the S1-ADP-AlF_4^- and S1-ADP-BeF_x complexes not only the regulatory domain and the motor domain are located close to each other due to rotation of the regulatory domain, but tight interaction may occur between both these domains of the myosin head. Thus, we suggest that during the ATPase cycle the myosin head undergoes global changes in its domain structure, which are expressed in the tight coupling between the two main parts of the head, the motor domain and the regulatory domain. It seems likely that this interaction between the two domains, which probably occurs during the ATPase cycle, may play a crucial role in functioning of the myosin head as a molecular motor. For instance, the immobilization of the lever arm on the surface of the motor domain may be important for stabilization of the pre-power stroke state of the myosin head in the course of the ATPase cycle. This is consistent with the previously proposed concepts and also reveals new interesting details of the molecular mechanism of the myosin ATPase cycle.

This work was supported by RFBR (grant 15-04-03037) and by the Program “Molecular and Cell Biology” of Russian Academy of Sciences.

References

1. Borejdo J., Ushakov D.S. Moreland R., Akopova I., Reshetnyak Y., Saraswat L.D., Kamm K. & Lowey S. (2001) “The power stroke causes changes in the orientation and mobility of the termini of essential light chain 1 of myosin”. Biochemistry 40, 3796–3803.
2. Dominguez R., Freyzon Y., Trybus K.M. & Cohen C. (1998) “Crystal structure of a vertebrate smooth muscle myosin motor domain and its complex with the essential light chain: visualization of the pre-power stroke state”. Cell 94, 559–571.
3. Logvinova D.S., Markov D.I., Nikolaeva O.P., Sluchanko N.N., Ushakov D.S., & Levitsky D.I. (2015) “Does interaction between the motor and regulatory domains of the myosin head occur during ATPase cycle? Evidence from thermal unfolding studies on myosin subfragment 1” PLoS ONE 10(9): e0137517. (doi:10.1371/journal.pone.0137517)

COMPARATIVE ULTRASTRUCTURAL ANALYSIS OF RIGHT AND LEFT VENTRICLE CARDIOMYOCYTES OF OLD JAPANESE QUAILS *Coturnix japonica*

T.V. Lipina, N.B. Serezhnikova, L.S. Pogodina

Biological Faculty, Lomonosov Moscow State University, Leninskie Gori, 1, Moscow, 119991, Russia

Nowadays many studies in gerontology aim at search and comparative evaluation of animal models for aging, not only mammalian. Japanese quail

Coturnix japonica is characterized by quick natural aging, so it can be one of potential model for research in this field. *Coturnix japonica* is a perspective object for retina age-related changes research because its retina structure is similar with human one. Subcellular aging markers of retina as well as choroid changes were described, which are general both for quails and mammals [Seryozhnikova et al., 2013; Sigaeva et al., 2015].

One of major problems of elderly patients – cardio-vascular diseases, so it is important to find animal model with similar to human features at heart during aging. Recently we studied left ventricle cardiomyocyte of 48–55 weeks old quails (that is equal to 70 years of human life); it was found that their heart structural changes were similar to primary aging changes in mammalian myocardium [Lipina et al., 2014]. But it is necessary to analyze more old bird hearts and also different myocardial parts for adequate estimation of this model.

So in present work the structure of left and right ventricle myocardium of 78-weeks old female *Coturnix japonica* was studied. Birds were kindly provided by Department of Photochemistry and Photobiology, Group of Visual adaptation at Emanuel Institute of Biochemical Physics of RAS. For transmission electron microscopy muscle fibers at the heart apex region were fixed in a mixture of 2.5% glutaraldehyde and 2% formaldehyde in 0.1 M PBS, post-fixed in osmium tetroxide, treated according to the standard method, and embedded in Epon 812. Ultrathin sections of predominately longitudinal cardiomyocyte fibers were contrasted with 2%- uranylacetate and citrate lead by Reynolds, analyzed using microscopes JEM-100B and JEM-1011.

Electron-microscopic study revealed that cardiomyocytes of both ventricles had one or two nuclei, located among myofibrils. The majority of nuclei had elongate shape and invaginated borders in cardiomyocytes of left and right ventricles, smooth nuclear edges were rarely seen. Very irregular nuclear forms were more frequently seen in left ventricle. Unfortunately, this feature can't be used as aging marker, as such nuclei are typical for quail and other bird cardiomyocytes regardless of age [McKenzie et al., 1972; Lipina et al., 2014]. But in mammals similar nuclei appeared only under pathology conditions [Michailov et al., 2001].

Contractile apparatus was formed by well-defined myofibrils, organized in parallel rows, they occupy major part of cytoplasm, their pattern was the same as in younger birds. Myofibril thickness was visually larger in left ventricle. However some disorders were noted, such as local myofibril thinning, disturbed parallel alignment of myofibrils at several regions of both ventricles. Such changes were reported for mammalian cardiomyocytes under different pathology conditions, including age-related heart failure [Nepomnyashchikh, 1991].

Mitochondria are well-known as very polymorphous heterogeneous organelles, in bird cardiomyocytes of different ages their profiles are rounded, elongated, rod-like, less frequently convoluted and irregular. Their ultrastructure in old quail heart is in general normal in both ventricles: matrix of medium electron density and numerous lamellar cristae. But some condensed mitochondria with increased electron-density matrix were observed in old heart. Besides, several groups

of mitochondria with densely packed deformed cristae were found in old left ventricle. Such mitochondria were absent in cardiomyocytes of young and mature birds. As a rule mitochondria profiles in quail heart muscle don't exceed 1 sarcomere (about 2 μm), but their length in old bird cardiomyocytes was sometimes more than 3 sarcomeres (> 6 μm), such organelles had normal ultrastructure in left and right ventricle. Our recent studies revealed increased number of elongated mitochondria profile in left ventricle of 47–52-weeks old birds [Lipina et al., 2014], so this reaction is typical for mature and very old quails. Such profile elongation was reported in human cardiomyocytes during aging and cardiovascular diseases [Hom, Sheu, 2009]. The number of mitochondria with increased sizes also raised in the pigment epithelium of the quail retina [Seryozhnikova et al., 2013], so this sign can be considered as a universal marker of age-related changes for organs with high oxidative stress (as eye and heart). A possible connection between eye and heart pathologies was demonstrated [Flammer et al., 2013], therefore comparative studies of aging in these organs have become more interesting.

The age pigment lipofuscin is a well-known cell aging marker. Its excessive accumulation compromises cell function, but the exact mechanism of this action is still unclear. Lipofuscin granules in old quail's cardiomyocytes of both ventricles were electron-dense heterogeneous structures, not only scattered in cytoplasm as in younger bird cardiomyocytes, but also clustered. Sometimes these clusters contained up to 8 granules, several granules exceeded mitochondria in length and width; that was never noted in 47–55 weeks old and younger quails. In mammalian heart muscle cells lipofuscin accumulation is usually associated with mitochondria, especially with enlarged mitochondria, with distorted cristae [Terman et al., 2004]. We found the same picture for quail myocardium.

Some myelin-like structures characterized by many concentric layers of membrane were observed in cytoplasm of left and right ventricle cardiomyocytes of 78-weeks old birds, they appeared more often and had larger size in left ventricle. These structures as well as the appearance of long mitochondria may indicate impairment of mitochondria utilization during aging [Terman et al., 2004].

Thus, our ultrastructural research showed that left and right ventricle cardiomyocytes of 78 weeks old Japanese quail *Coturnix japonica*, in comparison with younger birds, characterized by local disorganization of myofibrils, increased number of elongated mitochondria profiles, large lipofuscin accumulations, significant number of myelin-like structures. There was no obvious difference between left and right ventricles. Such structural quail myocardial reaction has much in common with changes in human heart during aging and some cardiovascular pathologies. So quail *C. japonica* could serve as one of the models for cardiovascular age-related research. But further studies, including morphometrical analysis, are necessary for proving validity of this animal model.

References

N. B. Seryozhnikova, P. P. Zak, L. S. Pogodina, N. N. Trofimova, T. V. Lipina, M. A. Ostrovsky. // Moscow University Biological Sciences Bulletin. 2013. V. 68. P. 149–155.

Sigaeva A. O., Seriozhnikova N. B., Pogodina L. S., Trofimova N. N., Gur'eva T. S., Zak P. P. // Sensornye sistemy. 2015. V. 29. P. 354-361.

T.V. Lipina, M.S. Dukhinova, N.B. Serezhnikova, L.S. Pogodina, Yu.S. Chentsov. // Doklady Biological Sciences. 2014. V.458. P. 295-297.
McKenzie B.E., Easterday B.C., Will J.A. // Am J Pathol. 1972. V.69. P.239–254.
Hom J., Sheu S.S. / / J Mol Cell Cardiol. 2009. V.46. P. 811–820.
Mikhailov, V.M., Komarov, S.A., Nilova, V.K., Shtein, G.I., and Baranov, V.S., // Tsitologiya, 2001, v. 43, P.729–733.
Nepomnyashchikh, L.M., Morfologiya vazhneishikh obshchepatologicheskikh protsessov v serdtse (The Morphology of the Most Important General Pathological Processes in the Heart), Novosibirsk: Nauka, 1991
J. Flammer, K. Konieczka, R. M. Bruno, A. Virdis, A.s J. Flammer, S. Taddei. // European Heart Journal. 2013. 34, 1270–1278.
Terman A., Dalen H., Eaton J.W., Neuzil J., Brunk U.T. // Ann. N.Y. Acad. Sci. 2004. 1019. P. 70-77.

PROPOSED INTERMOLECULAR AND INTRAMOLECULAR INTERACTIONS OF THE N-TERMINAL SEGMENT OF MYOSIN "ESSENTIAL" LIGHT CHAIN-1 WITH THE MOTOR DOMAIN OF MYOSIN HEAD

D. Logvinova[1,2], O. Nikolaeva[3], D.I. Levitsky[1,3]

[1]*A.N. Bach Institute of Biochemistry, Research Center of Biotechnology of the Russian Academy of Sciences, Moscow, Russia;*

[2]*Department of Biochemistry, School of Biology, Moscow State University, Moscow, Russia*

[3]*A.N. Belozersky Institute of Physico-Chemical Biology, Moscow State University, Russia*

In the previous works [1,2], we compared thermally induced denaturation and aggregation of two isoforms of the isolated myosin head (myosin subfragment 1, S1) containing different "essential" (or "alkali") light chains, A1 or A2. These light chains are nearly identical, except for first 41 additional amino acid residues of the A1 light chain, containing repeated Ala-Pro sequence and two pairs of lysine residues located near the *N*-terminus. The functional significance of this *N*-terminal extension of the A1 light chain is currently under investigation. It was shown by many authors that at low ionic strength the affinity of S1 containing light chain A1 (S1(A1)) for actin is significantly higher than that of S1 containing light chain A2 (S1(A2)), and this is due to direct interaction of the *N*-terminal extension of the A1 light chain with actin. Another interesting property of the A1 N-terminal extension is its putative ability to interact, at relatively low ionic strength, with the globular motor domain of the myosin head [3,4].

No appreciable differences were observed between the S1(A1) and S1(A2) in their thermal unfolding studied by differential scanning calorimetry (DSC) [1,2]. On the other hand, a significant difference between the two S1 isoforms was revealed in the temperature dependencies of their aggregation measured at low ionic strength. Under these conditions, the aggregation of S1 containing light chain A1 (but not A2)

was strongly dependent on protein concentration, the increase of which shifted the aggregation curve towards the lower temperatures [2]. It was concluded that these unusual aggregation properties of S1(A1) at low ionic strength are basically determined by intermolecular interactions of the N-terminal extension of the A1 light chain (which is absent in the A2 light chain) with other S1 molecules, and these interactions seem to be independent of the S1 thermal denaturation as they may take place even at low temperature [2].

In the present work, we applied other methods and approaches to investigate in more detail the intermolecular interactions of the N-terminal extension of the A1 light chain leading to unusual aggregation of S1(A1) at low ionic strength. We applied dynamic light scattering (DLS) which allows determining the size of particles formed in the process of protein aggregation by measuring the hydrodynamic radius (R_h) of these particles. Moreover, we compared by DLS the properties of S1(A1) and S1(A2) not only in the absence of added nucleotides, but also in the presence of ADP and in the ternary complexes S1-ADP-AlF_4^- and S1-ADP-BeF_x which mimic the S1 ATPase intermediate states $S1^{**}$-ADP-P_i and $S1^{*}$-ATP. The DLS experiments were performed at relatively low temperatures, either before the thermal unfolding of the protein or at the initial stages of this process. Under these conditions, we observed a significant growth in the R_h value for S1(A1), with no R_h changes for S1(A2). For instance, after 15 min heating at 35°C, the R_h value for S1(A1) attained ~800 nm, whereas the R_h for S1(A2) remained unchanged and equal to ~16–20 nm. Only 15–20% of S1(A1) molecules precipitated upon ultracentrifugation after such a heating, as was shown by SDS/PAGE analysis of supernatants and pellets. Similar although less pronounced difference between S1(A1) and S1(A2) in their aggregation properties was observed by DLS in the presence of ADP. In contrast, no differences in the aggregation properties were observed by DLS between these two S1 isoforms in their ternary complexes S1-ADP-AlF_4^- and S1-ADP-BeF_x.

We propose the following explanation for the results obtained. During the ATPase cycle, when the myosin head undergoes to considerable conformational changes, the N-terminal extension of the A1 light chain can form a contact with the motor domain of the same S1 molecule, which may be important for immobilization of this extension on the surface of the motor domain and stabilization of the pre-power stroke state of the myosin head. This intramolecular interaction can explain why the two S1 isoforms, S1(A1) and S1(A2), in the ternary complexes S1-ADP-AlF_4^- and S1-ADP-BeF_x do not differ from each other in their aggregation properties. In the absence of nucleotides (or in the presence of ADP), the *N*-terminal extension of the A1 light chain should directly interact with actin and form an additional actin-binding site on the myosin head. However, in the absence of actin, the *N*-terminal segment of the A1 light chains seems to be unable to intramolecular interaction, but it probably can interact with its contact point on the motor domain of another S1 molecule. These intermolecular interactions of the A1 N-terminal extension can explain unusual aggregation properties of the S1(A1) isoform.

This work was supported by RFBR (grant 15-04-03037) and by the Program “Molecular and Cell Biology” of Russian Academy of Sciences.

References

1. Markov D.I., Zubov E.O., Nikolaeva O.P., Kurganov B.I. & Levitsky D.I. (2010) «Thermal denaturation and aggregation of myosin subfragment 1 isoforms with different essential light chains». International Journal of Molecular Sciences 11, 4194–4226.
2. Markov D.I., Nikolaeva O.P. & Levitsky D.I. (2010) “Effects of myosin “essential” light chain A1 on the aggregation properties of the myosin head”. Acta Naturae 2(2), 77–81.
3. Borejdo J., Ushakov D.S. Moreland R., Akopova I., Reshetnyak Y., Saraswat L.D., Kamm K. & Lowey S. (2001) “The power stroke causes changes in the orientation and mobility of the termini of essential light chain 1 of myosin”. Biochemistry 40, 3796–3803.
4. Lowey S., Saraswat L.D., Liu HJ., Volkmann N. & Hanein D. (2007) «Evidence for an interaction between the SH3 domain and the N-terminal extension of the essential light chain in class II myosins». J. Mol. Biol. 371, 902–913.

eEF2K–eEF2 SIGNALLING CASCADE IS ACTIVATED IN *M. soleus* UNDER HINDLIMB SUSPENSION IN Ca^{2+}-DEPENDENT MANNER WITH L-TYPE CALCIUM CHANNELS INVOLVEMENT

Y.N. Lomonosova, B.S. Shenkman

Institute of Bio-Medical Problems, RAS,
Khoroshevskoe shosse 76a, Moscow, 123007, Russia

Profound decrease of muscle mass and contractile properties in postural (predominantly antigravitational m.soleus) and locomotor skeletal muscles due to functional unloading is characteristic not only for human being in zero gravity but for patients with traumatological and neurological diseases [Thomason et al., 1990; Chopard et al., 2001]. Decrease of protein synthesis rate and increase of proteolysis in skeletal muscle were shown under functional unloading [Loughna et al., 1986; Kandarian et al., 2002]. The mechanisms of protein synthesis rate, particularly ones exploring polypeptide elongation rate in the skeletal muscle under conditions of unloading are not known. Eukaryotic elongation factor 2 (eEF2) is one of the important member of eEF family catalyzing simultaneous translocation tRNA and mRNA on a 80S ribosome [Taylor et al., 2007]. It was shown that phosphorylation of eEF2 by its specific Ca^{2+}/CaM-dependent kinase (eEF2k) decreased 10-100 folds eEF2 affinity to ribosome, which led to protein synthesis rate drop [Carlberg et al., 1990]. We supposed that eEF2k was activated by increased [Ca^{2+}] which led to reduction in protein synthesis rate in m.soleus during hindlimb suspension. The hypothesis was tested by means of experiments with *in vivo* administration of calcium chelator BAPTA-AM and specific L-type calcium channels blocker nifedipine. Male Wistar rats were divided into 4 groups: control group (“CTR”, n=7), hindlimb suspended (HS) group during 3 days (“3HS”, n=7), HS group with nifedipine (“3HS-Nif”, n=7) or BAPTA-AM administration (“3HS-BAPTA”, n=7). Hindlimb suspension was

carried out according to Novikov-Ilyin's technique modified by Morey-Holton. The rats were sacrificed by avertin overdose (75 mg/kg body wt), each soleus muscle was weighed, immediately frozen in liquid nitrogen and stored at 80°C below zero until analysis. We didn't find decrease of soleus muscle wet mass in all unloaded groups. Moreover, there weren't any changes in myofibrillar and sarcoplasmic protein content. eEF2 mRNA expression and its protein content didn't change in all 3HS groups. However, phosphorylation level of eEF2 (Thr56) was significantly increased after 3HS. Nifedipine decreased P-eEF2 level partially after 3 days of HS, BAPTA-AM completely prevented the rise in P-eEF2 content, which did not differ from that in CTR group. Expression of eEF2k mRNA and content of its protein were greatly increased in all 3HS groups. It was shown that phosphorylation of p70S6k-related or p90rsk1-related site Ser366 of eEF2k could decrease its activity [Wang et al., 2001]. We showed that P-eEF2k (S366) content increased along with the eEF2k rise in 3HS. Nifedipine administration did not have any significant effect on this process. Unlike nifedipine, BAPTA-AM injection led to decrease in P-eEF2k (S366) level during the 3HS. When applying puromycin-labeling we observed 40 % reduction in protein synthesis rate after 3 days of HS. Despite the reduction of P-eEF2 level in 3HS-BAPTA group the protein synthesis rate in this group was as low as in 3HS group. It is concluded that eEF2 activation in m.soleus during HS is Ca^{2+}-dependent process with involvement of L-type calcium channels. eEF2 activation is not a limiting event for protein synthesis rate in soleus muscle during HS. Possibly Ser366 phosphorylation of eEF2k under HS displays additional compensatory regulation to reduce eEF2k activity.

The work was supported by grant RFBR 15-04-05729-a.

TENSION-LENGTH RELATION IN FAILING RAT MYOCARDIUM: COMPARATIVE STUDY ON MUSCLES AND ISOLATED CARDIOMYOCYTES

O.N. Lookin, Yu.L. Protsenko

Institute of Immunology and Physiology, Ural Branch of Russian Academy of Sciences, 106 Pervomayskaya str., Yekaterinburg, 620049, Russia

We evaluated tension-length relation in healthy and failing right ventricular myocardium of young rats on multicellular (muscle) and single-cell (cardiomyocyte) levels. This relation was obtained under isometric mode of contraction on muscle level and in auxotonically contracting isolated cardiomyocytes. On either level, tension-length relation was substantially suppressed in the failing myocardium. The two-level study supports an (intra)cellular origin of the deficiency in the Frank-Starling mechanism.

Methods

The study conforms to the Guide for the Care and Use of Laboratory Animals (NIH Publication No. 85-23, revised 1985) and has been approved by the

local Institutional Animal Care and Use Committee. Monocrotaline (MCT) was used to develop pulmonary hypertension followed by right ventricular heart failure in young rats. 4-week old Wistar rats of both sexes (weighted 80–100 g) were randomly divided to control and MCT-treated groups. Animals were injected either by MCT-containing (50 mg/kg, MCT groups) or MCT-free saline solution (CONT groups). MCT-treated rats were euthanized as soon as loss of body weight and apnea at rest has been prominent (7-to-8-week old age). Control rats were euthanized at the same age. The animals were further subdivided for separate studies on muscle or single-cell level: control male (CONT-male, n=12 for muscle level and n=4 for single-cell level, respectively), control female (CONT-female, n=9 and n=4), MCT-treated male (MCT-male, n=21 and n=5), MCT-treated female (MCT-female, n=17 and n=5).

The measurements on muscle level were conducted on thin right ventricular trabeculae, attached to force transducer and length servomotor in experimental chamber, continuously washed by modified Krebs-Henseleit solution (in mM: NaCl – 118.5; KCl – 4.2; $MgSO_4$ – 1.2; $CaCl_2$ – 2.5; glucose – 11.1, buffered with $NaHCO_3$ and KH_2PO_4 to maintain pH 7.35 and bubbled with 95%O_2+5%CO_2). These measurements were done at 25°C and 0.33 Hz pacing rate using Muscle Research System (Scientific Instruments GmbH, Heidelberg, Germany). Isolated right ventricular cardiomyocytes were harvested enzymatically by the perfusion of whole heart preparation with collagenase-containing solution (1 mg/ml Collagenase Type 2, Worthington Biochemical Corporation, USA). Cardiomyocytes were stored in Tyrode's solution (in mM): NaCl – 118.0, KCl – 4.7, $MgSO_4$ – 1.0, HEPES – 10.0, d-(+)-Glucose – 11.1, $CaCl_2$ – 1.25, 1 mg/ml bovine serum albumin, pH maintained to 7.3 with NaOH. The single-cell measurements were done at 25°C and 1 Hz pacing rate in laser confocal scanning system LSM 710 (Carl Zeiss, Germany). The stretch manipulation and measurement of auxotonic contraction of a cardiomyocyte were performed using carbon fiber technique [1]. Two 7-um thick carbon fibers (Tsukuba Materials Information Laboratory Ltd., Japan) were inserted into glass filaments and each mounted on precise micromanipulator (MP285, Sutter Instrument, USA). Single cell was attached to the tips of the carbon fibers and auxotonic shortening of the cell was measured optically as the bending of the fibers. This bending was converted into auxotonic force by knowing the stiffness coefficients of the fibers. Auxotonic force was then converted to tension by assuming cross-sectional area of a cardiomyocyte to be $S=\pi d^2/12$, where d – wider side of the cardiomyocyte. Cardiomyocytes were stretched by command unit (ROE200, Sutter Instrument, USA) which shifted micromanipulator(s) by desired degree.

The sample (muscle or isolated cardiomyocyte) was released to slack length and then progressively stretched to a certain extent. Several steady-state twitches were recorded at any new stretch. The muscle samples were stretched up to the length where maximal active force was obtained (L_{MAX}). The isolated cardiomyocytes were stretched as much as possible until they detach from carbon fibers. Therefore, the stretch degree was either provided as a % of L_{MAX} for muscles or measured as sarcomere length for isolated cardiomyocytes. The isometric tension-

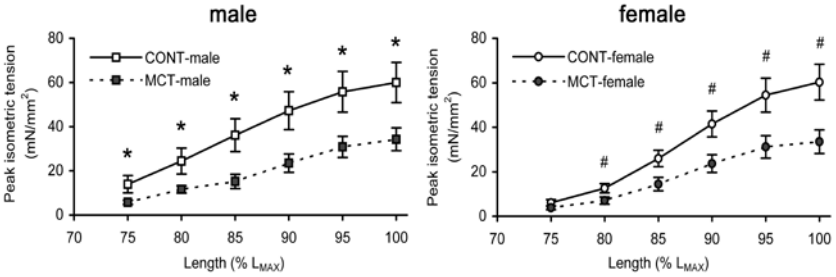

Fig. 1. The tension-length relations obtained for isometrically contracting right ventricular trabeculae from control and monocrotaline-treated young male and female rats. Relative length is expressed as a % of LMAX. Data presented as mean ± S.E.M. * – significant difference between CONT-male vs. MCT-male at the same relative length (P<0.05), # – significant difference between CONT-female *vs*. MCT-female at the same relative length (*P*<0.05). Adapted with permission from [2].

Results

length relations (peak isometric tension vs end-diastolic length) were obtained for muscles and auxotonic tension-length relations (peak auxotonic tension vs end-diastolic sarcomere length) were obtained for isolated cardiomyocytes. We compared either isometric or auxotonic tension-length relations obtained in CONT male/female rats and MCT-treated male/female rats. Two-tailed t-test was used to evaluate difference between mean values of peak tension measured in the same-sex CONT and MCT groups under the same degree of stretch of a sample. The differences were considered significant at $P<0.05$. Data are presented as mean ± S.E.M.

As we have shown previously [2], tension-length relation obtained in isometrically contracting right ventricular trabeculae are significantly blunted in both male and female MCT rats (fig. 1). The deficiency in peak active tension, observed in MCT-treated group vs. same-sex CONT group, was evaluated at each relative length (i.e. 75, 80, 85, 90, 95 and 100% of L_{MAX}). On average for this range of relative lengths, trabeculae from MCT-male and MCT-female developed only 48.8±2.7% and 57.5±1.2% of peak isometric tension in the same-sex CONT group, respectively (fig. 1, $P<0.05$ vs. same-sex CONT group). Due to the non-linear shape of the tension-length relations, we did not calculate slope values for individual relations.

As similar to the multicellular preparations of right ventricle, isolated right ventricular cardiomyocytes obtained from the hearts of male or female MCT-rats showed deficient tension-sarcomere length relation measured in auxotonic contraction under moderate load, compared to the same-sex CONT group (fig. 2). The male groups were not different in the peak auxotonic tension for sarcomere length ≤1.8 μm but the tension was significantly suppressed in isolated cardiomyocytes from MCT-male at sarcomere lengths above this value. The cardiomyocytes from

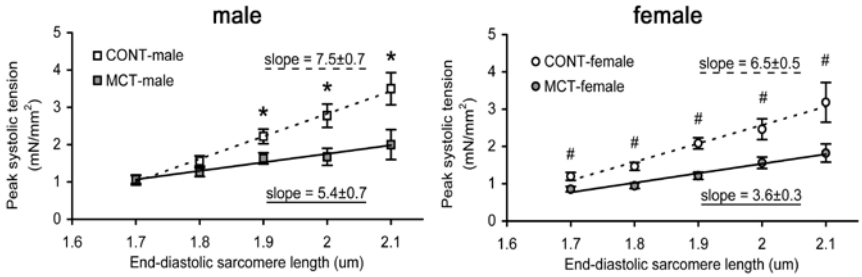

Fig. 2. The tension-sarcomere length relations obtained for auxotonically contracting right ventricular cardiomyocytes isolated from the hearts of control and monocrotaline-treated young male and female rats. Data presented as mean ± S.E.M. * – significant difference between CONT-male *vs.* MCT-male at the same sarcomere length (P<0.05), # – significant difference between CONT-female vs. MCT-female at the same sarcomere length (P<0.05). Individual tension-length relations were approximated by linear equation, the mean slope values for CONT and MCT male/female groups shown in the plot area.

MCT-female were significantly weaker for sarcomere lengths ranged between 1.7 and 2.1 µm, compared to the same-sex CONT group. As the tension-sarcomere length relations were quite linear, we calculated this linear slope for each individual relation. The mean slope in CONT-male was significantly larger, compared to the MCT-male (7.5±0.7 *vs.* 5.4±0.7 (mN/mm^2)/µm, P<0.05). Similarly, the mean slope in CONT-female was significantly larger, compared to the MCT-female (6.5±0.5 *vs.* 3.6±0.3 (mN/mm^2)/µm, P<0.05). The mean slopes were not different between CONT male and female rats while MCT-female showed substantially smaller mean slope vs MCT-male (P<0.05).

Conclusion

The length-dependent activation of contraction (evaluated as tension-length relation) was substantially suppressed in the failing right ventricular myocardium of young rats, regardless the sex. Our comparative study showed that the deficiency in the Frank-Starling mechanism is expressed on the level of single cell and virtually with the same extent as it was previously found in multicellular samples from right ventricle. Therefore, the blunting of the Frank-Starling mechanism in failing myocardium has an (intra)cellular origin, most likely due to the impaired Ca^{2+} regulation of contractile myofilaments [2-4].

The study was supported by Russian Foundation for Basic Research (grant #16-04-00545).

References

1. S. Sugiura, et al., Nat. Protoc. **1** (3), 1453 (2006).
2. O. Lookin, et al., Clin. Exp. Pharmacol. Physiol. **42** (11), 1198 (2015).
3. H. E. ter Keurs, Am. J. Physiol. Heart Circ. Physiol. **302**, H38 (2012).
4. M. L. Ward, et al., Clin. Exp. Pharmacol. Physiol. **38**, 711 (2011).

THE INFLUENCE OF RESISTANCE EXERCISE ON ANABOLIC SIGNALLING IN SKELETAL MUSCLES OF TRAINED AND UNTRAINED SUBJECTS

E.A. Lysenko[1,2], D.V. Popov[1,2], A.D. Butkov[1], T.F. Vepkhvadze[1], D.V. Perfilov[1]

[1]*SSC RF Institute of biomedical problems RAS, Moscow, 123007, Russia*

[2]*Lomonosov Moscow State University, Moscow, 119234, Russia*

It is well known that resistance exercise results in shift of protein balance toward anabolic response in skeletal muscles [Phillips et al., 2010]. Increase in protein synthesis rate particularly is due to activation of key regulator of translation initiation and elongation – mTORC1 [Proud, 2007]. Crucial role of mTORC1 in adaptation of a muscle to resistance exercise is confirmed by the experiments with its specific inhibitors [Bodine et al., 2001; Goodman et al., 2011]. It was shown that exercise-induced signaling events depend on fitness level: acute resistance exercise after training period could results in less pronounced effect on mTORC1 signalling in comparison with that after first exposure [Ogasawara et al., 2013; Phillips et al., 1999]. Thus in present study we compared the effects of single resistance exercise on signalling involved in regulation of protein synthesis in skeletal muscle of trained and untrained subjects.

The study was approved by the Human Ethics Committee of the Institute of Biomedical Problems (Moscow, Russia). Eight untrained subjects and eight powerlifters were involved in the experiment. They visited the laboratory three times separated by at least three days: familiarization visit, visit when their maximal voluntary contraction (MVC) was examined, and experimental session. In experimental day the subjects performed one leg press exercise with load corresponding to 65% of MVC. Venous blood samples were taken before, immediately after and 15 min after the exercise for evaluation of lactate and hormones level. Biopsy samples from *m. vastus lateralis* were taken before, 1, 5, 10 hours after the exercise. mRNA expression level and phosphorylated protein content were evaluated using q-PCR and Western blot, accordingly. All data are presented as median and interquartile range, statistical analisis has been performed using Wilcoxon matched pairs signed-rank test or Fisher criterion. The level of significance was set at $P < 0.05$.

Absolute and specific strength (ratio of MVC to volume of m. quadriceps femoris) of one leg extensors were 1.54 and 1.21 times higher in powerlifters accordingly compared with untrained persons. There was significant correlation between muscle volume and MVC. Basal testosterone and cortisol levels were not different between the groups, whereas the increase in testosterone level after exercise was observed in untrained subjects only. The phosphorylation level of mTORC1 downstream kinase p70S6k (site) was increased in both trained and untrained groups after exercise. On the other hand the phosphorylation level of another target of mTORC1 – 4EBP1 had just a tendency to increase after exercise only in trained group. The phosphorylation level of mechano dependent site of

p70S6k (421/424) was increased in both groups. The phosphorylation level of elongation factor 2 (eEF2) was significantly decreased in trained group and had a tendency to decrease in untrained group. The phosphorylation level of mitogen activated proteinkinase Erk1/2 was increased in both groups. The phosphorylation level of FOXO1, a key regulator of ubiquitin-ligase genes expression, was decreased only in trained group.

Thus the strength exercise results in activation of kinases regulating translation initiation and elongation. When exercise intensity is equalized by relative level these molecular events do not differ between trained and untrained skeletal muscles.

EFFECTS OF INTERCHAIN DISULFIDE CROSSLINKING OF TROPOMYOSIN ON ITS FUNCTIONAL PROPERTIES

A. Matyushenko[1,2], N. Artemova[1], D. Shchepkin[3], G. Kopylova[3], S. Bershitsky[3], D. Levitsky[1,4]

[1]*A.N. Bach Institute of Biochemistry, Research Center of Biotechnology of the Russian Academy of Sciences, Moscow, Russia;*

[2]*Department of Biochemistry, School of Biology, Moscow State University, Moscow, Russia;*

[3]*Institute of Immunology and Physiology, Ural Branch of the Russian Academy of Sciences, Yekaterinburg, Russia;*

[4]*A.N. Belozersky Institute of Physico-Chemical Biology, Moscow State University, Russia*

It is known that two chains of skeletal or cardiac α-tropomyosin (Tpm 1.1, onwards simply Tpm) can be cross-linked by formation of disulfide bond between Cys190 residues. Normally, the SH-groups of these residues are in a reduced state in skeletal or cardiac muscle [1,2]. However, the interchain cross-linking between Cys190 residues of cardiac Tpm was shown to occur upon human end-stage heart failure [3]. It was previously shown using differential scanning calorimetry (DSC) that the cross-linking between the two Cys190 residues strongly increases the thermal stability of C-terminal part of Tpm molecule [4]. However, until now it was unclear how this disulfide cross-linking affects the functional properties of Tpm. We have shown using cosedimentation assays that formation of the disulphide bonds strongly decreases the affinity of Tpm for F-actin. Moreover, this cross-linking strongly decreased the stability of preformed Tpm–F-actin complexes as was shown by measuring the temperature dependences of thermal dissociation of these complexes monitored with light scattering. On the other hand, the cross-linking of Tpm enhanced maximal sliding velocity of regulated actin filaments containing Tpm and troponin (Tn) in the *in vitro* motility assay at high Ca^{2+} concentrations, with no appreciable effect on Ca^{2+}-sensitivity of the actin-myosin interaction underlying this sliding. It should be noted that this effect was highly dependent on proteins, skeletal or cardiac, used in the motility assay. Initially, the experiments were performed in an assay containing rabbit skeletal muscle proteins – myosin, actin, and Tn. Under these condi-

tions, the interchain cross-linking of cardiac Tpm (which is identical to skeletal Tpm) enhanced the maximal sliding velocity of regulated actin filaments by 20%. When rabbit skeletal Tn was replaced by rabbit cardiac Tn, the maximal sliding velocity of the filaments was enhanced by 30%, and even a twofold increase in the velocity was observed when both skeletal myosin and skeletal Tn were replaced by rabbit cardiac proteins. Surprisingly, the effect of the Tpm cross-linking became negligible (i.e. the increase in the sliding velocity did not exceed 8-9 %) when all skeletal proteins in the system (Tn, myosin, and actin) were replaced by rabbit cardiac proteins. Thus, the most pronounced effect of the Tpm cross-linking on the velocity was observed when the following combination of proteins was used: cardiac Tn + cardiac myosin + skeletal actin. This situation seems to be quite possible during cardiac hypertrophy where increased expression of α-skeletal actin mRNA and protein were found, leading to partial replacement of cardiac α-actin isoform by skeletal α-actin [5].

In conclusion, our results indicate that interchain disulfide cross-linking between Cys190 residues may have a significant effect on the functional properties of cardiac Tpm, and this can explain, at least partly, why this cross-linking is associated with human heart diseases.

This work was supported by the Russian Foundation for Basic Research (grant 15-34-20136).

References

1. Lehrer S.S., Ly S. & Fuchs F. (2011) "Tropomyosin is in a reduced state in rabbit psoas muscle" J. Muscle Res. Cell Motil. 32, 19–21.
2. Lehrer S.S., Ly S. & Fuchs F. (2011) "Tropomyosin is in a reduced state in rat cardiac muscle" J. Muscle Res. Cell Motil. 32, 63–64.
3. Canton M., Menazza S., Sheeran F.L., de Laureto P.P., Di Lisa F., Pepe S. (2011) "Oxidation of myofibrillar proteins in human heart failure" J. Am. Coll. Cardiol. 57, 300-309.
4. Kremneva E., Boussouf S., Nikolaeva O., Maytum R., Geeves M.A., and Levitsky D.I. (2004) "Effects of two familial hypertrophic cardiomyopathy mutations in α-tropomyosin, Asp175Asn and Glu180Gly, on the thermal unfolding of actin-bound tropomyosin". Biophys. J. 87, 3922–3933.
5. Clement S., Chaponnier C., Gabbiani G. (1999) "A subpopulation of cardiomyocytes expressing α-skeletal actin is identified by a specific polyclonal antibody" Circulation Research 85, e51–e58 (doi: 10.1161/01.RES.85.10.e51).

THE ROLE OF Arp2/3 COMPLEX IN GLUTOXIM REGULATION OF Na^+ TRANSPORT IN FROG SKIN

A.V. Melnitskaya, Z.I. Krutetskaya, S.N. Butov, N.I. Krutetskaya, V.G. Antonov

Saint-Petersburg State University, 7/9 University emb., Saint-Petersburg, 199034, Russia

The barrier epithelia of amphibians such as frog skin and toad urinary bladder play an essential role in electrolyte, acid/base and water balance of the whole animal. The amphibian skin and urinary bladder share common Na^+ and H^+ transport proper-

ties with distal renal tubule, and have been used as models in studies of the mechanisms and regulation of ion transport across tight-junction epithelia [1]. Transepithelial Na^+ transport is a complex system that creates and maintains electrolytic and water homeostasis. The different protein components of this system can be targets for oxidative stress [2]. However, the mechanisms underlying the effect of oxidants and reducing agents on individual components of the Na^+ transport are still unknown.

Recently, new disulfide-containing agents with d-metals as nanoadditives, altering cell redox state, have been widely used in clinical practice. Thus, the drug glutoxim® (oxidized glutathione (GSSG) with d-metal nanoaddition, PHARMA-VAM, Saint-Petersburg) is widely applied as an immunomodulator and hemostimulator for the therapy of bacterial and viral diseases, psoriasis and the radio- and chemotherapy of oncological diseases [3]. We earlier demonstrated that Na^+ transport in the frog skin is modulated by various oxidants. This was the first finding to demonstrate that GSSG and glutoxim applied to the basolateral frog skin surface imitate the effect of insulin and stimulate Na^+ transport [4]. At the same time, almost nothing is known about the effects of these agents on Na^+ transport in native epithelial systems, such as the epithelium of the frog skin.

It is known that actin cytoskeleton is involved in the modulation of the activity of many Na^+ - transporting proteins colocalized with actin filaments and actin-binding proteins (ankyrin and spectrin), and is also involved in the regulation of transepithelial Na^+ transport by some hormones [5]. A key role in the formation of microfilaments from G-actin monomers plays the Arp2/3 complex (Actin-Related Proteins). Actin nucleation sites also include WASP proteins (Wiskott-Aldrich syndrome proteins) which activate Arp2/3complexes, provide their interaction with actin monomers, trigger actin polymerization and the formation of branched actin filaments [6]. We have previously shown that Na^+ transport in the frog skin depends on the structural and functional organization of the actin and tubulin cytoskeleton [7]. In this regard, it is interesting to investigate the possible involvement of growth processes and actin filaments branching in glutoxim effect on Na^+ transport in the skin of frogs. A selective inhibitor of N-WASP protein wiskostatin [8] and an inhibitor of the Arp2/3 complex compound CK-0944666 [9] were used in the experiments.

Materials and methods

Experiments were performed on frog Rana temporaria males. The skin from the frog abdomen was removed and placed in Ussing chamber (World Precision Instruments, Inc., Germany) with 12 mm inner orifice. Frog skin electrical parameters were measured with the automatic device for voltage-clamp and registration of current-voltage relations (*I–V* relations). To measure *I–V* relations, transepithelial potential V_T was changed periodically to a series of nonzero values. From skin *I–V* relations the electrical characteristics of frog skin were determined: the short – circuit current (I_{SC}), the open – circuit potential ($V_{OC} = V_T$ at the total transepithelial current $I_T = 0$), and transepithelial conductance (g_T). The transepithelial Na^+ transport was measured as amiloride – sensitive short – circuit current (I_{SC}). Wiskostatin and CK-0944666 were added 30–40 min before glutoxim application. Statistical analysis was

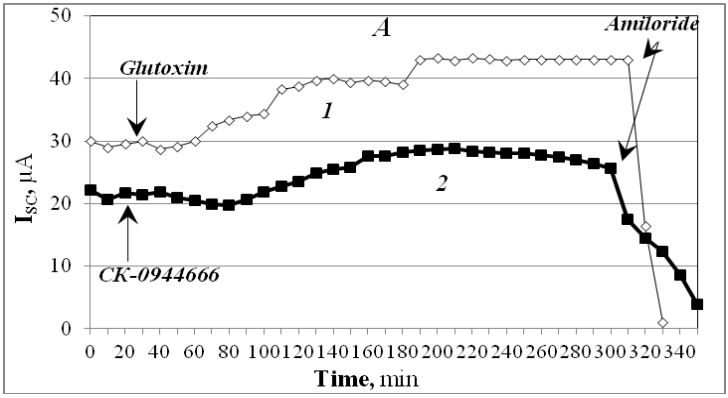

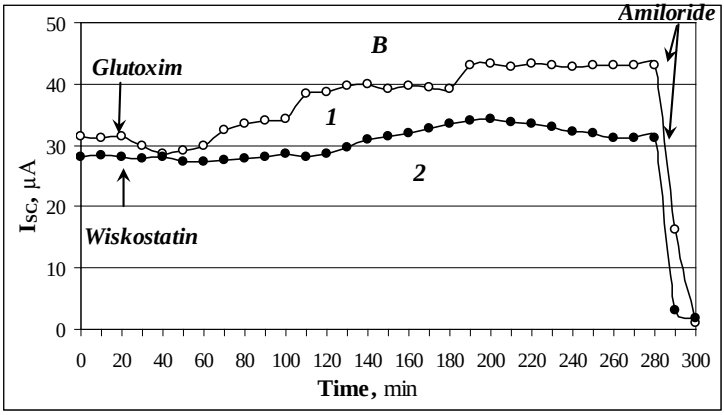

Dependence of the changes in short-circuit current, ISC, through the frog skin in response to glutoxim in the absence or presence of wiskostatin and CK-0944666.
A: (1) ISC after applying 100 μg/mL glutoxim to the basolateral surface of intact frog skin; (2) ISC after applying glutoxim to the frog skin pretreated (for 30 min) from the apical side with 100 μM CK-0944666;
B: (1) ISC after applying 100 μg/mL glutoxim to the basolateral surface of intact frog skin; (2) ISC after applying glutoxim to the frog skin pretreated (for 30 min) from the apical side with 10 μM wiskostatin; at the end of each experiment, the solution bathing the apical skin surface was supplemented with 20 μM amiloride, an ENaC blocker.

performed using Student's *t*-test. The data are presented as $x \pm s_x$. Figure illustrates the results of typical experiments.

Results and discussion

The mean values of frog skin electrical characteristics in control (from 10 experiments) are: $I_{SC} = 30.31 \pm 3.14$ μA, $V_{OC} = -52.28 \pm 6.25$ mV, and $g_T = 0.57 \pm 0.14$ mS. Glutoxim, applied to the basolateral surface of the intact frog skin, stimulated

Na^+ transport. After glutoxim application I_{SC} increased in average by 31.24 ± 8.32%; V_{OC} – by 38.04 ± 5.15%; and g_T did not change (the data from 10 experiments).

It has been found that wiskostatin and CK-0944666 decrease the glutoxim stimulatory effect on the Na^+ transport in frog skin (figure). On average (the results of 10 experiments), after the preincubation of skin apical surface with 10 μM wiskostatin or 100 μM CK-0944666 for 30 min before application of 100 μg/ml glutoxim to the frog skin basolateral surface, I_{SC} increased by 14.34 ± 3.12 or 18.75 ± 4.01%, V_{OC} increased by 16.09 ± 5.11 or 5.98 ± 0.34 %, and g_T – by 1.58 ± 0.32 or 13.47 ± 2.85 % for wiskostatin and CK-0944666, respectively.

It is known that key Na^+ transporting proteins, such as amiloride-sensitive epithelial Na^+ channels (ENaC), Na^+-K^+-ATPases and Na^+/H^+ exchangers, contain numerous cysteine residues that are targets for intra- and extracellular oxidizing and reducing agents [2,10]. However, when, at the end of each experiment, the ENaC-blocking agent amiloride (20 μM) was applied to the apical skin surface, the I_{SC} was almost completely inhibited, suggesting that the effect of glutoxim on Na^+ transport is mostly caused by modulation of the ENaC activity (figure).

Thus, we have shown that WASP protein inhibitor wiskostatin and Arp2/3 complex inhibitor CK-0944666 attenuate the stimulatory effect of glutoxim on Na^+ transport in frog skin. These results are in accordance with the data of literature. In various types of epithelial cells it has been found that in ENaC activity modulation actin - associated proteins are involved. Thus, using transfected Chinese hamster ovary (CHO) cells it was shown that Arp2/3 complex and actin-associated protein cortactin modulate ENaC gating characteristics reducing the open probability of the channel [11]. Furthermore, coexpression of ENaC with N-WASP significantly increases ENaC activity in CHO cells [12]. At the same time, in other types of epithelial cells such as immortalized rat cortical collecting duct (CCD) cells N-WASP inhibitor wiskostatin did not affect Na^+ reabsorption and ENaC activity [11].

We have previously shown that Na^+ transport in frog skin depends on the structural and functional organization of the actin and tubulin cytoskeleton. It was also found by us that any change in the structure of microtubules and microfilaments leads to a decrease of stimulating action of glutoxim on Na^+ transport [13]. The results of this study also indicate that inhibition of actin growth and branching processes decreases the effect of glutoxim on Na^+ transport in frog skin.

References

1. Koefoed- Johnsen V, Ussing HH. // Acta Physiol. Scand. 1958. V. 42. P. 298 – 308.
2. Firsov, D., Robert-Nicoud, M., Gruender, S., et al., // J. Biol. Chem. 1999. V. 274. P. 2743–2749.
3. Borisov A.E., Kozhemyakin L.A., Antushevich A.E., et al., // Vest. Hirurgii im. I.I. Grekova. 2001. V. 4. P. 32 – 38.
4. Крутецкая З.И., Лебедев О.Е., Мельницкая А.В., и др. // ДАН. 2008. Т. 421. № 5. С. 709–712.
5. Els W.J., Chou K.Y. // J. Physiol. 1993. V. 462. P. 447–464.
6. Bouma G., Burns S.O., Thrasher A.J. // Immunobiology. 2009. V. 214. P. 778-90.
7. Мельницкая А.В., Крутецкая З.И., Лебедев О.Е. // Цитология. 2006. V. 48. N. 10. P. 817–840.

8. Peterson J.R., Bickford L.C., Morgan D., et al // Nat. Struct. Mol. Biol. 2004. V. 11. P. 747-755.
9. Nolen B.J, Tomasevic N., Russell A., et al // Nature. 2009. V. 20. P. 1031-1034.
10. Boldyrev, A.A., Bulygina, E.R. // Ann. N.Y. Acad. Sci. 1997. V. 834. P. 666–668.
11. Karpushev A.V., Levchenko V., Ilatovskaya D.V., et al // Hypertension. 2011. V. 57. P. 996-1002.
12. Ilatovskaya D.V, Pavlov T.S., Levchenko V., et al // FASEB J. 2011. V. 25. P. 2688-2699.
13. Melnitskaya A.V., Krutetskaya Z.I., Lebedev O.E., et al // Cell Tissue Biol. 2012. V. 6. N. 3. P. 248–253.

DYNAMICS OF BIOENERGETIC PROCESSES IN MUSCLE TISSUE OF RATS AFTER PROLONGED INJECTION OF SIMVASTATIN

Z.I. Mikashinovich, E.S. Belousova, E.V. Vinogradova, I.A. Semenets

Rostov State Medical University,

29, Nakhichevanskiy street, Rostov-on-Don, 344022, Russia

Despite numerous studies, there is no consensus about the pathogenetic mechanisms of destruction of muscle fibers when taking statins. In modern publications, there are few data on the involvement of mitochondria in the pathogenesis of statin myopathy, the nature and extent of morphological changes in them.

The lack of clear understanding of the molecular mechanisms of statin myopathy significantly impedes the development of methods of metabolic correction and prevention of degenerative changes in skeletal muscle.

In this context, the aim of the work was to analyze the dynamics of indicators that reflect the state of the cell energy metabolism in myocytes of laboratory animals during prolonged administration of simvastatin (Zocor).

The study was conducted on 70 mongrel male rats aged 12-14 months (300–350 g). The animals were corresponded to sanitary rules SR 2.2.1.3218-14 “Sanitary requirements to the device, equipment and maintenance of experimental biological clinics (vivariums)” dated 08.29.2014. During 3 months, the animals were maintained on a diet enriched with animal fat (melted butter) and easily digestible carbohydrates (sugar cane, semolina). During the experiment, the animals were divided into two groups: a control group – 35 animals fed a diet without addition of drugs; Experimental group - 35 animals treated for 2 months, simvastatin (Zocor, 20 mg) at 0.001 g/100 g of body weight once daily as an aqueous slurry through an esophageal probe. The intact control group animals were kept on a general vivarium ration. The animals were taken out of the decapitation of the experiment.

There were selected of skeletal muscle fragments of the rear paw of the animal for the study. Concentration of the pyruvate acid was determined by reaction with 2,4-dinitrophenilhydrazin [2]. Lactate concentration was determined by reaction of acetaldehyde formed from lactic acid in the presence of sulfuric acid, phosphoric acid and copper ion from para-oxydiphenil [2].

Mitochondria were isolated by differential centrifugation after homogenization in saline (0.15 M KCl and 10 mM Tris-HCl). Homogenates were centrifuged for 15 min at 640 *g* to remove the nuclear fraction. Mitochondrial fraction was isolated for 25 minutes at 20000 *g* by washing twice with release medium. Active substrate dehydrogenases Krebs cycle: pyruvatedehydrogenase (PDH), alpha-ketoglutaratedehydrogenase (alpha-KG-DH), succinatedehydrogenase (SDH) was determined by spectrophotometric method in a model system for the reduction reaction of nitro tetrazolium in the presence of a specific substrate (pyruvate Na, α-ketoglutarate, succinate) [3]. The activity of cytochromeoxydase (CCO) was determined by reaction with paradinitrophenylendiamine [1].

Statistical processing of the experimental data was performed using STATISTICA 6.0 software. Statistically significant difference was considered appropriate assessment of the probability of error $p \leq 0{,}05$.

Animals on a diet enriched in carbohydrate and fat animals (control group), led to a significant increase in the level of cholesterol in blood serum to 75.38% (p <0,001) relatively to the control group.

The muscle tissue of comparison group animals revealed a significant increase in the levels of pyruvate and lactate – 247% (p <0.001) and 73% (p <0.001), respectively, relatively to the control group (table). Determination of the activity of enzymes of carbohydrate and energy metabolism showed an increase of PDH activity by 119% (p <0.001), α-KG-DH at 94.12% (p <0.001), CCO activity and SDH

The concentration of metabolites of glycolysis and energy metabolism enzyme activity in animal muscle tissue treatment groups ($M \pm m$)

Index	Control group n=35	Comparison group n=35	Experimental group n=35
Pyruvate [mkmol/mg of protein]	2.25 ± 0.024	7.81 ± 0.570 p<0.001	3.28 ± 0.269 p_1<0.001 p<0.001
Lactate [mkmol/mg of protein]	3.96 ± 0.447	6.86 ± 0.657 p<0.001	4.64 ± 0.491 p_1<0.01 p>0.05
SDH [mkmol/mg of protein]	2.14 ± 0.235	2.44 ± 0.261 p>0.05	0.79 ± 0.066 p_1<0.001 p<0.001
CCO [mkmol/mg of protein]	0.0039 ± 0.00056	0.0036 ± 0.00028 p>0.05	0.0011 ± 0.00011 p_1<0.001 p<0.001
alpha-KG-DH [mkmol/mg of protein]	0.884 ± 0.094	1.716 ± 0.085 p<0.001	0.779 ± 0.089 p_1<0.001 p>0,05
PDH [mkmol/mg of protein]	0.811 ± 0.096	1.774 ± 0.223 p<0.01	1.279 ± 0.137 p_1<0.05 p<0.001

Note: p - significantly relative to the control group; p_1 - significantly relative to the comparison group.

did not differ from the control group. These changes may be related to the biological effect of insulin. Thus, increased levels of lactate and pyruvate can be regarded as a measure of increasing the intensity of oxidative decomposition of glucose. At the same time, the significant increasing of PDH oxidation activity provides excess of pyruvate to acetyl-Co A.

Injection of simvastatin (experimental group) helped to reduce cholesterol levels in the blood serum to 1.637 ± 0.136 mmol/l, which was not significantly different from the control group.

The muscles of the animals of the experimental group showed a reduction in the concentration of pyruvate by 58% (p_1<0.001) and lactate at 32.36% (p_1<0.001) relatively to the comparison group. Regarding the control group the concentration of pyruvate has been increased by 45.8% (p<0.001), lactate concentration did not differ significantly. After administration of simvastatin in the muscles of animals, a decrease in PDH activity in 27.9% (p_1<0.05) and alpha-KG-DH at 54.6% (p_1<0.001) was observed relatively to the comparison group. Regarding the control group, PDH activity remained increased by 57.71 (p_1<0.001), and α-KG-DH did not differ significantly.

Given the close relationship of carbohydrate and lipid metabolism, it can be assumed that the reduction in cholesterol levels, despite the continuing nature of the food, supports eliminating glucose hypermetabolism, as indicated by the decrease in the concentration of lactate and pyruvate, while maintaining a high level pyruvate and activity of PDH, obviously, due to the regulatory effect of insulin.

At the same time, the animals' experimental group muscles showed a sharp decrease in SDH activity at 67.62% (p_1<0.001), CCO at 69.44% (p_1<0.001). When comparing the results with a control group SDH activity and CCO was reduced by 63% (p<0.001) and 71.8% (p<0.001), respectively. Decreased activity of the terminal portion of the respiratory chain may be caused by a deficiency ubiquinone biosynthesis and also performed with HMG Co-A reductase inhibitors.

Thus, the biochemical changes in the muscle tissue when administered simvastatin was characterized by decreased activity of the bioenergetic processes. Reducing the terminal region of the respiratory chain activity can be considered as indirect evidence of violations of exchange of ubiquinone, performing the function of collecting and providing further oxidation of NAD and FAD-dependent substrates [4,5]. Since the constant regeneration of ATP is a prerequisite for an act of muscle contraction, the violation of energy myocytes can be considered as a molecular basis for the formation of dystrophic changes when taking statins. These results give reason to use them as a theoretical basis for the development of metabolic correction circuits in the application by high-statin therapy to maintain functional state of skeletal muscles.

References

1. Krivchenkova R.S. Modern methods in biochemistry. M.: Medicine, 1977.
2. Mikashinovich Z.I., Letunovsky A.V., Volzhin O.O., Belousova E.S. Biochemical studies of saliva in clinical practice. Rostov-on-Don., 2004.

3. Nordmann I.N. Determination the activiti dehydrogenasique des mitochondries a 1-acid-dichloride-2,3,5-triphenyl-tetrazolium.// Bull. Sos. Chim. Biol. 1957. Vol. 33. P. 189-197.
4. Parker B.A., Gregory S.M., Lorson L. et al. A randomized trial of coenzyme Q10 in patients with statin myopathy: rationale and study design. // J. Clin. Lipidol. 2013. Vol. 7(3). P. 187-193.
5. Sirvent P., Fabre O., Bordenave S. et al. Muscle mitochondrial metabolism and calcium signaling impairment in patients treated with statins. // Toxicol. Appl. Pharmacol. 2012. Vol. 259(2). P. 263-268.

REVERSIBLE EYE OCCLUSION RESULTS IN PERSISTENT CHANGES OF GOLDFISH MOTOR LATERALITY

G.Z. Mikhailova, G.A. Alilova, N.A. Pen'kova, R.Sh. Shtanchaev

Institute of Theoretical and Experimental Biophysics of the Russian Academy of Sciences, Pushchino, Moscow region, 142290, Russia

Visual perception of different targets in the environment and their estimation in the brain from the aspect of danger or attraction play an important role in shaping of motor behavior of actively moving animals [1]. Various disorders of the eyesight involve a whole cascade of molecular and cellular events associated with neuroplastic morphofunctional transformations in the central nervous system. Abnormalities of neuronal homeostasis in CNS which have occurred after the transformations will inevitably be affect the motor behavior of the animal, providing a compensatory reactions of adaptive nature, which can be detected experimentally.

We showed previously that removal (enucleation) of one eye in fish (goldfish *Carassius auratus*) either by experimental way or after a trauma in early postnatal period resulted in a shift of preference in turns during free (not mediated by external stimuli) swimming in a narrow channel [2,3]. Animals preferred to turn toward the side of visual deprivation, with including development of motor asymmetry in fish initially had no the lateralized motor behavior ("ambidextrous"). It should be noted that the change in motor asymmetry of fish after eye enucleation was irreversible, that is, the level of motor asymmetry did not return to the original, pre-operative one, nor spontaneously, with the lapse of time, nor compulsively, by stimulating a healthy eye.

In this context, the aim of the study was to use such manipulations which would have reversible effects on visuomotor behaviors and allow to investigate alterations in the behavior and dynamics of the termination and renewal of the visual stimuli influx into the brain. This method of a temporary interruption of the visual information influx into one brain hemisphere called reversible monocular deprivation (RMD) was previously developed in mammals and successfully used as a model for studies of a number of visual pathologies such as amblyopia ("lazy" eye syndrome) [1,4–6]. Despite the fact that the method of RMD had never been used on fish because of the obvious methodological limitations it has certain opportunities when using fish as a model, primarily due to a simpler organization of the CNS neural networks involved in visuomotor relationships.

Using the techniques applied in conventional electrophysiological investigations on fish *in vivo* [7,8], a method of occlusion of the eye by its gluing with opaque, noninvasive mask on water-repellent vehicle has been developed. Eye's mask is held firmly enough on the skin around the eye, with protecting the eye itself from possible mechanical or toxic effects by vaseline containing hydrocortisone as an anti-inflammatory agent. Antisepsis of an operated animal is provided by special adhesive composition of the mask as well as by housing the fish in the water with antiseptic additives specifically designed for aquariums. The duration of eye's mask retention is 1–3 weeks; this period was enough for changing the motor behavior of fish after eye enucleation [2,3].

Testing of goldfish in the narrow channel was performed according to previously described procedure [2]. A coefficient of motor asymmetry, the ratio of the number of full turns in the preferable direction to the sum of turns in both directions, was calculated based on the observations of the motor behavior. To assess the state of the operated eye after peeling eye's mask an optomotor drum [9] modified by inner opaque wall, given mostly monocular vision of goldfish, was used. A method of adaptation to the optokinetic stimulation, which based on 15-day training sessions of the optomotor reaction (following the moving visual cues) [10], was used for recovery of the original motor behavior. During each session fish were contained in the test tank with a solution of glycine, concentration of which was gradually decreased accordingly the daily increasing of the session's duration.

It was shown that the eye gluing in ambidextrous fish leads to the development of preference of the turnings to the side of the closed eye ("blind" side). A shift of the CMA averaged 34% from the baseline after two weeks of RMD. In lateralized fish, the occlusion of ipsilateral eye intensified the initial motor asymmetry by an average of 30% within 1–2 weeks after surgery. In other words, the preference of fish to turn to the left, i.e., toward the side of blinded left eye, became greater. Occlusion of the eye contralateral to preffered side resulted in inversion of motor asymmetry and reduced its level by 45% within a week after the surgery. These results are consistent with experimental data obtained for irreversible monocular deprivation (enucleation of the eye) [3] and point to the applicability of this approach to the study of visual-motor relations in fishes.

Study of goldfish motor behavior after falling off the eye's mask (during a period of visual rehabilitation) showed that the motor asymmetry of fish does not completely return to the preoperative level. Thus, the CMA of the ambidextrous fish increased by 21%, on average, after 10 days postsurgically and remained at a higher level (8% of the initial average value) two weeks after peeling off the mask. Reduction of the CMA in individual fish after rehabilitation period ranged from 9 to 15% relative to the value after the eye occluding, remaining at 4–32% higher than the preoperative level of motor asymmetry. Thereby, the value of CMA in the rehabilitation period showed the maintenance of lateralized status in most individuals. At the same time operated fish showed the similar behavior with intact fish while following a moving optomotor drum, indicating the safety of the eye and the basic brain structures involved in shaping of the optomotor reaction. This probably

means that traumatic effects of surgery (in connection with RMD), that might be the cause of impaired vision or incomplete recovering of vision, are minimized in our work.

According to the traditional view [1], the visual cortex in mammals develops properly only if it receives signals from both eyes in the early stage of life [4]. If one eye is deprived during the critical (sensitive) period of postnatal development, it leads to amblyopia or lazy eye, a state near to blindness [5,6]. This can happen if person born with the cataract, the omission of the lower eyelid or other defects when the disorders were not corrected in time. If the eye is opened in adulthood the recovery can be long and incomplete [1]. In a series of experiments on modeling of delayed effects of the RMD we used goldfish at the age of about 1.5 years. Given that fish live up to 10-15 years in the aquarium environment (up to 30–40 years in ponds and pools) and their ability to reproduce begins around the age of 2–3 years, it can be concluded that experimental animals belonged to the group of actively growing ones and their sensitive period was not finished.

It is known that increased physical activity, combined with the visual stimulation activates the process of neuroplasticity in an area of visual cortex, associated with the eye closed temporarily in mice, improving the quality of perception of visual stimuli and generally rehabilitating the lazy eye [5]. Likewise, there are some manipulations with the inhibitory influences on the plasticity of neural networks, which can help to “return” a critical period for the formation of the visual perception [6]. In looking for ways to restore the motor behavior of fish after the RMD, we stopped at a traditional neurologic approach to functional recovery of the brain based on the combined therapeutic rehabilitation (“training” of impaired function) with pharmacological treatment. It has been found that adaptation to optokinetic stimulation (contralateral to the preferred side of turns and the side of deprivation [10]) in combination with treatment by increased concentration of glycine, on average, reduces the CMA up to the level of preoperative values. However, analysis of the recovery dynamics in fish motor behavior revealed that the CMA of some individuals did not differ from those for fish untreated after deprivation. Therefore, further research and perhaps new approaches based on used in this paper method of rehabilitation are needed for ensure in the beneficial effect of training optokinetic stimulation in combination with glycine on the motor behavior of goldfish and morpho-functional state of the nerve centers in the brain involved in visual-motor relationships.

This work was supported by Russian Foundation of Basic Research No. 12-04-00699-a and 16-04-01759-a.

References

1. Hubel D.H. (1988) Scientific American Library (N.-Y.). P.239.
2. Mikhailova G.Z. (2006) Neurophysiology. V.38. No.1. P.15-26.
3. Grigorieva E.E. et al. (2010) Neurophysiology. V.42. No.3. P.185-196.
4. Wiesel T.N. et Hubel D.H. (1963) Journal of Neurophysiology. V.26. No.6. P.978-93.
5. Kaneko M. et Stryker M.P. (2014) Elife. V.3. e02798. P.1-16.
6. Davis M.F. et al. (2015) Neuron. V.86. No.4. P.1055-1066.

7. DiDomenico R. et al. (1988) Brain Research. V.473. P.15-28.
8. Korn H. et Faber D.S. (2005) Neuron. V.47. P.13–28.
9. Shtanchayev R.Sh. et al. (2007) Neurophysiology. V.39. No.2. P.118-129.
10. Dektyareva N.Yu. et al. (2008) Neurophysiology. V.40. No.3. P.178-186.

ANTIASTHMATIC AGENT ZILEUTON MODULATES GLUTOXIM AND MOLIXAN EFFECT ON INTRACELLULAR Ca^{2+} CONCENTRATION IN MACROPHAGES

L.S. Milenina, Z.I. Krutetskaya, A.A. Naumova, N.I. Krutetskaya, S.N. Butov, V.G. Antonov

The Department of Biophysics, Saint-Petersburg State University, University emb. 7/9, Saint-Petersburg, 199034, Russia

The pharmaceutical agents glutoxim®, disodium salt of oxidized glutathione (GSSG) with a platinum nanoadditive, and molixan®, a complex of glutoxim and inosine nucleoside, (PHARMA-VAM, Saint-Petersburg, Russia) belong to a group of thiopoethins affecting cellular redox-status. Glutoxim has found clinical application as an immunomodulator and a hemostimulator in complex therapy in cases of bacterial and viral diseases, psoriasis and radio- and chemotherapies in oncology [1]. Molixan has immunomodulatory, hepatoprotective and antiviral effects [1]. However, the cellular and molecular mechanisms underlying these drugs action are poorly understood.

Earlier we found for the first time that GSSG, glutoxim, and molixan increase the intracellular Ca^{2+} concentration ($[Ca^{2+}]_i$) due to Ca^{2+} mobilization from the thapsigargin-sensitive Ca^{2+} stores and subsequent store-dependent Ca^{2+} entry in rat peritoneal macrophages [2,3]. Also, we have found that the key enzyme of arachidonic acid (AA) metabolism phospholipase A_2 [4], enzymes and/or products of cyclooxygenase, lipoxygenase [5] and epoxygenase [6] pathways of AA metabolism are involved in complex signaling cascade triggered by glutoxim or molixan in macrophages.

Enzymes of AA metabolism serve as targets for a wide spectrum of natural and synthetic pharmacological agents. These agents are important tools for investigation of the role of AA and its oxidation products in intracellular signaling. In addition, nowadays a lot of AA metabolism inhibitors are actively used in medicine in the therapy of inflammatory, allergic and infective diseases [7]. Thus, it is known that 5-lipoxygenase pathway products play a critical role in bronchial asthma pathogenesis. The first specific 5-lipoxygenase inhibitor used for chronic asthma treatment was zileuton (N-[1-(benzothien-2- ylethyl]-N-hydroxyurea), Zyflo®) [8]. Zileuton reduces sulfopeptide leukotrienes and leukotriene B_4 generation, causes bronchodilatation and prevents bronchoconstriction induced by cold air or aspirin [8]. Also, recent data suggest zileuton effectiveness in the treatment of acne [9].

Therefore, the aim of this work was to investigate the effect of 5-lipoxygenase specific inhibitor zileuton on $[Ca^{2+}]_i$ increase induced by glutoxim and molixan.

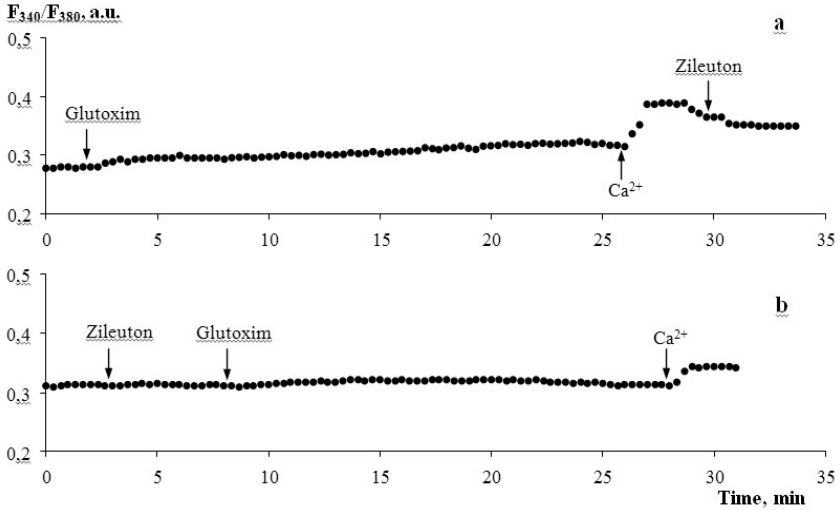

The effect of zileuton on Ca^{2+} responses induced by glutoxim in macrophages. Ordinate - the ratio of Fura-2AM fluorescence intensities F340/F380 at excitation wavelengths of 340 and 380 nm, respectively (arbitrary units, a.u.), abscissa – time, min. (a) – Macrophages were treated with 200 μg/ml glutoxim in Ca^{2+}-free solution, 25 min later Ca^{2+} entry was initiated by the addition of 2 mM Ca^{2+} to the external medium, then 4 μM zileuton was added; (b) – cells were preincubated with 1 μM zileuton for 5 min in Ca^{2+}-free solution, after that 200 μg/ml glutoxim was added, 20 min later Ca^{2+} entry was induced by addition of 2 mM Ca^{2+} to the external medium. Each recording was obtained for a group of 40–50 cells and is a typical variant of six or seven independent experiments.

Cultures of resident peritoneal macrophages from Wistar rats were preincubated for 1–2 days at the room temperature of 20–22°C. The cultivation procedure and $[Ca^{2+}]_i$ measurement using a fluorescent microscope Leica DM 4000B (Leica Microsystems, Germany) have been described in detail earlier [10]. The fluorescent probe Fura-2AM (Sigma-Aldrich, United States) was used for measuring of $[Ca^{2+}]_i$. After excitation of fluorescence of the object at wavelengths of 340 and 380 nm, emission was recorded at 510 nm. To avoid photobleaching, measurements were made every 20 s after irradiation of the object for 2 s. The $[Ca^{2+}]_i$ values were calculated according to the Grynkiewicz equation [11]. The results were processed statistically using Student's test. Figure 1 shows the results of typical experiments.

It has been demonstrated in control experiments that incubation of macrophages in the presence of 200 μg/ml glutoxim (figure, a) or 200 μg/ml molixan (not shown) for 25 min in a medium without calcium causes a significant increase in $[Ca^{2+}]_i$, which reflects mobilization of Ca^{2+} from intracellular Ca^{2+} stores. Addition of 2 mM Ca^{2+} to the external medium induces entry of Ca^{2+} into the cytosol, which is apparently mediated by depletion of the Ca^{2+} store (figure, a).

It has been found for the first time that preincubation of macrophages with 1 μM zileuton for 5 min before glutoxim administration led to a significant inhibition of Ca^{2+} mobilization from the stores (on average, by 79.2 ± 9.1%, according to the results of seven experiments) and subsequent Ca^{2+} entry into the cytosol (on average, by 63.4 ± 8.7%). The experiments with molixan yielded similar results (data not shown).

Also, it was shown that 4 μM zileuton application during developed glutoxim-induced Ca^{2+} entry significantly reduces Ca^{2+} entry in macrophages (by 45.9±9.7%, the mean value for eleven experiments) (figure, a). Similar results were obtained in experiments with molixan (data not shown).

Thus, we have demonstrated for the first time that zileuton inhibits both phases of Ca^{2+} response induced by glutoxim or molixan in macrophages. These results are in accordance with the data on zileuton-induced inhibition of Ca^{2+} responses in rat mast cells [12,13].

The results of this study confirm our earlier data on 5-lipoxygenases involvement in signaling cascade triggerred by glutoxim or molixan and leading to $[Ca^{2+}]_i$ increase in macrophages. The data on zileuton inhibition of already developed Ca^{2+} entry suggest the involvement of 5-lipoxygenases not only in generation but also in the maintenance of store-dependent Ca^{2+} entry in macrophages.

In addition, the results indicate that the combined clinical application of glutoxim or molixan with antiasthmatic agent zileuton is not recommended.

References

1. Борисов А.Е, Кожемякин Л.А., Антушевич А.Е, Кетлицкая О.С., Кащенко В.А., Чепур С.В., Кацалуха В.В., Васюкова Е.Л., Новиченков А.О., Мотущук И.Е. Клинико-экспериментальное обоснование регионарного и системного введения препаратов группы тиопоэтинов при циррозе печени. Вестник хирургии им. И.И. Грекова. 2001. Т. 4. С. 32 – 38.
2. Kurilova L.S., Krutetskaya Z.I., Lebedev O.E., Antonov V.G. The effect of oxidized glutathione and its pharmacological analogue glutoxim on intracellular Ca2+ concentration in macrophages. Cell Tissue Biol. 2008. V. 2. P. 322-332.
3. Курилова Л.С., Крутецкая З.И., Лебедев О.Е., Крутецкая Н.И., Антонов В.Г. Влияние препарата моликсан на процессы Ca^{2+}-сигнализации в макрофагах. Цитология. 2011. Т. 53. N 9. С. 708.
4. Krutetskaya Z.I., Milenina L.S., Naumova A.A., Antonov V.G., Nozdrachev A.D. Phospholipase A2 inhibitors modulate the effects of glutoxim and molixan on intracellular Ca^{2+} level in macrophages. Doklady Biochem. Biophys. 2015. V. 465. P. 374-376.
5. Krutetskaya Z.I., Kurilova L.S., Antonov V.G., Nozdrachev A.D. Cyclooxygenase and lipoxygenase inhibitors modulate the glutoxim and molixan effects on the intracellular Ca^{2+} concentration in macrophages. Doklady Biol. Sci. 2013. V. 452. P. 277-279.
6. Миленина Л.С., Крутецкая З.И., Наумова А.А., Бутов С.Н., Крутецкая Н.И., Антонов В.Г. Влияние ингибиторов эпоксигеназ на Ca^{2+}-ответы, вызываемые глутоксимом и моликсаном в макрофагах. Цитология. 2015. Т. 57. № 7. С. 518 – 525.
7. Машковский М.Д. Лекарственные средства. М.: Новая волна, 2010. 1216 с.
8. Dube L.M., Swanson L.J., Awni W. Zileuton, a leukotriene synthesis inhibitor in the management of chronic asthma. Clin. Rev. Allergy Immunol. 1999. V. 17. P. 213-221.

9. Zouboulis C.C. Zileuton, a new efficient and safe systemic anti-acne drug. Dermatoendocrinol. 2009. V. 1. № 3. P. 188-192.
10. Milenina L.S., Krutetskaya Z.I., Naumova A.A., Krutetskaya N.I., Butov S.N., Antonov V.G. Arp2/3 complex is involved in the effect of glutoxim and molixan on intracellular Ca^{2+}-concentration in macrophages. Biophysics. 2014. V. 59. № 5. P. 736-740.
11. Grynkiewicz, G., Poenie, M., Tsien, R.Y. A new generation of Ca^{2+} indicators with greatly improved fluorescence properties. J. Biol. Chem. 1985. V. 260. P. 3440 – 3450.
12. Di Capite J., Shirley A., Nelson C., Bates G., Parekh A.B. Intracellular Ca^{2+} wave propagation involving positive feedback between CRAC channels and cysteinyl leukotrienes. FASEB J. 2009. V. 23. P. 894-905.
13. Di Capite J., Nelson C., Bates G., Parekh A.B. Targeting Ca^{2+} release-activated Ca^{2+} channel channels and leukotriene receptors provides a novel combination strategy for treating nasal polyposis. J. Allergy Clin. Immunol. 2009. V. 124. P. 1014-1021.

FUNCTION OF VIMENTIN IN FIBROBLAST MIGRATION

A.A Minin

Institute of Protein Research, RAS, Moscow/Pushchino, Russia

The involvement of vimentin IF in cell migration is one of the old problems of cell biology. First, vimentin is expressed in mesenchymal cells - fibroblasts, leukocytes, endothelium cells – common property of which is ability to migrate.Second, vimentin expression is induced in epithelial cells during their transition to mesenchymal phenotype. The most important example of such transition is malignant transformation when cancer cells turn into metastases. That is why vimentin is used as probe in cancer diagnostics. However, the question “What is the role of vimentin IF in cell migration?” still remains unsolved and important. Our recent discovery of interaction of vimentin IF with mitochondria that increases their membrane potential allowed us to suggest that the role of vimentin in cell migration somehow connected with the effect on mitochondria. We have shown that PAK kinase, effector of Rac1 phosphorylate Ser-55 of vimentin and disrupts the interaction of mitochondria with VIF. Substitution of this serine for alanine blocked this effect of Rac1. Thus, our data predicted that mitochondria with decreased potential will accumulate in the front part of the migrating cell where Rac1 activity is elevated. Actually we demonstrated that mitochondria at the rear of cells are more energizied than at the front. This polarization of mitochondria properties in cells could be involved in the promotion of their migration. To test this hypothesis we generated the cell lines expressing mutants of vimentin mimicking phosphorylated and dephosphorylated forms at the PAK site responsible for regulation of its binding to mitochondria. To our surprise the analysis of lines with disrupted polarization of mitochondria in cells did not reveal any disturbance of cellular motility. Thus our hypothesis of vimentin effect on the migration of cells through mitochondria turned out to be wrong.

SIGNALING CONTROL OF PROTEIN SYNTHESIS IN MURINE SKELETAL MUSCLES FOLLOWING CHRONIC HYPERGRAVITY

T.M. Mirzoev[1], S.A. Tyganov[1], I.O. Petrova[1], L.Vico[2], B.S. Shenkman[1]

[1]*Institute of Biomedical Problems RAS (Moscow, Russia)*

[2]*Inserm U1059 Université Jean Monnet (St-Etienne, France)*

The long-term retention of organisms in increased acceleration fields is an experimental approach towards understanding the biological consequences of earth gravity. Such treatment, called chronic acceleration, simulates a change in gravity and requires exposed organisms to adapt physiologically to the new environment. Information from chronic acceleration supplements that from space physiology in understanding gravitational physiology [Smith, 1976].

As for muscle tissue adaptation to an altered gravity, it is well established that exposure to microgravity (zero-g) induces a decrease in protein synthesis resulting in a significant loss of muscle mass in mammalian postural muscles [Fitts et al., 2000]. However, anabolic signaling pathways regulating protein synthesis (PS) in skeletal muscle following an exposure to chronic hypergravity are still poorly studied. Therefore the aim of the study was to unravel signaling pathways implicated in PS regulation in mouse skeletal muscles following 30-day 2g-centifugation.

Soleus and tibialis anterior muscles of seventeen C57BL6J mice (Charles River,115 L'albresle France) from control group (C) and 2g-group (mice exposed to chronic 30-day 2g-centrifugation) were investigated. All procedures with the animals were conducted in accordance with the European Community Standards on the care and use of laboratory animals (Ministère de l'Agriculture, France, Authorization 04827) and approved by the local Animal Care Committee Université Jean Monnet (St-Etienne, France).

Phosphorylation level of the key signaling proteins of the various anabolic signaling pathways was determined by Western-blotting. The rate of protein synthesis was assessed using puromycin-based SUnSET technique.

Chronic hypergravity did not induce any significant changes in the phosphorylation status of p70s6k, 4E-BP1, GSK-3beta in soleus muscle. PS was significantly reduced in tibialis anterior ($p<0.05$). We also detected an increase in GSK-3beta ($p<0.05$) and p70s6k ($p<0.05$) phosphorylation, as well as a decrease in eEF2 phosphorylation ($p<0.05$) as compared to control values. We can conclude that chronic hypergravity can result in a different anabolic response in mouse hindlimb muscles.

The work was supported by RFBR grant No. 13-04-00888 and CNES.

CEREBROCHOLESTEROL ENHANCES SYNAPTIC VESICLE CYCLE ACTING AS AN ANTAGONIST OF NMDA-RECEPTOR-NO SYNTHASE PATHWAY AT THE MOUSE NEUROMUSCULAR JUNCTION

K.A. Mukhutdinova, M.R. Kasimov, M.R. Fathrahmanova, A.M. Petrov

Department of Normal Physiology, Kazan State Medical University, Butlerova st. 49, Kazan, 420012, Russia

Brain cholesterol has an extremely long live in myelin (5–10 years), but it is metabolized significantly faster (within 5–10 months) in the neuronal membrane, especially in the synaptic sites. Recently it has been revealed that intensive synaptic activity leads to a decrease in cholesterol availability due to activation of cholesterol-24-hydrolase (CYP46A1) converting cholesterol to 24-hydroxycholesterol (also referred cerebrocholesterol). Under these conditions, increased intracellular Ca^{2+} and endoplasmic protein STIM2 participate in the CYP46A1 stimulation. Afterwards, the oxidized cholesterol leaves the synaptic membranes and diffuses into extracellular space. 24-Hydroxycholesterol can permeate a cell wall and a blood brain barrier entering to systemic circulation. Currently, nuclear liver X (LX) receptor and postsynaptic glutamate NMDA-receptors are considered as the main molecular targets of 24-hydroxycholesterol in the mammalian brain [1]. Acting in the submicromolar range 24-hydroxycholesterol potentiates the Ca^{2+} current through NMDA-receptors in response to glutamate release, facilitating induction of long-term potentiation in the hippocampus [2]. Stimulation of LX-receptor (presumably glial) by 24-hydroxycholesterol increases expression of proteins involved in cholesterol metabolism (synthesis, delivery to neuron). However, little is known about both presynaptic action of 24-hydroxycholesterol and its effects on cells located out of brain. Recently using electrophysiological and optical methods we have found that 24-hydroxycholesterol (in the submicromolar concentrations) potentiates evoked neurotransmission in the mouse neuromuscular junctions owing to increases in both the amount of synaptic vesicle involved in exo-endocytosis and the rate of their recycling at high-frequency activity (unpublished data). In the present study we have investigated the underlying mechanism by which 24-hydroxycholesterol (0.4 μM) impacts on the synaptic vesicular exocytosis in isolated phrenic nerve-diaphragm preparations from the mice. FM1-43 dye was used to image the synaptic vesicle exocytosis. Initially, this dye was captured into the synaptic vesicles by compensatory endocytosis which followed the exocytosis evoked by high-frequency (20 Hz) motor nerve stimulation for 1 min. After a rest period (about 30 min) the motor nerve was re-stimulated with the same frequency (during 10 min) and the trapped dye was being released from the vesicles, which was accompanied by a decrease in the nerve terminal fluorescence (termed “unloading” of the dye). For detection of intracellular nitric oxide (NO) production a fluorescent marker DAF-FM DA was used. See for more details about the methods [3,4].

At submicromolar concentrations 24-hydroxycholesterol is a very potent, direct, and selective positive allosteric modulator of NMDA receptors with a mechanism that does not overlap that of other allosteric modulators [2]. NMDA receptor subunits specifically localize postsynaptically at the mice and rat neuromuscular junctions, but are not coincident with nicotinic acetylcholine receptors [5,6]. To test the possible involvement of the NMDA receptors in the effect of 24-hydroxycholesterol (0.4 μM), we applied two selective antagonists of these receptors, AP-5 and MK-801, having different mechanisms of action. Surprisingly, both the antagonists accelerated the FM1-43 unloading at 20 Hz stimulation. This indicates

that the antagonists of NMDA receptor modulate the FM1-43 unloadings in a similar way to that of 24- hydroxycholesterol. Moreover, under conditions of NMDA-receptor inhibition the application of 24-hydroxycholesterol had more profound effect on the rate of FM1-43 unloading. Conversely, activation of the glutamate receptors by exogenous glutamate (in the presence of glycine) led to a decrease in the rate of FM1-43 unloading and to a significant attenuation of the 24-hydroxycholesterol effect on the kinetics of FM1-43 unloading. These data suggest that the action of 24-hydroxycholesterol is dependent on the NMDA-receptors, whose activation could counteract the enhancement of synaptic vesicle exocytosis induced by this oxysterol.

Synaptic vesicles contain the peptide co-transmitter N-acetylaspartylglutamate at the vertebrate neuromuscular junctions. After release into the synaptic cleft, this peptide can be hydrolyzed to N-acetylaspartate and L-glutamate by the enzyme glutamate carboxypeptidase II expressed on membranes of the perisynaptic Schwann cells [7]. Therefore, a prolonged nerve activity should lead to an increase in cleft glutamate concentration and a further stimulation of the postsynaptic NMDA receptors. Low frequency nerve stimulation (0.2 Hz; 240 stimulus) for ~20 min before an unloading stimulus train only slightly decreased the initial FM1-43 fluorescence (by ~5%), but it slowed the rate of the dye loss during the 20 Hz train. This inhibition of the FM1-43 unloading was abolished by both the NMDA receptor antagonist AP-5 and 24-hydroxycholesterol. On the other hand, the low-frequency stimulation prevented the enhancement in FM1-43 unloading caused by AP-5 or 24-hydroxycholesterol under control conditions (without the 0.2 Hz stimulation). Of note, simultaneous treatment with AP-5 and 24-hydroxycholesterol, in conjunction with the low frequency activity, increased the rate of the FM1-43 unloading compared to the control. In sum, these results show that endogenous released glutamate could (1) suppress synaptic vesicle exocytosis induced by high-frequency activity through activation of NMDA-receptors and (2) counteract the effect of 24-hydroxycholesterol on the exocytosis.

Another possible target for 24-hydroxycholesterol is liver X receptor that regulates cholesterol homeostasis and lipid metabolism in skeletal muscle [1]. However, antagonist of liver X receptor did not interfere with the effect of 24-hydroxycholesterol on the FM1-43 unloading. But the agonist itself slightly increased the rate of the dye unloading.

To estimate the NO production at the synaptic region labeled by α-bungarotoxin, we used a fluorescent indicator DAF-FM. The high frequency stimulation lead to a slight, but statistically significant, increase in the DAF-FM fluorescence. This enhancement in the fluorescence was almost completely prevented by 24-hydroxycholesterol (0.4 μM), but enhanced in the presence of glutamate (with glycine). Simultaneous treatment with 24-hydroxycholesterol and glutamate resulted in little effect on the changes in DAF-FM fluorescence in response to the 20 Hz stimulus train. These data indicate that 24-hydroxycholesterol could attenuate the NO production during synaptic activity, while glutamate has the opposite effect and can compete with 24-hydroxycholesterol in the regulation of NO level. Note that we revealed relatively small changes in DAF-FM fluorescence, but

even small increases in NO level can significantly affect the neurotransmission though activation of signal transduction cascades [4].

Synaptic transmission generally depends on locally produced NO. In the mouse neuromuscular junctions retrograde NO signaling could reduce the evoked neurotransmitter release [8]. To test the possibility that 24-hydroxycholesterol is able to act by decreasing NO production, we interfered with NO signaling using L-NAME (inhibitor of all NO synthase isoforms), caveolin-1 scaffolding domain peptide / cavtratin (inhibitor of endothelial NO synthase) and hemoglobin (scavenger of extracellular NO). It was found that L-NAME, cavtratin and hemoglobin significantly enhanced the rate of FM1-43 unloading. Under conditions of NO signaling inhibition (by L-NAME, cavtratin or hemoglobin), the 24-hydroxycholesterol had little or no additional effect on the kinetics of FM1-43 unloading. Collectively, these results suggest that the mechanism by which 24-hydroxycholesterol potentiates synaptic vesicle exocytosis during high-frequency activity could be linked with a decrease in NO synthase activity localized postsynaptically in conjunction with caveolin-1.

Taken together observed data indicate that effect of 24-hydroxycholesterol on synaptic vesicle exocytosis depends on activity of glutamate NMDA-receptor and NO production. We now propose that activation of postsynaptic NMDA-receptor –NO synthase axis attenuates the synaptic vesicle exocytosis during high-frequency activity, while 24-hydroxycholesterol acts as antagonist of this pathway by hindering the increase in NO synthase activity. Since 24-hydroxycholesterol had the effect at the low concentration (0.4 μM) in the neuromuscular junctions located far from endogenous sites of 24-hydroxycholesterol origin (brain), we speculate that brain-derived 24-hydroxycholesterol in the systemic circulation can regulate neuromuscular transmission, especially when its plasma level becomes more, for example, due to an elevated synaptic activity of the brain neurons. Further studies are needed to understanding physiological and/or pathological relevance of 24-hydroxycholesterol in the neuromuscular transmission.

The research is supported by RFBR # 14-04-00094 and # 16-34-00127.

References

1. Petrov AM, Kasimov MR, Zefirov AL. // Acta Naturae. 2016; 8 (1) – in print.
2. Paul SM, Doherty JJ, Robichaud AJ, Belfort GM, et al. // J Neurosci. 2013; 33(44):17290-300.
3. Kasimov MR, Giniatullin AR, Zefirov AL, Petrov AM. // Biochim Biophys Acta. 2015; 1851(5):674-85.
4. Odnoshivkina UG, Sytchev VI, Nurullin LF, Giniatullin AR, Zefirov AL, Petrov AM. // Eur J Pharmacol. 2015; 765:140-53.
5. Malomouzh AI, Nurullin LF, Arkhipova SS, Nikolsky EE. // Muscle Nerve. 2011; 44(6):987-9.
6. Mays TA, Sanford JL, Hanada T, Chishti AH, Rafael-Fortney JA. // Muscle Nerve. 2009; 39(3):343-9.
7. Walder KK, Ryan SB, Bzdega T, Olszewski RT, Neale JH, Lindgren CA. // Eur J Neurosci. 2013;37(1):118-29.
8. Yakovleva OV, Shafigullin MU, Sitdikova GF // Neurochem J. 2013; 7(2): 103-110.

SPINAL MECHANISMS OF THE DIRECTION CONTROL DURING LOCOMOTOR ACTIVITY

P. Musienko[1,2], N. Merkulieva[1,2], Y. Gerasimenko[1]

[1]*Pavlov Institute of Physiology RAS, Russia, Saint-Petersburg, Makarov emb., 5, 199034*

[2]*Institute of Translational Biomedicine, St Petersburg State University, Russia, Saint-Petersburg, Universitetskaya nab. 7-9, 199034*

Most bipeds and quadrupeds, in addition to forward walking, are capable of backward and sideward walking. The direction of locomotion is determined by the direction of stepping movements of individual limbs in relation to the front-to-rear body axis. Our goal was to assess the functional organization of the system controlling the direction of stepping. The experiments were carried out on decerebrated cats walking on the treadmill with their hindlimbs, whereas the head and trunk were rigidly fixed. We performed a detailed mapping of the lumbosacral enlargement (spinal segments L4-S1) to compare the locomotion patterns in different directions evoked by electrical spinal cord stimulation (ES) of the local network. Forward locomotion was initiated when any tested segments were stimulated; however, the motor pattern characteristics were different. Stimulation of the rostral segments (L4-L5) induced a coordinated walking with a predominance of the flexor component. Stimulation of the caudal segments (L7-S1) induced more pronounced extension during gait. It was shown that only during stimulation of specific area of the spinal cord, a reverse of the treadmill belt direction (at constant parameters of electrical stimulation) resulted in backward locomotion. This area was distributed in different cats from caudal part of L5 to rostral part of L7 spinal segments. It confirms the specific rostrocaudal distribution of spinal neural networks responsible for locomotor control in different directions. While the spinal circuitry responsible for forward stepping are widely distributed, the neural networks that control backward stepping are apparently more localized. Thus, ES can activate limb controllers, which are able to generate stepping movements in different directions. The direction of steps was opposite to the treadmill motion, suggesting that this direction was determined by sensory input from the limb during stance. By contrast, stimulation of the brainstem (the mesencephalic locomotor region, MLR) evoked well-coordinated stepping movements only if the treadmill was moving in the front-to-rear direction. The MLR can be considered as a command center for forward locomotion, which is the main form of progression in bipeds and quadrupeds. We conclude that supraspinal commands (caused by MLR stimulation) select one of the numerous forms of operation of the spinal limb controllers, namely, the forward walking.

The study was supported by Russian Science Foundation (RSF grant No. 14-15-00788).

HYDROGEN SULFIDE INCREASES THE ACTIVITY OF TRIGEMINAL NERVE BY ACTIVATION OF TRP RECEPTORS

A.N. Mustafina[1], K.S. Koroleva[1], R.A. Giniatullin[1,2], G.F. Sitdikova[1]

[1]*Institute of fundamental medicine and biology, Kazan Federal University, Kremlevskaya 18, Kazan 420008, Russia*

[2]*A.I. Virtanen Institute for Molecular Sciences, University of Eastern Finland, Neulaniementie 2, Kuopio 70211, Finland*

Migraine – a neurological disorder characterized by episodic or regular strong attacks of headaches in one (rarely both) sides of the head. Dura mater plays a key role in the pathophysiology of headache, where the activation of trigeminal afferent neurons innervating the meninges, is the first stage of pain in migraine [1]. There is increasing data on the involvement of the new gasotransmitter – hydrogen sulfide (H_2S) in nociception. Endogenously H_2S is produced by enzymes cystathionine β-synthase and cystathionine γ-lyase in trigeminal neurons. It was shown that, H_2S causes depolarization of the membrane of neurons, leading to increased generation of action potentials, which in turn leads to an increase in the excitability of trigeminal neurons [3]. It is known that donor of H_2S - sodium hydrosulfide NaHS activates capsaicin-sensitive sensory neurons in the isolated rat bladder through the activation of TRPA1 – channels [2], but the effects of H2S on TRPV receptors in trigeminal neurons are unknown. Therefore, the aim of our study is investigation the influence donor of H_2S – NaHS on responses of TRPV receptors and spontaneous electrical activity in the trigeminal neurons.

The recordings of electrical activity of trigeminal nerve were performed on male rats aged 40-42 days. Animal experiments were approved by the Ethics Committee of Kazan Federal University. Before starting the experiment, preparations were stored in saline solution with the following composition (in mM): NaCl 119, KCl 2.5, $NaHCO_3$ 30, $CaCl_2$ 2, $MgCl_2$ 1, $NaHPO_4$ 1, glucose 11; pH 7.2–7.4; oxygenated by carbogen (95% O_2/5% CO_2). Immediately before the experiment, peripheral process of the trigeminal nerve was cut from dura mater and is sucked into the glass electrode with the appropriate diameter. Substances were applied in the region of dura mater vessels branching. Signals were recorded using an amplifier DAM 80 (World Precision Instruments, Sarasota, FL), electrical events were digitized on a PC using NI PCI6221 board (National Instruments, Austin, Texas, United States). Signals were visualized and analyzed using WinEDR v.3.2.7 software (University of Strathclyde, Glasgow, United Kingdom).

The TRPV-mediated currents were recorded in trigeminal neurons isolated from 9–12 day rats. The animals were decapitated, the trigeminal ganglia was removed and placed in a cooled solution. For dissociation of neurons, the ganglion was added in an enzymatic solution containing trypsin, collagenase and DNAse, and placed in an incubator for 25 min. Dissociated neurons were placed on glass covered with poly-L lysine and kept in the incubator for 12 hours before the experiments.

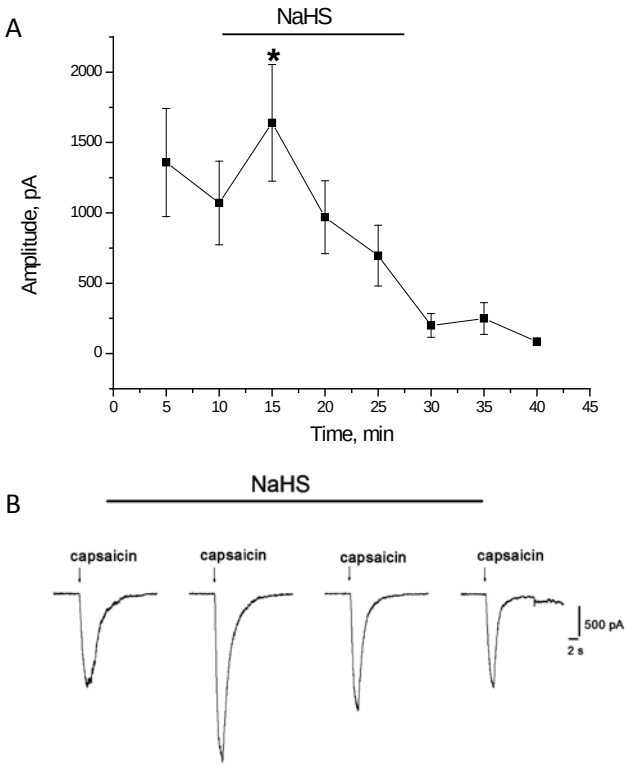

Fig. 1. NaHS increases the TRPV-mediated currents in rat trigeminal neurons A. The average amplitudes of TRPV-currents in the control and during application of NaHS (100 mkM). B. Original recordings of TRPV currents in the control and during application of NaHS.

To register currents of TRPV receptors in response to application of the agonist capsaicin the patch-clamp technique in the whole-cell configuration at holding potential –70 mV was used. Cells were continuously perfused with a solution of the following composition (in mM): 148 NaCl, 5 KCl, 1 $MgCl_2$, 2 $CaCl_2$, 10 Hepes, 10 D-Glucose, pH 7.2. Intracellular solution contained (in mM): 145 KCl, 1 $MgCl_2$, 10 Hepes, 5 EGTA, 0.5 $CaCl_2$, 2 Mg-ATP, 0.5 Na-GTP, 5 KCl, pH 7.2. Capsaicin in a concentration of 1 mkM was applied using a system of fast application for 2 sec. For preventing desensitization of receptors the agonist was applied at intervals of 5 min. NaHS was used as donor of H_2S, since in aqueous solution it dissociates to sodium ion (Na^+) and anion hydrosulfide (HS^-), which reacts with protons (H^+) to form H_2S.

Application of the TRPV receptor's agonist – capsaicine induced the inward currents with amplitude of 2470.9 ± 1168.9 pA (n = 5). In the conditions of

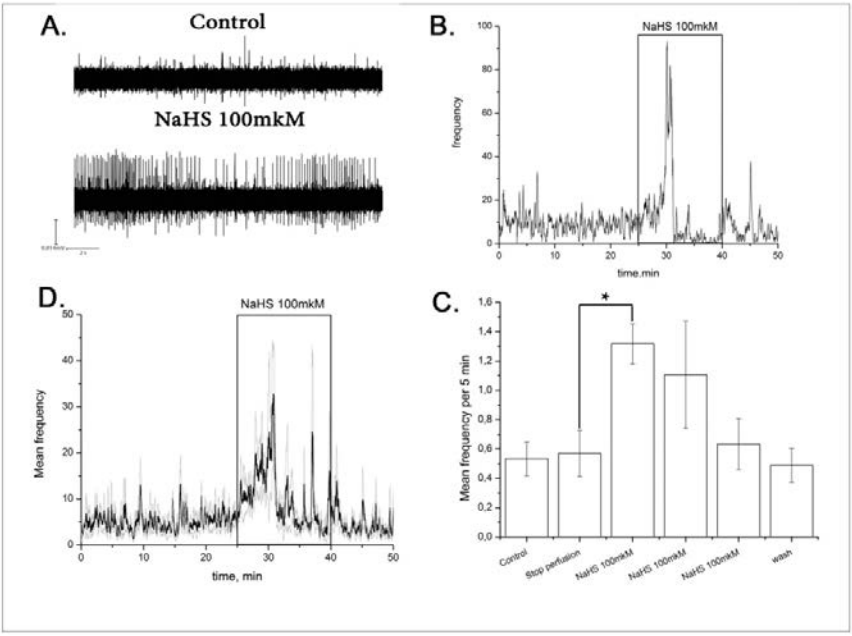

Fig. 2. Effect donor of hydrogen sulfide (NaHS 100 mkM) on spontaneous electrical activity in the trigeminal nerve A. An example of the original trace in control and in the presence of NaHS 100mkM; B. Changes in the frequency of electrical activity (AP) during the experiment; C. Histogram average frequency AP for 5 minutes. D. Diagram of the averaged frequency (*p< 0.05, n = 8)

cell perfusion solution containing NaHS in concentrations of 100 mkM, an increase in the amplitude of TRPV currents within 5 minutes was observed which achieved 3680.4 ± 1689.4 pA (n = 5). However, by the 15 minutes of application NaHS the TRPV-currents amplitude decreased to 273.5 ± 139.1 pA (n = 5), which is 76.8 ± 12.7% less than the control values (n = 5, p <0.05) (fig. 1).

During electrophysiological experiments on the trigeminal nerve we have shown that the application donor of H_2S in concentration of 100 mkM, induced significant increase in the frequency of action potentials in the first 5 minutes (control 0.57 ± 0.16; in the presence of NaHS 100 mkM - 1.32 ± 0.14; p > 0.05, n = 8), which corresponding to the data obtained in cell culture. By the 10th minute the frequency returned to control values (Fig. 2). To confirm the target of action of H_2S, series of experiments were carried out with a capsazepine, blocker of TRPV1 receptors. Capsazepine prevented the increase of electrical activity by NaHS.

It was suggested that H_2S induce the increase of electrical activity of trigeminal nerve by activation of TRP receptors of trigeminal neurons.

The work was supported by Russian Science Foundation No. 14-15-00618.

References

1. Cortical spreading depression induces oxidative stress in the trigeminal nociceptive system / A. Shatillo,K. Koroleva,R. Giniatullina,N. Naumenko,A.A. Slastnikova,R.R. Aliev,G. Bart,M. Atalay,C. Gu,R. Khazipov,B. Davletov,O. Grohn,R. Giniatullin // Neuroscience. Elsevier.3 December 2013. pp. 341-349
2. Hydrogen sulfide causes vanilloid receptor 1-mediated neurogenic inflammation in the airways/ Marcello Trevisani, Riccardo Patacchini, Paola Nicoletti, Raffaele Gatti, David Gazzieri, Nicola Lissi, Giovanni Zagli, Christophe Creminon, Pierangelo Geppetti, Selena Harrison // British Journal of Pharmacology (2005) 145, 1123–1131
3. Physiological role of hydrogen sulfide in nervous system/ A.V. Yakovlev, G.F. Sitdikova// Genes and Cells. V.9, № 3-2014

STUDY OF THE EFFECT OF TROPOMYOSIN ON THE STRENGTH OF ACTIN-MYOSIN CONTACT

S.R. Nabiev[1], A.K. Tsaturyan[2], S.Y. Bershitsky[1]

[1]*Institute of Immunology and Physiology, Ural Branch of RAS, Yekaterinburg, 620049, Russia*

[2]*Institute of Mechanics, Moscow State University, Moscow, 119992, Russia*

Stiffness of the bond of myosin head with actin filament during their interaction is an important characteristic of force-generating ability of a myosin head. During this interaction, some conformational changes occur in the myosin head, which cause either sliding of thick and thin filaments relative to each other or generation of force. Energy of this conformational transition in myosin head is stored in an elastic element [Huxley, Simmons, 1971] to be released as mechanical work of myosin head. Maximal force that myosin head can develop is restricted by strength of the contact of myosin head with thin filament where the strength can be affected by mutations in the proteins participating in the interaction particularly in tropomyosin.

The stiffness of actomyosin cross-bridge was measured in single muscle fiber and its value in those experiments was in the range from 0.25 to 3.3 pN/nm [Huxley, Simmons, 1971; Linari *et al.*, 2007; Decostre *et al.*, 2005; Piazzesi *et al.*, 2007]. It was found that compliance of myofilaments may significantly affect stiffness measurements.

The cross-bridge stiffness was also measured at single molecule level with the use of an optical trap. In earlier works it was underestimated (0.2 and 0.6 pN/nm, [Molloy *at al.*, 1995, Nishizaka *et al.*, 1995], respectively) due to a compliance in bead-actin links. More recent works with advanced experimental protocols and data analysis reported the stiffness value of 1.3–2.9 pN/nm, which is comparable with that obtained in muscle fiber experiments [Takagi *et al.*, 2006; Capitanio *et al.*, 2006; Lewalle *et al.*, 2006; Kaya, Higuchi, 2010].

All measurements of the stiffness of actomyosin cross-bridge in the optical trap were done only with F-actin and did not consider the effect of tropomyosin on the contact strength of myosin head with thin filament. Recently was shown [Lu *et al.* 2006] that some tropomyosin mutants reduce the rigor stiffness of bovine heart

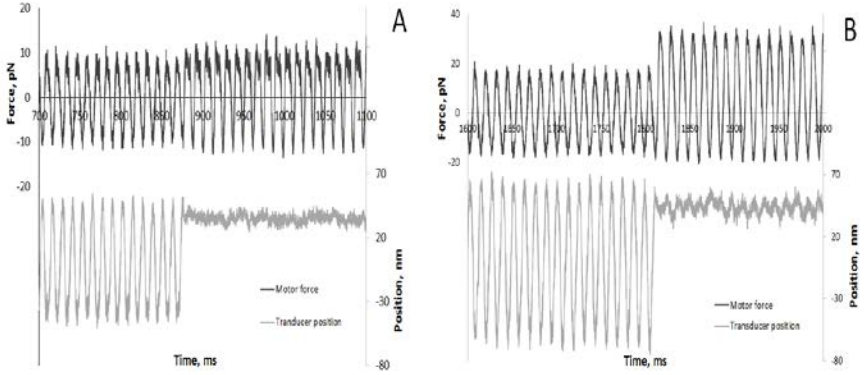

Example of experimental recordings of oscillations of the beads in movable (motor bead) and unmovable (transducer bead) beams. Panel A shows interaction of myosin head with F-actin and panel B shows that with reconstructed thin filament (containing F-actin, troponin and tropomyosin). Interactions are seen by reduction in oscillation amplitude of transducer bead.

trabeculae as compared with native tropomyosin. The authors supposed that tropomyosin in the presence of troponin and calcium strengthens the hydrophobic interactions actin filament with myosin head. This modulating effect can be caused by a positive allosteric influence of tropomyosin on actin that involves a higher amount of hydrophobic residues in the myosin-binding site on actin. This in turn may affect stereospecific docking of myosin head on actin filament. However, it is not clear whether the stiffness of a single complex or amount of these complexes is changed. Single muscle fiber studies cannot answer this question, but the optical trap makes it possible.

To understand whether tropomyosin does affect the strength of myosin-thin filament contact we measured the cross-bridge stiffness in the optical trap using three beads assay [Finer *et al.* 1994]. Two polystyrene beads of one micrometer in diameter were held in two independent beams of infrared laser. A 5-9-nanometer fragment of F-actin or reconstructed thin filament (F-actin, troponin and tropomyosin) was glued to these beads forming a dumbbell-like probe. The dumbbell was pre-stretched by force of ~10 pN and 100 Hz sinusoidal oscillations of about 300 nm amplitude were applied by moving one of the beams using acousto-optical deflector. In the absence of interaction of myosin head with F-actin or thin filament the oscillations of the both beads of the dumbbell were almost equal. During the interaction, the amplitude of oscillations of the bead in unmovable beam sharply decreased. To estimate the reduction in amplitude of its oscillations, we decreased ATP concentration to extend the duration of interactions. At 50 nM the duration lasted for several seconds. An example of experimental recording of the bead oscillations in the presence and the absence of interactions is shown in figure. We esti-

mated the stiffness of the bond of myosin with F-actin or reconstructed thin filament by the ratio of the oscillation amplitude in attached and detached state. Thus, we have elaborated an approach of testing the effect of tropomyosin on the strength of actomyosin contact.

Work is supported by the RFBR grant 16-34-00493 mol_a.

AROUSAL FROM HIBERNATION INDUCES THE REGION-SPECIFIC INCREASE IN CYCLIN-DEPENDENT PROTEINKINASES IN THE BRAIN OF GROUND SQUIRREL (SPERMOPHILUS UNDULATUS)

M.V. Onufriev[1], T.P. Semenova[2], E.P. Volkova[1], M.A. Sergunkina[1], A.A. Yakovlev[1], N.M. Zakharova[2], N.V. Guljaeva[1]

[1]*Institute of Higher Nervous Activity and Neurophysiology Russian Academy Sciences, ul. Butlerova 5a, Moscow, 117485, Russia*

[2]*Institute of Cell Biophysics Russian Academy Sciences, ul. Institutskaja 3, Pushchino, Moscow region, 142290, Russia*

Recent studies demonstrated that cell cycle proteins play an important role in the functioning of the central nervous system [Steward et al., 2003]. It was shown that cell cycle-related proteins are involved in regulation of migration process, transmission of pain impulses [Piper et al., 2004, Gomazkov, 2013]. Cdk 1 protein, when with cyclin B1, participates in triggering mitosis and, when alone, it is involved in the morphological transformations of cells [Knight et al., 2003]. In the nervous system Cdk 5 kinase, structurally similar to Cdk 1, regulates specifically protein activity associated with neuron morphology, cytoskeleton, cell motility [Gomazkov, 2013], has an impact on synaptic plasticity through its up-regulation of NMDA-receptors [Hawasli et al., 2007]. We have shown the involvement of Cdk 5 in the development of dendritic spines in the neocortex and hippocampus [Pappas et al., 2001], in the regulation of intracellular responses to dopamine signals [Bibb et al., 1999]. In our previous studies we revealed a regional specificity of distribution of actin mRNA expression in the brain of Yakutian ground squirrel (*Spermophilus undulatus*). It has been established that the level of expression of this protein in the hippocampus was 4-5 times higher as compared with that one in another brain regions through the whole yearly life cycle of hibernators [Onufriev et al., 2016]. The pattern of actin mRNA changes during arousal of animals from their torpid state was compared with neuron changes revealed in morphological [Magarin et al., 2006, Popov et al., 2007] and physiological studies [Semenova 2004; Semenova et al., 2014, Semenova, Zakharova, 2015].

The present study was undertaken to investigate the pattern of changes in the brain of hibernators.

The object and methods of investigation

Three groups of mature adult Yakutian long-tailed ground squirrels (*Spermophilus undulatus*) of both sexes with the body weight of 600–800 *g* (*n*=28) were used in the experiments. The animals for the experiment were trapped at the differ-

ent phases of year life cycle of these mammals (Zakharova, 2014). Group 1 included summer active animals (n=8, t_{brain}= 37–38ºC, mid June – start July); Group 2 consisted of winter animals trapped for the experiment by 6–7 day of torpor bout (n=10, t_{brain}= 1–2ºC, the end of January –start February), Group 3 was composed of winter animals which were roused in the mid of torpor bout, in particular, taken for the experiment at emergence from torpid state (n=10, t_{brain}= +10ºC, the end of January – start February).

Immediately after decapitation the brain of ground squirrel was excised, chilled in an ice cold isotonic solution of NaCl and the frontal neocortex, cerebellum, hippocampus and brain stem were dissected on ice. Western blotting was performed to determine the amounts of cell cycle proteins: cyclin-dependent protein kinases Cdk 1, Cdk 2, Cdk 4, which were directly involved in up-regulation of the cell cycles and Cdk2, that participated in processes of neuronal maturity and neuromigration, and also cyclin A, cyclin B1 which like kinases were involved in different processes except control of the cell cycle. Biochemical methods used in this study we described in detail in our article [Onufriev et al., 2016].

Data have been statistically processed using Exel 2003 and Statistica 8.0 software packages. RESULTS AND DISCUSSION

When the brain temperature of torpid hibernators was getting as low as +1-2ºC, the expression level of Cdk 1 in the hippocampus was truly decreased by 30% ($P<0.05$) compared with that in summer animals. The reduction of Cdk 1 level in the frontal portion of neocortex and stem appeared as a tendency. Arousal of the animals from the hibernating state is associated with the increased expression level of Cdl 1 in the cortex and hippocampus ($P<0.05$).

A decrease in the level of cyclin-dependent kinase Cdk 2 expression during torpor by 37.2% ($P<0.05$) compared to that one in summer animals was observed only in the hippocampus, in the rest brain regions its level remains virtually unchangeable. An increase in the Cdk 2 expression by 72.6% in the animals who emerged from hibernation was seen also only in the hippocampus, changes in the other brain region are of tendency nature.

The expression level of Cdk 4 in animals who are in a torpor state (Group 2) declines by 22.1 ($P<0.05$) in the hippocampus compared to that in summer animals, although the decrease in the stem and neocortex is negligible. In animals who emerged from torpid state we observe real increase in the expression level of this protein kinase in the hippocampus and the frontal neocortex.

The decrease in the expression level of Cdk5 in torpor during winter was shown in the hippocampus (by 30,9%, $P<0.05$) and in the caudal region of the brain stem (by 44,8%, $P<0.05$). In the frontal region of neocortex the decrease was weakly pronounced and was shown as a tendency, In animals who roused from the torpor the real increase in the expression level of Cdk 5 (by 31,9%, $P<0,05$) is developed only in the hippocampus.

Low expression values of cyclins B1 and A compared to the other proteins we studied point to poor abundance of these cyclins in the brain that is, probably, caused by rare cell division in it.

Thus, having analyzed the results of our study it was shown that a pattern of protein expression in the cell cycle and in Cdk 5 is significantly distinguished by the level of expression in different regions of the hibernator brain. We showed that in active summer animals the values of the expression level of one and the same protein can be different by a factor of 3–5 between the frontal neocortex, hippocampus and caudal region of the brain stem. This gives evidence of distinctive region-specific features of cell cycle protein regulation in the brain of mammals who hibernate in winter. Data on the regional difference in the pattern of protein regulation changes when temperature decreases or increases in the brain of ground squirrel are also indicative.

The event, that the highest level of expression of cell cycle protein is recorded in the hippocampus, is presumably related to the fact that in the subgranular zone of the fascia dentate this brain region of mammals retains the ability to produce new nerve cells throughout life [Parent et al., 1997, Kernie, Parent, 2010]. In this brain region progenitor neural cells continue their cell division to produce new novel neurons [Viktorov, 2001; Scheider-Mizell et al., 2010].

In our experiments the increase in brain temperature of the animals who emerged from hibernation was accompanied by the elevation of the expression level of the studied cyclin-dependent protein kinases in the hypocampus. In addition, many authors noted that in ground squirrels when they came out of hibernation state a restoration process of spine apparatus occurs in CA1 and CA3 hippocampal areas as the animals warm up [Magarin et al., 2006; Popov et al., 2007], sensitivity of opioid [Semenov et al., 2015], NMDA-[Zhao et al., 2006] and adrenoreceptors [Semenova, 2004] enhances, the activity of NO synthase [Onufriev et al., 2002] increases. Probably, these changes in animals after arousal point to a rapid, within several hours, restoration of the parameters of the studied behavioral activity, training ability and memory up to the level that is illustrative for the animal behavior during the period of its maximum activity in summer [Semenova et al., 2001, Semenova et al., 2014]. So we can hypothesize that cell cycle protein could be involved in realization of morpho-functional alterations which are necessary for the formation of new or restoration of old interneuronal relations [Semenova et al., 2001, 2014, 2015] providing an adequate functioning of this cell cycle in a new functional state of the hibernating animal.

References

1. Bibb J.A., Snyder G.L., Nishi A. et al. Phosphorylation of DARPP-32 by Cdk5 modulates dopamine signalling in neurons». // Nature. 1999. 402 (6762): 669 - 671.
2. Gomazkov O.A. Neurogenesis as adaptive function of brain. Moscow. IKAR. 2013. 136 P.
3. Hawasli A.H., Benavides D.R., Nguyen C. et al. Cyclin - dependent kinase 5 governs learning and synaptic plasticity via control of NMDAR degradation. // Nat. Neurosci. 2007. 10 (7): 880 - 886.
4. Kernie S.G., Parent J.M. Forebrain neurogenesis after focal ischemic and traumatic brain injury. // Neurobiol. Dis. 2010. 37(2): 267-274.
5. Knights C.D., Pestell R.G. The cell cycle. Therapeutic targeting of cell cycle regulatory components and effector pathways in cancer // Cancer drug discovery and devel-

opment: molecular targeting in oncology. Ed. Kaufman H.L., Walder S., Antman K. New Jersey: Humana Press, 2003. 1: 1-32.
6. Magarin A.M., McEwen B.S., Saboureau M., Pevet P. Rapid and reversible changes in intrahippocampal connectivity during the course of hibernation in European hamsters // PNAS. 2006. 103(49): 18775-18780.
7. Onufriev M.V., Semenova T.P., Kolaeva S.G. et al. NO synthase activity in brain regions of ground squirrel Citellus undulates in different phases of the hibernation cycle.// Neurochemical Journal. 2002. 19(2):264-268. In Russian.
8. Onufriev M.V., Semenova T.P., Volkova E.P. et al. Seasonal features of actin expression and protein cdk 5 in different regions of the brain Yakut squirrel (Spermophilus undulatus).// Neurochemical Journal. 2016. № 2. In Russian. In Press.
9. Pappas G.D., Kriho V., Pesold C. Reelin in the extracellular matrix and dendritic spines of the cortex and hippocampus: a comparison between wild type and heterozygous reeler mice by immunoelectron microscopy. // J. Neurocytol. 2001. 30 (5): 413 - 425.
10. Parent J.M., Timothy W.Yu., Leibowitz R.T., Geschwind D.H., Sloviter R.S., Lowenstein D.H. Dentate granule cell neurogenesis is increased by seizures and contributes to aberrant network reorganization in the adult rat hippocampus. // J. of Neuroscience. 1997. 17(10): 3727 – 3738.
11. Piper M., Holt C. RNA translation in axons. // Annu.Rev. Cell. Dev.Biol. 2004. 20: 505 – 523.
12. Popov V.I., Medvedev N.I., Patrushev I.V., Ignat'ev D.A., Morenkov E.D., Stewart M.G. Reversible reduction in dendritic spines in CA1 of rat and ground squirrel subjected to hypothermia-normothermia *in vivo*: a three-dimentional electron microscope study // Neuroscience. 2007. 149: 549-560.
13. Schneider-Mizell C.M., Parent J.M., Ben-Jacob E., Zochowski M.R., Sander L.M. From network structure to network reorganization: implications for adult neurogenesis. // Phys. Biol. 2010. 7(4): 046008.
14. Semenova T.P., Anoshkina I.A., Khomut B.H., Kolaeva S.G. Seasonal peculiarities of behavior, of ground squirrels Citellus undulatus in the holeboard and open field tests. // Behav. Processes. 2001. 56(1): 195–200.
15. Semenova T.P. Specifics of monoaminergic regulation of the central nervous system of hibernating animals (Citellus undulatus)// Zh Vyssh Nerv Deiat Im I P Pavlova. 2004. 54(2):174-182.
16. Semenova T.P., Spiridonova L.A., Zakharova N.M. Seasonal peculiarities of the ground squirrel (Spermophilus undulatus) and Wistar rats circadian activity// Ross Fiziol Zh Im I M Sechenova. 2014. 100(9):1068-1076.
17. Semenova T.P., Zakharova N.M. Seasonal features of the effects of blockade of opioide receptors on adaptive behavior in hibernating animals // Neurosci. and Behav. Physiol. 2015. 45(6): 658- 663.
18. Steward O., Shuman E.M. Compartmentalized synthesis and degradation of proteins in neurons. // Neuron. 2003. 40(2): 347 – 359
19. Viktorov I.V. Stem cells of mammalian brain: biology of the stem cells *in vivo* and *in vitro*// Izv Akad Nauk Ser Biol. 2001. № 6. P. 646-655. In Russian
20. Zhao H.W., Christian S.L., Castillo M.R., Buno-Ito B., Drew K.L. Distribution of NMDA receptor subunit NR1 in Arctic ground squirrel central nervous system. // J. Chem. Neuroanat. 2006. 32: 196-207.

ALLOSTERIC INTERACTIONS IN ACTIN: HOW A POINT MUTATION CAN CHANGE THE STRUCTURE OF THE ACTIN FILAMENT

A. Orlova[1], P.M. Fagnant[2], H. Lu[2], K.M. Trybus[2], E.H. Egelman[1]

[1]*University of Virginia, Charlottesville, VA, USA*

[2]*University of Vermont, Burlington, VT, USA*

Muscle actin has been exquisitely conserved over vertebrate evolution, with not a single amino acid change between humans and chickens in the striated muscle isoform. Most variations that are seen in actin are tissue-specific, rather than species-specific, with a small number of substitutions occurring, for example, between the smooth muscle and striated muscle isoforms. The origin of the extreme selective pressure on every residue, particularly buried residues that cannot be directly interacting with actin-binding proteins, is unknown. Mutations in actin have been shown to lead to hereditary myopathies, such as the Arg256Cys substitution in smooth muscle actin (R258C in the *ACTA2* gene), which causes thoracic aortic aneurysms and dissections (TAAD). While this mutation has been shown *in vitro* to affect actin's interactions with cofilin, profilin, tropomyosin and myosin [Lu et al., PNAS, 2015], all of these effects must be allosteric as this residue is buried in the actin filament. We have used electron cryo-microscopy (cryo-EM) to compare expressed wild-type smooth muscle actin with the Arg256Cys mutant. We show that the mutation causes an allosteric shift of the 262–274 "hydrophobic loop" between the two strands of the actin filament, which plays an important role in filament formation and stabilization. Because the conformation of this buried loop has previously been shown to be coupled to myosin binding on the surface of the actin filament, a picture emerges of large allosteric networks of buried actin residues that communicate information across the actin filament.

CHARACTERIZATION OF HUMAN VASCULAR ENDOTHELIAL CELLS EA.HY926 AS A MODEL TO STUDY INSULIN RESISTANCE

K.A. Palkina, M.V. Samsonov, V.P. Shirinsky, A.V. Vorotnikov

Laboratory of Cell Motility, Institute of Experimental Cardiology, Russian Cardiology Research Center, Moscow 121552, Russia

Obesity and type 2 diabetes associated with increased cardiovascular risks are the most threating metabolic diseases in the modern society. Insulin resistance (IR) is the earliest feature of these metabolic disorders. It develops as a result of dysregulated insulin signaling in insulin-sensitive cells and underlies inability of insulin to lower the blood glucose level in organism. How and why insulin signaling becomes dysregulated is not completely understood. Neither is clear whether the mechanisms of IR development are different in the insulin-sensitive cells. These include the striated muscle, liver, and fat cells, which normally respond to insulin by increased accumulation of glucose and its conversion into glycogen and

fat, respectively. In addition, vascular endothelium is the primary target of blood insulin. Instead of glucose utilization, it functions to regulate vascular contractility and permeability in insulin-sensitive manner. Thus, dysregulated insulin signaling in these cells may provide a link to cardiovascular disorders associated with obesity and type 2 diabetes.

Studying mechanisms of IR development in endothelium at the cellular level is problematic because no cultures of vascular endothelial cells are available. Recently, immortalized EA.Hy926 cells have been introduced that are a hybrid of human umbelical vein endothelial cells (HUVEC) and lung carcinoma A-549 cells. Whether these cells is a suitable model to explore mechanisms of IR is unknown. We study this possibility by measuring insulin signaling, NO production and endothelial barrier function in these cells. To stimulate IR we apply several protocols similar to those used for cultured adipocytes, including hyperlipidemia, hyperglycemia, and hyperinsulinemia models. Thus, EA.Hy926 cells are cultured in the presense of high concentrations of BSA-conjugated palmitate, D-glucose or human insulin. Insulin signaling is typically measured by western blots of cell lysates and phospho-specific antibodies to the key members of insulin cascade. Endothelial NO-synthase (eNOS) activation is measured by phosphorylation response of Ser1177 in eNOS, and NO production by these cells is assessed using 4-Amino-5-methylamino-2',7'-difluorofluorescein diacetate (DAF) as NO probe. The full electric impedance of EA.Hy926 cell monolayers grown on gold electrodes is used as a measure of endothelial permeability and the barrier function.

We found that insulin signaling is functional in EA.Hy926 cells. Phosphorylation of Akt (Ser473) and eNOS (Ser1177) was increased in response to insulin treatment indicating that EA.Hy926 cells possess insulin-sensitive receptors coupled to PI3-kinase pathway that sequentially targets Akt and eNOS. Surprisingly, insulin-stimulated phosphorylation of Akt and eNOS was not lower in IR-treated than in control cells. However, IR cells displayed increased basal phosphorylation of Akt (i.e., not stimulated by insulin) indicating reduction in the fold-stimulation of insulin signaling by IR. Whether these cells have reduced NO production and permeability is currently under investigation.

OXYSTEROL-DRIVEN CHANGES IN SYNAPTIC TRANSMISSION RELATED WITH SYNAPTIC VESICLE CYCLING. LESSONS FROM NEUROMUSCULAR JUNCTIONS

A.M. Petrov, M.R. Kasimov, K.A. Mukhutdinova, M.R. Fathrahmanova

Department of Normal Physiology, Kazan State Medical University, Butlerova st. 49, Kazan, 420012, Russia

Neurotransmitter release occurs due to fusion of synaptic vesicle containing neurotransmitter and other service molecules. After exocytosis the synaptic vesicle membrane is captured into the nerve terminal by endocytotic machine. Newly

formed vesicle is filled by neurotransmitter in two steps process which involved proton pump and the neurotransmitter transporter. The synaptic vesicle then is included in one of three synaptic vesicle pools having different properties. Small population of synaptic vesicles, docked to the presynaptic membrane (at specific region named active zone), makes up the ready releasable pool (RRP). Vesicles from RRP release the neurotransmitter in response to single stimuli. Majority of undocked synaptic vesicle (~80–90%) constitutes the reserve ("resting") pool, vesicles from it reluctantly undergo exocytosis (only under conditions of strong stimulation) and use slow ("bulk") pathway of endocytotic recycling. Some synaptic vesicles (~10–20%) are able to fuse rapidly and then recycle through a fast endocytosis. These vesicles can maintain the neurotransmitter release during a slight to moderate synaptic activity owing to continuous reuse (recycling). A population of the vesicles is referred to as recycling pool and usually comprises the RRP. Synaptic vesicle cycling is required to maintain a neurotransmission during prolonged activity under natural and experimental conditions. Involvement of the vesicular pools in neurotransmitter release depends on activity mode (frequency of action potentials) and intracellular signaling network.

Vertebrate neuromuscular junctions have a relatively large common synaptic vesicle population. One active zone is served by from a few hundred to thousand synaptic vesicles. This gives us a good opportunity to investigation of the vesicular cycling using combination of optical and electrophysiological recordings. Styryl (FM) dyes provide powerful instrument for monitoring of synaptic vesicle exo- and endocytosis. FM dye reversibly binds with the surface membrane and enters into the nerve terminal due to compensatory endocytosis following exocytosis evoked by nerve stimulation (loading of FM dye). After washout period the FM-loaded nerve terminal can be re-stimulated and a decrease in FM- fluorescence indicate on the dye loss due to synaptic vesicle exocytosis. Note that FM dye fluorescence in the solution is very low, and it is significantly increased by interacting FM dye with the membrane. Recording of postsynaptic events (end plate potentials and currents) allows indirectly quantifying the neurotransmitter release. Comparative analysis of optical and electrophysiological data could give the additional information about synaptic vesicle recycling.

Cholesterol is a long-lived molecule in the membrane, especially neuronal, and can be oxidized by specific enzymes or reactive oxygen species [1]. Numerous cholesterol oxidation products (oxysterol) have been described previously, but their physiological or pathological relevance has only begun to emerge recently [1,2]. Cholesterol has a particular importance for synaptic transmission and synaptic membranes are enriched in cholesterol [3–6]. Production of some oxysterols could be significantly increased during neurotransmission [1]. That is why it seems interesting to clarify the role of the oxysterol in regulation of synaptic transmission. In contrast to central synapses, the neuromuscular junctions are deprived of the oxysterol-rich microenvironment. So we can study the fundamental aspects of oxysterol-driven changes in synaptic transmission without a lot of interferences from other oxysterols produced endogenously *in situ*. We have chosen to study three oxyster-

ols (5α-cholestan-3-one, olesoxime/cholest-4-en-3-one oxime, 24-hydroxycholesterol) of different origin and used these cholesterol derivatives in the submicromolar range (0.2–0.4 μM). In case of rare hereditary disorder *cerebrotendinous xanthomatosis*, caused by the defects in sterol-27-hydroxylase enzyme (CYP27A1), 5α-cholestan-3-one appears in blood plasma. In the CYP27A1 -/- mice the plasma level of this oxysterol is about 0.2 μM. Features of *cerebrotendinous xanthomatosis* include neurological problems in adulthood (such as dementia, seizures, hallucinations, depression, ataxia, dysarthria) and myopathy [2]. In contrast, being structurally similar to 5α-cholestan-3-one, an experimental drug olesoxime has powerful neuroprotective properties in various experimental models of neurodegenerative disorders, including amyotrophic lateral sclerosis, Parkinson and Alzheimer diseases [7]. 24-Hydroxycholesterol is the main metabolite of brain cholesterol that can cross the brain blood barrier. The plasma concentration of 24-hydroxycholesterol (from nano- to low micromolar range) may reflect size, activity, age and health of the brain relative to the capacity of the liver to eliminate the substance [1]. There are many oxysterol-binding proteins which potentially can be involved in the intracellular signaling, vesicular traffic, mitochondrial function and organization of both membrane lateral domain and membrane contact sites [1,2]. In addition, some oxysterols modulate membrane and nuclear receptors. Particularly, 24-hydroxycholesterol serves as potent allosteric positive modulator of glutamate NMDA-receptor and selective activator of nuclear LX-receptor in brain [1]. Olesoxime interacts with two outer mitochondrial membrane proteins, TSPO and VDAC, implicated in control of mitochondrial permeability transition [7]. No molecular targets of 5α-cholestan-3-one are known. In sum, the study of oxysterol-dependent regulation is still in its infancy and much investigation needs to be conducted to understand role of oxysterol in cellular function, especially synaptic transmission.

In our research we have revealed that in the frog and mouse neuromuscular junctions the oxysterols modulate neurotransmission acting on synaptic vesicle exo- and endocytosis. Moreover, the oxysterols change the synaptic membrane properties, probably altering lipid raft stability. In the mouse muscles, application of 5α-cholestan-3-one (0.2 μM) slightly decreased evoked neurotransmitter release in response to the single stimuli (without affecting the spontaneous secretion), whilst significantly accelerated the depression of neurotransmitter release (exocytosis) during high frequency activity. In last case, this oxysterol reduced the amount of synaptic vesicles which are actively involved in exo-endocytosis, but time needed for synaptic vesicle recycling remained the same as that in control [2]. In frog neuromuscular junctions, 5α-cholestan-3-one induced the similar changes in neurotransmission, but specific features were a slight increase in spontaneous release and a marked decrease in the synaptic vesicle recycling time at high frequency stimulation. In contrast, olesoxime (0.2 μM) potentiated evoked neurotransmission in the frog neuromuscular junctions by enhancing neurotransmitter release in response to both single stimuli (slightly) and high-frequency stimulation (strongly). The changes in transmitter release during high-frequency activity were

caused by increasing of both the synaptic vesicle population, which actively engages in the exo-endocytosis, and the velocity of the synaptic vesicle cycling. Note that olesoxime had no influence on spontaneous transmitter release. In the mouse neuromuscular junction 24-hydroxycholesterol (0.4 μM) upregulated the neurotransmitter release evoked by the motor nerve stimulation, especially when high frequency was used. Under these conditions more synaptic vesicles were involved in exo-endocytosis and recycling time of these vesicles became shorter than the control. Increasing concentration of 24-hydroxycholesterol to 4μM resulted in a significant enhancement of the effect of the oxysterol on the neuromuscular transmission, while 24-hydroxycholesterol in lower concentration (0.04μM) did not facilitate the neurotransmission significantly. At all concentration 24-hydroxycholesterol did not modify spontaneous exocytosis of synaptic vesicles. Note that inhibitor (voriconazole 0.1, 1 or 10 μM) of CYP46A1 (24-hydroxycholesterol synthesizing enzyme) [8] had no any influence on the synaptic vesicle exocytosis during high-frequency stimulation. It indicates that local production of 24-hydroxycholesterol is absent in the mouse neuromuscular junctions and probably brain-derived 24-hydroxycholesterol can increase the efficiency of evoked synaptic transmission.

Synaptic cholesterol participates in organization of lipid rafts which seems to be involved in synaptic vesicle exocytosis and receptor-mediated signaling. Using fluorescent-labeled lipids (22NBD-cholesterol, ganglioside GM1) and cholera toxin B-subunit, we test the possibility that oxysterols can influence on the lipid raft stability. It was found that olesoxime and 24-hydroxycholesterol (which facilitate neurotransmission) enhanced staining of the synaptic lipid rafts, while 5α-cholestan-3-on (having a depressant action on the neurotransmitter release) caused the opposite changes in the fluorescence of the reporter molecules. Probably, the oxysterol-induced shifts in the membrane properties can modulate the synaptic vesicle cycling, at least partially. Double-immunofluorescent labeling of the synaptic proteins (syntaxin 1, synaptophysin) is shown a typical distribution of these proteins in the neuromuscular junction treated with olesoxime or 5α-cholestan-3-on. In sum, further studies are necessary to revealing of underling mechanisms by which the oxysterols impact the synaptic communication.

The research is supported by RFBR grant # 14-04-00094a.

References

1. Petrov AM, Kasimov MR, Zefirov AL. // Acta Naturae. 2016; 8 (1) – in print.
2. Kasimov MR, Giniatullin AR, Zefirov AL, Petrov AM. // Biochim Biophys Acta. 2015; 1851(5):674-85.
3. Petrov AM, Zakyrjanova GF, Yakovleva AA, Zefirov AL. // Biochem Biophys Res Commun. 2015; 456(1):145-50.
4. Petrov AM, Yakovleva AA, Zefirov AL. // J Physiol. 2014;592(22):4995-5009.
5. Petrov AM, Naumenko NV, Uzinskaya KV, Giniatullin AR, et al. // Neuroscience. 2011; 186:1-12.
6. Petrov AM, Kasimov MR, Giniatullin AR, Tarakanova OI, Zefirov AL. // Neurosci Behav Physiol. 2010; 40(8):894-901.

7. Bordet T, Buisson B, Michaud M, Drouot C, et al. // J Pharmacol Exp Ther. 2007; 322(2):709-20.
8. Shafaati M, Mast N, Beck O, Nayef R, et al. // J Lipid Res. 2010; 51(2):318-23.

cGMP-SPECIFIC PHOSPHODIESTERASE OF BOVINE RETINAL ROD OUTER SEGMENTS, ACTIVATED BY TRANSDUCIN-GUANOSINE 5`-O-(3-THIO-TRIPHOSPHATE) COMPLEX. MAGNESIUM ION DEPENDENCE

O.V. Petrukhin, A.R. Nezvetsky, T.G. Orlova, N.Ya. Orlov

Institute of Theoretical and Experimental Biophysics Russian Academy of Sciences, Pushchino, Moscow region, 142290 Russia

The kinetics of cyclic nucleotide hydrolysis by cGMP–specific phosphodiesterase (PDE6) in a bovine retinal rod outer segment (ROS) suspension have been studied by the pH-metric method [Yee, Liebman, 1978; Orlov et al., 1988] in 50 мМ HEPES-NaOH, pH 8,0, 28 мМ NaCl, 0,7 мМ KCl, 0,1 мМ $CaCl_2$ over a wide range of magnesium ion concentrations ($[Mg^{2+}]$ = 0,4 – 20 мМ). PDE6 in totally bleached ROS suspensions was activated about 7 to 10 times by 2 μM GTP[S] (a pure-hydrolyzed analog of GTP guanosine 5'-O-(3-thiotriphosphate), which was comparable with the concentration of G protein transducin (Gt), whose GTP-binding α-subunit (Gtα) is the intrinsic activator of PDE6.

The initial rate of PDE substrate hydrolysis activated by the Gt-GTP[S] complex reached values close to maximum ones at Mg^{2+} ion concentrations higher than 15 mM and was semi-maximal at 2.5–3.0 mM Mg^{2+}. In a close proximity with earlier data [Yee, Lieberman, 1978], the basal activity of the enzyme was practically constant over the whole range of Mg2+ ion concentrations studied (0.2–20 mM), but diminished by 30–50% in a medium containing no free Mg^{2+} ions upon addition of 2 mM EDTA.

These results were obtained at rather small concentration of NaCl and KCl. Some other results were gained on addition to the reaction mixture of NaCl or KCl up to a final concentration of 100 mM: the PDE6 activity reached its maximum already at much lower Mg^{2+} ion concentrations (3–5 mM) and was by 25–30% higher, than at their absence, the half-maximum value was reached at a concentration of magnesium ions of 0,5–0,6 mM.

Thus, in media of a high ionic strength (100 mM KCl or NaCl), 3–5 мМ Mg^{2+} was enough for the maximum activation of PDE6 by transducin. It corresponds well to the conditions used in earlier works (see [Angleson, Wensel, 1993,1994; Orlov et al., 1988, 2011; Bennett, Clerk, 1989; Miki et al., 1973, 1975; Baehr, Dewlin, Applebury, 1979; Fawzi, Northup, 1990)]). However, at low ionic strengths, the efficient activation of PDE6 by transducin demands a much higher concentration (15–20 mM) of Mg^{2+}.

Mg^{2+} ions are necessary for the functioning of PDE6 and other members of the PDE superfamily [Bender A.T., Beavo J.A., 2006; He et al., 2000] and can also have impact on the efficiency of interaction between transducin and PDE6. The

activity of PDE6 in ROS is usually measured in the majority of works at 2–5 mM of Mg^{2+} and by using various reaction media [Angleson, Wensel, 1993, 1994; Orlov et al.,1988, 2011; Bennett, Clerk,1989; Miki et al., 1973, 1975; Baehr, Dewlin, Applebury, 1979; Fawzi, Northup, 1990]. Therefore it remains unclear, whether the used concentrations of Mg^{2+} are sufficient to achieve the maximum activity of PDE6 in various modes of its work, and a more efficient functioning of the phototransduction system in general. The results of our study help us to resolve this question and gain additional value in attempts to elucidate the influence of Ca^{2+} ions on photo- and transducin-dependent activation of PDE6 in ROS. In such types of experiments, the Ca-chelator EGTA is used for the maintenance of certain concentrations of free Ca^{2+} ions. Because of its incomplete specificity, EGTA can also change the concentration of free Mg^{2+} ions.

References

Angleson J.K., Wensel T.G. (1993) A GTPase-accelerating factor for transducin, distinct from its effector cGMP phosphodiesterase, in rod outer segment membranes. Neuron **11**(5), 939-949.

Angleson J.K., Wensel T.G. (1994) Enhancement of rod outer segment GTPase accelerating protein activity by the inhibitory subunit of cGMP phosphodiesterase. J. Biol. Chem. **269**(23), 16290–16296.

Baehr W., Dewlin M.J., Applebury M.L. (1979) Isolation and characterization of cGMP phosphodiesterase from bovine rod outer segments. J. Biol. Chem. **254**(22), 11669-11677.

Bender A.T., Beavo J.A. (2006) Cyclic Nucleotide Phosphodiesterases: Molecular Regulation to Clinical Use. Pharmacol. Rev. **58**(3), 488–520.

Bennett N., Clerk A. (1989) Activation of cGMP phosphodiesterase in retinal rods: mechanism of interaction with the GTP-binding protein (transducin). Biochem. **28**(18), 7418-7424.

Fawzi A.B., Northup J.K. (1990) Guanine nucleotide binding characteristics of transducin: essential role of rhodopsin for rapid exchange of guanine nucleotides. Biochem. **29**(15), 3804 - 3812.

He F., Alexander B. Seryshev A.B., W. Cowan C.W., and Theodore G. Wensel T.G. (2000) Multiple Zinc Binding Sites in Retinal Rod cGMP Phosphodiesterase, PDE6 αβ. J. Biol. Chem. **275**(27), 20572–20577, 2000.

Miki N., Keirns J.J.,Marcus F.R., Freeman J., Bitensky M.W. (1973) Regulation of Cyclic Nucleotide Concentrations in Photoreceptors: An ATP-Dependent Stimulation of Cyclic Nucleotide Phosphodiesterase by Light. Proc. Nat. Acad. Sci. USA **70**(12), 3820-3824.

Miki N., Baraban J.M., Keirns J.J., Boyee J.J., Bitensky M.W. (1975) Purification and properties of the cyclic nucleotide phosphodiesterase of rod outer segments. J. Biol. Chem. **250**(16), 6320-6327

Orlov, N.Ya., E.V. Kalinin E.V., Orlova T.G., Freidin A.A.(1988) Properties and content of cyclic nucleotide phosphodiesterase in photoreceptor outer segments of ground squirrel retina, Biochim. Biophys. Acta **954**(3), 325-335.

Orlov N.Ya. (2011) Phototransduction systems of vertebrate retinal rods and cones. Molecular mechanisms. LAP LAMBERT Academic Publishing GmbH & Co KG.

Yee R., Liebman P.A. (1978) Light-activated phosphodiesterase of the rod outer segments. Kinetics and parameters of activation and deactivation. J. Biol. Chem. **253**(24), 8902-8909.

MODELLING OF PHOTOTRANSDUCTION PROCESSES IN THE PHOTORECEPTOR DISK MEMBRANES BY THE MONTE-CARLO METHOD

O.V. Petrukhin, N.Ya. Orlov

Institute of Theoretical and Experimental Biophysics Russian Academy of Sciences, Pushchino, Moscow region, 142290 Russia

A version of the Monte-Carlo method was used and realized in the C^{++} language to model the diffusion of functionally important proteins of the retinal rod outer segment phototransduction system. The purpose of the model consists in calculating the number of collisions of enzymes with effectors and the numbers of products of these reactions. This allows us to estimate the influence of diffusion on the kinetics of photoactivation processes, when each collision of enzyme with an effector leads to chemical interaction.

Our model is an improvement of the approach offered earlier by Trevor Lamb [Lamb, 1994]. The essence of improvements isn't reduced to the fact that we have applied modern computer facilities to calculations. We have tracked events on a photoreceptor disk membrane up to 2000 ms, have considered existence of an unitary and a double complex of a phosphodiesterase with an alpha-subunits of a transducin, and have applied (as we believe) a more exact algorithm of calculation.

A number of results, which differ slightly from those of the Lamb model, and also from dot (ODE) models, have been received and discussed. The conclusion about need to create composite (including both diffusive, and kinetic components) models for a more adequate description of processes occurring in rod outer segment membranes has been made.

Reference

Lamb T.D. (1994) Stochastic simulation of activation in the G-protein cascade of photo-transduc-tion. Biophys J. 67(4), 1439-1454.

DECREASE IN LIGHT SENSITIVITY OF ISOLATED FROG ROD PHOTORECEPTOR IN THE PRESENCE OF THE PHOSPHORYLATION-RESISTANT GDP ANALOGUE GUANOSINE-5'-O-(2-THIO-DIPHOSPHATE) CAN BE EXPLAINED IN A FRAMEWORK OF THE HYPOTHESIS ABOUT TRANSDUCIN ACTIVATION VIA TRANSPHOSPHORYLATION MECHANISM

O.V. Petrukhin, T.G. Orlova, A.R. Nezvetsky, N.Ya. Orlov

Institute of Theoretical and Experimental Biophysics Russian Academy of Sciences, Pushchino, Moscow region, 142290 Russia

Analogues of GTP and GDP provide a powerful biochemical tool for investigating G-protein function [Liebman, Pugh, 1982]. To investigate the functions of photoreceptor G protein transducin (Gt) under physiological conditions, the analogues were introduced into single isolated retinal rods. Lamb and Matthews [Lamb, Matthews, 1988] introduced analogues of GDP into isolated salamander rod photore-

ceptors using the whole-cell patch clamp technique, while simultaneously recording the photocurrent with a suction pipette. After several minutes of whole-cell recording the patch pipette was disengaged, thus trapping the analogue inside the cell. It was shown that introduction of the phosphorylation-resistant GDP analogue guanosine-5'-O-(2-thio-diphosphate) (GDP[S]) resulted in a decrease in light sensitivity and a reduction in the slope of the rising phase of the flash response. Similar results have also been obtained by Sather and Detwiler [Sather, Detwiler, 1987] using a different technique. No satisfactory explanation of this rather unusual effect of GDP[S] were done in these works.

We attempted to suggest our explanation, which may be briefly summarized in follow: 1) It is well-known that in a dark photoreceptor the complex Gt-GDP is very tight to decrease the intrinsic noise of a phototransduction system. The dissociation time of Gt-GDP complex was estimated to be of the order of several hours at 37ºC [Fawzi, Northup, 1990; Faurobert et al., 1993]. It means that incubation of a photoreceptor cell with 2 mM GDP[S] during the time of experiment (10–20 min) will provide a very low percent (0.1–1.0%) of Gt-GDP[S] formed.

2) Transphosphorylation hypothesis (see review [Orlov, Orlov, 2008] as the example) predicted that transducin is activated in the presence of bleached rhodopsin (R*) via the phosphorylation of bound GDP to GTP. But when phosphorylation-resistant GDP analogue is used the intermediate complex between R* and Gt-GDP[S] cannot convert to the GTP state and release R* in a free state to continue further activation of transducin molecules.

3) It is usually assumed [Orlov, 2011] that one bleached rhodopsin molecule activates about 1000 molecules of Gt. It seems to be clear that as low as about 1% of molecules of Gt-GDP[S] would be sufficient for a significant decrease (about 10 times) in production of active Gt and in light sensitivity of photoreceptor cells.

So it is possible that the decrease in light sensitivity of photoreceptor cells in the presence of phosphorylation-resistant GDP[S] may be explained in the framework of the transphosphorylation hypothesis and looks like one of its confirmation.

References

Fawzi A.B., Northup J.K. (1990) Guanine nucleotide binding characteristics of transducin: essential role of rhodopsin for rapid exchange of guanine nucleotides.- Biochem., **29**(11), 3804 - 3812.

Faurobert E., Otto-Bruc A., Chardin P., Chabre, M. (1993) Tryptophan W207 in transducin T-alpha is the fluorescence sensor of the G protein activation switch and is involved in the effector binding. EMBO J., **12**(11), 4191-4198.

Lamb T., Matthews H.R. (1988) Incorporation of analogues of GTP and GDP into rod photoreceptors isolated from the tiger salamander. J. Physiol., **407**, 463-487.

Liebman P.A., Pugh Jr, E. N. (1982) Gain, speed and sensitivity of GTP binding vs PDE activation in visual excitation. Vision Research **22**(5), 1475-1480.

Sather W. A., Detwiler P. B. (1987) Intracellular biochemical manipulation of phototransduction in detached rod outer segments. Proc. Natl. Acad. Sci. USA **84**(24), 9290–9292.

Орлов Н.Я. Системы фототрансдукции палочек и колбочек сетчатки позвоночных. Молекулярные механизмы. (LAP LAMBERT Academic Publishing GmbH & Co KG, Saarbrücken, Deucschland, 2011).
Орлов Д.Н., Орлов Н.Я. (2008) Нуклеозиддифосфаткиназа и ГТФ-связывающие белки. Возможные механизмы сопряжения. Биофизика **53**(6), 922-928.

EXPLORING MECHANISMS OF INSULIN RESISTANCE IN PREADIPOCYTES

N.V. Podkuychenko, Yu.S. Stafeev, M.Yu. Menshikov, A.V. Vorotnikov

Institute of Experimental Cardiology, Russian Cardiology Research Center, Moscow, 121552, Russia

Insulin resistance is the earliest event in pathogenesis of type 2 diabetes mellitus. It is defined as inability of insulin to decrease postprandial glucose levels in blood. At the cellular level, it is due to inability of insulin to stimulate glucose uptake by insulin-sensitive skeletal muscle, liver and fat cells. At the molecular level, this is caused by disruption of intracellular cascade initiated by insulin receptor in these cells. Physiological conditions that promote IR include obesity, inflammation, chronic hypoxia, oxidative and cellular stresses. However, the intimate mechanisms linking to dysregulated insulin signaling remain largely unclear. Furthermore, it is unknown whether these mechanisms are typical only for differentiated muscle, liver and fat cells, whereas their precursor cells are less affected and have a potential against IR. We explore this possibility using mouse preadipocytes 3T3L1 that can be maintained in culture or fully differentiated into adult adipocytes.

To compare the effects of IR on insulin-stimulated signaling in pre- and adult adipocytes we use several protocols of IR induction based on hyperlipidemia, hypoxia, hyperinsulinemia, hyperglycemia, and oxidative/cellular stress. Typically, cells are cultured in the absence or presense of corresponding inductors (BSA-conjugated palmitate, Co2+ ions, insulin, brefeldin A, etc), then are briefly stimulated by insulin and lysed to compare, by western blots, the phosphorylation responses of insulin receptor substrate (IRS) and Akt, the downstream target of the insulin-induced PI3-kinase pathway. We will present and discuss the ongoing results.

NADPH-oxidases that generate reactive oxygen species (ROS) are thought to contribute to IR development through the oxidative/celluar stress mechanism. ROS are known to modulate activity of insulin receptor, PI3-kinase and MAP-kinase downstream pathways. To test their involvement in IR, we aim to silence NADPH-oxidase expression in cultured adipocytes and explore the effects on insulin-dependent signaling. As a preliminary research, we here determined, by RT-PCR, which of NADPH-oxidases are expressed in 3T3L1 cells and whether their expression changes during adipogenesis.

Preadipocytes 3T3L1 were differentiated to adult adipocytes during 10 days according to standard protocol using high glucose, insulin, IBMX, dexamethasone, and rosiglitazone as adipogenic inductors. mRNA was isolated using RNeasy® Kit

before, after, and in the middle (4th day) of differentiation. The RevertAid First Strand cDNA Synthesis Kit was used to obtain cDNA. The NADPH-oxidase expression was determined by RT-PCR, using specific primers and extracted cDNA as a matrix. We found that expression of the major NADPH-oxidases (NOX4, DUOX1, DUOX2) was significantly reduced in these cells during adipogenesis. Western blotting of Nox4 and Duox2 confirmed the RT-PCR data, indicating that NADPH-oxidase expression is almost lost in the adult adipocytes. These results suggest that NADPH-oxidases are the markers of, and may maintain the undifferentiated phenotype of preadipocytes. Further silencing studies will demonstrate whether they affect adipogenesis and susceptibility to IR in these cells.

Supported by RFBR grant 14-04-01746a.

INDIRECT EFFECT OF ACTIVE TRANSPORT INHIBITION ON INTRACELLULAR Na/K BALANCE

M. Pogorelova[1], A. Panait[1], V. Pogorelova[1], V. Balashov[2], A. Pogorelov[1]

[1]*Institute of Theoretical and Experimental Biophysics, RAS, Pushchino, Moscow Region, 142290, Russia*

[2]*Moscow Institute of Physics and Technology (State University) Dolgoprudny, Moscow Region, Russia*

In this work Electron Probe Microanalysis (EPMA) was applied to study changes of potassium and sodium concentrations in muscle cells of isolated heart from Wistar rat during experimental ischemia. Hypoxic perfusion without glucose was shown to evoke the potassium deficiency and sodium accumulation in cardiac myocells. Short-term (10 min) inhibition by strophanthin (0.1 mM/l) recovered intracellular Na/K balance in cells.

It is known that in the absence of substrate influx against the back ground of prolonged hypoxia, one registers growing de-energization of the heart muscle cell [6]. As a result, Na^+/K^+-ATPase inactivates, that causes dissipation of the membrane gradient of electrolytes [4,6]. As a consequence, the electric potential on the cytoplasmic membrane declines, which comes to be one of the causes of electromechanical uncoupling of contraction [3]. For the described sequence of events, apparently paradoxical is the use in clinical practice of a Na^+/K^+-ATPase blocker strophanthin for stimulating the activity of the heart in ischemia [10]. This phenomenon, when inhibition of active potassium transport abolishes cardiac ischemia, is likely to be explained by the indirect action of cardiac glycoside on the cardiomyocyte. Search for a target of such nonspecific action of the drug was the aim of the given work.

Details of specimen preparation and of the method for measuring the cytoplasmic concentration of elements in the rat heart muscle cell have been described by us earlier [7]. This approach for isolated rat (Wistar) heart perfused according to Langendorff was recently discussed [8].

Results and Discussion

The role of strophanthin, a plant cardiac glycoside, in regulation of the cytoplasmic Na/K balance was checked on isolated rat heart in ischemia environments modeled by hypoxic perfusion without glucose. The cytoplasmic content of K and Na at different intervals of ischemia and the effects of the drug are shown in table.

The cardiac glycoside was shown to affect Na^+/K^+-ATPase in isolated cells [1,9]. Bearing in mind the specific effect of the inhibitor, one should expect, upon suppression of active transport in the cardiomyocyte, a still more pronounced K^+ deficit and Na^+ accumulation as compared with ischemia. Contrary to such expectation, strophanthin exerts an opposite effect, raising the K^+ and reducing the Na^+ levels (table). In other words, a relatively short action of strophanthin (10 min) stops the disturbance in Na/K balance emerging in ischemia. Therewith the intracellular concentration of elements (K, Na) tends to the initial level, which is especially obvious at the late terms of ischemia. Such a tendency may signify restoration of the state of the heart in the presence of strophanthin.

Possibly, the discrepancy in the effect of the drug at different steps of hypoxic perfusion without glucose is caused by activation of different transmembrane ion transport complexes over time [3–5]. Thus, low doses of Na^+/K^+-ATPase inhibitor, contrary to expectations, have a stimulating effect on cardiac function, which is consistent with clinical practice. So what does stimulate the nonspecific action of strophanthin on the cardiomyocyte in ischemia? Possibly, the reason hides in active involvement of the capillary endothelium in regulating the myocell homeostasis (figure).

Figure 1A demonstrates the cascade of events evoked by ischemia, which causes a deficit of K^+ in the heart muscle cell. First of all, the K^+ level rises in the intercellular space because of the K^+release from cardiomyocyte through a system of channels. As a result, there takes place activation of Na^+/K^+-ATPase of the endothelial cell at the side of the basal membranes, with subsequent passive transcellular transport of potassium into the capillary lumen. Figure 1B illustrates the situation developing in the

Changes of elemental (K, Na) concentrations in cardiac myocells of rat (Wistar) evoked by hypoxic perfusion (38°C) without glucose and in the absence of strophanthin or with strophanthin (0.1 mM) action during the last 10 min of perfusion *

Hypoxic perfusion duration	Intracellular elemental concentrations, mM (without strophanthin)		Intracellular elemental concentrations, mM (with strophanthin, last 10 min.)	
	potassium	sodium	potassium	sodium
15 min	96±3	44±3	115±3	45±2
30 min	91±2	40±1	99±2	39±1
45 min	71±2	56±2	101±2	54±2
60 min	54±2	66±3	123±3	52±3

(*) data are presented as mean + sem over at least 80 cells from five rats.

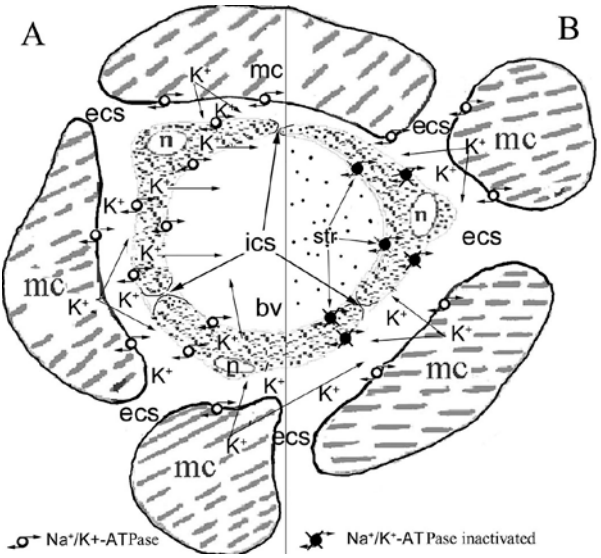

Scheme of cardiac capillary assembly (From [8]). (A) – Events sequence of K^+ transport from the muscle cell via the intercellular space and endothelium into the capillary lumen under ischemia. (B) – Nonspecific effect of short-term exposure to strophanthin, caused by inhibition of endotheliocyte membrane Na^+/K^+-ATPase. Designations: bv – blood vessel; n – nucleus of vascular endotheliocyte; ecs – extracellular space; mc – muscle cell; str – strophanthin in the capillary lumen; ics – pores (fenestrae) in the capillary endothelium.

presence of strophanthin. Upon short-term perfusion of the heart with a solution containing the drug at low concentration, the target of its action in the first places comes to be the more spatially accessible Na^+/K^+-ATPase of the capillary wall endothelium. As the result, the endothelial cell loses the function of active regulator of the ionic homeostasis of the interstitium. In the given case, K^+ transport from the intercellular space into the capillary lumen is interrupted, and endothelium becomes a morphological barrier to potassium leakage from the muscle tissue into blood [2].

In the scenario described above, not only conservation of the state is possible but also reverse diffusion of K^+ into the intercellular space through the fenestrae between endothelial cells. Passive transport of substances from the capillary into the intercellular space together with active Na^+/K^+-ATPase on the membrane of the myocell promote restitution of the Na/K balance in cytoplasm at ischemia followed with short-term exposure to strophanthin.

Such an effect of low doses of cardiac glycoside has been denoted by us as a “mechanism of indirect impact”. For its realization, necessary is the fulfillment of the following conditions: (1) inhibition of Na^+/K^+ substances from the capillary lumen into the extracellular space of the muscle cells; (3) active Na^+/K^+-ATPase

on the cardi omyocyte membrane. To attain direct action of strophanthin on the myocyte in an isolated heart perfusion experiment, one perhaps should raise the drug concentration above that used in cell culture (0.1 mM) and/or prolong the exposure. Above we have discussed mechanism of "mediated impact" of strophanthin, the effect of low temperature may be actualized via the same mechanism, based on suppression of active K^+ transport through the capillary endothelium. In conclusion, the task of microanalysis of elements in the cytoplasm of the heart muscle cell can be regarded as solved; this model allows testing the influence of various substances on the state of cardiomyocyte by changes in the intracellular elemental composition.

Acknowledgments

In part of EPMA approach development this work was supported by the Russian Science Foundation (project no. 16-16-00020).

References

1. Balazs I., 1981. Cardiac Toxicology, 1: 39-48.
2. Lindinger M. I., 1995. J. Mol. Cell. Cardiol., 27: 1011-1022.
3. Pierce G. N., Czubryt M. P., 1995. J. Mol. Cell. Cardiol.: 27, 53-63.
4. Pogorelov A. G., Pogorelova V. N., Dubrovkin M. I., et al., 2002. Biofizika, 47: 744-752.
5. Pogorelov A. G., Pogorelova V. N., Khrenova E. V., et al., 2004. Zh. Evol. Biokh. Fiziol., 40: 353-358.
6. Pogorelov A. G., Rusakov A. V., Pogorelova V. N., 2006. Biofizika, 51: 852–858.
7. Pogorelov A. G., Pogorelova V. N., Pogorelova M. A., 2010. Biofizika, 55: 875-879.
8. Pogorelova V. N., Panait A.I., Pogorelov A. G., 2014. Biofizika, 59: 946-950.
9. Pribe L., Friedrich M., Benndorf K., 1996. J. Physiol., 23 492:405-417.
10. Therien A. G., Blostein R., 2000. Am. J. Physiol., 279: C541-C566.

MOLECULAR MECHANISMS OF SKELETAL MUSCLE ADAPTATION TO ACUTE EXERCISE WITH METFORMIN ADMINISTRATION

D.V. Popov, A.D. Butkov, P.A. Makhnovskii, E.A. Lysenko, T.F. Vepkhvadze, D.V. Perfilov

Institute of Biomedical Problems, Russian Academy of Sciences, Khoroshevskoye shosse 76A, Moscow, 123007, Russia

The Diabetes Prevention Program Outcomes Study has shown that either lifestyle intervention (i.e. an increase in moderate-intensity physical activity) or metformin therapy (the most commonly used drug to treat type 2 diabetes) reduce the risk of diabetes in individuals with impaired glucose tolerance. Endurance exercise improves skeletal muscle insulin sensitivity and induces mitochondrial biogenesis via the upregulation of AMPK and PGC-1a. In resting human diabetic muscle, metformin treatment has been reported to induce AMPK activation. Indeed, studies have shown that metformin treatment induces increases in PGC-1a mRNA and protein levels, expression of PGC-1a-responsive genes, and activation of mitochondrial proteins in skeletal myotubes, as well as in mouse and rat muscles. However, a study in prediabetic individuals reported that met-

formin treatment has been found to ablate the increase in insulin sensitivity gained after acute endurance exercise and exercise training alone, the combination of metformin treatment and endurance training has been reported to have a lower impact on aerobic performance in insulin-resistant individuals, or even to not affect these indices. The goal of our study was to investigate the effect of metformin on the expression of *PGC-1a* gene isoforms and PGC-1a-responsive genes in human skeletal muscle.

Nine healthy men participated in this study. We obtained samples from m.vastus lateralis before and 0, 4 and 8 h after acute endurance exercise bouts, with or without administration of a single dose of metformin (2 g). Dynamic muscle contractions rapidly increase muscle blood flow, therefore, in order to improve metformin delivery to skeletal muscle, the exercise bouts were performed when the level of metformin in the blood was near maximal (2 h after administration). On the other hand, to avoid exercise-induced activation of AMPK, we used low-intensity exercise (40% *V*'O2max). Total RNA was taken from samples of three subjects for RNA sequencing by Illumina HiSDefault 2000 instrument prior to exercise, and at 4 and 8 h after (18 samples in total). The differential expression of individual genes was confirmed by quantitative PCR using samples from all subjects (n=9). The phosphorylation levels of kinases were evaluated by Western blot.

The administration of a single dose of metformin had systemic effects: compared with placebo, the lactate level was higher (by 0.8 mmol/l, $P < 0.05$) during exercise, while the blood glucose level was lower (by 1.2 mmol/l, $P < 0.01$) after exercise. The phosphorylation level of AMPKThr172 did not change immediately after the exercise bout in either the metformin or placebo trials. However, ACCSer222 (the substrate of AMPK, i.e. an endogenous marker of AMPK activity) showed a 2.6-fold ($P < 0.01$) increase in phosphorylation level immediately after exercise in the metformin trial. 236 and 234 genes changed expression level (Padj < 0.1) at the 4 and 8 h after exercise accordingly; and only 86 genes displayed overlap. The exercise bout in the metformin trial changed expression level (Padj < 0.1) of 30 and 31 genes at the 4 and 8 h after exercise accordingly; and only 8 genes displayed overlap. Comparison of changes in transcriptome after aerobic exercise alone and with metformin administration showed that metformin suppresses noticeably exercise-induced change of genes expression. Gene Ontology Analysis revealed than this effect may be explained by metformin-induced activation of expression of genes participating in inflammatory and stress responses.

Having in mind that metformin and exercise are recommended as countermeasures against metabolic disturbances and for treating of these illnesses, study of molecular mechanisms of metformin action seems to be an important component for constructing optimal strategy of treatment, particularly for combination of metformin therapy with physical loads.

This work was supported by the Russian Science Foundation (grant № 14-15-00768).

SESONAL CHANGES OF CALPAIN ACTIVITY IN STRIATED MUSCLES OF GROUND SQUIRREL (*Spermophilus undulatus*)

S.S. Popova[1], I.M. Vikhlyantsev[1], N.M. Zakharova[2], Z.A. Podlubnaya[1,3]

[1]*Institute of Theoretical and Experimental Biophysics, Russian Academy of Sciences, Pushchino, Moscow region, Russia*

[2]*Institute of Cell Biophysics, Russian Academy of Science, Pushchino, Moscow region, Russia*

[3]*Pushchino State Institute of Natural Science, Pushchino, Moscow region, Russia*

It is known that mammalian skeletal muscles exhibit significant atrophy and loss in contractile proteins during prolonged unloading or disuse (hindlimb suspension, bed rest and spaceflight) [1]. Hibernation is characterized by prolonged periods of inactivity, yet, hibernators consistently emerge from winter with very little atrophy, that accompanied by a shift in fiber ratios to more oxidative fiber types [2–4]. One of the mechanisms clarifying the stability of muscle of hybernants to atrophy, can be hyper-activation of protein synthesis in different organs and tissues of arousing and active interbout animals [4–6]. It is known that calpains (calcium-dependent proteases) are initiators of myofibrillar protein turnover [7]. Calpains are nonlysomal, calcium-activated cysteine proteases [8,9]. Two ubiquitous isoforms are well characterized (μ- and m-calpain), and several tissue-specific isoforms have also been reported [9,10]. Striated muscles contain significant amounts of the 2 ubiquitous well-characterized calpains, the micromolar Ca^{2+}, requiring Ca^{2+}-dependent protease (μ-calpain), and the millimolar Ca^{2+}, requiring Ca^{2+}-dependent protease (m-calpain), and their specific inhibitor, calpastatin [9]. Calpains initiate the digestion of individual myofibrillar proteins, including desmin, filament, C-protein, tropomyosin, troponin T, troponin I, titin, nebulin, vimentin, gelsolin, and vinculin [9], which then are degraded to amino acids by ubiquitin-proteasome pathway [7]. Probably, that increased activity of these proteses will be observed in muscles of hibernants in period of interbout activity, when hyperactivation of protein synthesis is observed. The aim of this work was study of seasonal changes of content and proteolytic activity of μ-calpain in the heart (left ventricle) and skeletal (*m. soleus*, *m. longissimus dorsi*, *m. quadriceps femoris*) muscles of *Spermophilus undulatus*.

Material and methods

The long-tailed ground squirrels (*Spermophilus undulatus*) were used. The weight of animals was 450–650 g. Ground squirrels were trapped during August or September in the Lena river valley of the Yakutsk region and shipped by air to Pushchino, the Moscow region. In October, when the endogenous cycle of the animals reached the hibernating phase, animals of either sex were transferred to a darkened cold room (about 4°C) to prepare them for hibernation. Animals were provided with food, water and nesting material *ad libitum.* The following animal groups were used in experiment: active summer animals (May–September, *n*=4, "AS" group); torpid animals (November–March, heart muscle temperature is 2–

5ºC, duration of torpor is 7–14 days, *n*=4, "T" group); and active winter animals (10–13 hours after torpor, *n*=4, "AW" group). Control of physiological state of ground squirrels was conducted according to [11]. Calpain activity was studied by casein zymography method [12]. SDS-PAGE and Western blot analysis of μ-calpain from muscle tissues was carried out by method [13]. Protein samples were electrophoresed in 6.5% polyacrylamide slab gels [14]. Measurements of protein concentration were made by using NanoDrop 1000 (Thermo Scientific, USA), then equal amount of protein (30–45 μg/line) was applied. Transfer of proteins to the PVDF membrane was carried out by the method [15]. Membranes were blocked with a blocking buffer (5% nonfat milk powder, PBS pH 7.4, and 0.05% Tween-20) and incubated for 2 h at room temperature with the primary rabbit monoclonal antibodies against μ-calpain (Abcam, 1:4000). Secondary antibodies conjugated to alkaline phosphatase (goat antirabbit Ig, Abcam, 1:3000) were used. The content of μ-calpain was determined by densitometry method (Total Lab v.1.11). The results obtained during the experiments were statistically processed using the Mann-Whitney *U*-test with the confidence levels $P \leq 0.05$ to evaluate the significance of differences between groups. The data were represented as $M \pm SD$, where M is the mean value and SD is the standard deviation.

Results

The aim of this study was verifying hypothesis about increase of calpain activity in striated muscles of ground squirrels in periods of interbout activity. It is known that in periods of wake up and interbout activity of hibernants, increase of protein synthesis is observed [4–6]. In particular, mTOR activity are increased during arousal bouts, supporting the idea that increased muscle protein synthesis occurs during periodic arousal bouts [16,17]. Probably, an increase of activity of calpain, initiating turnover of proteins in muscles, is observed in these periods. This hypothesis was confirmed in our study. Increase of μ-calpain activity in heart (in 2.5 times, $P \leq 0.01$), in *m. soleus* (in 1.7 times, $P \leq 0.01$), in *m. longissimus dorsi* (in 1.5 times, $P \leq 0.01$) and in *m. quadriceps femoris* (in 1.2 times) was observed by casein zymography in "AW" animal group. Significant changes of μ-calpain activity in the muscles of "T" and "AS" animal groups were not detected. Data of Western blot analysis of μ-calpain isoform content in the striated muscles of ground squirrels confirm these results. It is known that Western blot analysis of μ-calpain content is one of the methods for assessment of calpain activity. In particular, it was shown, that activation of full-length μ-calpain (80 kDa) involves autolysis to a 78-kDa and then to a 76-kDa protein, with both of these autolysed isoforms being proteolytically active [13]. The results of our Western blot analysis revealed significant increase relative content of autolysed isoform (78 kDa) of μ-calpain in two of the four studied muscles: in heart (in 2 times, $P \leq 0.01$) and in m. soleus (in 2.6 times, $P \leq 0.05$) of active winter ground squirrels. Significant seasonal differences in content of autolysed isoform (78 kDa) of μ-calpain in *m. quadriceps femoris* and *m. longissimus dorsi* of ground squirrels were not found. Nevertheless, data of casein zymography point out increasing proteolytic activity of calpains in ground squirrel muscles in period interbout activity. Interesting to

note that in “slow” *m. soleus* and in *m. longissimus dorsi*, containing up to 40% of “slow” fibers [3], calpain activity was higher, than in *m. quadriceps femoris*, containing, mostly, “fast” fibers. These data indicate that protein synthesis in period of interbout activity occurs mainly in “slow” fibers of skeletal muscles of long-tailed ground squirrels. The obtained results correspond to hibernation strategy, aimed at increase of content of “slow” filaments being more energetically favorable and more enduring, than “fast” filaments. This adaptation is aimed at saving of energy resources during hibernation in order to survival in unfavorable environmental conditions.

This work was supported by the Russian Foundation for Basic Research (Grants nos. 14-04-00112 and 14-04-92116).

References

1. Ulanova A, Gritsyna Y, Vikhlyantsev I, Salmov N, Bobylev A, Abdusalamova Z, Rogachevsky V, Shenkman B, Podlubnaya Z. Isoform composition and gene expression of thick and thin filament proteins in striated muscles of mice after 30-day space flight. Biomed Res Int. 2015;2015:104735. doi: 10.1155/2015/104735.
2. Lee K, Park JY, Yoo W, Gwag T, Lee JW, Byun MW, Choi I. Overcoming muscle atrophy in a hibernating mammal despite prolonged disuse in dormancy: proteomic and molecular assessment. J Cell Biochem. 2008 May 15;104(2):642-56. doi: 10.1002/jcb.21653.
3. Lazareva MV, Trapeznikova KO, Vikhliantsev IM, Bobylev AG, Klimov AA, Podlubnaia ZA. Seasonal changes in the isoform composition of the myosin heavy chains in skeletal muscles of hibernating ground squirrels Spermophilus undulates. Biofizika. 2012 Nov-Dec;57(6):982-7.
4. Cotton CJ. Skeletal muscle mass and composition during mammalian hibernation. J Exp Biol. 2016 Jan;219(Pt 2):226-34. doi: 10.1242/jeb.125401.
5. Zhegunov GF, Mikulinskiĭ IuE. Activation of protein synthesis in tissues of gophers after arousal from hibernation. Ukr Biokhim Zh (1978). 1987 May-Jun;59(3):69-73.
6. Zhegunov GF. Protein synthesis in cardiac cells and the ultrastructural dynamics of cardiomyocytes of hibernating animals during the hibernation cycle. Tsitologiia. 1988 Feb;30(2):157-62.
7. Goll DE, Neti G, Mares SW, Thompson VF (2008) Myofibrillar protein turnover: the proteasome and the calpains. J Anim Sci 86(14 Suppl):E19–35. Epub 2007 Aug 20.
8. Dayton WR, Goll DE, Zeece MG, Robson RM, Reville WJ (1976) A Ca2+-activated protease possibly involved in myofibrillar protein turnover. Purification from porcine muscle. Biochemistry 15(10):2150–2158.
9. Goll DE, Thompson VF, Li H, Wei W, Cong J (2003) The calpain system. Physiol Rev 83(3):731–801.
10. Sorimachi H, Saido TC, Suzuki K (1994) New era of calpain research. Discovery of tissue-specific calpains. FEBS Lett 343(1):1–5.
11. N.M. Zakharova. Some features of body heating at provoked awakening of hibernating ground squirrels Spermophilus undulatus . J. Fundamental research. 2014. № 6. P. 1401-1405.
12. Raser KJ, Posner A, Wang KK. Casein zymography: a method to study mu-calpain, m-calpain, and their inhibitory agents. Arch Biochem Biophys. 1995 May 10;319(1):211-6.
13. Murphy RM, Verburg E, Lamb GD. Ca2+ activation of diffusible and bound pools of mu-calpain in rat skeletal muscle. J Physiol. 2006 Oct 15;576(Pt 2):595-612.

14. Laemmli UK. Cleavage of structural proteins during the assembly of the head of bacteriophage T4. Nature. 1970 Aug 15;227(5259):680-5.
15. Towbin H, Staehelin T, Gordon J. Electrophoretic transfer of proteins from polyacrylamide gels to nitrocellulose sheets: procedure and some applications. Proc Natl Acad Sci U S A. 1979 Sep;76(9):4350-4.
16. Lee K, So H, Gwag T, Ju H, Lee JW, Yamashita M, Choi I. Molecular mechanism underlying muscle mass retention in hibernating bats: role of periodic arousal. J Cell Physiol. 2010 Feb;222(2):313-9. doi: 10.1002/jcp.21952.
17. Wu CW, Storey KB. Regulation of the mTOR signaling network in hibernating thirteen-lined ground squirrels. J Exp Biol. 2012 May 15;215(Pt 10):1720-7. doi: 10.1242/jeb.066225.

STRUCTURAL AND FUNCTIONAL STUDIES ON αβ-HETERODIMERS OF TROPOMYOSIN

K. Popruga[1,2], A. Matyushenko[1,2], A. Pivovarova[1], D. Shchepkin[3], G. Kopylova[3], S. Bershitsky[3] and D.I. Levitsky[1,4]

[1] *A. N. Bach Institute of Biochemistry, Research Center of Biotechnology of the Russian Academy of Sciences, Moscow, Russia*

[2] *Department of Biochemistry, School of Biology, Moscow State University, Moscow, Russia*

[3]*Institute of Immunology and Physiology, Ural Branch of the Russian Academy of Sciences, Yekaterinburg, Russia*

[4]*A.N. Belozersky Institute of Physico-Chemical Biology, Moscow State University, Moscow, Russia*

Tropomyosin (Tpm) is one of the key components of the regulatory apparatus of thin filaments in all types of muscles. The Tpm molecule is a dimer of α-helices forming a left-handed superhelix ('coiled-coil'). In fast skeletal muscle, two different isoforms of Tpm – α-Tpm (Tpm 1.1) and β-Tpm (Tpm 2.2) are present, which are expressed from different genes (TPM1 and TPM2, respectively). Accordingly, Tpm molecules can exist either as αα-Tpm homodimers or as αβ-Tpm heterodimers (ββ-homodimers are very unstable, and therefore they are rarely found). The properties of αα-Tpm homodimers have been studied in detail, while the functional significance of αβ-Tpm heterodimers has not been defined because these studies were hindered by the difficulty of isolating or reconstituting the Tpm heterodimers. It seems likely that αα-homodimers and αβ-heterodimers can significantly differ from each other in their structure and functions. Importantly, a significant increase in the expression of β-Tpm (Tpm 2.2) leading to an increase in the content of αβ-Tpm heterodimers was often observed at pathological states of skeletal or cardiac muscles. All these imply a necessity of detailed analysis of structural and functional properties of αβ-Tpm heterodimers.

Recently a novel effective method has been reported for purifying bacterially expressed Tpm as αβ-heterodimers using a cleavable N-terminal His-tag on one of the two chains [1]. The same method can be used to isolate αα-Tpm homodi-

mers in which only one chain carries a mutation [2]. We applied this method, with some modifications, to purify αβ-Tpm heterodimers carrying stabilizing substitutions D137L, G126R, and D137L/G126R in the middle part of α-chain, as well as to obtain αα-Tpm homodimers with these substitutions in only one of the two chains. We investigated the effects of these substitutions in the middle part of the α-chain on structural and functional properties of both αβ-Tpm heterodimers and αα-Tpm homodimers in which only one chain carried these mutations. Circular dichroism (CD) was applied to measure the temperature dependences of the thermal unfolding of these Tpm species. It was shown that stabilizing substitutions D137L, G126R, and D137L/G126R in the middle part of the α-chain increased the thermal stability of both αβ-Tpm heterodimers and αα-Tpm homodimers with these mutations in only one of two α-chains (although to a lesser extent than for αα-Tpm homodimers with these mutations in both α-chains). Moreover, the stabilizing substitutions in the α-chain strongly increased the stability of preformed Tpm–F-actin complexes as was shown by measuring the temperature dependences of thermal dissociation of these complexes monitored with light scattering. These effects were observed for both αβ-Tpm heterodimers and αα-Tpm homodimers with stabilizing substitutions in only one α-chain; however, they were less pronounced than those observed for αα-Tpm homodimers with stabilizing substitutions in both α-chains.

Interesting and even surprising results were obtained in experiments performed using the *in vitro* motility assay, in which we studied the effects of stabilizing substitutions D137L and D137L/G126R in the middle part of the α-chain on maximal sliding velocity (measured at high Ca^{2+} concentration, i.e. at pCa 4) of regulated actin filaments containing αβ-Tpm heterodimers and troponin (Tn). It has been shown that these mutations in the α-chains of αβ-heterodimers strongly decreased the sliding velocity, by 25–30 % in comparison to that of control αβ-Tpm heterodimers. The results obtained with αβ-Tpm heterodimers were quite different from those obtained earlier on αα-Tpm homodimers with stabilizing substitutions in both α-chains, when these mutations strongly increased the sliding velocity of regulated actin filaments [3,4].

In conclusion, our results indicate that functional properties of αβ-Tpm heterodimers with mutations in the α-chain (and, probably, αα-Tpm homodimers with mutations in only one α-chain) can be quite different from those of αα-Tpm homodimers with mutations in both α-chains.

This work was supported by RFBR (grant № 16-34-00654_mol_a) and by the Program “Molecular and Cell Biology” of the Russian Academy of Sciences.

References

1. Kalyva A., Schmidtmann A., and Geeves M.A. (2012) “*In vitro* formation and characterization of the skeletal muscle α β tropomyosin heterodimers”. Biochemistry **51**, 6388–6399.
2. Janco M., Kalyva A., Scellini B., Piroddi N., Tesi C., Poggesi C., and Geeves M.A. (2012) “α-Tropomyosin with a D175N or E180G mutation in only one chain differs from tropomyosin with mutations in both chains”. Biochemistry **51**, 9880–9890.

3. Shchepkin D.V., Matyushenko A.M., Kopylova G.V., Artemova N.V., Bershitsky S.Y., Tsaturyan A.K. & Levitsky D.I. (2013) “Stabilization of the central part of tropomyosin molecule alters the Ca^{2+}-sensitivity of actin-myosin interaction”. Acta Naturae **5**, 126–129.
4. Matyushenko A.M., Artemova N.V., Shchepkin D.V., Kopylova G.V., Bershitsky S.Y., Tsaturyan A.K., Sluchanko N.N. & Levitsky D.I. (2014) “Structural and functional effects of two stabilizing substitutions, D137L and G126R, in the middle part of alpha-tropomyosin molecule”. FEBS J. **281**, 2004-2016.

ARCHAELLAR FILAMENTS IN TWO RELATED *HALORUBRUM* SPECIES ARE QUITE DIFFERENT

M.G. Pyatibratov, T.N. Melnik, A.S. Syutkin, S.N. Beznosov, A.K. Surin, A.V. Galeva, O.V. Fedorov

Institute of Protein Research, Russian Academy of Sciences, Institutskaya Str. 4, Pushchino, Moscow Region, 142290, Russia

The Domain Archaea is a unique group of organisms combining bacterial, eukaryotic and archaeal-specific characteristics. Recent studies identified archaea that could be the direct ancestors of eukaryotes [1]. Archaea often exist in the most extreme environments on Earth, such as salt lakes, hot springs and surroundings with extreme pH values, they have also been found in the oceans, soil, and even in the human gut [2,3]. In order to survive in a changing environment archaea like bacteria use rotating motility organelles called flagella. Interestingly, the archaeal flagella structurally resemble type IV pili rather than bacterial flagella. There is now no doubt that the archaeal flagella are a unique system of biological motility [4], and in a recent study it was proposed to call them “archaella” [5]. The extracellular part of archaella is an extended protein filament (up to a few microns) which consists of a plurality of copies of one or more proteins. Structural proteins of these appendages have a conserved hydrophobic N-terminus, forming an extended alpha helix. Hydrophobic interactions between these alpha helices keep the subunits together in the filament. These subunits are synthesized in the cytoplasm and then exported across the cytoplasmic membrane by the Sec translocation pathway, whereupon they are incorporated in the growing filament.

Our research group investigates the motility apparatus of the extremely halophilic archaea. These organisms thrive in environments with salt concentrations approaching saturation. As a rule, archaellar filaments are composed from several archaellin (flagellin) molecules with different amino acid sequences. We first showed that the Antarctic haloarchaea *Halorubrum lacusprofundi*, unlike previously studied euryarchaeota *Halobacterium salinarum* and *Methanococcus maripaludis*, forms functional helical filaments from a single archaellin gene product [6]. *H. lacusprofundi* was the first member of the *Halorubrum* genus, which genome was sequenced. Later the genome sequences of 12 more *Halorubrum* species were published. It turned out that unlike *H. lacusprofundi* in other *Halorubrum* genomes as a rule there are two archaellin genes organized into one operon. The amino acid

sequences of FlaB1 and FlaB2 archaellins, encoded by these genes are substantially different from each other and FlaB1 has a high homology with single *H. lacusprofundi* archaellin. We investigate role of FlaB2 archaellin in archaella formation which may consist of: (I) to form individual filaments functionally different from FlaB1 filaments, (II) to stabilize the supramolecular structure of the bicomponent FlaB1/FlaB2 filaments. As an object of the research we selected *Halorubrum saccharovorum* strain isolated from salterns in California evolutionarily closest to *H. lacusprofundi*. We observed that at growth in the liquid medium *H. saccharovorum* cells unlike *H. lacusprofundi* aggregate to form larger granular cell agglomerates and characteristic biofilm at the inner surface of the glass flask. SDS-electrophoresis of *H. saccharovorum* archaellar filaments demonstrates two major bands corresponding to FlaB1 and FlaB2 archaellins. The molar ratio FlaB1:FlaB2 in archaella samples was approximately 2:3 and does not depend on the method of archaella isolation and cultivation conditions. To separate FlaB1 and FlaB2 archaellins and detect their possible isoforms, the *H. saccharovorum* archaella were dissociated using 8 M urea and a nonionic detergent Triton X-100 and subjected to anion exchange chromatography. The resulting elution profile shows, as in the case of *H. lacusprofundi*, the presence of several non-identical forms for both archaellins. Our attempts to identify the archaellin localization using immunoelectron microscopy specific antibody were unsuccessful. However, the use of indirect methods indicates that both FlaB1 and FlaB2 archaellins are present in each of the filaments. Using scanning microcalorimetry and limited proteolysis we found that *H. saccharovorum* filaments are much more resistant to external factors (temperature increase and decrease in salinity) than the *H. lacusprofundi* filaments constructed from a single archaellin. While *H. lacusprofundi* filaments are resistant to trypsin and cooperatively melt only at NaCl concentrations of 10% and above, for the *H. saccharovorum* filaments this range is much wider and starts from 1% NaCl. In a solution of 10% NaCl the melting temperatures were about 45^{o}C for *H. lacusprofundi* and 85^{o}C for *H. saccharovorum* filaments. By lowering the NaCl concentration in *H. lacusprofundi* archaella samples we observed a significant decrease in the enthalpy of transition and split of the heat absorption peak. In the case of *H. saccharovorum* despite the marked difference in aliphatic index which characterizes protein thermostability [7] of FlaB1 and FlaB2 (91.1 and 99.1, respectively), there was only one asymmetric heat absorption peak. Our findings point to the interdependence of the thermal denaturation process in *H. saccharovorum* archaellins FlaB1 and FlaB2, which may indicate their colocalization in the filaments. Our results demonstrate that the presence of the second FlaB2 archaellin may be important to stabilize the supramolecular structure of the archaellum. In our view, lack of second archaellin gene in *H. lacusprofundi* may be related with unique habitat conditions of this organism (Deep Lake in Antarctica), while the habitat area of the remaining known *Halorubrum* species includes warmer salt ponds in the regions of Turkmenistan and Tibet to Chile and Australia.

The work was supported by the RFBR grant № 14-04-01604-a.

References

1. Spang, A., Saw, J. H., Jørgensen, S. L., Zaremba-Niedzwiedzka, K., Martijn, J., Lind, A. E., ... & Ettema, T. J. (2015). Complex archaea that bridge the gap between prokaryotes and eukaryotes. Nature, 521(7551), 173-179.
2. Chaban, B., Ng, S. Y., & Jarrell, K. F. (2006). Archaeal habitats-from the extreme to the ordinary. Canadian Journal of Microbiology, 52(2), 73-116.
3. Mihajlovski, A., Alric, M., & Brugère, J. F. (2008). A putative new order of methanogenic Archaea inhabiting the human gut, as revealed by molecular analyses of the mcrA gene. Research in Microbiology, 159(7), 516-521.
4. Syutkin, A. S., Pyatibratov, M. G., & Fedorov, O. V. (2014). Flagella of halophilic archaea: Differences in supramolecular organization. Biochemistry (Moscow), 79(13), 1470-1482.
5. Jarrell, K. F., & Albers, S. V. (2012). The archaellum: an old motility structure with a new name. Trends in Microbiology, 20(7), 307-312.
6. Syutkin, A. S., Pyatibratov, M. G., Beznosov, S. N., & Fedorov, O. V. (2012). Various mechanisms of flagella helicity formation in haloarchaea. Microbiology, 81(5), 573-581.
7. Ikai, A. (1980). Thermostability and aliphatic index of globular proteins. Journal of Biochemistry, 88(6), 1895-1898.

CHOLINESTERASE IN CONTRACTILE STRUCTURES OF PLANTS AND ANIMALS: HISTOCHEMICAL EXPERIMENTS WITH AZOCOMPOUNDS

V.V. Roshchina, N.E. Shvirst

Institute of Cell Biophysics, Russian Academy of Sciences, Institutskaya Str. 3, Pushchino, Moscow region, 142290, Russia

At a neuro-muscle junction acetylcholine triggers a contraction and enzyme acetylcholinesterase brokes its down that allows a neuron to return to the resting state after activation. Therefore cholinesterases play an important role in controlling acetylcholine-induced contractions of muscle. The finding of contractile elements, acetylcholine and cholinesterase in any cell not only in animal, but in plants and microorganisms [1] needs us to study a location of a cholinesterase activity in cells and their connection with motile systems. Fist histochemical reseach in animals was based on the color reactions with some azo compounds [2,3]. Cholinesterase activity in muscle of mammalians was studied by the method from 60 th years of 20 centhury, but today there are few data related to histochemical analysis of the cholinesterase location of in non-mammalian cells [4]. This work to devote the histochemical studies of the enzyme in contractile structures worms as model to study muscles and some plant cells based on the known reactions with azo compounds (fig. 1).

Materials and Methods

A choose of objects was connected with the possibility to analyze a cholinesterase activity in stuctures able to motile and contactile like whole body of planarians and whole plant secretory cells (hairs) or pollen (table). At cellular

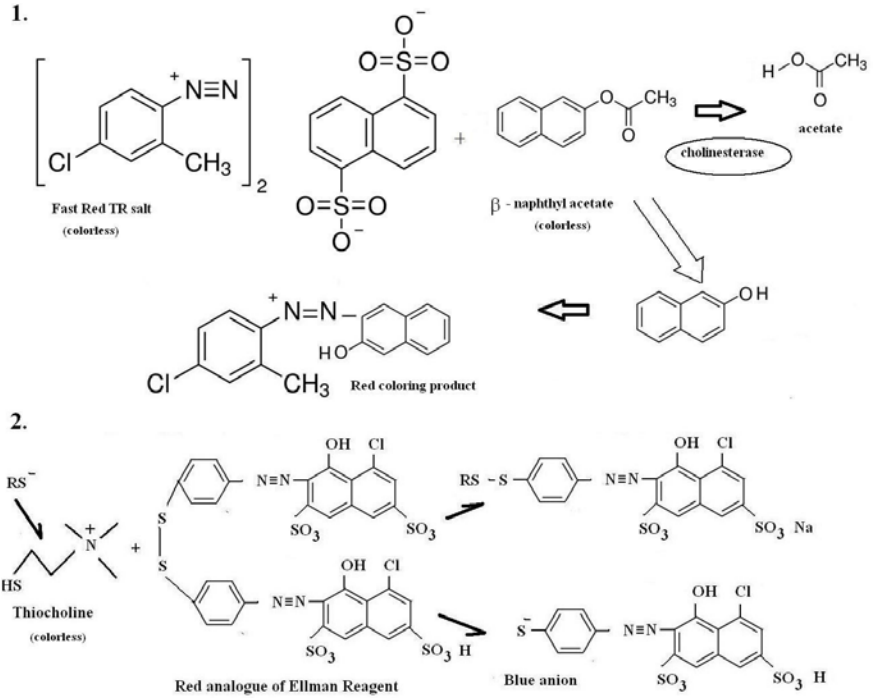

Fig. 1. Proposed histochemical reactions (1) with Fast Red TR salt that adapted from [3] and (2) with Red analogue of Ellman reagent [4].

level similar structures may be membranes such as plasmatic membranes or outer membranes of cellular organelles isolated as described in [5]. Histochemical staining of the objects for the cholinesterase activity determination was carried out with 1. Fast Red TR salt and β-naphthyl acetate as substrate (Sigma, USA) or 2.with Red analogue of Ellman reagent named 2,2-dithio-bis-(p-phenyleneazo)-bis-(1-oxy-8-chlorine-3,6) -disulfur acid in form of sodium salt according to proposed reactions on Fig.1. First group of reagents were prepared and used as described in [6] whereas second group – as in [4]. Histochemical reactions for the cholinesterase assays were done by staining of vital samples with above-mentioned azo dyes solved 0.01M K/Na phosphate buffer pH 7.4 (w/w 1:5) [2–4]. The 1% β-naphthyl acetate or 10^{-3} M acetylthiocholine were used in the same buffer as substrates for cholinesterase at the exposure 1 h, and for special variants 10^{-4} M neostigmine or physostigmine as inhibitors of the enzyme for 20 min before the addition of the substrate. Cholinesterase activity was also controlled in water extracts from samples [4,5]. For the analysis of the extracts from native or homogenized tissues were used. Enzyme solution (50 μL) and β-naphthyl-acetate (50 μL; 20 mmol·L^{-1}) were incubated in 350 μL of 50 mmol·L^{-1} phosphate buffer, pH 7.0, at 22°C in the pres-

ence of Fast Red TR (50 μL;10 mmol·L^{-1} in 50 mmol·L^{-1} hosphate buffer, pH 7.0) [6]. The activity was assayed at 560 nm by measuring the degree of substrate hydrolysis. Reaction basing on the substrate of acethylthiocholine 10^{-3} M lasted 1 h and then staining with another azo dye contained 6 mg red analog of Ellman reagent (Chemanalit, Russia) 120 ml 96% ethanol, 50 ml 0.1 M Na/K-phosphate buffer (pH 7.4), and 50 ml distilled water. The optical density of the blue product between thiocholine and Ellman red analogue were measured with a Perkin-Elmer model spectrophotometer at 620 nm – vacuoles, nuclei and chloroplasts. The observation of colored samples occurred both in transmitted light and ultra-violet light (400 nm).

Results

In table and fig.2 there are objects which demonstrated red or/and blue coloring after the incubation with substrates β-naphthyl acetate or acethylthiocholine. Moreover the color may be absent or weak after the preliminary treatments of the samples with 10^{-4} M inhibitors of cholinesterase neostigmine or physostigmine. As shown on Fig.2 after the staining with Fast Red TR red non-soluble product was seen in the junctions of bicellular secretory hair of *Hibiscus rosa-sinensis* – at contacting cells (images 1–3), and this dense material fluoresced in blue at ultra-violet light (image 3). The reaction with Red analogue of Ellman reagent led to the surface of planarian body coloring in blue (fig. 2, images 4,5), and the product in outer cell layer fluoresced in red under the UV-light (image 5). Pollen of *Hippeastrum hybridum* after similar staining demonstrated the location of blue product in plasmatic membrane that is under the cell wall (fig. 2, image 6). This procedure was applied to isolated organelles – nuclei from *Dolichothele albescens* (fig.2, image 7), vacuoles from bracts of *Euphorbia milii* (image 8) and chloroplasts from

The samples which are clear coloring in red or blue after the staining with azo dyes Fast Red TR (*)or Red analogue of Ellman reagent (**), relatively after the hydrolysis of the substrate used

Object	Contractile element	Object	Contractile element
Worm *Planaria tigrina*	Muscle**	Pollen of *Hippeastrum hybridum*	Pollen tube**
Bracts of *Humulus lupulus*	Veins***	Pollen of *Epiphyllium hybridum*	Pollen tube**
2 days-old Seedlings of *Raphanus sativus*	Growing tip***	Vacuole of petals from *Begonia acetosa*	Tonoplast*
Leaf secretory hairs of *Hibiscus rosa-sinensis*	Hairs ***	Vacuole of *Euphobia milii*	Tonoplast**
Trap of *Utricularia sp.*	Trap**	Nuclei of *Dolichothele albescens* flower petals	Outer membrane**
Secretory hairs of *Drosera capensis*	Head of secretory hair **	Chloroplasts of *Euphobia milii*	Outer membrane**

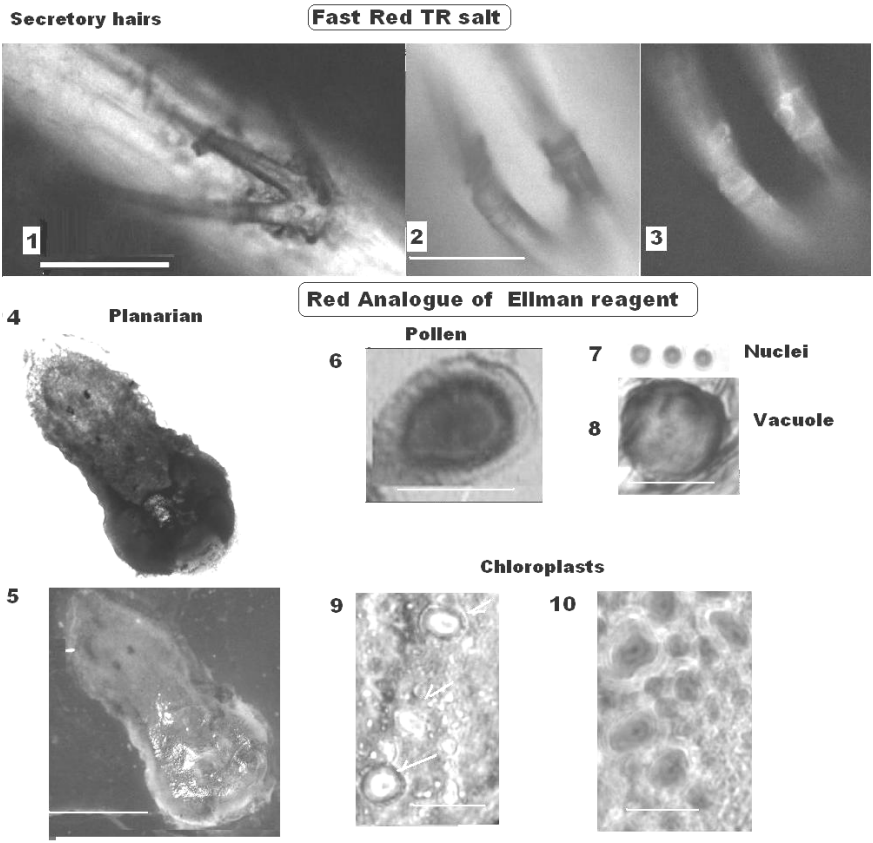

Fig. 2. Examples of the cell staining with azo dyes at the reactions for cholinesterase actiity. 1, 4, 6–10 – images under transmittent light, 2, 3, 5 – under UV-light (400 nm) of luminescence microscope DM 6000 Leica (USA-Germany). Bars = 200, 100, 500, 100, 5, 30, 8 μm for 1, 2–3, 4–5, 6, 7, 8, 9, 10, relatively.

leaves of *E. milii* (images 9 control and 10 experiment, relatively) where also outer membranes were colored.

The sensitivity of plant contractile elements to acetylcholine and the connection with cholinesterase activity was earlier demonstrated as in phloem transport and chloroplasts [8–10]. Pollen tube growth is also connected with the actin polymerization and may be described as motile reaction which is also sensitive to acetylcholine [4]. Although contraction and motility of vacuoles at the cell growth is known [7], only motility within cell and reversed swelling are peculiar to nuclei and chloroplasts that demonstrated a link with actomyosin fibrils of cytoplasm. We believe that using azocompounds may help to analyse the connections between cholinesterase activity and cellular systems elated to contraction and motility.

References

1. Roshchina V.V. New Tendency and Perspectives in Evolutionary Considerations of Neurotransmitters in Microbial, Plant, and Animal Cells. In: Advances in Experimental Medicine and Biology, 2015 ,Vol. 874 . Series: Microbial Endocrinology: Interkingdom Signaling in Infectious Disease and Health. Lyte M, (Ed).New York, Heidelberg: Springer. pp. 25-77.
2. Menten M.L, Junge J., Green M.H. A coupling histochemical azo dye test for alkaline phosphatase in the kidney. J. Biol. Chem. 1944. 153, 471-477.
3. Nachlas M.M., Seligman A.M. The histochemical demonstration of esterase. J Nat. Cancer Inst. 1949.9, 415-425.
4. Roshchina V.V. Neurotransmitters in Plant Life. 2001. Enfield, Plymouth: Science Publisher, 284 pp.
5. Roshchina V.V., Yashin V.A., Kuchin A.V. Флуоресценция нейротрансмиттеров и их рецепция в растительной клетке. Биологические мембраны. 2016. 33(1): 105-112.
6. Kakariari E, Georgalaki M, Kalantzopoulos G, Tsakalidou E. Purification and characterization of an intracellular esterase from *Propionibacterium freudenreichii* ssp. freudenreichii ITG 14. Le Lait, 2000, 80 (5): 491-501.
7. Roshchina V.V., Roshchina V.D. Excretory function of higher plants. Berlin, Heidelberg, Springer, 1993. 314 p.
8. Yang C.J, Zhai Z.X, Guo Y.H, Gao P. Effects of acetylcholine, cytochalasin B and amiprophosmethyl on phloem transport in radish (*Raphanus sativus*). J Integrative Plant Biol 2007, 49(4): 550-555.
9. Roshchina, V.V. Characterization of pea chloroplast cholinesterase: Effect of inhibitors of animal enzymes. Photosynthetica1988. 22 (1): 20-26.
10. Gorska Brylass A., Rascio N.,Mariani P. Cytochemical localization of cholinesterase in the thylakoids of chloroplasts of *Marchantia polymorpha*. Cell Biology International Reports. 1990. 14(abstr. Suppl): 208.

THE EFFECT OF THE CONGENITAL MYOPATHY-CAUSING MUTATION E139del IN TPM2 GENE ON MOVEMENT OF β-TROPOMYOSIN STRANDS AND ACTIN-MYOSIN INTERACTION DURING THE ATPase CYCLE

N.A. Rysev[1], S.V. Avrova[1], O.E. Karpicheva[1], A. Piers[2], C.S. Redwood[2], Y.S. Borovikov[1]

[1]*Institute of Cytology, Tikhoretsky Pr., 4, Saint Petersburg, 194064, Russia*

[2]*University of Oxford, John Radcliffe Hospital, Oxford OX3 9DU, United Kingdom*

Tropomyosin (TM) is a two-chained α-helical coiled-coil protein. Its rod-like molecules associate head-to-tail to form continuous strands that run along the entire length of F-actin. Amino acid sequence of the TM molecule reflects the presence of 7 pseudo-repeats (about 40 amino acids each) that has been postulated to relate to the binding sites for the 7 actin monomers along the length of a TM molecule, conforming to the F-actin helix. The position of TM strands in troponin-free actin filaments was found to be correlated with the number of the switched on

actin subunits, and the amount of the strongly bound myosin heads during the ATPase cycle. In skeletal muscles there are three main tropomyosin isoforms, α-TM, β-TM and γ -TM, which are encoded by the TPM1, TPM2 and TPM3 genes, respectively. Mutations in the TPM2 gene demonstrate a wide spectrum of clinically, histologically and genetically variable neuromuscular disorders. One of these mutations is E139del. The mutation causes cap disease, characterized by cap-like structures located under the sarcolemma. We have investigated how the E139del mutation in TPM2 gene of β-tropomyosin affects TM's position on actin filament and the spatial arrangement of actin subunits and myosin heads at different mimicked stages of the ATPase cycle in ghost muscle fibres by polarized fluorimetry. We labelled recombinant wild-type and mutant E139del TMs with 5-IAF, F-actin with FITC-phalloidin and myosin S1 with 1.5-IAEDANS and incorporated them into ghost muscle fibres. The reconstructed actin filaments of the fibres were decorated by myosin S1 and polarized fluorescence was measured at different stages of the ATPase cycle. It was found that at transition from the weak-binding to the strong-binding actomyosin states actin monomers turned to the filament periphery and the TM strands moved towards the inner domains of actin subunits. The E139del mutation kept the TM strands near the inner domains of actin but decreased the number of the switched on actin monomers throughout the cycle. This mutation inhibits the amount of strongly bound myosin heads throughout the ATPase cycle. The aberrant movement of the E139del TM causes abnormal response of the contractile system that may result in muscle weakness observed in patients with the E139del mutation.

This work was supported by the Russian Foundation for Basic Research (grants №16-34-00865mol and № 14-04-00454).

NEUROMUSCULAR SYNAPSE OF *Drosophila melanogaster* LARVAE ALTERATIONS IN RESPONSE TO HUMAN *APP* GENE EXPRESSION

E.A. Saburova[1], A.N. Vasiliev[1], V.V. Kravtsova[1], O.I. Bolshakova[2], S.V. Sarantseva[2], I.I. Krivoi[1]

[1]*Saint-Petersburg State University, Saint-Petersburg, Russia;*

[2]*B.P. Konstantinov Petersburg Nuclear Physics Institute, National Research Centre "Kurchatov Institute", Gatchina, Russia*

Accumulation and increased synthesis of amyloid-β-protein (Aβ) that occurs as a result of proteolytic processing of Amyloid precursor protein (APP) by β- and γ-secretases is considered to be a major reason for Alzheimer's disease. Regarding APP, physiological role of this protein itself remain incompletely understood. Data obtained on mammals indicate that APP takes part in synapse formation and in regulation of synaptic and neuronal function, alteration of APP expression affects cognitive and memory processes. Notably, APP is located in active zones and interacts with exocytosis cascade proteins (Kohli et al., 2012; Laβek et al., 2013). However, present mammal experimental models do not al-

low to study the effects of APP and Aβ separately. One of the convenient models in this regard is *Drosophila melanogaster*, which does not contain *APP* and *β-secretase* genes. In *Drosophila*, all components of the protein complex responsible for the activity of γ-secretase are present, but the activity of β-secretase is extremely low or negligible. So in transgenic lines of *Drosophila* it is possible to separate and study effects of APP and Aβ independently. Experiments with expression of human *APP* gene in *Drosophila melanogaster* demonstrated neurodegenerative changes, altered cognition and memory processes, changes in locomotion behavior as well as multiple morphofunctional changes in neuromuscular junction (Sarantseva et al., 2009; Sarantseva et al., 2012; Mhatre et al., 2014). In addition, altered presynaptic function and decreased level of synaptic vesicle exocytosis proteins, synaptotagmin and synaptobrevin, were observed (Sarantseva et al., 2009; Ting et al., 2007; Tyan et al., 2012).

Materials and Methods

In our study, neuromuscular junctions of transgenic *Drosophila melanogaster* lines with different level of APP were investigated. To express human *APP* genes in neuronal cells of *Drosophila*, we used the UAS/Gal4 system (Brand, Perrimon, 1993). Line *Gal4-D42* was used as control; line expressing human *APP* gene was able to produce APP only; line expressing both human *APP* and *β-secretase* genes could produce Aβ with corresponding reduce in APP level; and line with direct expression of Aβ only also was used (Table).

The experiments were performed on freshly prepared 3rd instar level *Drosophila* larvae placed into 2-ml Plexiglas chamber. The chamber was continuously perfused with a HL3 solution using BT-100 two-channel peristaltic pump (Leadfluid Co). The solution was continuously aerated with 95% O_2 and 5% CO_2 gas mixture and maintained at 22° C using CL-100 bipolar temperature controller equipped with SC-20 heating/cooling element (Warner Instruments, USA). Resting membrane potentials and miniature excitatory junction potentials (mEJPs) were recorded intracellularly from 6 and 7 muscle fibers using glass microelectrodes with internal capillaries BF150-110-10, made with a P-97 microforge (Sutter Instrument, Co., USA). The electrodes were filled with 3 M KCl, their resistance was less than 10 mOhm. Recordings were made in junctional membrane regions within visually identified terminal branches of the motor nerve. For visual control the binocular PZMTIII (WPI) equipped with TK-092 video camera (JVC) were used. The resting membrane potentials and mEJPs were amplified and digitized using Axoclamp 900A and Digidata 1440A (Molecular devices, USA), with automated data statistics processing (PC Clamp 10.0). Confocal microscopy with cytochemistry was also used.

Results

It was observed that the resting membrane potentials (~ –65 mV) as well as mean peak amplitude, rise time and time to decay half-amplitude of mEJPs (1.04 mV, 7.5 ms and 29.6 ms respectively), obtained in control line, were not significantly changed in all transgenic lines (table). Thus, no postsynaptic alterations were observed. The mEJPs amplitude distribution in control was bimodal

Parameters of mEJPs in control and transgenic Drosophila melanogaster lines with different level of APP production

mEJPs parameter	**Control** (*Gal4-D42*)	**APP** (*UAS-APP; Gal4-D42*)	**APP/BACE** (*UAS-APP; UAS-BACE; Gal4-D42*)	**Aβ** (*UAS-Aβ42; Gal4-D42*)
Peak amplitude, mV	1.04 ± 0.05	0.99 ± 0,06	1.06 ± 0.09	1.06 ± 0.06
Rise time, ms	7.5 ± 0.3	9.2 ± 0.4	9.4 ± 0.4	9.2 ± 0.3
Decay time, ms	29.6 ± 0.8	33.8 ± 0.8	33.4 ± 1.3	34.0 ± 0.9
Number of fibers	44	30	15	34
Number of larvae	16	12	6	14

with peaks at 0.68 mV and 1.15 mV, presumably due to mEJPs generated from Ib and Is presynaptic boutons respectively (Karunanithi et al., 2002). These peaks of mEJPs amplitudes bimodal distribution in all lines never differs significantly from control line and only rare giant mEJPs were observed. Human *APP* gene expression in motor neurons decreased mean mEJPs frequency ($p<0.01$) from 2.6/s in control up to 1.6/s. In addition, enhanced axon branching and decreased expression of synaptobrevin was observed. Co-expression of human *APP* and *β-secretase* genes (production of Aβ and decrease in APP level) slightly recovered mean mEJPs frequency up to 1.9/s. In line with direct expression of Aβ there was no any alteration in mEJPs frequency compare to control. Distribution of mEJPs latencies in all lines fit the mono-exponential equation predicted by the Poisson model well, thus confirming that under all experimental conditions the random nature of spontaneous quantal release is conserved. However, as expected on the basis of the higher frequency of control mEJPs, the latency values were shorter in control line than in APP line.

Conclusions

In sum, our observations indicate that human *APP* gene expression decreases the spontaneous mEJPs frequency and this effect is specific for APP. These data give evidences for involvement of APP in synaptic vesicle exocytosis mechanism and in regulation of quantal transmitter release from nerve endings. Presumably, human *APP* gene expression specifically disturbs molecular machinery of vesicular exocytosis without alteration in the random nature of spontaneous quantal release; an alteration in synaptobrevin distribution, a component of the SNARE protein complex engaged in synaptic vesicle fusion, might be involved.

Supported by St. Petersburg State University grants #1.50.1621.2013 and #1.38.231.2014.

References

Brand A.H., Perrimon N. (1993). Targeted gene expression as a means of altering cell fates and generating dominant phenotypes. Development. 118: 401–415.

Karunanithi S., Marin L., Wong K., Atwood H.L. (2002). Quantal size and variation determined by vesicle size in normal and mutant Drosophila glutamatergic synapses. J. Neurosci. 22: 10267–10276.

Kohli B.M., Pflieger D., Mueller L.N., Carbonetti G., Aebersold R., Nitsch R.M., Konietzko U. (2012). Interactome of the amyloid precursor protein APP in brain reveals a protein network involved in synaptic vesicle turnover and a close association with Synaptotagmin-1. J. Proteome Res. 11: 4075–4090.

Laβek M., Weingarten J., Einsfelder U, Brendel P., Muller U., Volknandt W. (2013). Amyloid precursor proteins are constituents of the presynaptic active zone. J. Neurochem. 127: 48–56.

Mhatre S.D., Satyasi V., Killen M., Paddock B.E., Moir R.D., Saunders A.J., Marenda D.R. Synaptic abnormalities in a Drosophila model of Alzheimer's disease. (2014). Dis. Model. Mech. 7: 373–385.

Sarantseva S., Timoshenko S., Bolshakova O., Karaseva E., Rodin D., Schwarzman A.L., Vitek M.P. (2009). Apolipoprotein E-mimetics inhibit neurodegeneration and restore cognitive functions in a transgenic Drosophila model of Alzheimer's disease. PlosOne. 4: e8191. doi: 10.1371/journal.pone.0008191.

Sarantseva S.V., Kislik G.A., Tkachenko N.A., Vasil'ev A.N., Shvartsman A.L. (2012). Morphological and functional abnormalities in neuromuscular junctions of Drosophila melanogaster induced by the expression of human APP gene. Cell and Tissue Biology. 54: 421–429.

Ting J.T., Kelley B.G., Lambert J.T., Cook D.G., Sullivan J.M. (2007). Amyloid precursor protein overexpression depresses excitatory transmission through both presynaptic and postsynaptic mechanisms. Neurosci. 104: 353–358.

Tyan S.H., Shih A.Y.J., Walsh J.J., Maruyama H., Sarsoza F., Ku L., Eggert S., Hof P.R., Koo E.H., Dickstein D.L. (2012). Amyloid precursor protein (APP) regulates synaptic structure and function. Mol. Cell. Neurosci. 51: 43–52.

NO-DEPENDENT REGULATION OF TITIN EXPRESSION AND ITS PHOSPHORYLATION LEVEL IN RAT *soleus* DURING FUNCTIONAL UNLOADING

N.N. Salmov[1], Y.V. Gritsyna[1], I.M. Vikhlyantsev[1], Y.N. Lomonosova[2], T.L. Nemirovskaya[2], B.S. Shenkman[2], Z.A. Podlubnaya[1,3]

[1]*Institute of Theoretical and Experimental Biophysics, Russian Academy of Sciences, Pushchino, Moscow region, Russia*

[2]*State Scientific Center RF Institute of Bio-medical Problems, RAS, Khoroshevskoye Shosse, 76A, Moscow, 123007, Russia*

[3]*Pushchino State Institute of Natural Science, Pushchino, Moscow region, Russia*

Nitric oxide (NO) is an essential trigger of signaling processes, which leads to structural and metabolic changes in muscle fibers [1]. Nitric oxide is produced by NO-synthases during oxidation of amino acid L-arginine. Unloading is known leads to atrophy of skeletal muscles, that accompanied by heightened degradation of cytoskeletal and contractile proteins [2]. The role of calcium-dependent cysteine

proteases calpains in the initiation of proteolysis of cytoskeletal proteins, in particular titin, is known [3,4]. However, it was found that NO inhibited proteolytic activity of skeletal muscle μ-calpain in vitro [5]. Recently it was shown that L-arginine administration reduced atrophy of unloading soleus muscle [6]. Moreover, L-arginine supplementation prevented content decrease of several cytoskeletal proteins (desmin and dystrophin) in rat soleus muscle during functional unloading [6].

The purpose of this study was to clarify the role of NO in change of expression of titin and its phosphorylation level in rat soleus during functional unloading (7-day hindlimb suspension). The decrease (by 23.2%, $p \leq 0.01$) in content of intact titin-1 (T1) and increase (by ~66%, $p \leq 0.01$) of T2-fragment content in m. soleus of hindlimb suspension rats were detected. These changes have been accompanied by an increase of phosphorylation level of T1 (5.5%) and T2 (23%, $p \leq 0.01$). The increased degradation of titin is undoubtedly a consequence of the enhanced proteolytic activity of calpains. A decrease (by 10%) of titin mRNA level could contribute to the reduction of T1 content in atrophied rat soleus. L-arginine administration prevented enhanced titin degradation and leaded to an increase (by 75%, $p \leq 0.01$) of its mRNA level in hindlimb suspension rat soleus. At the same time, a decrease in phosphorylation level of T1 (by 5.4%) and T2 (by 14.4%, $p \leq 0.01$) was observed. This is first results showing a significant role of NO-dependent regulation in change of titin expression and phosphorylation level of the giant protein in rat skeletal muscle during functional unloading. Molecular mechanisms of the regulation are not clear. However, the indirect role of NO in decreasing degradation of titin through the change in its phosphorylation level is not excluded.

This work was supported by the Russian Foundation for Basic Research (Grants nos. 14-04-00112) and RAS Presidium program “Basic studies for the innovative medical technologies”.

References

1. Shenkman BS, Nemirovskaya TL, Lomonosova YN No-dependent signaling pathways in unloaded skeletal muscle. Front Physiol. 2015 Oct 31;6:298. doi: 10.3389/fphys.2015.00298.
2. Ulanova A, Gritsyna Y, Vikhlyantsev I, Salmov N, Bobylev A, Abdusalamova Z, Rogachevsky V, Shenkman B, Podlubnaya Z Isoform composition and gene expression of thick and thin filament proteins in striated muscles of mice after 30-day space flight. Biomed Res Int. 2015;2015:104735. doi: 10.1155/2015/104735.
3. Goll DE, Neti G, Mares SW, Thompson VF. Myofibrillar protein turnover: the proteasome and the calpains. J Anim Sci. 2008 Apr;86(14 Suppl):E19-35.
4. Shenkman BS, Nemirovskaya TL. Calcium-dependent signaling mechanisms and soleus fiber remodeling under gravitational unloading. J Muscle Res Cell Motil. 2008;29(6-8):221-30. doi: 10.1007/s10974-008-9164-7.
5. Michetti M, Salamino F, Melloni E, Pontremoli S. Reversible inactivation of calpain isoforms by nitric oxide. Biochem Biophys Res Commun. 1995 Feb 27;207(3):1009-14.
6. Lomonosova YN, Kalamkarov GR, Bugrova AE, Shevchenko TF, Kartashkina NL, Lysenko EA, Shvets VI, Nemirovskaya TL Protective effect of L-Arginine admin-

istration on proteins of unloaded m. soleus. Biochemistry (Mosc). 2011 May;76(5):571-80. doi: 10.1134/S0006297911050075.

THE ROLE OF 210 kDa MYOSIN LIGHT CHAIN KINASE AND RhoA-ACTIVATED PROTEIN KINASE IN CONTROL OF MICROVASCULAR ENDOTHELIAL CELL STIFFNESS

M.V. Samsonov[1], M.M. Khalisov[2,3], A.Y. Khapchaev[1], V.A. Penniyaynen[2], A.V. Ankudinov[3,4], B.V. Krylov[2], V.P. Shirinsky[1]

[1]*Institute of Experimental Cardiology, Russian Cardiology Research and Production Center, Moscow, 121552, Russia*

[2]*Pavlov Institute of Physiology, Russian Academy of Sciences, Saint Petersburg, 199034, Russia*

[3]*Saint Petersburg National Research University of Information Technologies, Mechanics and Optics (ITMO University), 197101, Russia*

[4]*Ioffe Physical Technical Institute, Saint Petersburg, 194021, Russia*

Endothelial cells (EC) are inherently mechanosensitive. These cells receive mechanical signals in the form of shear stress or stretch and transform them into chemical responses such as synthesis of NO, endothelin, prostanoids, etc. Mechanosensitivity of EC depends on the stiffness of their cytoplasm, which mainly reflects the status of endothelial cytoskeleton. It is generally accepted that three major cytoskeletal subsystems including microfilaments, intermediate filaments and microtubules as well as physical interactions between them, contribute to the overall stiffness of EC. However, the relationship between cytoskeletal dynamics and cell stiffness has been minimally addressed so far.

In this work, we focused on the role of the microfilament (actomyosin) subsystem in control of endothelial cell stiffness. Myosin type II is the major molecular motor in endothelial cells capable of changing cell rigidity through the formation of contractile microfilament bundles and meshes. It requires activation of regulatory light chains by phosphorylation to exhibit motor activity. The key activators of myosin motor in endothelial cells are the 210 kDa myosin light chain kinase (MLCK210) and RhoA-activated protein kinase (ROCK) whereas myosin light chain phosphatase (MLCP) antagonizes their stimulatory action on myosin. We applied protein kinase inhibitor analysis and atomic force microscopy (AFM) to investigate MLCK210 and ROCK involvement in control of stiffness of microvascular endothelial cells isolated from mouse lungs using immunomagnetic selection.

We subjected live endothelial cells to tactile AFM scanning and obtained stiffness maps of cell nucleus and cortical cytoplasm. In many cases, we observed the bimodal distribution of stiffness, which prompted us to analyze these data sets separately. Performing analysis of the lower value stiffness distribution we found that in non-stimulated cell the cytoplasm Young modulus is about 170±40 кPa whereas the nucleus is several-fold softer (23±10 kPa). Inhibition of endothelial MLCK catalytic activity by 10 μM ML7 led to the reduction of cortical cytoplasm stiffness down to

99±50 kPa while the stiffness of nucleus remained unaffected. Endothelial cells from mice with genetic knockout of MLCK210 (kindly provided by Dr. D.M. Watterson, Northwestern University, Chicago IL, USA) demonstrated reduced stiffness of cortical cytoplasm similar to that observed in wild type endothelium with inhibited MLCK (102±37 kPa). Nucleus stiffness in MLCK210-/- EC was not significantly different from that of the wild type EC (29±20 kPa). Treatment of MLCK210-/- EC with ML7 produced no changes in cell stiffness consistent with the absence of the molecular target for this inhibitor in these cells. Inhibition of ROCK by 10 μM Y27632 led to the reduction in stiffness of both endothelial cytoplasm and nucleus to 75±8 kPa and 13±3, respectively. Thrombin (100 nM) produced no alterations in the lower value endothelial stiffness distribution but affected the high value stiffness distribution leading to substantial softening of both peripheral cytoplasm and nucleus within 20 min. However, when ROCK was inhibited such effect of thrombin was attenuated suggesting that high local stiffness of EC is also regulated by ROCK. At present time, we launched experiments to elucidate the nature of the cytoskeletal structures responsible for the high local stiffness of EC cytoplasm and nucleus. It could not be excluded that such stiffness is generated by microtubules, which are known to undergo depolymerization following EC challenge by thrombin.

Overall, our studies allow conclude that MLCK210 and ROCK control EC cytoplasm stiffness but MLCK does not affect nucleus stiffness. Thus, MLCK and ROCK seem important players in transduction of mechanical signals in EC and may modulate mechanochemical reactions of endothelium.

Supported by RFBR grant 14-04-01813 to VPS.

EFFECTS OF DISEASE-RELATED ALDEHYDES ON ENDOTHELIAL CELLS: A COMPARATIVE STUDY AND PROBING POSSIBLE MOLECULAR MECHANISMS

M.V. Samsonov[1], M.M. Khalisov[2,3], A.Y. Khapchaev[1], A.V. Vorotnikov[1], V.A. Penniyaynen[2], A.V. Ankudinov[3,4], B.V. Krylov[2], V.Z. Lankin[1], V.P. Shirinsky[1]

[1]*Institute of Experimental Cardiology, Russian Cardiology Research and Production Center, Moscow, 121552, Russia*

[2]*Pavlov Institute of Physiology, Russian Academy of Sciences, Saint Petersburg, 199034, Russia*

[3]*Saint Petersburg National Research University of Information Technologies, Mechanics and Optics (ITMO University), 197101, Russia*

[4]*Ioffe Physical Technical Institute, Saint Petersburg, 194021, Russia*

Malonic dialdehyde (MDA), glyoxal (G), methylglyoxal (MG) and several other aldehydes that accumulate in blood and tissues of patients with atherosclerosis and diabetes adversely affect vascular endothelium. A number of studies demonstrated that these agents increase vascular permeability, however, the comparison of their relative efficacy was not extensively addressed in the literature and

insights into possible molecular mechanisms of their action on endothelium are mainly lacking.

In this work, we compared the effects of MDA, G, MG, and dimethylglyoxal on the basal permeability of EA.hy926 human endothelial cell line. Cells were grown on a gold-plated electrode and full electric impedance of the endothelial monolayer was monitored for 24 hours under control conditions (Hank's buffer) and in the presence of 50-250 μM aldehydes. We observed a concentration-dependent irreversible decrease of impedance of the monolayer in the presence of 100-250 μM MDA indicative of endothelial barrier dysfunction. At equimolar concentrations, neither G nor MG produced such an effect on EA.hy926 cells suggesting that a mere attachment of aldehyde molecules to endothelial proteins is not sufficient for alterations in permeability. Glutaraldehyde, a dialdehyde not present in human organism, decreased EA.hy926 monolayer impedance more effectively than MDA. These finding allowed suggesting that the bifunctionality of the aldehyde and the length of the carbon chain spacer between two aldehyde groups are the main determinants of its negative effect on a barrier function of EA.hy926 cells. Hence, cross-linking of endothelial proteins by a bifunctional aldehyde like MDA or glutaraldehyde but not G (which appears to be too short as a cross-linker) could be the cause of increased monolayer permeability.

We checked whether MDA and G treatment of EA.hy926 cells affects the activation of key proteins involved in a stress-response (p38 MAPK), intercellular contacts (Cx43) and NO production that is required for normal barrier function (Akt, eNOS). We used phosphospecific antibodies to assess the relative activation of these proteins in cells treated with 250 μM aldehydes as compared to control cells. We observed significant activation of p38 MAPK but very moderate or no effect on Cx43, Akt, and eNOS activation. Next, we sought to find out what other proteins could be affected by MDA-dependent cross-linking in EA.hy926 cells. We separated whole cell extracts using gradient SDS-PAGE and stained the gels with Coomassie Blue R-250. Side-by-side comparison of control and MDA-treated separated protein bands allowed identifying bands that are missing in MDA samples probably due to cross-linking and shifting the band mobility in the gel. Protein bands from control cells that correspond to missing bands in MDA-treated samples were excised from the gels and subjected to proteomic analysis.

In parallel, we elucidated the stiffness of EA.hy926 cells treated with either MDA or G. In order to do this, we used a tactile atomic force microscopy to obtain stiffness maps of live endothelial cells and determined Young modulus of the nucleus region and cortical cytoplasm. We found that in MDA-treated cells, in comparison to control cells, the stiffness of nucleus was reduced (48.75 ± 11 kPa *vs* 69 ± 7.6 kPa, $n>11$, $p<0.05$) while the stiffness of cortical cytoplasm increased 1.5-fold (88 ± 17 kPa *vs* 59.3 ± 7.5 kPa, $n>11$, $p<0.01$). Treatment of cells with G did not affect nucleus stiffness and only slightly increased the rigidity of cortical cyto-

plasm. These findings suggested that alterations in the properties of the cortical cytoplasm in MDA-treated cells along with other possible alterations brought about by this aldehyde but not by G might be responsible for the effects of MDA on EA.hy926 cell permeability.

To address an issue of peripheral cytoplasm dynamics in MDA-treated endothelial cells, we studied EA.hy926 cells using a video microscopy and analyzed their motile behavior. In preliminary experiments, we found that MDA-treated cells were more compact than control cells. They had less side-to-side contacts with neighboring cells and exhibited reduced ruffling activity at cell edges. The overall motile activity at their edges, both free and those engaged in intercellular contacts, seemed depressed.

Thus, the possible mechanism of the MDA-induced increase in permeability of EA.hy926 endothelial cells appears to be a cross-linking of cellular proteins essential for motile behavior of the cortical cytoplasm and for maintaining contacts between endothelial cells. The identity of these proteins may be resolved in the course of our proteomic studies. Although it sounds counterintuitively, additional covalent cross-linking by MDA does not enhance endothelial barrier but rather disorganize the dynamic intra- / intermolecular protein interactions required to support endothelial monolayer integrity.

Supported by RFBR grant 14-04-01813 to VPS and RSF grant 14-15-00245 to VZL.

EFFECTS OF HYDROGEN SULFIDE ON GASTRIC AND INTESTINAL MOTILITY IN RATS

I.F. Shaidullov, M.U. Shafigullin, G.I. Sabirullina, D.M. Gabitova, G.F. Sitdikova

Institute of Fundamental Medicine and Biology, Kazan Federal University, 18 Kremlevskaya Str., Kazan, 420008, Russia

Hydrogen sulfide (H_2S) is endogenously produced gasotransmitter having different effects in many mammalians organ systems. In recent years, H_2S was identified as messenger molecule in the digestive system, as its synthesizing enzymes are expressed in every part of gastrointestinal tract (GIT). Besides the enzymatic and nonenzymatic ways of H_2S synthesis in these tissues, here presented a large source of gas by sulfate-reducing bacteria, excreting H_2S as metabolic waste. Mechanisms of hydrogen sulfide action are difficult to reveal because of its gaseous nature: it is a small reactive molecule that can easily penetrate the plasma membrane and can interact with all cell structures. Many studies indicate that H_2S participate in regulation of contractile activity of GIT [1]. Motility of digestive system carried out by the contraction of circular and longitudinal muscular layers of GIT. These muscular layers consist of smooth muscle cells (SMC), neuronal cells, and interstitial cells of Cajal (ICC). In this study, we investigated hydrogen sulfide effects on motility of stomach, small and large intestine in rats.

We measured isometric contractions of longitudinal muscle on Biopac system with TSD125C force transducer (Biopac Systems Inc., USA). Muscle strips from stomach and large intestine (8x2 mm), jejunum segments (8 mm) were fixed in vertical bath with 20 ml Krebs solution containing (mM): NaCl – 121.0; KCl – 5.9; $CaCl_2$ – 2.5; $MgCl_2$ – 1.2; $NaHCO_3$ – 25.0; NaH_2PO_4 – 1.2; $C_6H_{12}O_6$ – 8.0 (pH 7.2–7.4, 37°C, bubbled with mixture of O_2 95% and CO_2 5%). Preparations were equilibrated before the experiment for 30 min under preload of 1.0–1.4 g and washed every 10 min with Krebs solution. The data were presented as mean±SEM with n-values representing the number of experiment performed. Statistical significance was evaluated using Student's *t*-test.

After equilibration, spontaneous contractions (SC) of stomach and large intestine strips and jejunum segments were recorded. The stomach preparation had a phasic SC with average amplitude 0.67±0.24 g and frequency 5.17±0.38 contractions per minute (n=25), jejunum segments had amplitude 0.57±0.50 g and frequency 27.0±0.6 contractions per minute (n=20). The large intestine strips had spontaneous non-rhythmic contractions. We measured amplitude, basic tension and frequency of contractions of stomach and large intestine. Area under the curve (AUC) was measured to evaluate the changes of large intestine non-rhythmic contractions. NaHS was used as a donor of H_2S.

NaHS (200 μM) led to relaxation of stomach and jejunum smooth muscles. To 10^{th} minute of addition NaHS reduced the stomach contractions amplitude (100% before *vs*. 16.84±2.39% after the administration of NaHS), the frequency (100% before *vs*. 22.12±4.84% after the administration of NaHS), and basic tension (by 0.40±0.06 g), (n=25, p<0.05). To 3^{rd}-5^{th} minute of addition NaHS reduced the jejunum contractions amplitude (100% before *vs*. 28.79±5.44% after the NaHS administration), frequency (100% before *vs*. 70.61±6.87% after the NaHS administration) and basic tension by 0.21±0.05 g (n = 14, p<0.05). During initial two minutes in 50% of experiments NaHS caused increase of amplitude (100% before *vs*. 119.55±10.3% in stomach strip and 125.5±10.9% in jejunum segment) and basic tension (100% before *vs*. 114.73 ± 6.5% in stomach strip and 121.9±3.6% in jejunum segment).

NaHS (200 μM) increased AUC in large intestine strips (100% before *vs*. 132.87±22.95%), although the basic tension reduced by 0.070±0.027 g from control rates (n=6, p<0.05). Following application of NaHS (300 μM) reduced the AUC in large intestine (100% before *vs*. 63.17+13.98% after the NaHS administration) and basic tension by 0.119±0.038 g from control rates (n=6, p<0.05).

Carbachol (1 μM) induced long term contractions (LTC). NaHS (200 μM) reduced this carbachol-induced contractions: AUC of stomach LTC (100% before *vs*. 59.43±5.49% after NaHS (200 μM) administration) (n=5, p<0.05), AUC of jejunum LTC (100% before *vs*. 17.3±2.11% after NaHS (200 μM) administration), (n=14, p<0.05), and AUC of large intestine LTC (100% before *vs*. 60.7±4.2% after NaHS (300 μM) administration), (n=15, p<0.05).

In the next series of experiments we investigated the target cell for hydrogen sulfide action on jejunum segments. Firstly, we used gap junction blocker Car-

benoxolone (1 μM), that lead to the inhibition of spontaneous activity of the preparation. Subsequent application of NaHS (200 μM) caused two-component change of basic tension: during firs minute the increasing by 0.20±0.03 g and then in 5 minutes the reducing by 0.25±0.04 g (n=8, p<0.05). Assuming that Carbenoxolone blocks the gap junctions between ICC and smooth muscle cells, we suppose that the contraction facilitation on the beginning of application and the following inhibition of motility caused by the effect of H_2S directly on smooth muscle cells.

Secondly, we used a sodium channel blocker Tetrodotoxin (0.5 μM) (TTX) to block a neuronal activity on the gastrointestinal wall. TTX inhibits intrinsic neurotransmission by binding to the voltage-gated sodium channels in nerve cell membranes and usually uses to examine the effects independent of neural influences [1]. Application of TTX caused a facilitation of contractions of the preparations (data not provided), indicating the presence of the tonic activity in some neurons. NaHS inhibits motility of the preparation as in control, but basic tension was more effectively reduced (0.33±0.06 g vs. 0.17±0.04 g after the NaHS administration in control; n=7, p<0.05). Overall picture of NaHS effect not changed, so we suppose that the effect of H2S on smooth muscle cells is not mediated by neuronal activity.

After that we examined the effect of NaHS (200 μM) in the background of carbenoxolone (100 μM) with pre-added TTX (0.5 μM). NaHS increased the basic tension by 0.60±0.09 g (n=7), which was significantly more than without TTX (0.20±0.03 g; n=8, p<0.05). Following decrease of the basic tension was by 0.12±0.04 g (n=7), which was also smaller compared to data obtained without TTX (0.25±0.04 g; n=8, p<0.05).

In conclusion, hydrogen sulfide donor inhibits motility of the stomach, small and large intestine preparations. In some cases, NaHS increases motility during initial period of application in stomach and jejunum or in large intestine preparations during whole application time. Carbenoxolone and TTX not prevented the effects of NaHS, indicating the direct effect of NaHS on smooth muscle cells, probably due the activation of myosin light chain phosphatase [3]. However, it does not exclude the effect of NaHS to the neuronal cells and ICC. For instance, inhibition of the frequency of spontaneous contractions may indicate its effect on ICC.

References

1. Gallego D. et al. The gaseous mediator, hydrogen sulphide, inhibits *in vitro* motor patterns in the human, rat and mouse colon and jejunum //Neurogastroenterology & Motility. – 2008. – Т. 20. – №. 12. – С. 1306-1316.
2. Blair P. J. et al. The significance of interstitial cells in neurogastroenterology //Journal of Neurogastroenterology and Motility. – 2014. – Т. 20. – №. 3. – С. 294-317.
3. Nalli A. D. et al. Inhibition of RhoA-dependent pathway and contraction by endogenous hydrogen sulfide in rabbit gastric smooth muscle cells //American Journal of Physiology-Cell Physiology. – 2015. – Т. 308. – №. 6. – С. C485-C495.

STRUCTURAL AND FUNCTIONAL STUDIES OF TROPOMYOSIN SPECIES WITH NOVEL CARDIOMYOPATHIC MUTATIONS

D.V. Shchepkin[1], G.V. Kopylova[1], A.M. Matyushenko[2,3], K.E. Popruga[2,3], A.V. Pivovarova[2], D.I. Levitsky[2,4], S.Y. Bershitsky[1]

[1]*Institute of Immunology and Physiology, Russian Academy of Sciences, Yekaterinburg, Russia;*

[2]*A. N. Bach Institute of Biochemistry, Russian Academy of Sciences, Moscow, Russia;*

[3]*Department of Biochemistry, School of Biology, Moscow State University, Russia;*

[4]*A.N. Belozersky Institute of Physico-Chemical Biology, Moscow State University, Russia*

Tropomyosin (Tm) is a coiled-coil actin-binding protein that plays a key role in the regulation of muscle contraction. The region around highly conserved Glu180 residue in tropomyosin (Tm) molecule is of particular interest as it is located at a troponin T–binding site of Tm. Mutation E180G of Tm is associated with Hypertrophic Cardiomyopathy (HCM) which leads to severe cardiac hypertrophy [Thierfelder *et al*., *Cell*, 1994]. More recently, novel mutations, E180V, L185R, and I172T, associated with HCM were described in the cardiac α-Tm gene [Regitz-Zagrosek *et al., Circulation*, 2000]. In previous works, the effects of E180G mutation on the structural and functional properties of Tm were studied in detail. In particular, it was shown with a differential scanning calorimetry (DSC) that this mutation decreases stability of the C-terminal part of the molecule [Kremneva *et al*,. *Biophys. J.*, 2004]. However, until now the properties of Tm with these novel HCM mutation were not studied.

Using DSC we showed that E180V mutation unlike E180G substantially increases the thermal stability of the C-terminal part of Tm molecule, whereas mutation L185R have no appreciable influence on the thermal unfolding of Tm (fig 1A). Mutations E180V and E180G demonstrated opposite effects on the stability of Tm–F-actin complexes as was shown by measuring the dependences of thermal dissociation of these complexes monitored with light scattering (fig 1B). Mutation E180G significantly decreased stability of these complexes while E180V mutant dissociated from F-actin at much higher temperature (by 3^{o}C compared to the WT Tm and by 6°C compared to Tm E180G). Both E180G mutation and all novel HCM mutations increased calcium sensitivity of "*p*Ca-velocity" relationship in the *in vitro* motility assay (fig. 2).

These results indicate that the changes in the region around the Glu180 residue in a troponin T–binding site of the Tm molecule may exert a significant influence on the structural and functional properties of Tm and thus take part in genesis of heart diseases.

Supported by Russian Foundation for Basic Research (15-34-20136, 15-04-01558).

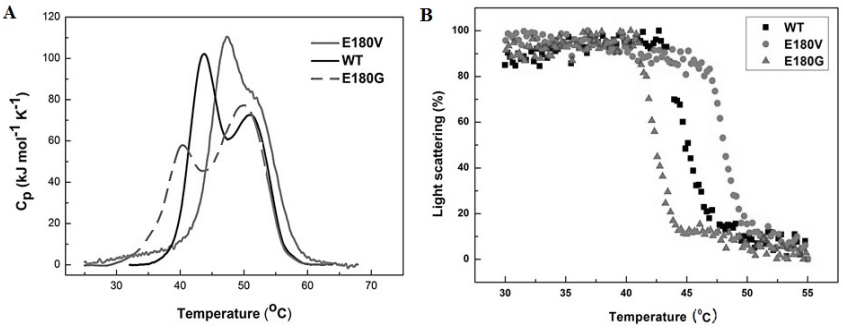

Fig.1. (A) DSC studies on Tpm mutants E180G and E180V. (B) Normalized temperature dependence of dissociation of the F-actin complexes with Tpm mutants E180G and E180V.

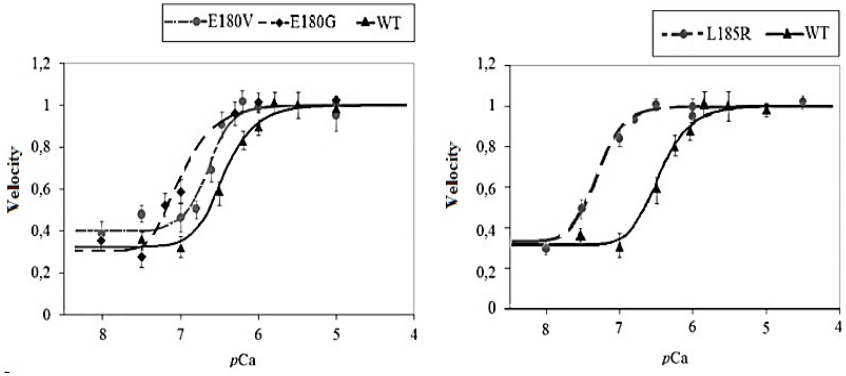

Fig. 2. The sliding velocity of the regulated thin filaments containing E180V Tpm, E180G Tpm or L185R Tpm over the myosin-coated surface as a function of the Ca^{2+} concentration in the *in vitro* motility assay.

SLOW TO FAST. PHYSIOLOGICAL CONTROL OVER SLOW MYOSIN EXPRESSION IN *soleus* MUSCLE UNDER GRAVITATIONAL UNLOADING

B.S. Shenkman, Yu.N. Lomonosova, Ch.A. Lyubimova, K. Ptitsyn

SSC RF Institute of Bio-Medical Problems, Russian Academy of Sciences, Moscow, Russia

Under actual or simulated μG conditions there were observed the decrease of expression of myosin heavy chain (MyHC) of slow type, and sometimes of IIa type, as well as upregulation of expression of IIb and IId/x isoforms. Calcineurin/NFATc1 signaling pathway promotes upregulation of the slow MyHC expression by dephosphorylation and entry of NFAT molecules to the nucleus. But the

NFAT myonuclear import can be prevented by means of calsarcins I and II(also referred to as myozenin II and I), which are known to be calcineurin inhibitors. The other factor preventing from NFAT entry to myonuclei the glycogen synthase kinase GSK3β. It facilitates the NFAT phosphorylation thereby providing NFAT export from myonuclei. We supposed that downregulation of calcineurin pathway took place during unloading. The study was aimed to analyze the states of the myonuclear NFAT inhibitors calsarcin I (CSI) and calsarcin II (CSII) and GSK3β in rat soleus during hindlimb suspension (HS).

Male Wistar rats were subjected to 3, 7 and 14 day HS. We found that after 3 days of HS the content of CSII mRNA two-fold increased in soleus as compared to the controls. This level was increased by more than 5-fold (as compared to controls) after two weeks of HS. The increase of CSII RNA may be explained as the mechanism of stabilization of fast phenotype [Shenkman et al., 2014]. We found that from the 3 day till 14 day of HS the content of MuRF-1 and MuRF-2 in the nuclear fraction 4-5 fold increased in HS soleus. We supposed that nuclear import of the MuRFs allows to promote CSII expression during unloading. We also observed the decline of the phosphorylated GSK3β content (i.e. increase of NFATc1 phosphorylating activity) in the nuclear extract of the soleus tissue after 3 and 7 days of unloading [Lomonosova ety al, 2015]. It is known that the activity of GSK3β inhibiting the MyHCIβ expression can be suppressed by nitric oxide (NO) through cGMP pathway. Earlier we found the reduction of NO content in rat soleus muscle under HS conditions [Lomonosova et al., 2011]. In the 7 day rat HS study we used the i.p. daily injections of L-arginine, the activator of NO-synthase (500 mg per kg of animal BW). In the L-arginine supplemented rats we didn't find any reduction in the GSK3β phosphorylation and downregulation of MyHC Iβ mRNA as in saline injected suspended animals. Thus the NO accumulation may suppress the inhibiting activity of GSK3β and prevent the decline in slow myosin expression. We believe that reduced level of NO content during unloading may participate in the slow-to-fast myosin shift. It is concluded that the decline of slow MyHC expression characteristic for the unloading conditions is associated with the increased expression and activation of the factors known to prevent NFAT accumulation in the myonuclei.

The study was supported by the grant of the Russian Science Foundation #14-15-00358

THE SKELETAL MUSCLE RESPONSE TO ALCOHOL ABUSE: MEN *vs.* WOMEN

B.S. Shenkman[1], O.E.Zinovyeva[2], T.M. Mirzoev[1], E.G. Altaeva[1], O.V. Turtikova[1], T.L.Nemirovskaya[1,3]

[1]*Institute of Biomedical Problems RAS, Moscow, Russia*

[2]*I.M. Sechenov First Moscow State Medical University*

[3]*Faculty of Basic Medicine, Lomonosov Moscow State University, Moscow, Russia*

Clinical examination of women abusing alcohol and analyses of the reasons for changes occurring in muscle tissue were carried out. In the study methods of electromyography, magnetic resonance imaging, western-blotting, immunohistochemistry and RT-PCR were used. Using the method of magnetic resonance imaging, we for the first time established that degenerative changes in women, abusing alcohol, are more pronounced in the posterior muscles of the femur and tibia than in the anterior group of muscles. Thus, we identified the groups of muscles subjected to the greatest impact of alcohol intoxication. It will help us to develop new preventive measures for the most affected muscles. *We for the first time showed that* **1)** among women abusing alcohol, muscle atrophy occurs much faster than in men and the atrophy is more pronounced. Both fast and slow muscle fibers are affected. The period of development of atrophic processes is much shorter than in male patients. The causes and mechanisms of the development of alcohol-induced atrophy of skeletal muscles were discovered. **2)** In women the anabolic mTORC1 signaling pathway is damaged to a greater extent than ERK1/2. **3)** In women abusing alcohol, signaling system of the protein degradation works more intensely than in men. Calpain1 content and the ubiquitylation of proteins are higher than in the control group. This may be the reason for the more rapid and profound atrophy of skeletal muscle in women who abuse alcohol. This finding is important for the development of (i) prevention systems against the lowering of working capacity and (ii) pharmacological and physiological methods for correction of atrophic processes in skeletal muscle in a socially significant disease, such as alcoholic myopathy.

The work was supported by Russian Science Foundation, grant no. 14-15-00392.

EFFECTS OF SUPPORT UNLOADING ON POSTURAL MUSCLES MOTOR UNITS' ACTIVITY

T.A. Shigueva, A.Z. Zakirova., E.S. Tomilovskaya, I.B. Kozlovskaya

State Scientific Center of the Russian Federation – Institute of Biomedical Problems of the Russian Academy of Sciences, Khoroshevskoe sh., 76A, Moscow, 123007, Russia

The purpose of the study was to investigate the effect of support unloading on changes of recruitment order of motor units` (MU) activity of shin extensor muscles (m.soleus *и* m.gastrocnemius lat.) and intensity of spinal excitatory and inhibitory processes in motoneurons pools.

Conditions of support unloading were reproduced by "dry" immersion (DI). The experiments were performed with participation of 18 healthy men. All the subjects were divided into 2 groups. In the control group the subjects stayed in DI without any other influences; DI the mechanical stimulation of soles' support zones in the regimen of locomotion was applied daily in the experimental group in the course of DI. MUs' activity of shin muscles was recorded with needle concentric electrodes during execution of the task of maintaining a small plantar flexion

effort. Single electrical pulses 0,1 ms of duration were applied to n.tibialis. Duration of interspike intervals (ISI) as well as H-response threshold, the duration of the silent period (SP) following H-reflex response and presence of rebound phenomenon – an increase of MU activity at the end of SP, the events that are usually observed under normal conditions reflecting trace of inhibitory and excitatory processes in motoneurons pools, were analyzed.

The activity of MUs characterized by low amplitude and small ISI was recorded during the performance of the task before DI. Under DI conditions characteristics of MUs' activity changed distinctly in the control group: the number of MUs characterized high amplitude and long ISIs grew up significantly. These changes were also observed in the experimental group but their intensity was less expressed. Exposure to the conditions of support unloading was followed also by significant decline the duration of SP. The rebound phenomenon in the course of DI in this group was not observed. In the group with mechanical stimulation of the soles' support zones the duration of SP in m. soleus remained close to that of control. The rebound phenomenon in the experimental group was also unchanged. Thus, withdrawal of support was followed by decline of strength of inhibitory processes that followed evoked responses. Under these conditions application of artificial support eliminated the described above effects.

The study is supported by project RSF №14-25-00167.

NOVEL APPROACHES TO RESTORATION OF MYOCARDIAL CONTRACTILITY IN ISCHEMIA-REOXYGENATION CONDITIONS AND CARDIAC FAILURE

V.P. Shirinsky, N.A. Undrovinas, A.A. Abramov, V.L. Lakomkin, Zh.D. Bespalova, M.V. Sidorova, V.I. Kapelko

Institute of Experimental Cardiology, Russian Cardiology Research and Production Center, Moscow, 121552, Russia

Acute and chronic cardiac ischemia negatively affect contractile function of myocardium and provoke arrhythmia. One of the immediate causes of poor cardiac performance is the dysfunction of the molecular system responsible for Ca^{2+} transport in cardiomyocytes. Striated muscles including heart muscle demonstrate almost linear dependence of generated contractile force on the levels of free ionized Ca^{2+} in the sarcoplasm. Ca^{2+} proportionally binds to troponin complex on thin filaments and induces unmasking of myosin binding interface on actin. When Ca^{2+} is removed from the sarcoplasm actin - myosin interaction is again inhibited. Ion channels of sarcolemma and sarcoplasmic reticulum mediate the rise of ionized Ca^{2+} in the sarcoplasm. It is fast and energy-independent process. To the opposite, the removal of Ca^{2+} from the sarcoplasm requires energy (ATP) and its speed critically depends on the overall function of Ca-ATPases of sarcolemma (PMCA) and sarcoplasmic reticulum (SERCA). The main Ca^{2+} pump of cardiomyocytes is SERCA2.

We observed that in isolated rat cardiomyocytes subjected to experimental hypoxia and in cardiomyocytes obtained from rats with experimental cardiac failure SERCA2 function is depressed. While the influx of Ca^{2+} in the sarcoplasm remains relatively intact its withdrawal is attenuated leading to prolonged accumulation of free Ca^{2+} in the sarcoplasm accompanied by intermediate level contraction and the lack of full relaxation. Moreover, these cardiomyocytes fail to respond to rhythmic stimulation by electric impulses and develop arrhythmic contractions. We tested several pharmacologic approaches to improve SERCA2 function and overall Ca^{2+} transport in disease-modeled cardiomyocytes. We used the peptide apelin-12 and its synthetic derivatives, designed and produced at the Cardiology Research and Production Center, to restore SERCA2 function. We found that nanomolar concentrations of apelin-12-2 analog (Methylin) within 15 min after application restored normal Ca^{2+}-transits in cardiomyocytes isolated from the hearts of rats with isoproterenol-induced cardiac failure. Another compound that was able to rescue SERCA2 function in hypoxic conditions was Oxacom®, a dinitrosyl iron complex with glutathione, which currently undergoes phase 3 clinical trials as hypotensive drug. Additionally, nanomolar Oxacom® produced more sustained effect then Methylin on SERCA2 function in cardiomyocytes from rats with doxorubicin-induced heart failure. Our findings obtained in cardiomyocytes were confirmed using the model of isolated perfused rat heart. Indeed, both Methylin and Oxacom® reduced stiffening of the heart and promoted more profound relaxation after ischemia-reperfusion. Oxacom® effectively prevented reoxygenation-associated arrhythmias while Methylin also increased contractile and relaxation indices in isolated hearts with cardiac failure as well as in the whole animals.

While further studies of Methylin and Oxacom® are underway, it is clear that both compounds have a strong potential to become novel cardioprotective drugs that stimulate myocardial contractility, in particular, by normalizing cardiomyocyte relaxation.

DESIGN AND INITIAL CHARACTERIZATION OF CELL PERMEABLE AND PEPTIDASE RESISTANT MYOSIN LIGHT CHAIN KINASE INHIBITOR PEPTIDES BASED ON MYOSIN REGULATORY LIGHT CHAIN SEQUENCE

M.V. Sidorova, A.A. Az'muko, A.S. Molokoedov, V.N. Bushuev, M.V. Samsonov, O.A. Kazakova, A.Y. Khapchaev, A.V. Nikashin, V.P. Shirinsky

Institute of Experimental Cardiology, Russian Cardiology Research and Production Center, Moscow, 121552, Russia

Myosin light chain kinase (MLCK) is the key Ca^{2+}-calmodulin-dependent regulator of actomyosin-based cell motile reactions such as cytokinesis, receptor capping, adhesion and migration, endothelial and epithelial monolayer permeabil-

ity to macromolecules, smooth muscle contraction, etc. Inhibition of MLCK catalytic activity is a widely used research tool in biomedical applications and is considered as a potential approach for treatment of disease conditions such as acute microvascular hyperpermeability that leads to lung and brain edema.

We designed the set of nonapeptides based on the sequence of MLCK substrate, the 20 kDa myosin regulatory light chain (RLC) ^{11}KKRAARAT^{19}S ($RLC_{11–19}$). This peptide is a competitive inhibitor of smooth muscle myosin RLC phosphorylation by MLCK [Pearson et al., 1986]. The peptide $RLC_{11–19}$ was also shown to penetrate in neutrophils [Chilcoat et al., 2008] apparently due to the presence of a positively charged N-terminal amino acid cluster KKR. We synthesized RLC_{11-19} peptide using automated solid phase synthesis and Fmoc technology and demonstrated by ^{1}H-NMR spectroscopy that this peptide is rather unstable in human blood plasma (half-life is 45 min). Hence, $RLC_{11–19}$ is not an optimal compound to use on cultured cells or in vivo in the presence of serum / plasma. Therefore, a peptide analog of $RLC_{11–19}$ that retains its inhibitory activity and penetrate plasma membrane while being less prone to degradation will be more preferable as a research tool and a potential drug candidate.

^{1}H-NMR spectroscopy analysis allowed us establish the degradation pattern of $RLC_{11–19}$ in plasma and suggested focused modifications of its structure in order to protect the peptide from peptidase attack. We designed and synthesized acetylated $RLC_{11–19}$ analog (Ac-$RLC_{11–19}$) and peptides modified with non-protein amino acid ornithine (Orn-$RLC_{11–19}$) or D-amino acid (D-$RLC_{11–19}$) incorporated in critical positions in the parent peptide. Additionally, an amide group at C-terminus protected all synthesized peptides. Subsequent ^{1}H-NMR spectroscopy analysis of degradation patterns of the novel peptides revealed that Ac-$RLC_{11–19}$ and D-$RLC_{11–19}$ were 8-fold more resistant to degradation in human blood plasma than the original $RLC_{11–19}$ and Orn-$RLC_{11–19}$, which stability was not improved.

Next, we elucidated whether Ac-$RLC_{11–19}$ and D- $RLC_{11–19}$ are able to penetrate cell membrane and affect the state of myosin RLC phosphorylation in cultured cells. We preincubated human endothelial cells EA.hy926 with 20 μM peptides for 1 hour and analyzed the levels of monophosphorylated RLC using immunoblotting with commercial P-RLC(Ser19)-specific antibodies. We found that in the presence of D-$RLC_{11–19}$ P-RLC level decreased 1.3-fold compared to that in control cells while Ac-$RLC_{11–19}$ produced no P-RLC decrease, perhaps, because of its poor penetration in endothelial cells.

Thus, we produced a novel peptide D-$RLC_{11–19}$ that is able to inhibit MLCK activity in cultured endothelial cells and is substantially more stable than a parent peptide $RLC_{11–19}$. This original peptide may be used in a biomedical research to manipulate cell motile reactions and could be a prototype structure for the development of the novel antiedemic drugs.

ROLE OF HYDROGEN SULFIDE IN REGULATION OF VASCULAR SMOOTH MUSCLE CELLS CONTRACTILE ACTIVITY

L.V. Smagliy[1], J.G. Birulina[1], I.V. Kovalev[1], S.V. Gusakova[1], S.N. Orlov[2]

[1]*Siberian State Medical University, Moskovskiy trakt 2, Tomsk, 634050, Russia*

[2]*Faculty of Biology MV Lomonosov Moscow State University, Leninskiye Gory 1/12, Moscow, 119991, Russia*

We studied the mechanisms of hydrogen sulfide (H2S) action on vascular smooth muscles (VSM). The study was performed on endothelium-denuded ring segments of male Wistar rats thoracic aorta by method of mechanography.

Contractions of VSM were induced with highpotassium solution (30 mM KCl) or activator of α_1-adrenoreceptors phenylephrine (PE, 10 μM). The amplitude of contractile responses was calculated as a percentage of control highpotassium contraction or PE-induced contraction, which was taken as 100%. We used sodium hydrosulfide (NaHS) as a donor of H2S. NaHS solution was prepared immediately before use; pH of the solution was maintained at the range 7.35-7.40.

NaHS at concentrations of 5, 10, 50 μM induced an increase in VSM mechanical tension (MT) of 9.1 ± 2.5%, 15.9 ± 3.4% and 18.5 ± 3.5%, respectively (n = 9, p <0.05).

NaHS at concentration of 100 μM caused biphasic response of VSM: transient increase in MT to 27.5 ± 5.7% with its subsequent decrease to 15.3 ± 2.4% (n = 9, p <0.05).

500 and 1000 μM NaHS led to decrease of MT to 35.1 ± 7.5% and 51.7 ± 5.0% (n = 9, p <0.05), respectively, of the amplitude of control highpotassium contraction. Constrictive effect of NaHS (5-100 μM) was eliminated by pretreatment of VSM with an inhibitor of Na^+, K^+, $2Cl^-$ -cotransporter (NKCC) bumetanide (100 μM).

This findings were confirmed by radionuclide studies where the NKCC activity was assayed as the bumetanide-sensitive component of 86Rb + input in freshly isolated aortic smooth muscle cells from Wistar rats: NaHS at concentrations of 50 and 100 μM increased NKCC activity to 46.0 ± 7.0% and 38.0 ± 11.0%, respectively. The subsequent addition of NaHS at concentrations of 500 μM reduced NKCC activity to its initial level.

In VSM precontracted with PE NaHS (5–1000 μM) caused a dose-dependent relaxing effect.

A blocker of voltage-dependent and calcium-activated potassium channels tetraethylammonium (10 mM) and a blocker of voltage-dependent potassium channel 4-aminopyridine (1 mM) significantly reduced relaxing action of NaHS (100 μM) in VSM precontracted with PE.

The blocker of ATP-sensitive potassium channels glibenclamide (10 μM) completely abolished the relaxing effect of NaHS (100 μM). The blocker of calci-

um-activated potassium channels of big conductivity charybdotoxine (0,1 μM) had no significant influence on NaHS-induced vasorelaxing action.

Relaxing action of NaHS (500 μM) on highpotassium contraction of VSM was also depend on the potassium conductance of smooth muscle cells membranes and significantly reduced in presence of tetraethylammonium (10 mM) and 4-aminopyridine (1 mM), but not glibenclamide (10 μM) and charibdotoxine (0,1 μM).

Conclusion: constrictive action of H2S on aortic segments of Wistar rats precontracted with 30 mM KCl, is due to the activation of NKCC, and relaxing action of H2S caused by activation of voltage-dependent potassium channels. H2S-induced relaxation of vascular segments, precontracted with PE, is due to preferential activation of ATP-sensitive potassium channels of smooth muscle cells membranes.

TO THE ISSUE ABOUT MODELLING OF SCALABLE STRUCTURES OF VISCOELASTIC BIOLOGICAL TISSUES

A.T. Smoluk, L.T. Smoluk, Y.L. Protsenko

Institute of Immunology and Physiology of the Ural Branch of the RAS, 620049, Pervomayskaya st., building 106, Ekaterinburg, Russia

In this study the approaches for calculating the viscoelastic properties of scalable model structures of soft biological tissues were analyzed. Since the standard numerical methods for calculating the scalable structures become more cumbersome and difficult to verify (difficult debugging) with an increase in the number of structural units, the use of physically based methods are the most popular.

The proposed method is a modification of the "mass-spring" method for systems consisting of many massless structural elements whose behaviour cannot be calculated analytically or difficult to calculate with the standard numerical methods, including finite element method [4]. Finite element method is the most complete and qualitative method to solve biomechanical tasks. However surgeons need to watch modelling result as fast as possible so executable speed is also a key point. Because of complex calculations finite element model works slowly. So nowadays together with it the new mass-spring model [1], the main criteria of which is modelling speed, also becomes widely used. This approach was successfully implemented to model different biomechanical tasks: heart, lungs and muscles [2].

The developed approach was applied to describe the strained state of the model of myocardial morphofunctional units [3] to test of its adequacy. The model is a structural combination of massless elastic and viscous elements. The behaviour of this basic model can be calculated from ab initio conditions (ie, solving nonlinear equations describing the expected deformed state). However, in the model composed of four basic blocks (fig. 1A), taking into account the shear deformation of the biological tissue, using ab initio approach results in a significant complication of the calculation algorithm. This fact indicates that this approach cannot be used to describe the viscoelastic behaviour of heterogeneous biological tissue, comprising a

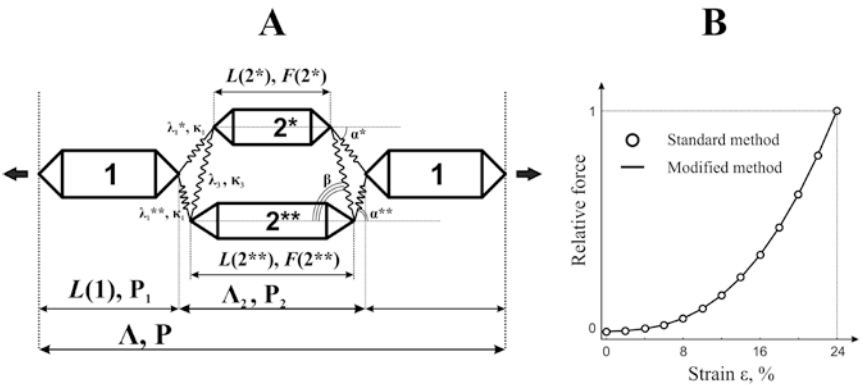

(A) Structural diagram of the simplest model of an inhomogeneous biological tissue. $L(i)$ – current length of i-th unit, λ_m – current length of m-th junction between 1 and 2 units, κ_m – current length of m-th junction between 1 and 2 units, ρ_m – force developed by m-th junction between 1 and 2 units, Λ_2 - current length of the central part of whole model, Λ - the total length of the whole model, P – force developed by the whole model.

(B) Representative example of "force-strain" dependence. Point-curve was obtained with standard method of calculating, line-curve – with modified method.

plurality of structural elements. Thus, there is a problem of scalability of the original base model. Therefore, it has been suggested that the use of the modified «mass-spring» approach would be most effective for this task.

"Mass-spring" method does not imply analytical or numerical solution of the constraint equations between the structural elements when setting the deformation, and, instead, includes a series of iterations required to achieve equilibrium of the entire model (based on a pre-selected "conditional zero") on the basis of presentation of the model as a physical object. The main feature of our modified method is to use a massless model elements. The calculation algorithm involves the following steps:

1) Longitudinal deformation is set to the entire model.
2) Longitudinal structural model element / block is deformed artificially by a value equal to the deformation of the entire model.
3) Characteristic nodes of the model (points of forces application that determine the behaviour of the model as a physical system) are selected.
4) For each node, the components of the resultant force is calculated.
5) Depending on the direction of the resulting force coordinate vectors and the magnitude of the vector module defining elements in each node are resized.
6) Steps 1–5 are repeated as long as the resultant force module for each node is less than the selected "conditional zero". The resulting state of the model is considered to be the equilibrium.

The differential discrete changes in the lengths of the model elements is used to optimize and for convergence of the method. Then the question arises, how to simulate the response to the deformation of a larger structure? We know the behaviour of a single unit, so it is necessary to repeat the same algorithm, considering the individual blocks nonlinear viscoelastic elements ("super springs") with known characteristics.

The results of mathematical modelling on a single unit showed coincidence of the corresponding "force – deformation" dependency of the traditional and modified approaches. A representative example is shown in fig. 1B. Obtained data indicate the consistency of the modified method of calculating our structural and functional model of a biological tissue. The main advantage of the proposed modification of the method is the possibility to use of parallel programming algorithms to optimize our computational scheme.

This work is supported by RFBR grant 16-34-00037 and the Program of fundamental research of Presidium of the RAS №43 on strategic areas of science in 2016 year "Fundamental problems of mathematical modeling".

References

1. Jarrousse O. Modified Mass-spring System for Physically Based Deformation Modeling. 2012. Karlsruhe. KIT Scientific Publishing C.
2. Nikolaev S.N. Non-linear mass-spring system for large soft tissue deformations modeling. // Scientific and technical journal of information technologies, mechanics and optics. 2013. V. 5(87). P. 88-94.
3. Smoluk L., Protsenko Y. Viscoelastic properties of the papillary muscle: experimental and theoretical study. // Acta Bioeng Biomech. 2012. V. 14(4). P. 37-44.
4. Jarrousse O., Fritz T., Dossel O. A modified Mass-Spring system for myocardial mechanics modeling. // 4th European Conference of the International Federation for Medical and Biological Engineering. 2009. V. 22(1-3). P. 1943-1946.

TWO ISOFORMS OF EXTRACELLULAR HEAT SHOCK PROTEIN 90 (HSP90) ARE INVOLVED IN MIGRATION AND INVASION OF HUMAN TUMOR CELLS *in vitro*

A.V. Snigireva, V.V. Vrublevskaya, Y.Y. Skarga, O.S. Morenkov

Institute of Cell Biophysics, Russian Academy of Sciences, 142290, Russia, Pushchino, Moscow Region, 3 Institutskaya Str.

Heat shock protein 90 (Hsp90) is one of the most abundant and ubiquitously expressed proteins. Hsp90 plays an important role in cell functioning under normal and stress conditions. Hsp90 acts inside cells as a chaperone that regulates folding, maturation, transport, and degradation of a diverse set of client proteins, in particular, signaling molecules, steroid receptors, and transcription factors. There are two cytoplasmic isoforms of Hsp90, Hsp90α (the inducible form) and Hsp90β (the constitutive form), which share a high sequence homology but show some differences in biochemical properties, expression, and function. In addition to intracellular localization, Hsp90 can be found at the cell plasma membrane and in the

extracellular space. Extracellular Hsp90 was shown to participate in cell motility, invasion and metastasis of tumor cells. The data concerning the role of particular extracellular Hsp90 isoforms, Hsp90α and Hsp90β, in cell migration and invasion are contradictory. The aim of this work was to investigate the role of two isoforms of extracellular Hsp90 (Hsp90α and Hsp90β) in migration and invasion of human glioblastoma (A-172) and fibrosarcoma (HT1080) cells *in vitro*.

We investigated the effects of native total Hsp90, Hsp90α, and Hsp90β on migration and invasion of human tumor cells *in vitro*. Native total Hsp90 was purified from murine brain using the thiophilic chromatography-based method developed earlier in our laboratory. Native total Hsp90 consisted of Hsp90α and Hsp90β isoforms at a ratio of approximately 40% and 60%, respectively. Native Hsp90α and Hsp90β isoforms were purified from total Hsp90 using immunoaffinity chromatography based on agarose gels coupled with Hsp90α- and Hsp90β-specific antibodies. To prepare these antibodies, rabbits were immunized with conjugates of Hsp90α- and Hsp90β-specific peptides with proteins. Antibodies directed to Hsp90α and Hsp90β were purified from hyperimmune rabbit sera using sorbents with immobilized Hsp90α- and Hsp90β-specific peptides. Native total Hsp90, Hsp90α, and Hsp90β preparations were of at least 95% purity. Hsp90α preparation contained no Hsp90β, Hsp90β preparation contained less than 5% of Hsp90α which was shown by immunoenzyme assay and immunoblotting assay. The purified native proteins did not affect cell proliferation and had no cytotoxicity. Heat shock protein 70 (Hsp70), isolated from murine brain, and BSA were used as controls.

The effects of native total Hsp90, Hsp90α, and Hsp90β on migration of tumor cells *in vitro* were investigated using transwell migration assay. The inserts with polyethylene terephthalate (PET) membrane (pore size 8 μm) were used in the assay. Cell culture inserts were placed in the wells of multiwell cell culture plates. The migration chamber consisted of an upper and lower compartment with a porous PET membrane in-between. Cells actively migrated from the upper to the lower compartment along a chemoattractant gradient. The effects of native total Hsp90, Hsp90α, and Hsp90β on cell invasion *in vitro* were investigated using inserts with PET-membrane coated with Matrigel Basement Membrane Matrix (Becton Dickinson). Matrigel is a solubilized basement membrane preparation extracted from the Engelbreth-Holm-Swarm mouse sarcoma, a tumor rich in extracellular matrix proteins to include laminin, collagen IV, heparan sulfate proteoglycans, entactin. In transwell invasion assay, Matrigel occludes the pores of the PET-membrane and serves as a reconstituted basement membrane *in vitro*, imitating extracellular barriers in tissues.

Native total Hsp90, Hsp90α, and Hsp90β reliably stimulated migration of human glioblastoma and fibrosarcoma cells *in vitro* at concentrations of 10–100 μg/ml. For both cell cultures, native total Hsp90 at a concentration of 50 μg/ml increased migration of cells by 35–50%. Hsp90α and Hsp90β at a concentration of 50 μg/ml also stimulated migration of A-172 and HT1080 cells by 40–45% and 25–32%, respectively. Control proteins, Hsp70 and BSA, had no effect on cell

migration at a concentration of 100 μg/ml. These data indicated an important role of both isoforms of extracellular Hsp90 in activation of a process of tumor cell migration. Native Hsp90α demonstrated more pronounced stimulating effects on migration of cells as compared to Hsp90β. The specificity of effects of Hsp90α and Hsp90β on cell migration was confirmed using antibodies. Hsp90α-specific antibodies inhibited the stimulating effects of Hsp90α but not Hsp90β while Hsp90β-specific antibodies decreased the effects of Hsp90β but not Hsp90α.

An addition of native total Hsp90, Hsp90б, and Hsp90в to culture medium (10–100 μg/ml) also stimulated invasion of human glioblastoma and fibrosarcoma cells *in vitro*. At a concentration of 25 μg/ml, total Hsp90 stimulated the invasion of human A-172 and HT1080 cells by 75–130%. Native Hsp90α and Hsp90β at a concentration of 25 μg/ml also stimulated invasion of A-172 and HT1080 cells by 45–90% and 90–145%, respectively. Control proteins, Hsp70 and BSA, had no effect on cell invasion at a concentration of 100 μg/ml. Hsp90β had more profound stimulatory effect on invasion of both human tumor cells *in vitro*. The specificity of effects of Hsp90α and Hsp90β on cell invasion was confirmed using antibodies.

Previously, the role of two isoforms of Hsp90 in migration and invasion was studied using recombinant Hsp90α and Hsp90β and the results were rather contradictory. Recombinant proteins may have alterations in secondary and tertiary structure which may impair their functionality and lead to unreliable results. Here, we showed for the first time direct stimulatory effects of Hsp90α and Hsp90β on migration and invasion of tumor cells using purified native proteins. It is noteworthy that the results were obtained using two different tumor cell lines, human glioblastoma A-172 and human fibrosarcoma HT1080. Thus, we convincingly demonstrated that both isoforms of Hsp90, Hsp90α and Hsp90β, stimulate migration and invasion of tumor cells *in vitro*. It is known that metastasis is a complex process that includes migration and invasion of tumor cells through tissue barriers inside the surrounding tissues. In this context, the obtained results suggest that both isoforms of extracellular Hsp90, Hsp90α and Hsp90β, can be considered as a promising molecular targets to suppress metastasis of tumor cells.

THALLIUM INDUCES AN INCREASE IN INTRACELLULAR CALCIUM OF RAT NEONATAL CARDIAC MYOCYTES AND REDUCES THE FORCE OF CARDIAC CONTRACTIONS

C.V. Sobol, G.B. Belostotskaya, V.P. Nesterov, S.M. Korotkov

Sechenov Institute of Evolutionary Physiology and Biochemistry, RAS, Thorez 44, St.-Peterburg, 194223, Russia

$^{201}Tl^{+}$ is used in medicine as a radioisotope in clinical cardiology, heart imaging, for planar and SPECT imaging, myocardial perfusion and cellular dosimetry [Amin et al., 2006]. Thallium is also used in medicine in tumor imaging [Nadel, 1993; Abdel-Dayem et al., 1994]. The normal distribution of thallium within the body is choroid plexus of the lateral ventricles, lacrimal glands, salivary

glands, thyroid, myocardium, liver, spleen, splanchnic areas, kidneys, and testes. Thallium produces one of the most complex and serious patterns of toxicity known to humans, involving a wide range of organs and tissues. Because of the accumulation of Tl^+ in the myocardium, we investigated the effects of Tl^+ in cardiac cells. Many authors have investigated how Tl^+ affects total calcium in various tissues, but the dynamics of intracellular calcium in the cells after Tl^+ application has not been investigated. The aim of this work was to investigate the effects of Tl^+ on intracellular Ca^{2+} dynamics in rat neonatal cardiac myocytes and on force of cardiac contractions.

Female Wistar rats (250–300 g) were used in the research. Methods of cultivation and Ca^{2+} registration have been described in detail [Sobol et al., 2013]. During Ca^{2+} experiments in Ca^{2+}-free EGTA solution, all Ca^{2+} was replaced with 2 mM EGTA. $[Ca^{2+}]_i$ was measured using a computer analysis system for intracellular ion content (Intracellular Imaging & Photometry System, USA). Spontaneous contraction of frog atrium was registered as described earlier [Sobol et al., 2014].

Application of Tl^+ to cardiac myocytes led to an increase in $[Ca^{2+}]_i$. The effects of Tl^+ on $[Ca^{2+}]_i$ depended on the Tl^+ concentration and duration of Tl^+ application. 1mM Tl^+ did not initiate an increase in $[Ca^{2+}]_i$ in cardiomyocytes over at least 5 min. A concentration of 1.5 mM Tl^+ may induce an increase in $[Ca^{2+}]_i$ within 5 min. Inhibition of Ca^{2+} influx with Ca^{2+}-free EGTA solution prevented a sustained increase in $[Ca^{2+}]_i$. Therefore, the increase in $[Ca^{2+}]_i$ was due to the influx of Ca^{2+} across the plasmatic membrane, rather than due to a release of calcium from intracellular stores. Tl^+-induced increase in $[Ca^{2+}]_i$ was not inhibited by calcium-channel blocker, nifedipine. We observed that 1 mM Tl^+ exerted negative inotropic effects on spontaneous frog atrium contraction.

Being a K^+ surrogate, owing to a similarity in ion radii, Tl^+ belongs to the group of trace elements and lightly penetrates mammals through the skin and respiratory and digestive systems [Mulkey & Oehme, 1998; Korotkov, 2013; Rodriguez-Mercado & Altamirano-Lozano, 2013]. Thallium poisoning in humans was accompanied by tachycardia, hypertension, alopecia, and axonal neuropathy, detected as axonal loss and myelin degeneration, as well as distended mitochondria and vacuoles, swelling and fragmentation in peripheral nerve fibers and some chromatolytic changes in neurons of cranial nerves and spinal cord were found [Tanaka et al., 1978; Davis et al., 1981; Dumitru & Kalantri, 1990; Mulkey & Oehme, 1998]. Tl^+ increased the concentration of Ca^{2+} and Na^+ in isolated rat hepatocytes [Zierold, 2000]. The mechanistic basis of thallium toxicity is the ability of Tl^+ to replace K^+ in K^+-dependent biochemical processes, penetrating easily the inner mitochondrial membrane, releasing Ca^{2+} from intracellular compartments, and changing cell cycle regulation [Saris et al., 1981; Mulkey & Oehme, 1998; Zierold, 2000; Rodriguez-Mercado & Altamirano-Lozano, 2013].

In this study, we showed for the first time that Tl^+ stimulated the uncontrolled influx of extracellular calcium ions into the cardiac myocytes and exerted negative inotropic effects on spontaneous frog atrium contraction, thereby showing its toxic effect.

Work was supported by governmental grant for 2013–2017 years (N of state registration 01201351570). $[Ca^{2+}]_i$ was measured using of Research Resource Center equipment for the physiological, biochemical and molecular-biological studies (Sechenov Institute of Evolutionary Physiology and Biochemistry, the Russian Academy of Sciences).

EFFECT OF LACTOBACILLI AND THEIR METABOLIC PRODUCTS ON MYOCARDIAL CONTRACTILITY AND ON MITOCHONDRIAL MEMBRANE POTENTIAL

C. V. Sobol, S. M. Korotkov, V. P. Nesterov

Sechenov Institute of Evolutionary Physiology and Biochemistry, RAS, Thorez 44, St.-Peterburg, 194223, Russia

The prevalence of cardio-vascular diseases (CVDs) is increasing in magnitude across the globe and presents an immense burden to health care systems worldwide. It became obvious that there is a link between microbes and cardiovascular health [Sobol et al., 2011; 2013; 2014; Ettinger G et al., 2014; Rogler G, Rosano G, 2014; Kitai T et al., 2016]. The interaction of heart and gut, or heart-intestine axis [Sobol 2014], has emerged as a novel concept to provide new insights into the intricate mechanisms of CVDs [Nagatomo Y, Tang WH, 2015]. More and more data is evidencing about complex interdependence of intestinal and cardiovascular diseases [Rogler G, Rosano G, 2014; Kitai T et al., 2016]. Some intestinal diseases are reported to be associated with elevated risk of development of ischemic heart disease [Rogler G, Rosano G, 2014]. Some authors is considering chronic heart failure in complex with disorders of the gastrointestinal tract [Krack A., et al., 2005; Kitai T et al., 2016], at that the intestine microflora plays an important role [Rogler G, Rosano G, 2014; Sobol CV, 2014]. Disturbance of intestinal microflora is observed in 90% patients with cardiovascular diseases [Grinevich VB, Zakharchenko MM, 2005]. Also excessive bacterial growth and translocation of intestinal microflora lead to activation of systemic inflammatory response connected with pathogenesis of chronic heart failure [Arutyunov GP et al., 2004]. An association between infectious organisms and atherosclerosis has previously been postulated [Shah PK, 2001]. However anti-microbial therapy in preventing disease progression has been disappointing [Grayston JT, et al 2005].

Until recently, probiotic applications for cardiovascular health were limited to metabolic and diet-associated processes. An accumulating body of evidence has demonstrated that intervention of microbiota by a probiotic product can favorably affect cardiac morphology and function in nonhuman animals. Treatment with probiotics that contain the leptin-suppressing bacteria Lactobacillus plantarum led to the attenuation of ischemia-reperfusion injury in rats [Lam V, et al., 2012]. In addition, in a rat myocardial infarction model, probiotic administration (Lactobacillus rhamnosus GR-1) attenuated left ventricular (LV) hypertrophy and improved LV ejection fraction [Gan XT, et al., 2014].

We examined the influence of Lactobacilli, lipopolysacharides and new fermented probiotic product (PP) on the myocardial contractile force and on mitochondrial membrane potential. We used spontaneous contraction of circular atrium muscle isolated from heart of male frog Rana Redibunda. Mitochondria were isolated from rat heart and mitochondrial membrane potential was measured using safranin.

PP and lipopolysacharides were observed to exert positive inotropic effects on spontaneous frog atrium contraction. The contractile force remained high for approximately 2 h after wash-out, while, Lactobacilli may inhibit spontaneous frog atrium contraction. PP did not change mitochondrial potential. However, PP stimulated mitochondria respiration and exerted a mild uncoupling effect on electronic transport and oxidative phosphorylation in mitochondria [Sobol et al., 2013]. Additionally, PP and Lactobacilli increased in $[Ca^{2+}]_i$ in cardio-vascular cells and potentiated contraction of vessels in hyperpotassium solution [Sobol et al., 2011; 2013].

It is not excluded that PP may stimulate intracellular signaling cascades, which may increase the excitability of cardio-vascular cells. Demonstrating typical properties of mild uncoupler of mitochondrial oxidative phosphorylation [Sobol et al., 2014], PP may be considered as non-toxic cardioprotector. Since mild uncoupling is one of the main mechanisms of ischemic preconditioning at the cellular level and is quite important for cardioprotection [Minners J. et al., 2001].

Work was supported by governmental grant for 2013–2017 years (N of state registration 01201351570). $[Ca^{2+}]_i$ and mitochondrial membrane potential was measured using of Research Resource Center equipment for the physiological, biochemical and molecular-biological studies (Sechenov Institute of Evolutionary Physiology and Biochemistry, the Russian Academy of Sciences).

INTERRELATION BETWEEN PROTEOLYTIC ACTIVITY IN BASAL NUCLEI OF THE BRAIN AND MOTILITY OF RATS IN THE OPEN FIELD TEST UNDER THE CONDITIONS OF ALTERED PHOTOPERIOD

I.Yu. Sopova, V.V. Sheremet

Bukovinian State Medical University,
Teatralnaya pl. 2, Chernovtsy, 58002, Ukraine

Motility is a component of adaptive behavior. It is known that basal nuclei of the brain are involved in the organization of various forms of adaptive behavior. To this end, our goal was to investigate the changes in metabolic rate under the influence of the changed photoperiod, particularly proteolytic activity in these brain structures, and projecting of changes on the mobility of rats in the open field test.

The research was executed on the 48 juvenile male rats. For the study were extracted: the caudate nucleus, globus pallidus, accumbens, the amygdala. The state of proteolysis was evaluated based on the reaction with azo compounds. At the same time the intensity of proteolysis by azoalbumin and azocasein was determined. In the open field within 3 minutes the next parameters were registered: horizontal activity, vertical locomotor reactions, mink reflex. The animals were contained during one week in conditions of usual (natural conditions of illumination) and altered (constant darkness, constant light) photoperiod after preliminary passage of the open field test. Then the behavior of animals was studied again in the open field.

Research has shown that the physical activity of rats in the darkness was declined: the horizontal activity in 2.3 times ($F_{1,12}$=90,24, p=0,00001), vertical movements in 3.7 times ($F_{1,12}$=76,56, p=0,000001), mink reflex in 2-fold ($F_{1,12}$=30,27, p=0,0001). Reduced mobility of the animals in the dark was supplemented by decreasing of proteolytic activity in basal nuclei: in accumbens the casein lysis decreased by 32,9% ($F_{1,12}$=27,41, p=0,0002), in the caudate nucleus the albumin lysis decreased by 26.4 % ($F_{1,12}$=22,28, p=0,0005).

The correlation parameters of locomotor activity with previous data were changed in animals that were in the continuous light: horizontal locomotion increased in 1.5 times ($F_{1,12}$=44,42, p=0,00002) and vertical activity decreased in 1.7 times ($F_{1,12}$=17,47, p=0,013). Increased motor activity was associated with an increase in the activity of enzymes that degrade casein: in the pallidum on 11,4% ($F_{1,12}$=21,83, p=0,0005) and the amygdala on 16,2% ($F_{1,12}$=7,33, p=0,019); lysis of albumin was increased in accumbens on 22,1% ($F_{1,12}$=6,72, p=0,024).

Thus, it may be concluded that altered photoperiod simulates the functional state of basal nuclei, which in turn affects the mobility of animals.

EVALUATION OF HUMAN SKELETAL MUSCLE VS. LIQUID BIOPSIES FOR EARLY DETECTION OF INSULIN RESISTANCE

A.V. Stepanova, K.O. Koksharova, A.Yu. Mayorov, A.V. Vorotnikov, V.A. Tkachuk

Faculty of Fundamental Medicine, Lomonosov Moscow State University, Moscow, 117192; Russian Endocrinology Research Center, Moscow, 117036, Russian Cardiology Research Center, Moscow 121552, Russia

Insulin resistance (IR) is a common pathophysiological condition characterized by higher than normal concentration of insulin required to exert biological effects in target tissues such as skeletal muscle, fat and liver. IR is a major public health issue; it is frequently associated with major diseases, including obesity, type 2 diabetes mellitus (T2DM), increased cardiovascular risk and atherogenic dyslipidaemia. The early insulin resistance is a reversible stage in the pathogenesis of T2DM, otherwise it leads to hyperinsulinemia and delayed sequela. Thus, the development of tools to quantify insulin sensitivity/resistance has been the aim of many studies. There are many various clinical measurements by which IR can be estimated in individuals and in population studies, but all of

them are either not accurate enough or too complex and resources/cost consuming (e.g. hyperinsulinemic-euglycemic clamp). Ranging from just a single fasting blood sample for simple indices, such as the HOMA or QUICKI, to elaborated gold-standard hyperinsulinaemic–euglycaemic clamp test, these methods are nonetheless imperfect and indirect reflecting the pathological changes in target tissues.

Reliable and affordable diagnostic methods for early insulin resistance in target tissues are yet to be developed. The basis for the development of new methods may be to study features of change in muscle tissue of patients with T2DM and other metabolic disorders. In the early stages of development of the type 2 diabetes impaired glycogen synthesis in muscle is the primary defect responsible for the insulin resistance. The initial step in muscle glucose metabolism involves activation of the glucose transport system, leading to influx of glucose into insulin target tissues. The free glucose that has entered the cell is then metabolized by a series of enzymatic steps under insulin control.

Normally, insulin promotes glucose uptake by skeletal muscle and fat cells by activating intracellular signaling downstream of insulin receptor. The key molecules of this pathway are insulin receptor substrate (IRS), phosphatidylinositol (PI)-3 kinase, and Akt kinase, which relays the signal via AS160 (160 kDa Akt substrate) and Rab GTPase to exocytotic machinery. This triggers vesicle fusion and exposure of glucose transporter type 4 (GLUT4) to facilitate the glucose uptake. Many studies have consistently demonstrated that insulin resistance is associated with defects in insulin signaling at the IRS level. In contrast to tyrosine phosphorylation needed for insulin signal transduction, IRS has been identified as a target for inhibitory phosphorylation by several Ser/Thr-kinases that block IRS function and results in less activation of Akt and glucose transport. Thus, phosphorylation level of IRS and Akt at specific Ser/Thr residues may serve as potential markers of insulin resistance.

We aim to find whether Ser/Thr-phosphorylation of IRS and Akt is detectable in biopsy material of (pre)diabetic patients and correlates to their body mass index (BMI) and the extent of insulin resistance. The skeletal muscle (vastus lateralis) biopsies of approximately 10-15 mg of wet mass are obtained by the standard needle technique from the patients that have been categorized by BMI and insulin resistance measured by hyperinsulinemic-euglycemic clamp. In addition, the liquid biopsies are taken as the blood samples and immediately processed for leukocyte isolation. We attempt to determine if insulin signaling in these cells displays same abnormalities as in skeletal muscle of diabetic patients. Thus, mononuclear cells are separated and appropriately fixed for a further analysis by flow cytometry and western blots. Here we will present the current results and discuss their relevance and clinical applications.

Supported by RCF grant 14-35-00026.

EXPERIMENTAL SUBSTANTIATION OF STEM CELLS DELIVERY TO THE BRAIN THROUGH CEREBRAL NERVES ENDINGS

Yu.P. Stukach[1], Yu.G. Shanko[2], V.A. Kulchitsky[1]

[1]*Institute of Physiology, National Academy of Sciences of Belarus, Akademicheskaya Str. 28, Minsk, 220072, Belarus*

[2]*Republican Scientific and Practical Center of Neurology and Neurosurgery, Ministry of Health of the Republic of Belarus, Skaryna Str., 24, Minsk, 220114, Belarus*

Brain traumas and their treatment still remain an unsolved problem in the whole world. Scientists try to solve this problem using stem cell therapy in recent years. Stem cells administration into different parts of bloodstream or cerebrospinal fluid pathways is well known [1–4]. These techniques have some limitations, namely the risk of homeostasis impairment, when stem cells are introduced to internal milieu from outside. The technique of intracentral (directly into brain tissue) stem cells administration is used to overcome scattering of implanted cells, but it is accompanied with increased trauma (skull trepanation) [2,4]. Therefore, the time is ripe for development of more effective technique of stem cells implantation, based on their natural migration into the brain from different parts of peripheral nervous system.

Taking into account the ability of stem cells to migrate to damaged area as well as the presence of perineural tracing along central projections of cranial nerves [3] and topography of major nerve endings and ganglia inside skull one can define a hypothesis of targeted migration of stem cells introduced into receptive fields of olfactory and trigeminal nerves to different brain areas of anterior and posterior cranial fossae.

Materials and Methods

White mature rats weighing 220–300 g were used for experiments. Mesenchymal stem cells (MSC) were isolated from adipose tissue of female rats weighing 300–350 g and cultivated using Dulbecco's Modified Eagle's Medium with low glucose content and 10% fetal calf serum for 8–10 days for cell mass gain. The cells were stained with PKH67 Green Fluorescent Cell Linker at the operation day. The final concentration of cells was 700 thousand cells per 1 ml. The operation of brain injury modelling (2–3 mm2 of brain tissue removing with micropipette) was made on anesthetized rats.

5 groups of animals were formed: unilateral injury of sensorimotor zone with intranasal administration of MSC (group 1, n=8); bilateral injury in sensorimotor zone with intranasal administration of MSC (group 2, n=6); unilateral cerebellar injury with ipsilateral administration of MSC into Meckel cavity (group 3, n=6); unilateral cerebellar injury and contralateral administration of MSC into Meckel cavity (group 4, n=6); bilateral cerebellar injury and unilateral administration of MSC into Meckel cavity (group 5, n=6). Brain tissue aspiration from anterior cranial fossa was performed in sensorimotor zone (2.5 mm lateral from midline, 2.5 caudal to bregma and 2.5 mm from brain surface). Injury in posterior cranial fossa was made at the

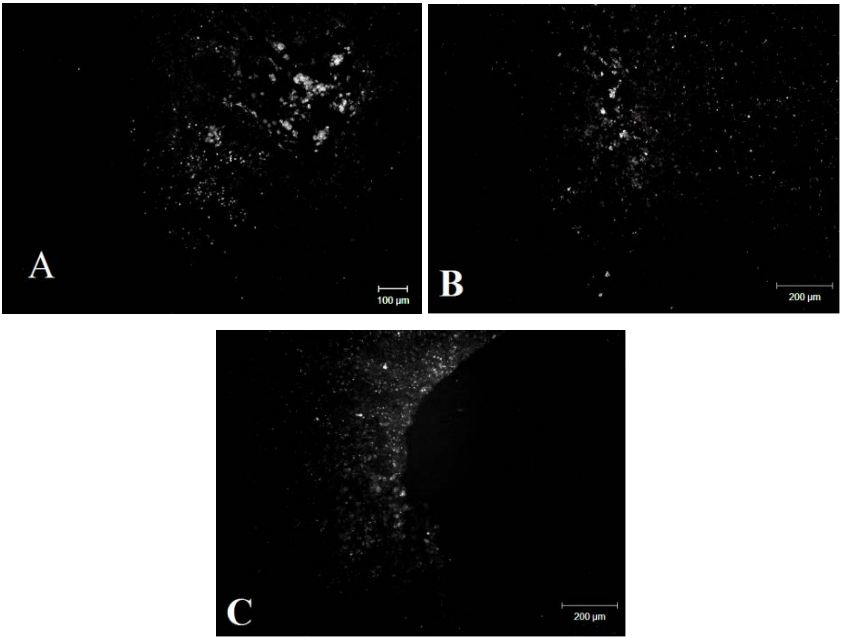

Fig. 1. Fluorescent cells in 10 days after unilateral destruction of precentral gyrus in right hemisphere (A), and after bilateral destruction of precentral gyrus in left (B) and right (C) hemispheres.

level of cerebellar cortex (2.0 mm lateral from midline, 1.5 caudal to lambda and 2.5 mm from brain surface). 50 µl of cell suspension (35 thousand cells) was injected under nasal mucosa of animals or into Meckel cavity in 10 days after local destruction of brain regions. Longitudinal sections of brain (8 µm in thickness) were made using cryostat in one, three, five and ten days after the operation and studied using fluorescent microscope.

Results and Discussion

Fluorescent cells were detected both in olfactory bulbs and around the damaged sensorimotor brain area as well as caudal parts of brain stem and damaged cerebellar region (in the form of areola) in 1 day after the implantation. The amount of fluorescent cells increased in the damaged areas of anterior and posterior cranial fossae in three-five days after injury modelling. Large clusters of fluorescent cells were detected in damaged areas in ten days after stem cells implantation, some of them penetrating deep into damaged tissue, but the majority surrounding it (figs 1,2).

It was found that intranasally administered stem cells migrated generally to anterior cranial fossa, while mesenchymal cells from Meckel cavity – to posterior one.

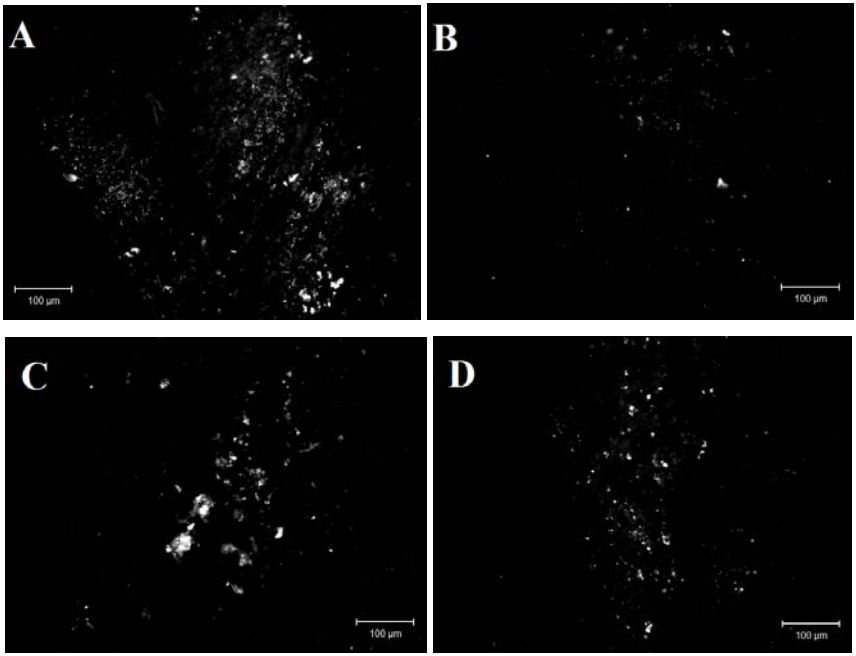

Fig. 2. Fluorescent cells in 10 days after unilateral destruction of cerebellar cortex region and ipsilateral administration of stem cells into Meckel cavity (A), after unilateral destruction of cerebellar cortex region and contralateral administration of stem cells into Meckel cavity (B), after bilateral destruction of cerebellar cortex region in left (C) and right (D) hemispheres.

The tracing analysis of intranasally administered stem cells did not reveal fundamental differences between the amount of cells reaching damaged sensorimotor areas of left and right cerebral hemispheres (fig. 1).

Efficiency of ipsi- and contralateral migration of stem cells from Meckel cavity differs (fig 2A,B). Priority of ipsilateral migration began to appear at 5^{th} day after the operation. That effect was present at 10^{th} day of the experiment. Bilateral injury also showed the same priority of ipsilateral tracing compared to contralateral one (fig 2C,D).

Therefore, the hypothesis of use of stem cells natural migration from receptive fields of olfactory and trigeminal nerves to anterior or posterior cranial fossae was proven. Intranasally administered stem cells were spread out mainly in anterior cranial fossa, while the cells implanted into Meckel cavity – in the tissues of posterior one.

References

1. Andrade C. Intranasal drug delivery in neuropsychiatry: focus on intranasal ketamine for refractory depression. J. Clin. Psychiatry. 2015. Vol. 76, No 5. P. 628-631.

2. Li Y.H., Feng L., Zhang G.X., Ma C.G. Intranasal delivery of stem cells as therapy for central nervous system disease. Exp. Mol. Pathol. 2015. Vol. 98, No 2. P. 145-151.
3. Ninomiya K., Iwatsuki K., Ohnishi Y., Ohkawa T., Yoshimine T. Intranasal delivery of bone marrow stromal cells to spinal cord lesions. J. Neurosurg Spine. 2015. Vol. 23, No 1. P. 111-119.
4. Wei Z.Z., Gu X., Ferdinand A., Lee J.H., Ji X., Ji X.M., Yu S.P., Wei L. Intranasal delivery of bone marrow mesenchymal stem cells improved neurovascular regeneration and rescued neuropsychiatric deficits after neonatal stroke in rats. Cell Transplant. 2015. Vol. 24, No 3. P. 391-402.

A CYLINDRICAL MODEL OF THE LEFT VENTRICLE AND ITS APPLICATION TO THE ANALYSIS OF HEART PERFORMANCE

F.A. Syomin, M.V. Zberia

Institute of Mechanics, Moscow State University,
Mitchurinsky prosp. 1, Moscow, 119992, Russia

The model of the left ventricle of the heart used here is an improved version of our earlier model [1,2]. The ventricle was approximated by a thick-walled cylinder that consisted of myocardial (cardiac muscle) tissue [1]. We considered myocardium to be incompressible anisotropic material in which axes of anisotropy were specified by the orientation of muscle fibers. We supposed the fibers to be aligned along helices with helical angle changing linearly from sub-endocardium to sub-epicardium. Only radial, axial and twist deformations were allowed. Stress-strain relations were specified by isotropic properties of myocardium and forces generated by muscle fibers. Those forces included the passive stress of elastic protein titin and active forces of muscle contraction. We defined the last ones with our kinetic model of cardiac muscle contraction and its regulation [3,4]. In the absence of inertial forces the one-dimensional model was set by the only equilibrium equation and boundary conditions, which are presented in detail in [1], and by ordinary differential equations of the kinetic model, which were written down for the model variables considering their dependences on radial coordinate. A blood circulation of the model was initially (ref. [1]) defined by a simple null-dimensional windkessel model.

The complete model described quite well the time-courses of its main hemodynamical and geometrical parameters. It also gave some explanation of the role of fibers orientation in cardiac muscle and reproduced changes in the ventricle geometry in some cases of simulated cardiomyopathies in which contractile properties of muscles were disturbed [1]. However, the model had some inconsistencies in description of the heartbeat hemodynamics. In particular, the end of the outflow from the ventricle occurred at the moment when the ventricular pressure reached its maximum. Therefore we have improved the hemodynamic model in accordance with [5] introducing several parts of arterial bed with different elastic properties of their walls and different values of flow and inertial resistance. Another improve-

ment was that we had taken into account the inertial resistance of aortic valve. A final system of hemodynamic equations is as follows:

$$L_i \frac{dO_i(t)}{dt} + R_i O_i(t) = P_V(t) - P_{LV}(t),$$

$$L_{o1} \frac{dO_{o1}(t)}{dt} + R_{o1} O_{o1}(t) = P_{LV}(t) - P_{A1}(t),$$

$$L_{o2} \frac{dO_{o2}(t)}{dt} + R_{o2} O_{o2}(t) = P_{A1}(t) - P_{A2}(t),$$

$$C_{A1} \frac{dP_{A1}(t)}{dt} = Q_{o1}(t) - Q_{o2}(t),$$

$$C_{A2} \frac{dP_{A2}(t)}{dt} = Q_{o2}(t) - \frac{P_{A2}(t) - P_V(t)}{R_{per}} - \frac{P_{A2}(t) - P_C(t)}{R_C},$$

$$C_C \frac{dP_C(t)}{dt} = \frac{P_{A2}(t) - P_C(t)}{R_C},$$

$$C_V \frac{dP_V(t)}{dt} = \frac{P_{A2}(t) - P_V(t)}{R_{per}} - Q_i(t).$$

Here P_{LV}, P_{A1}, P_V, P_{A2} и P_C are pressures in the left ventricle, aorta, pulmonary veins, and other parts of arterial bed respectively; Q_i, Q_{o1}, Q_{o2} are inflow through the mitral valve, and outflows through different parts of major arteries; R_{per}, R_i, R_{o1}, R_{o2}, R_C are peripheral resistance, resistances to ventricular inflow and outflow, and viscous component of arterial compliance; L_k and C_k are inertial resistances and compliances of referenced parts of the vascular bed.

A numerical simulation of a heartbeat by the improved model [2] reproduces time-course of model hemodynamical parameters much more correctly than the initial model [1]. The results are shown in fig. 1.

The ventricle model with the new model of hemodynamics was used for simulation of ventricular performance at various values of preload (end-diastolic ventricular pressure) and afterload (peripheral resistance) [2]. Results of the simulation were in accordance with known experimental data. In particular, during examination of the dependence on preload the model reproduced the Frank-Starling law of heart: the stroke volume increased with the increase in the end-diastolic pressure. On the other hand, the stroke volume weakly depended on an increase in peripheral resistance.

We have also applied the model to the numerical simulation of aortic valve stenosis and its insufficiency. For that purpose we introduced quadratic resistance term into the differential equation for ventricular outflow and considered dependence of inertial and flow resistances on relative open area of aortic valve:

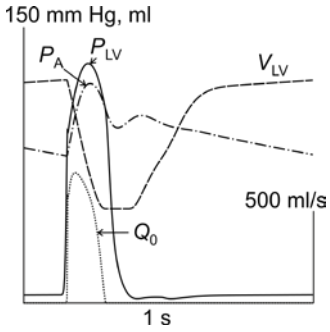

Fig. 1. A time course of hemodynamical parameters of the model during a heartbeat. The left scale is for ventricular and arterial pressures as well as for the volume of the ventricle (VLV). The right one is for ventricular outflow.

$$L_{o1}\left(\frac{S}{S_0}\right)\frac{dO_{o1}(t)}{dt}+R^{a}_{o1}\left(\frac{S}{S_0}\right)O_{o1}(t)+R^{B}_{o1}\left(\frac{S}{S_0}\right)O_{o1}(t)\left|O_{o1}(t)\right|=P_{LV}(t)-P_{A1}(t).$$

It is shown that the decrease in the relative open area during the simulation of stenosis results in the significant increase in the maximal ventricular pressure and the decrease in stroke volume. Under condition of insufficiency of the valve the increase of regurgitant orifice area results in the increase in end-diastolic ventricular pressure and stroke volume while the system blood flow reduces. Results of the numerical simulation are shown in figs 2,3.

In conclusion, the model adequately reproduces the dependencies of the performance of the ventricle on pre- and afterload as well as provides good qualitative description for some heart diseases, namely, aortic valve stenosis and its insufficiency.

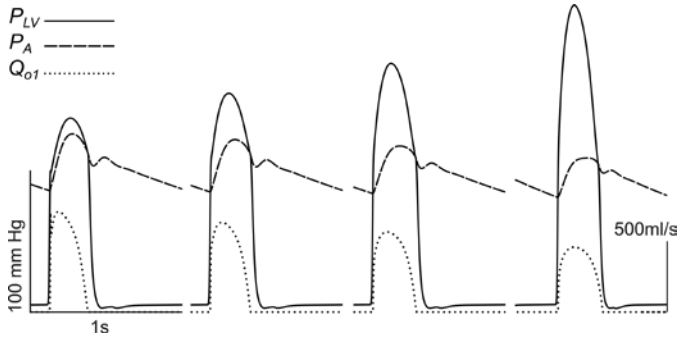

Fig. 2. A time course of hemodynamic parameters in the case of stenosis of aortic valve. Relations of maximal open area of aortic valve to its area are 1, 0.55, 0.4, 0.28, from left to right. The left scale is for ventricular and arterial pressures. The right one is for ventricular outflow.

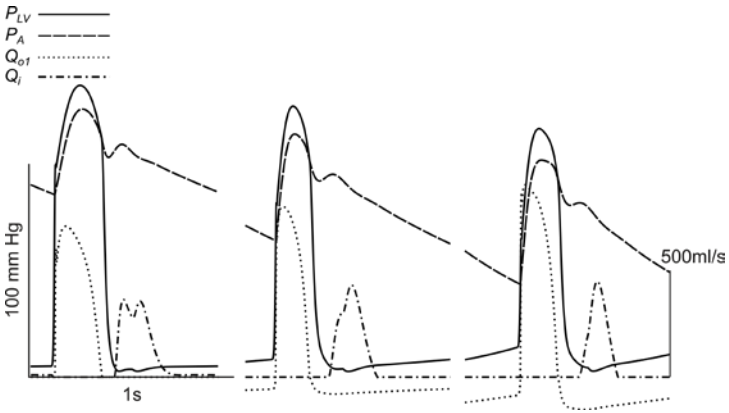

Fig. 3. A time course of hemodynamic parameters in the case of insufficiency of aortic valve. Relations of the regurgitant orifice area of aortic valve to its total area are 0, 0.1, 0.15, from left to right. The left scale is for ventricular and arterial pressures. The right one is for ventricular inflow and outflow.

The work is supported by RFBR grants 16-04-00693, 15-04-02174, and by RSF grant 14-35-00005.

References

1. F. A. Syomin, A. K. Tsaturyan, Doklady Biochemistry and Biophysics, 2015, V. 462 (1), pp. 158-162.
2. F. A. Syomin, M. V. Zberia, N. A. Koubassova, A. K. Tsaturyan, Biophysics, 2015, V. 60 (6), pp. 983-987.
3. F. A. Syomin, A. K. Tsaturyan, Biophysics, 2012, V. 57 (5), pp. 651-657.
4. F. A. Syomin, Biophysics, 2014, V. 59 (5), pp. 772-779.
5. Burattini R., Gnudi G., Med. Biol. Eng. Comput., 1982, V. 20 (2), pp. 134-144.

THE INFLUENCE OF SUCCINATE AMMONIUM ON AEROBIC WORK OF ATHLETES

R.V. Tambovtseva, O.S. Zhumaev, I.S. Walter

Russian State University of Physical Culture, Sport, Youth and Tourism, Lilac boulevard, 4, Moscow, 105122, Russia

Currently, the search for new ergogenic tools to enhance athletic performance, development of endurance, speed-strength, speed up recovery processes, extension of sports longevity, maintaining the health of athletes practicing is a very urgent task. Of greatest interest in this regard is succinic acid and salts of succinic acid. This metabolite is the subject of many papers, the most important is the research of M.N Kondrashova school [1–5]. According to M.N. Kondrashova research, succinic acid has antioxidant, antihypoxic, antiatsidoticheskim and membrane-stabilizing effect. Human body, in the course of various metabolic transformations, generates a lot of endogenous succinic acid. Meanwhile, the question on the impact of small amounts of exogenous succinic acid on metabolic processes

arises. Succinic acid – is a weak acid and its rate of passage through the membrane of mitochondria is very low. It is known, that the succinic acid formed in the mitochondria is quickly used by the very same mitochondria and does not go beyond it (with the exception of damaged mitochondria). Succinic acid appears in the bloodstream in the case of hypoxic conditions or the absence of oxygen. This is a serious signal response of the body, which warns about the lack of energy and the oxygen starvation. Such processes are often associated with physical exertion particularly in anaerobic conditions. The subject of our study was to investigate the effect of small doses of exogenous succinate on the possibility of expanding the aerobic performance of athletes and on preventing premature deployment of anaerobic glycolytic process.

Purpose of the study

To study the influence of ammonium succinate on high qualification athletes' aerobic performance.

Methods and Organization of Studies

The study was conducted on the basis of laboratory of bio-energy muscle activity at the Department of Biochemistry and Bioenergetics of sport named after N.I. Volkov. The experiment was carried out with no risk to human health, in compliance with all the principles of humanity and ethics (Helsinki Declaration of 2000, the European Community Directive 86/609). The experiment was attended by 22 sportsmen of high qualification (weightlifters, wrestlers, cyclists, footballers). 30 minutes before the step-load increase test on the cycle ergometer, the tested sportsmen once per os got the standard dose of ammonium succinate (30 mg per 1 kg of body weight) (by the decision of the State Committee for Sanitary and Epidemiological Supervision of the Russian Federation the drug is approved for use as a food supplement (SanPiN 2.3.2. 1078-01). We detected indices performed power, time, heart rate, respiratory parameters: oxygen consumption, respiratory rate, pulmonary ventilation, respiratory rate, the percentage of oxygen utilization.

The study results are statistically processed by programme Statistica 6.0 and by built-in analysis function in the program Microsoft Excel 2007.

Results and discussion

The value of the threshold of anaerobic metabolism (ANSP) was determined by the method of specialized program V-slope, by a graphical method of the ratio VE / VO2 and VE / HR.

Analysis of the data showed a significant increase of the number of parameters that characterize the anaerobic threshold. It is demonstrated, that the use of the succinic acid promoted a significant increase of the absolute and relative power of the anaerobic threshold at 29 W (17.5%) and 0.35 W/kg (16.1%), respectively. Considering the indicator, which characterizes the activity of the cardiovascular system (heart rate ANP), we can note a tendency to increase the value of this parameter after administration of succinic acid. Differences between the values of the absolute and relative indices ANP PC obtained after the experiment from "control group" (2.3 l/min and 28.6 ml/min/kg, respectively) and from "experimental

group" (2.7 l/min and 33.8 ml/min/kg respectively) are authentic. Furthermore, there was a significant increase in value (p <0.05) of absolute and relative PC ANP indicators after the treatment at 0.26 l/min (12.2%) and 2 ml/min/kg (7%), respectively. It was noted that the function of external respiration increased slightly – by 2 respiratory acts, but the pulmonary ventilation increased significantly on 12 l/min, which makes 22% increase after the intake of succinic acid. Significant, 4% increase in respiratory exchange ratio (RER) shows the relation between carbon dioxide gas and oxygen consumption. Increasing RER greater than unity, results from the formation of "Non-metabolic excess" of carbon dioxide due to the activation of anaerobic glycolysis and neutralization of moved into blood hydrogen ions (H^+) with the producing of carbon dioxide. The emergence of "Non-metabolic surplus" of CO_2 leads to a sharp increase in pulmonary ventilation and to reduction of the efficiency of the respiratory system. According to this indicator one can indirectly judge the activation of anaerobic glycolysis. Our research shows that as a result of taking the salt of succinic acid the process of anaerobic glycolysis occurs later. The percentage of oxygen utilization at anaerobic threshold was significantly reduced (by 8.9%), which is characterized by greater sensitivity to oxygen by the body and lower content of oxygen in the exhaled air.

Following the method of the step test, the work was being provided by the athlete up to his failure to continue and in this case, there is a tendency of increasing for work time. On average, the work duration of the group increased by 28 s (4%).

When considering the absolute and relative IPC W there was detected an increase of this indicator after taking the drug, but no significant differences were found. At the same time there is a significant increase of 2.8% (p <0.05) of the absolute performance of the IPC, meanwhile the relative IPC remains unchanged. In addition, a trend of increasing the maximum heart rate is revealed. The situation with lung function is similar situation to that recorded at the level of the anaerobic threshold: respiratory rate slightly increased by 3 respiratory acts, but it significantly increases the pulmonary ventilation of 14 l/min, which is 12% increase after administration of succinic acid salts. Due to the increasing of the oxygen consumption at the anaerobic threshold and stable BMD, significantly by 9% (p <0.05) increased the percentage of consumption relative to the maximum oxygen consumption. From the results of the study one can see that the change in the percentage of utilization of oxygen takes a significant decrease of 8.7%, which is characterized by greater sensitivity to oxidant by the body and lower content of oxygen in the exhaled air.

Conclusions

1. A single injection of the drug succinate ammonium has a positive effect on aerobic performance of athletes of high qualification.

2. Use of the drug succinate ammonium contributed to significant increase in absolute and relative power of the anaerobic threshold.

3. As a result of the drug salt of succinic acid intake, process of anaerobic glycolysis occurs later.

4. Within the test load there is a tendency of an increase of the work time.

5. Due to the increase of oxygen consumption at the anaerobic threshold and stable BMD significantly increased the percentage of consumption relative to the maximum oxygen consumption.

References

1. Majewski E.I., Grishin E.V., Rosenfeld A., Zyakun A.M., Kondrashova M.N., Vereshchagin Anaerobic formation of succinate and facilitate its oxidation - Possible mechanisms of cell adaptation to hypoxia // Biophysics. - 2000. - V. 45. - № 3. - S.509 - 513.
2. Majewski E.I. Correction of metabolic acidosis by maintaining mitochondrial function / A. Rosenfeld, Grishin EV Kondrashov MN - Pushchino, 2001. - 155 p.
3. Sand A.B., Majewski E.I., Teacher M.L., Kondrashov M.N. Placebo-controlled study sympathicotonic effects of dietary supplements on the basis of succinic acid salts // Biomedical Journal. - 2005 - 6 T - S. 508 - 514.
4. Severin E.S. Biochemistry: the textbook. - Moscow: GEOTAR Media, 2014. - 759 p.
5. The therapeutic effect of succinic acid / ed. M.N. Kondrashova - Pushchino, 1976. - 234 p.

FUNCTIONAL ALTERATIONS OF VASCULAR SMOOTH MUSCLE IN RATS WITH ANTENATAL AND EARLY POSTNATAL HYPOTHYROIDISM

O.S. Tarasova, D.K. Gaynullina. S.I. Sofronova, E.K. Selivanova, D.S. Kostyunina, A.A. Shvetsova, A.A. Borzykh, A.A.Martyanov

SRC RF Institute for Biomedical Problems RAS and Faculty of Biology, Lomonosov Moscow State University, Moscow, Russia

Thyroid hormones are key regulators of the developmental processes. Their deficiency during early stages of development (prenatal and early postnatal) delays growth and functional maturation of different body systems, including cardiovascular system. However, hypothyroid-associated alterations of vascular smooth muscle during early postnatal period are poorly understood and their mechanisms are not explored at all. We hypothesized that the deficiency of thyroid hormones in antenatal and early postnatal periods will affect the regulation of contractile responses in arteries of young progeny, in particular, by affecting smooth muscle cell differentiation processes as well as Rho-kinase pathway activity (this pathway is particularly important for vasomotor control in perinatal age).

To test this hypothesis we used the model of antenatal and early postnatal hypothyroidism. Dams were treated with propylthiouracil (PTU) in drinking water (0.0007%) during the whole gestation period and two weeks after delivery. Two-week-old male offspring from dams treated with PTU (PTU group) in comparison with the control offspring demonstrated a marked reduction of thyroid hormones in the blood: total T_4 concentration was reduced by 79%, free T_4 – by 87%, total T_3 – by 94% and free T_3 – by 68%. Blood concentration of thyroid stimulating hormone was compensatory increased by 50 times in PTU group compared to the control.

Vasoregulatory effects of thyroid deficiency in 2-week-old offspring were studied using small mesenteric arteries, where we measured: (i) contractile re-

sponses to α_1-adrenoceptor agonist methoxamine (wire myography); (ii) mRNA contents of actin isoforms (markers of smooth muscle cell maturation), RhoA (Rho-kinase activator) and CPI-17 (one of Rho-kinase targets) (qPCR); and (iii) the content of Rho-kinase α protein (Western Blotting).

The isometric contractility (maximum active force) of the vascular wall was smaller in arteries of PTU group in comparison to the control group. Maximum active force is mainly determined by the thickness of smooth muscle layer in the wall. Along with that, the contractility of developing arteries is known to depend on the maturity of their contractile apparatus. Vascular smooth muscle differentiation is marked by the switch of actin isoforms expression, so that β-actin is replaced by smooth muscle α-actin. In mesenteric arteries of PTU rats the ratio of α-actin mRNA to β-actin mRNA was two-fold smaller compared to that in control rats.

To evaluate the role of Rho-kinase in the regulation of contraction in control and PTU rats we used Rho-kinase inhibitor Y27632 (3 μM). Incubation with Y27632 significantly reduced the contractile responses to methoxamine in both groups. However, the effect of Y27632 was more prominent in PTU group compared to control, which indicates an increased contribution of Rho-kinase to the regulation of arterial contraction. The increased functional role of Rho-kinase in mesenteric arteries of PTU rats was observed along with elevated Rho-kinase protein content and elevated level of CPI-17 mRNA, while the level of RhoA mRNA was similar in both groups.

In conclusion, our data show that antenatal and early postnatal hypothyroidism delays vascular smooth muscle cells differentiation and augments the functional role of Rho-kinase in small mesenteric arteries. Notably, the increased activity of Rho-kinase pathway is a hallmark of various cardiovascular pathologies. In this study, we demonstrated, for the first time, its association with antenatal and early postnatal hypothyroidism.

Supported by the Russian Science Foundation (Grant N 14-15-00704).

ROLE OF CALCINEURIN AND ADENOSINE RECEPTORS IN REGULATION OF ACETYLCHOLINE RELEASE IN MOUSE NEUROMUSCULAR JUNCTIONS

E.O. Tarasova, A.S. Miteva, A.E., Gaydukov, O.P. Balezina

Moscow State University, Leninski Gory, Moscow, Russia

Evoked acetylcholine (ACh) release in peripheral mouse neuromuscular junctions (NMJs) depends on elevation of intracellular calcium concentration. The main source of calcium is the influx through P/Q-type calcium channels [1]. Under certain conditions acetylcholine secretion can be enhanced, for example, when L-type calcium channels are being activated. Normally they do not contribute to ACh release in mammalian NMJs and stay in a “silent” state [2,3].That arises the question what the functional mechanisms of the inhibition of this calcium input are.

As it has been shown in our previous research, L-type calcium channels of the mouse NMJ are being continuously downregulated by a Ca^{2+}/CaM-dependent

phosphatase – calcineurin (CaN). Therefore it is of particular interest, whether a counteracting enzymatic influence on L-type calcium channels exist.

One of the kinases known for their ability to upregulate L-type calcium channel activity in different cell types is PKA [4,5]. The activity of this kinase is calcium-independent, but may be altered by signalization from two main types of metabotropic adenosine receptors present on the nerve terminal of mice: A1 and A2A-receptors [6,7]. This could be a way to link the metabolic needs of the nerve cell and intensity of ACh release.

Our work was focused on unraveling the relative roles of adenosine signalization through its specific receptors (A1- and A2A-type) and calcineurin in L-type calcium channel regulation, resulting in changes of ACh secretion.

Methods

Experiments were conducted on "cut" mouse diaphragm preparations. We registered both spontaneous and evoked (50 Hz) activity of NMJs in form of miniature end plate potentials (mEPP) and short trains of end plate potentials (EPP) respectively using standard microelectrode technique of biopotential registration. EPP amplitude was corrected for nonlinear summation. Quantal content of the EPPs was calculated as following: A (EPP)/A(mEPP), A(EPP) – corrected EPP amplitude, A (mEPP) – mEPP amplitude. Statistical analysis of the obtained data was performed using the Student's *t*-test or Mann-Whitney criterion. Difference between sample means was considered significant at $p<0,05$ (n – number of studied synapses).

Results and discussion

In our previous work we showed that calcineurin downregulates evoked transmitter release in mouse neuromuscular junctions [8]. We sought to find endogenous ways to overcome this calcineurin-mediated effect – either by diminishing the activity of this phosphatase, or by strengthening the possible counteracting influences on its targets.

Since it is widely known that calcineurin activity depends as well as on Ca^{2+}, as on CaM levels, we decided to investigate the effects of a blocker of CaM – W-7 (10 μM) on ACh release. Surprisingly we did not see any change in synaptic activity upon W-7 application. Neither EPP amplitude, nor QC were different from control levels. This might be due to the wide involvement of CaM in different kind of processes, not only CaN activity regulation, so that inhibition of this molecule might result in masked effects of CaN inactivation. But this might also indicate that blocking CaM by W-7 doesn't result in any changes of CaN activity, indicating that in mouse nerve terminals a persisting CaM-independent activity of calcineurin exist. In crayfish neuromuscular junctions a tonic activity of CaN was the result of its partial proteolysis by calpain – a calcium-dependent proteinase – leading to the production of Ca^{2+}/CaM-independent forms of CaN [9]. Therefore we tested whether calpain inhibition would lead to changes in the quantal secretion of ACh in mammal NMJs.

Calpain inhibitor PD150606 (100 μM) lead to an about 32% increase in QC of every single EPP in train, while mEPP amplitude and frequency remained at

control level (mEPP amplitude: 1,00±0,06 mV (n=22) in control and 1,11±0,08 mV (n=19, p<0,05) after PD150606 application; mEPP frequency: 1,02±0,17 Hz in control and 1,43±0,23 Hz after PD150606 treatment). This increase was comparable with the potentiating effect (also about 30%) of CaN inhibitors on evoked ACh release.

Combined with our findings that CaM inhibition doesn't affect neuromuscular transmission, this leads us to the suggestion that the presynaptic activity of calpain in mouse NMJs might be directed on calcineurin, leading to the appearance of a tonically active, CaM-independent form of this phosphatase.

But because of the wide range of calpain substrates the long-lasting effects of its inhibition on NMJ function still remain a matter of investigation.

Another way of ACh release potentiation without altering the activity of CaN itself might be due to strengthening counteracting influences on common targets. Previously we established that one of CaN targets are L-type calcium channels, which are being continuously downregulated by this phosphatase. Upregulation of L-type calcium channel activity, for example through phosphorylation by PKA, might lead to increased ACh release.

Inhibition of PKA activity by H-89 (1 μM) didn't cause changes neither in spontaneous, nor in evoked activity of mouse neuromuscular junctions. Thus, basal PKA activity doesn't contribute to ACh release regulation. This might be due to the fact that its main target seem to be L-type calcium channels, which normally do not participate in transmitter release regulation in NMJs of mice. So we tried to attenuate PKA activity through changes in basal adenosine signalization.

Blocking A2A-receptors with ZM241385 (1 μM) had no effect on EPP QC and the form of the EPP train. This could be a basis for the conclusion, that A2A-receptors do not play a role in transmitter release regulation in mouse NMJs. Nevertheless, ZM241385 application prevents transmitter release potentiation mediated by a CaN inhibitor – CsA (1 μM). In other words, continuous activation of A2A-receptors by endogenous adenosine is necessary for increased ACh release during CaN inhibition and calcium influx through L-type calcium channels.

A2A-receptor agonist CGS-21680 (1 μM) application lead to an 28% increase in EPP QC, thus providing evidence that A2A-receptor activation may enhance evoked transmitter release. Interestingly, after CsA treatment there was no additional increase in EPP amplitude and QC during following exposure to CGS-21680 (1 μM).

The increase in EPP QC following CGS-21680 treatment was completely abolished by PKA inhibitor H-89 (1 μM) or by L-type calcium channel blocker nitrendipine (1 μM) application. Taken together, this data indicate that A2A-receptor activation by CGS-21680 leads to increased ACh release through the following pathway: A2A-receptors → PKA → L-type calcium channels → ACh quanta release. This facilitation of neurotransmission takes places even though CaN continues to act on L-type calcium channels. In this case, upregulated PKA activity might be essential to overcome the downregulation of L-type calcium channels by CaN.

Activation of A1-receptors by adenosine is known to have an inhibitory effect on ACh secretion.

A1-receptor inhibition by DPCPX caused an increase in EPP QC by approximately 28%, while spontaneous release remained unchanged.

Similarly to the facilitation of transmitter secretion driven by A2A-receptor activation, the potentiating effects of A1-receptor inhibition by DPCPX are completely prevented by H-89 or nitrendipine. This leads us to the conclusion that A1 and A2A-receptors affect transmitter release by modulating the same intracellular pathway, which includes PKA and L-type calcium channels.

We also investigated how A1-receptor agonist 2-CADO (1 μM) influences ACh release and saw an about 38% decrease in QC of every single EPP in train, once more supporting the idea that A1-receptor negatively control neuromuscular transmission in mice.

So, intensity of acetylcholine release in mice neuromuscular junctions can be regulated by different kind of pathways. Normally, there is a tonic CaN-mediated inhibition of transmitter secretion, which, according to our speculation, is due to a CaM-independent form of CaN generated by partial proteolysis by presynaptic calpain. CaN action can be overcome by strengthening the activity of PKA through an adenosine-dependent pathway through modulating the activity of A1- and A2A-type of adenosine receptors. Activation of A2A-receptors and inhibition of A1-receptors causes a substantial increase in evoked neurotransmitter release even in the presence of functionally active CaN.

References

1. Nudler S. Ca^{2+} channels and synaptic transmission at the adult, neonatal, and P/Q-type deficient neuromuscular junction / Nudler S., Piriz J., Urbano F., Rosato-Siri M., Renteria E., Uchitel O. // Ann. NY Acad. Sci. - 2003. - V. 998. - P. 11-7.
2. Flink M., Atchison W. Iberiotoxin-induced block of Ca^{2+}-activated K^+ channels induces dihydropyridine sensitivity of ACh release from mammalian motor nerve terminals // J. Pharmacol. Exp. Ther. - 2003. - V. 305. - P. 646-652.
3. Pagani R. Differential expression of alpha 1 and beta subunits of voltage dependent Ca2+ channek at the neuromuscular junction of normal and P/Q Ca^{2+} channel knockout mouse / Pagani R., Song M., McEnery M., Qin N., Tsien R., Toro L., Stefani E., Uchitel O. // Neuroscience. - 2004. - V. 123. - P. 75-85.
4. Tandan S. Physical and functional interaction between calcineurin and the cardiac L-type Ca2+ channel / Tandan S., Wang Y., Wang T. T., Jiang N., Hall D. D., Hell J. W., Luo X., Rothermel B. A., Hill // J. A. Circ Res. – 2009 – V. 105, № 1 - P. 51–60.
5. Murphy J.G. AKAP-anchored PKA maintains neuronal L-type calcium channel activity and NFAT transcriptional signaling / Murphy J.G., Sanderson J.L., Gorski J.A., Scott J.D., Catterall W.A., Sather W.A., Dell'Acqua M.L. // Cell Rep. – 2014. – V. 7. - №5. – P. 1577-88.
6. Garcia N. Adenosine A_1 and A_2A receptor-mediated modulation of acetylcholine release in the mice neuromuscular junction / Garcia N., Priego M., Obis T., Santafe M.M., Tomas M., Besalduch N., Lanuza M.A., Tomas J. // Eur. J. Neurosci. - 2013. - Vol. 38. - №2. - P. 2229-41.

7. Oliveira L., Correia-de-Sá P. Protein kinase A and Ca(v)1 (L-Type) channels are common targets to facilitatory adenosine A2A and muscarinic M1 receptors on rat motoneurons // Neurosignals – 2005. Vol. 14, №5. – P.262-72.
8. Gaydukov A.E., Tarasova E.O., Balezina O.P. Calcium-dependent phosphatase calcineurin downregulates evoked neurotransmitter release in neuromuscular junctions of mice // Neurochem. J. – 2013. – V.7. - №1. – P. 35-40.
9. Silverman-Gavrila L.B. Calcium, calpain, and calcineurin in low-frequency depression of transmitter release / Silverman-Gavrila L.B., Prayer M., Mykles D.L., Charlton M.P. // J. Neurosci. – 2013. – V.33. - №5. – P. 1975-90.

PHYSICOCHEMICAL MECHANISMS OF THE SPATIOTEMPORAL SELF-ORGANIZATION OF MOTIVE ACTIVITY IN THE *Physarum* PLASMODIUM

V.A. Teplov

Institute of Theoretical and Experimental Biophysics, Russian Academy of Sciences, Pushchino, Moscow region, 142290, Russia

The ability to move in space themselves is among the most fundamental functions of cells. This report will focus on elucidating mechanisms of the spatiotemporal self-organization of motive activity in the cells with amoeboid type of movement, which plays an important role in processes of wound healing and metastasis, immunity, embryogenesis and morphogenesis. The most common and essential attribute of biological motility are mechanochemical oscillations since no organism is capable of traveling great distances, if its contractile apparatus would not function in an oscillatory mode. It probably explains why the most well-known cell oscillators were found in the cells with very pronounced contractile activity. But the matter perhaps is not only in the obviousness of such oscillations.

Another essential element of the amoeboid locomotion is endoplasmic streaming towards the cell front. So the question arises what processes provide the highly coordinated functioning of myosin molecular motors within a network of cross-linked actin filaments attached to the unexcitable membrane that leads to spatially well-ordered local contractions of the ectoplasm necessary for creating a intracellular hydrostatic pressure gradient and endoplasmic streaming. Activation of actomyosin system in nonmuscle cells mostly relies on phosphorylation of the myosin II regulatory light chains by their kinases in the presence of Ca^{2+} ions.

A very wide range of cellular processes can be responsible for the oscillatory behavior of cells. A great number of the graphically represented schemes describing the main mechanisms of various cell signaling pathways may be found in the excellent work by Berridge [1]. It is usually supposed that autooscillations with a minute period are solely chemical and arise because of oscillatory instabilities in the circuits of biochemical reactions. It leads to locally autonomous autooscillations of the concentration of Ca^{2+} ions, regulating the actin-myosin interaction and coupled in space by diffusion and advection. Numerous

mathematical models for the cell autooscillatory dynamics basing on the equations of the reaction-advection-diffusion type and on the assumption of existing autocatalytic chemical variable were created. It is the presence in the models of autocatalytic terms leads to instability of the stationary state and a self-excitation of autooscillations in well stirred 0D systems, and also causes instability of the homogeneous state and an emergence of traveling autowave or dissipative structures in distributed systems. However the mechanical properties of cells are not taken in account in such models.

But it is quite possible that basic oscillatory instability is in the mechanochemical system of cells. Autooscillations with participation of the contractile system may be excited as a consequence of a feedback between deformation and stress and the relationship between them depends on the state of the system. Such autooscillations arise in insect flight muscles, which have a resonant mechanical load and energy pumping occurs at a certain phase of autooscillations due to a direct effect of the strain on ATPase activity of actomyosin [2, 3]. It is indicative that not only live muscles of this type have the ability to oscillate, but also their glycerinated fibers. However, unlike this case, the forces of inertia in cells are negligibly small compared with viscoelastic ones. Therefore to excite autooscillations in amoeboid cells, the feedback between deformation and stress should be mediated by some chemical processes. But the assumption of autocatalysis of chemical variable is no longer obligatory.

The advantage of such mechanochemical oscillators is the possibility of interaction not only by diffusion and advection of chemical regulators, but also due to mechanical (hydrodynamic) connections, which are especially important for large cellular systems with unexcitable membranes. These interactions ensure rapid spatial coordination of contractile activity, which is necessary for creating a gradient of hydrostatic pressure causing a flow of the endoplasm and amoeboid locomotion of the cell. Although mechanical signals in ordinary cells are difficult to uncouple from chemical-based transduction pathways, this assumption is now confirmed by a large number of experimental data about influence of mechanical forces on various cellular processes both at the sub-cellular and tissue level [4]. Thus an important difference that emerges between modeling reaction-diffusion-advection chemical systems and modeling mechanochemical systems is that the mechanical coupling, either hydrodynamic or viscoelastic or both, as well as chemical feedback, may be essential components of the contractile dynamics of cytoplasm.

Although many of the molecular components of the cytoskeleton and associated motor proteins are now identified, it seems there is no clear linkage between the molecular biology of cytoskeleton and the behavior of amoeboid cells. This is primarily a problem of mechanics, and requires realistic models of cells as mechanical entities and a willingness to contemplate problems involving both elasticity and viscosity. Unique opportunities for studying the problems of amoeboid motility, the physics of self-organization, and mechanochemical autooscillations are provided by a giant multinucleated cell, the *Physarum poly-*

cephalum plasmodium. All hundred million nuclei in its protoplasmic sheet divide with precise synchrony every ten hours. Owing to uncoupling of nuclear and cell division, this unicellular organism with an unexcitable membrane, growing on a nutritive medium, is capable of reaching gigantic dimensions area, a square meter and thickness, 2 mm.

Actomyosin-based rhythmic contractions of the gelled ectoplasm and vigorous reciprocating (shuttle) endoplasmic streaming with the period 1–3 min are easily monitored in this cell. Synchronous oscillations of the membrane potential and intracellular concentration of Ca^{2+} ions and a series of other intermediators along with the oscillations of mechanical parameters occur in the plasmodium [5]. Migrating plasmodia are organized into a front region, i.e. a fan-like protoplasmic sheet, and in the rear region into a tree-type network of protoplasmic veins (called strands). Standing autowaves and peristaltic contractions can be set up in these strands. Autowave motile activity of the plasmodium manifests itself most vividly in its frontal sheet.

An important property of plasmodia is presented by its mechanical activation [5, 6]. Stretching of a strand by 10–20% in the isometric mode of contraction causes not only an increase of the tension but also of its oscillation amplitude. Then slow relaxation of tension with a simultaneous decrease of the oscillation amplitude usually occurs. Increasing load under isotonic conditions also increases the amplitude of strand length oscillations. Strong longitudinal stretching of strands leads also to an increase of the number of actomyosin fibrils in the ectoplasm and even their appearance in the region of the endoplasm [7]. However these fibrils disappear within several seconds if a stretch-activated strand is transferred into isotonic conditions without load. These data testify to an important role of mechanical stresses in the regulation of the contractile dynamics, and therefore one needs knowledge of the real rheological parameters of the strand for its adequate modeling [6].

Stretch activation plays a fundamental role also in our models [8–13] formulated in terms of deformation and stress of ectoplasm. The third variable is the intracellular Ca^{2+} concentration. Stretching the ectoplasmic wall is assumed to promote an increase in the Ca^{2+} concentrations through mechanosensitive Ca^{2+} channels. It is also supposed that sequestration of calcium ions into their storages obeys first-order kinetics. Since the contractile apparatus is capable only of contracting, its stretching is executed by an external load in our minimal 0D model [10] or by intracellular hydrostatic pressure in 1D and 2D models [11–13].

The 0D model deals with longitudinal dynamics of spatially uniform fragments of the strands wherein there occurs complete averaging of the concentration of Ca^{2+} on a time scale much smaller than the autooscillation period as a result of efficient mixing of endoplasm. In this case the longitudinal dynamics of strands can be described by a set of three ordinary differential equations of first order. According to the model when the load exceeds some critical value, there occurs the Andronov–Hopf bifurcation and self-excitation of mechanochemical autooscillations.

The distributed 1D and 2D models are systems of the differential equations in partial derivatives describing the undulating contractions of ectoplasm and the shuttle flows of endoplasm along strands and discoid spreading plasmodia. For simplicity the rheological behavior of ectoplasm in these models is described by the Voigt model. But in the 0D model the Kelvin model is used because the undamped elasticity cannot be ignored, as otherwise it would be impossible to simulate the longitudinal oscillatory dynamics under the isometric conditions, although in the isotonic mode, autooscillations in the reduced model are possible. The adequacy of the models has been evaluated by the correspondence of the results of their numerical solutions to the existing data on the dynamics of real strands. At empirically determined values of viscoelastic parameters [6], the 0D model well imitates the form and duration of the transient mechanochemical processes observed after isolation of strands. It also quantitatively simulates a subsequent excitation of the longitudinal contractile autooscillations and their stretch activation under isotonic and isometric conditions [10].

It has long been established that the autooscillatory contractions continue even when endoplasm in strand is replaced by artificial media [14]. Hence in the 1D model describing the radial dynamics of long strands attached to the substrate, only hydrodynamic interactions via liquid endoplasm have been taken into account because an exclusively advection seems unlikely. Consequently such a simplified model can well simulate an excitation of standing contractile autowaves and shuttle endoplasmic streaming. This model also explains the independence of the oscillation frequency on the plasmodium sizes and a low-frequency modulation of the autooscillations with a period of 15–20 minutes, which is frequently observed in real strands. According to the model it is due to the fact that the viscosity of endoplasm many orders of magnitude less than that of ectoplasm. Furthermore, the 2D model can simulate a circulation of contractile waves around the cell periphery just as it really occurs in the frontal sheet of spreading plasmodia [15–16].

Based on these data one can conclude that actomyosin network localized within ectoplasm may not only play a role of an executive mechanism, but also can be an essential part of the cellular control system, i.e. be a certain analogue of nervous system at the cellular level. In particular, it performs in the capacity of a crucial element responsible for appearing of oscillatory instability and standing autowaves that are impossible in purely chemical systems.

References

1. Berridge M.J. (2014) Cell Signalling Biology; doi:10.1042/csb0001001.
2. Pringle J.W.S. (1975) Insect Flight. Oxford Biology Readers, Vol. 52 London: Oxford University Press.
3. Deshcherevsky V.I. (1977) Mathematical Models of Muscle Contractions. Moscow: Nauka (in Russian).
4. Bukoreshtliev N.V., Haase K., Pelling A.E. (2013) Mechanical cues in cellular signalling and communication. Cell Tissue Res. 352, 77–94; doi: 10.1007/s00441-012-1531-4.
5. Kamiya N. (1981) Physical and chemical basis of cytoplasmic streaming. Ann. Rev. Plant Physiol. 32, 205-236.

6. Teplov V.A. (1988) Autooscillations in *Physarum* plasmodium. Correlation between force generation and visco-elasticity during rhythmical contractions of protoplasmic strand. Protoplasma (Suppl. 1), Cell Dynamics 1, pp. 81-88.
7. Fleischer M., Wohlfarth-Bottermann K.E. (1975) Correlation between tension force generation, fibrilogenesis and ultrastructure of cytoplasmic actomyosin during isometric and isotonic contraction of cytoplasmic strands. Cytobiologie, 10, 339-365.
8. Teplov V.A., Beylina S.I., Evdokimov M.V., Priezzhev A.V., Romanovsky Yu.M. (1981) Autowave mechanisms of intracellular motility. In: "Autowave processes in systems with diffusion". Ed. Grekhova M.T., Inst. Appl. Phys. USSR Acad.Sci.Press, Gorky, pp.190-201 (in Russian).
9. Romanovsky Yu.M., Chernyaeva E.B., Kolin'ko V.G., Khors N.P. (1981) Mathematical models of the protoplasmic movement. In: [8], pp. 202-209 (in Russian).
10. Teplov V.A. (2010) Cytomechanics of oscillatory contractions. Modeling the longitudinal dynamics of *Physarum polycephalum* protoplasmic strands. Biophysics, 55 (6), 987-995.
11. Teplov V.A., Romanovsky Yu.M., Latushkin O.A. (1991) A continuum model of contraction waves and protoplasmic streaming in strands of *Physarum* plasmodium. BioSystems, 24: 269-289.
12. Romanovsky Yu.M., Teplov V.A. (1995) The physical bases of cell movement. The mechanisms of amoeboid motility selforganization. Physics-Uspekhi, 38 (5), 521-542.
13. Teplov V.A., Mitrofanov V.V., Romanovsky Yu.M. (2005) Synchronization of mechano-chemical autooscillations within the *Physarum polycephalum* plasmodium by periodical external actions. Biophysics, 50 (4), 618-626.
14. Ueda T., Gotz von Olenhusen K., Wohlfarth-Bottermann K.E. (1978). Reaction of the contractile apparatus in *Physarum* to injected Ca2+, ATP, ADP, and 5' AMP. Cytobiologie 18, 76-94.
15. Pavlov D.A., Romanovsky Yu.M., Teplov V.A. (1996) Two-dimensional mechano-chemical autowaves in the amoeboid cell", Biophysics, 41 (1), 153-159.
16. Teplov V.A., Romanovsky Yu.M., Pavlov D.A., Alt W. (1997) Auto-oscillatory processes and feedback mechanisms in *Physarum* plasmodium motility In: Dynamics of Cell and Tissue Motion. Eds. Alt W., Deutsch A., Dunn G.A., Basel: Birkhaeuser, pp. 83-92.

LOCOMOTOR PROJECTIONS OF BRAIN CORTEX: EFFECTS OF LONG TERM SPACE FLIGHTS

E.S. Tomilovskaya[1], I.N. Nosikova[1], I.V. Rukavishnikov[1], A.D. Rumshiskaya[2], L.D. Litvinova[2], E.V. Pechenkova[2], E.A. Mershina[2], V.E. Sinitsin[2], A. Van Ombergen[3], F. Wuyts[3], I.B. Kozlovskaya[1]

[1]*Institute of Biomedical Problems, Moscow, Russia*

[2]*Federal Center of Treatment and Rehabilitation, Moscow, Russia*

[3]*Antwerpen Research Center, University of Antwerp, Belgium*

It is well known, that long time exposure to altered gravity environment is accompanied by wide disturbances of the activities of motor control systems. The mechanisms of this disorder are still unclear. Even less is known how much

these adaptive changes are connected with the activity of the central part of the motor control system – motor cortex.

Specialists of IBMP RAS and Scientific Center of Neurology RAMS using functional magnetic resonance imaging (fMRI) have described during mechanical stimulation of soles support zones in locomotor regimens the activation areas of the cerebral cortex similar to that of imaginary stepping movements (Kremneva et al., 2013).We have suggested that topography of cortical projections of the mechanical stimulation of support zones should be changed during long term exposure to conditions of supportlessness.

In this research we have studied the topography of cortical activities to the mechanical stimulation of the support zones in healthy volunteers and cosmonauts pre- and post- long term flight. The group of volunteers included 6 healthy men of age 37-55 years old with no signs of the central nervous system pathology. Three cosmonauts were examined in 2 session 60-90 days before flight and 2 sessions 7-8 and 180-200 days after it`s accomplishment. Scanning of volunteers was performed with the same six-month interval. fMRI-investigations were carried out using a 3T MRI General Electrics scanner with a specially developed protocol, where 20-seconds stimulation alternated with 20 seconds of rest (Chernikova L.A. et al., 2012). Mechanical stimulation of the soles support zones with parameters of locomotion (75 steps per minute) was performed using the "Korvit" device ("VIT" company, St. Petersburg). The pressure on the heel and metatarsal areas of feet varied about 40 kPa.

Preliminary results of the study in healthy volunteers group consisted fully with the data published before on topography of cortical projections zones connected to execution of locomotions (Chernikova L.A. et al., 2013; Kremneva E.I. et al., 2013). The changed topography of these locomotor projections was observed in the group of cosmonauts after space flight. The next session of the experiment which was carried out 6 month later have shown that all the changes observed shortly after flight were reversible.

The study is supported by RSF grant №14-25-00167.

NITRIC OXIDE REGULATES PROLIFERATION OF RAT *soleus* MUSCLE SATELLITE CELLS EARLY IN THE RECOVERY AFTER SIMULATED GRAVITATIONAL UNLOADING

O.V. Turtikova[1], E.G.Altaeva[1], T.M. Mirzoev[1], A.E. Bugrova[2], T.F. Shevchenko[2], B.S. Shenkman[1]

Institute of Biomedical Problems RAS, 123007, Khoroshevskoe shosse, 76-a, Moscow, Russia

Emanuel Institute of Biochemical Phisics RAS, 119991, Kosygina street,4 ,Moscow, Russia

The aim of this work was to evaluate the impact of the nitric oxide (NO) on satellite cells (SC) of soleus muscle at early recovery after simulated microgravity.

We assumed that at the beginning of the recovery period NO content increased, which in turn activates satellite cell proliferation. Rats were hindlimb suspended for 14 days, then recovered for 1 or 3 days with inhibition of NO synthesis by nonselective NO-synthase inhibitor N_{ω}-nitro-L-arginine methyl ester (L-NAME).

Rats were randomly divided into 6 groups: control (*C*), hindlimb suspension 14 days (*HS14*); HS14 +1 day recovery – *R1*; HS14+1 day recovery+L-NAME – *R1+L-NAME*; HS14 + 3 days recovery – *R3*; HS14+3 days recovery+L-NAME – *R3+L-NAME*. Rats were injected i.p. by L-NAME in a dose of 90 mg/ kg of body weight for the last 2 days of hindlimb suspension (HS) and within 1 (R1+L-NAME) or 3 (R3+L-NAME) days in early recovery period. *Soleus* muscle NO level was measured by electron paramagnetic resonance (EPR).

NO content in the control group was maximum as compared with other groups, was decreased in HS14 by half compared with the control, was still lower by 17% than the control after 1 day recovery, while R3 group did not significantly differ from control. L-NAME administration significantly reduced NO levels by 26% after the first day of recovery. There was no significant difference between R3+L-NAME and R3 group ($p = 0.17$). We observed a slight increase in NO content also on the background of L-NAME administration; NO content was higher in R3 + L-NAME group than in R1 + L-NAME.

We also measured protein level and mRNA expression of hepatocyte growth factor (HGF), which could be expressed by SCs or released by matrix metalloproteinases from the extracellular matrix in NO-dependent manner and activate satellite cells. HGF protein level was not changed in HS and R1 group and was significantly higher in R3 group by 94% as compared with control group. There were no significant differences in HGF protein level in L-NAME groups as compared to the groups without drug. Maximum HGF mRNA expression (near the control level) was observed on the 1st day of recovery and was decreased in subsequent days. However HGF mRNA expression in R1+L-NAME group was reduced by 0.4 times compared with the R1 group. On day 3 of the recovery no differences were observed.

NOS inhibition decreased proliferation marker Mki67 mRNA expression on day 1 of reloading. In R3+L-NAME group total number of BrdU + nuclei and the number of BrdU + nuclei outside the dystrophin layer was significantly lower than in the group without L-NAME. The number of BrdU+ nuclei inside the dystrophin layer (incorporated SCs nuclei) did not change ($p = 0.17$). So the NO – induced onset of proliferative activity on the day 3 of the recovery period, which was suppressed by L-NAME in the absence of significant changes of HGF protein in muscle. Apparently not total but released from extracellular matrix HGF involved in SC activation.

Pax7 expression (which is a nonambiguous satellite cell marker, usually observed in undifferentiated SCs, actively – in self-renewal cells, required for myogenic commitment and suppressed at differentiation) was stable to the changes in NO concentration and NO-synthase inhibition. Myogenin expression tended to decrease in R1+L-NAME and R3+L-NAME groups. Thus NO affected SC population during recovery towards to stimulation of differentiation.

According to immunohistochemistry data, SCs fusion occurred most intensively on the 3rd day of recovery. There was a tendency of decrease in SC fusion in R3 + L-NAME compared with the R3 group (p = 0.17). The relative amount of included BrdU+ nuclei remained constant through the recovery period, so there was no effect of L-NAME on satellite cells fusion with myofibers.

We conclude that nitric oxide played an important role in the activation of satellite cell pool during the recovery from gravitational unloading. NO synthase inhibition did not affect SCs fusion in early recovery period.

Supported by RFBR project no.13-04-01891-a.

SIGNAL SWITCHING IN MESENCHYMAL STROMAL CELLS: NORADRENALINE DOWNREGULATES β-ADRENERGIC RECEPTORS LEADING TO UPREGULATION OF α1-RECEPTORS

Tyurin-Kuzmin P.A., Fadeeva J.I., Kanareykina M.A., Kalinina N.I., Sysoeva V.Yu. , Stambolsky D.V., Tkachuk V.A.

Department of Biochemistry and Molecular Medicine, Faculty of Fundamental Medicine, M.V. Lomonosov Moscow State University, Moscow, Russia

Sympathetic neurons are important component of mesenchymal stem cells (MSC) niche. Catecholamines regulate proliferation, differentiation and secretion of bone marrow mesenchymal stromal cells (MSCs) acting through β1- and β2-adrenergic receptors. However, the expression of adrenergic receptors (AR) on adipose-derived MSCs (ADSCs) as well as their regulation on those cells remains poorly understood. We examined the mechanisms of regulation of MSC responsivity to noradrenaline. Using flow cytometry, we demonstrated that α1A adrenergic receptors isoform was the most abundant in adipose tissue-derived MSCs. Using calcium imaging in single cells, we demonstrated that only 6.9 ±0.8% of MSCs responded to noradrenaline by intracellular calcium release. Noradrenaline increases MSC sensitivity to catecholamines in a transitory mode. Within 6 hrs after incubation with noradrenaline the proportion of cells responding by Ca^{2+} release to the fresh noradrenaline addition has doubled but declined to the baseline after 24 hrs. Increased sensitivity was due to the elevated quantities of α1A adrenergic receptors on MSCs. Such elevation depended on the stimulation of β-adrenergic receptors and adenylate cyclase activation. These data for a first time clarify mechanisms of regulation of MSC sensitivity to noradrenaline.

EFFECTS OF SHORT-TERM HINDLIMB UNLOADING ON ANABOLIC SIGNALING PATHWAYS IN RAT *soleus* MUSCLE

N.A. Vilchinskaya, T.M. Mirzoev, S.A. Tyganov, B.S. Shenkman

SSC RF-Institute of Biomedical Problems RAS, Khorochevskoe Shosse 76 a, Moscow, 123007, Russia

It is well known that gravitational unloading results in a significant atrophy of mammalian postural muscles such as *soleus*. In a number of human and animal

studies it has been shown that disuse-induced muscle atrophy is associated with a decrease in the rate of protein synthesis and an increase in proteolysis. To date little is known about changes in signaling pathways regulating protein synthesis in the rodent *soleus* muscle during early stages of gravitational unloading. The goal of the study was to estimate the amount of rRNA and phosphorylation status of the key signaling molecules of anabolic signaling pathways controlling protein synthesis in rat *soleus* after 1 day of hindlimb unloading. Gravitational unloading was simulated by hindlimb suspension model. The content of total-p70S6k, phospho-p70S6k, 4E-BP1, phospho-AMPK in rat *soleus* after 1-day hindlimb suspension (HS) was determined by Western-blotting. The amount of 18S+28S rRNA in rat *soleus* after 1-day HS was evaluated by RT-PCR.

After 1-day HS a 62% ($p<0.05$) decrease of phospho-AMPK content was observed in rat *soleus* compared to control group. Also, there was a 35% ($p <0.05$) decrease of phospho-4E-BP1 compared to control value. Besides, after 1-day HS we detected a 72% ($p <0.05$) increase of phospho-p70s6k content in rat *soleus* compared to control group. Also we observed a significant decrease in the amount of 28S rRNA in rat *soleus* after 1-day HS.

The results of the study indicate that an inactivation of AMPK and a decrease in ribosome biogenesis occur as soon as after 1 day of HS. We assume that at the early stage of hindlimb unloading p70s6k activation can play a compensatory role by attenuating a reduction in muscle protein synthesis.

This work was supported by RFBR grant no. 16-34-60055.

SELECTIVE REMOVAL OF PARAMYOSIN FROM CATCH-MUSCLE MYOFIBRILS: AN OPPORTUNITY FOR STUDYING THE MECHANOCHEMICAL PROPERTIES

I.G. Vyatchin

A.V. Zhirmunsky Institute of Marine Biology, Far East Branch of Russian Academy of Sciences, Palchevsky St. 17, Vladivostok, 690041, Russia

The mechanochemical study of the suspension contractile models – myofibrils, synthetic and natural actomyosins- has made a great contribution to our knowledge of the mechanisms of contraction and regulation of vertebrate skeletal muscles. This approach allowed to link optical properties of skeletal muscles suspension models with the functional state of the contractile apparatus. Addition of calcium and Mg^{2+}-ATP to suspension models causes superprecipitation, while addition of Mg^{2+}-ATP in the absence of calcium results in clearance of the suspension. It appeared, however, that these phenomena are not observed in myofibril preparations from molluscan catch muscles, though these myofibrils possess the regulated Mg^{2+}-ATPase activity. We have found that response of molluscan myofibrils to addition of Mg^{2+}-ATP with Ca/EGTA became optically detectable after a selective removal of paramyosin – the core protein of thick filaments. The new opportunity to register changes in the optical properties of catch muscle suspension

models offers further advances in research of these interesting muscles, capable of being in three functional states: contraction, relaxation and catch.

STUDY OF VARIOUS TYPES OF ENDOCYTOSIS IN THE NERVE ENDING MOUSE IN EXPERIMENTAL DIABETES

O.V. Yakovleva

Institute of Fundamental Medicine and Biology, Kazan Federal University, Kremlevskaya st.18, Kazan, 420008, Russia

Diabetes mellitus is a heterogeneous endocrine metabolic disorder, due to absolute or relative defective insulin secretion and sensitivity [1]. One of the major complications of diabetes mellitus are peripheral neuropathy, characterized by muscle weakness, decreased sensitivity, muscle atrophy and functional disorders are the result of sensory and motor nerve fibers, as well as changes in neuromuscular transmission [1]. Several studies have shown morphological and functional changes of the neuromuscular synapse at both pre -and postsynaptic levels [2].

GSK-3 is a protein kinase with diverse physiological functions in mediating intracellular signaling, regulating neuronal plasticity, gene expression, and cell survival [3]. It may also play important roles in protein synthesis, cell proliferation, cell differentiation, microtubule dynamics and cell motility by phosphorylating initiation factors, components of the cell-division cycle, transcription factors and proteins involved in microtubule function and cell adhesion. Disfunction of the GSK-3 may be involved with some disorders, as cancer and diabets [3]. GSK-3 can regulation of excitatory synaptic transmission.

The maintenance of neurotransmission at nerve terminals is dependent on the efficient retrieval and recycling of synaptic vesicles across a wide range of stimuli. During mild synaptic activity the dominant endocytosis mode is clathrin-mediated endocytosis (CME), which retrieves single SVs from the nerve terminal membrane. However, when neuronal activity increases, an additional endocytosis mode is triggered to provide a rapid and immediate increase in synaptic vesicle retrieval capacity, called activity-dependent bulk endocytosis (for gross changes in nerve terminal surface area via the rapid generation of endosomes direct from the plasma membrane [4]). GSK -3 controls endocytosis via regulation of diynamin 1 activity [5].

Materials and Methods

Experiments were performed on isolated neuromuscular preparations diaphragmatic muscle laboratory white mice. To investigate the process of endocytosis of synaptic vesicles in motor nerve ending a fluorescent marker FM 1-43 (3 μM), which reversibly binds to the presynaptic membrane during endocytosis of synaptic vesicles is inside nerve terminals (“load” terminal). We used three protocols “loading” terminals: first – FM 1-43 is present in the solution for 1 minute during stimulation, second- FM 1-43 is present in the solution for 1 minute during stimulation and 7 minutes afterwards, and third – FM 1-43 is present

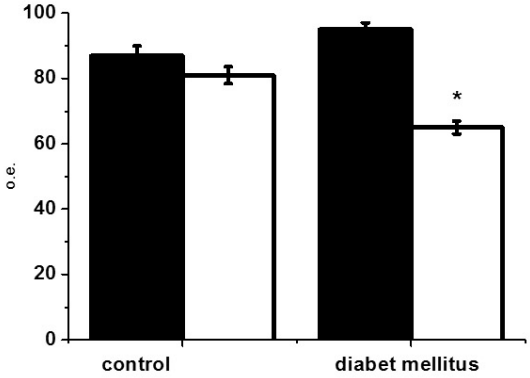

Change of glow in blocking nerve teminaley slow endocytosis in normal and experimental diabetes mellitus. Black bars – control, white bars – blocking GSK-3.

only 7 minutes after. Registration glow nerve was performed using a microscope AxioScope A1 equipped with high-speed black-and- white camera AxioCam MRm ("Carl Zeiss", Germany). All observations were made only on the surface-lying nerve endings. Estimated average intensity of luminescence in the area nervous long terminal 10–20 microns in relative units (r.u.), evaluating the pixel glow from 0 to 256. In experiments using synthetic blocker GSK3 – 1 azakenpaullone 2 mkM (Sigma, США).

For the development of type 1 diabetes using alloxan (200-250 mg/kg Sigma), which is has two mechanisms of action on the tissue of the pancreas: it selectively inhibits glucose-insulin secretion through the inhibition of glucokinase sensor glucose β-cells and causes the formation of free radicals, resulting in necrosis of the cells is observed [1]. Mouse of the control group was administered saline.

On day 45 animals with elevated glucose levels (> 9 mmol/l) were taken out of the experience for fluorescence studies. Blood sampling was carried out from the tail vein, changes made Meter "Accu-Chek Active" (Germany).

Results

An indicator dye loading in the nerve endings at the synaptic vesicle endocytosis is the appearance of the characteristic glow of nerve terminals.

In control at first protocol glow nerve terminals was 85 ± 1 pu (n = 14); at second its completion - 87 ± 1 pu (n = 13, figure), and the third its completion - 56±1 pu (n = 15). It is known that nerve ending mouse characterized by intensive processes of endocytosis with a predominance of short, quick way of recycling of synaptic vesicles. Thus exo- and endocytosis are almost parallel, and a reserve pool vesicles do not participate in the secretion of mediator. Therefore, the glow of nerve terminals were not significantly different at the two kinds of procedure.

In animals with experimental diabetes adding FM 1-43 at first protocol glow nerve terminals was 99 ± 3 pu (n = 5, p <0.05); and at second its completion

– 96 ± 2 pu (n = 8, p <0.05, figure), and the third its completion – 65±2 pu (n=7, n<0.05). The findings point to strengthening the processes of endocytosis of synaptic vesicles in nerve endings mouse model of diabetes.

For the study of slow endocytosis in the nerve endings of the mouse, we used a blocker GSK-3, an enzyme regulating the activity of dynamin 1 [5] – 1 azakenpaullone in concentration of 2 mkM.

In control animal, at first procedure glow nerve terminals was 81±2 pu (n = 5, figure), that no significant change in control of nerve terminals. Indeed, in normal conditions, even with a high-frequency stimulation in mammals slow processes of endocytosis does not contribute significantly [4].

In animals with experimental alloxan diabetes mellitus under the same conditions shows a strong reduction of emission of nerve terminals to 65 ± 2 pu (n = 7, p <0.05, figure).

Thus, one mechanism may be a quick way of recycling inhibition / enhancement or slow endocytosis due to disturbances, or mobilization of synaptic vesicles.

References

1 Lenzen, S The mechamisms of alloxan- and streptozocin-induced diabetes / S. Lenzen // Diabetologia — 2008 — V. 51 — P. 216-226.

2 Garcia, C.C. Acetylcholinesterase deficiency contributes to neuromuscular junction dysfunction in type 1 diabetic neuropathy / C.C. Garcia, J.G. Potian, K. Hognason, B. Thyagarajan [et al] // AmJ Physiol Endocrinol Metab – 2012 – V. 303 – P. E551–E561.

3 Frame, S. GSK3 takes centre stage more than 20 years after its discovery / S. Frame, Ph. Cohen // Biochem J. – 2001 – V. 359 – P. 1-16.

4 Rizzoli, S.O. Synaptic vesicle pools. / S.O. Rizzoli, W.J. Betz // Nature rev. Neurosci. – 2005 – V.6 – P. 57-69.

5 Clayton, E.L. Dynamin 1 phosphorylation by GSK3 controls activity-dependent bulk endocytosis of synaptic vesicles. / E.L Clayton., N. Sue, K.J. Smilie, N Bache. [et al] // Nat Naurosci. – 2010 – V. 13(7) – P. 845-851.

SMOOTH MUSCLE TITIN (500 KDa) FORMS *in vitro* AMYLOIDS

E.I. Yakupova[1], A.G. Bobylev[1], L.G. Bobyleva[1], I.M. Vikhlyantsev[1], N.V. Penkov[2], S.N. Udaltsov[3], Z.A. Podlubnaya[1]

[1]*Institute of Theoretical and Experimental Biophysics, Russian Academy of Sciences, 142290, Pushchino, Moscow Region, Russian Federation*

[2]*Institute of Cell Biophysics, Russian Academy of Sciences, 142290, Pushchino, Moscow Region, Russian Federation*

[3]*Institute of Physico-Chemical and Biological Problems in Soil Science, Russian Academy of Sciences, 142290, Pushchino, Moscow Region, Russian Federation*

Amyloids are insoluble fibrous protein aggregates sharing specific structural features: high content of β-sheet structure, ability to bind to Congo red (CR) and thioflavin T (ThT), birefringence in polarized light, insolubility in most solvents and resistance to proteases [1–3]. More than 50 proteins had been described to form amy-

loids which are involved in pathogenesis of amyloidosis in different organs and tissues: for example tau-protein, hantingtin, amylin, amyloid-β (Aβ) peptide, alpha-synuclein, insulin, lysozyme, myoglobin, transthyretin. [3,4]. Amyloid deposits were found in cross-striated muscles muscles and many were shown to contribute to the development of "amyloid cardiomyopathy" or "cardiac amyloidosis" [5]. It was also found that myosin subfragment-1 from rabbit skeletal muscles can form *in vitro* spherical oligomers with amyloid-like dye-binding properties [6]. Amyloid depositions were also revealed in vessels [7,8].

In 2002 smooth muscle titin (initially called smitin) was found in the smooth muscle extract of chicken gizzard [9]. Further studies showed that titin from smooth and cross-striated muscles is a product of the same gene, alternative splicing of which leads to the formation of titin isoforms with molecular mass 700–2000 kDa in the smooth muscle tissue [10].

Herein we present our experimental data for the 500 kDa smooth muscle titin (SMT) isoform, supporting the above proposal, and also the results of examination of cytotoxicity of SMT amyloid aggregates in order to clarify their potential negative effect like Aβ(1-42)-peptide oligomers.

SMT aggregates were studied *in vitro* using the electron microscopy. After 24-h incubation at 4°C in solution containing 0.15 M glycine-KOH, pH 7.0–7.5, smooth muscle titin formed amorphous aggregates as well as compact bundles of linear fibrils. These bundles extend up to several micrometers in length and 100 nm in width. It should be noted that bundles of SMT fibrils occurred very seldom, and the electron microscope field of view contained mostly amorphous aggregates, the formation of which was also observed in solution containing 0.2 M KCl, 10 mM imidazole, pH 7.5.

To clarify the putative amyloid nature of the formed SMT aggregates, their ability to bind to CR and ThT was studied. Upon measuring spectral characteristics of the CR solution in the presence of SMT aggregates, a shift of the absorption spectrum of the staining agent to the long-range region from ~490 nm to ~500 nm was observed that is characteristic to all known amyloid proteins. The fluorescence intensity of ThT increased (7-fold) in the presence of SMT aggregates as compared to the fluorescence intensity of the staining agent in the presence of the molecular (monomeric) form of this protein. This also indicates the amyloid nature of these aggregates.

Using CD analysis we show what no changes in the SMT secondary structure upon formation of their aggregates, though the protein released from the chromatographic column contained 6.1% of alpha-helical regions, while their content in aggregated titin was 5.5%. However these differences were within the limits of error. Thus, the results of the CD analysis suggest that the presence of disordered regions in the SMT secondary structure as well as a high content of regions with beta-structure may be the reason for an insignificant increase in ThT fluorescence in the presence of the molecular form of this protein. The obtained data may also explain the readiness of formation of SMT aggregates.

X-ray diffraction analysis of smooth muscle aggregates of titin revealed the presence of the following reflections: 8.04, 6.09, 5.67, 4.89, 4.11, 3.94, 3.74 and 3.48 Å. The pronounced reflection 8.04 and reflection 4.89 can be ascribed to cross-β-like reflections inside crystals of SMT aggregates. The presence of a cross-β structure identified by X-ray diffraction analysis confirms that SMT aggregates are amyloids.

To investigate the dynamics of SMT amyloid aggregates formation we chose a DLS technique, a non-invasive approach to detect and characterize aggregates of different sizes depending on the time of their formation [11]. We found the change in the autocorrelation function of the scattered light upon formation of SMT aggregates at pH 7.0 for 180 min. During the first 60-min incubation, almost mono-exponential decay of the correlation function $g_2(t)$ was observed with the subsequent emergence of a shoulder at high correlation times. This indicates the formation of large titin aggregates characterized by a smaller diffusion coefficient. After 180 min the correlation function $g_2(t)$ had a more pronounced shoulder at high correlation times which indicated the increase of the proportion of SMT aggregates.

Several peaks reflecting the dimensions of the aggregates were obtained after the correlation function analysis. Prior to the formation of aggregates, the presence of only two well resolved peaks with the average hydrodynamic radii (R_h) ~12–15 nm (the dominating peak of ~90%) and 45 nm (the minor peak of ~10%) was observed in the titin preparations. The first peak corresponds, most likely, to SMT molecules, whereas the second peak may be evidence for insignificant the presence of other proteins in the preparation, for example, more high-molecular titin isoform (m.m. ~1.5 MDa), the insignificant presence of which was recorded by the SDS-PAGE method in the purified titin preparations. The third peak, indicating the formation of titin aggregates (R_h ~700 nm) appears after 20-min incubation. The size of this fraction increased during incubation with the subsequent emergence (at 180 min) of the fourth peak (R_h ~4500 nm). These fourth peaks indicate the appearance of larger protein aggregates, the number of which increased during the following incubation period. When the experiment terminated (in 21 h), the presence of two main protein fractions with R_h ~ 4500 nm (the main peak corresponding to protein aggregates) and R_h ~ 40 nm (the minor indefinite peak that present during the whole experiment) was observed. It should be noted that the peak with hydrodynamic radius R_h ~ 4500 nm was on the boundary of the measuring range of this method. Therefore the formation of larger SMT aggregates cannot be excluded.

To summarize the above results, our *in vitro* studies show that under conditions close to physiological at neutral pH, the isoform of smooth muscle titin generates amyloid aggregates that have a pronounced cytotoxic effect on smooth muscle cells accompanied by distortions of the actin cytoskeleton and cell adhesion. As titin aggregates are readily formed *in vitro*, their emergence in human and animal organs and cells cannot be excluded. Further research is needed to establish the

possible role of SMT amyloid depositions in development of amyloidosis muscle tissue.

The research was performed with the financial support of RFBR grant №14-04-00283.

References

1. Dobson, C.M. (2004) Experimental investigation of protein folding and misfolding. Methods. 34, 4–14.
2. Ross, C.A., Poirier, M.A. (2004) Protein aggregation and neurodegenerative disease. Nat. Med. 10, Suppl:S10–7.
3. Uversky,V.N., Fink, A.L.(2004) Conformational constraints for amyloid fibrillation: the importance of being unfolded. Biochim. Biophys. Acta. 1698, 131–153.
4. Chiti, F., Dobson, C.M. (2006) Protein misfolding, functional amyloid, and human disease. Annu. Rev. Biochem. 75, 333–366.
5. Guan, J., Mishra, S., Falk, R.H., Liao, R. (2012) Current perspectives on cardiac amyloidosis. Am. J. Physiol. Heart Circ. Physiol. 302, H544–H552.
6. Komatsu, H., Shinotani, N., Kimori, Y., Tokuoka, J., Kaseda, K., Nakagawa, H., Kodama, T. (2006) Aggregation of partially unfolded Myosin subfragment-1 into spherical oligomers with amyloid-like dye-binding properties. J. Biochem. 139, 989–996.
7. Rosenthal, C.J., Franklin, E.C., Frangione, B., Greenspan, J. (1976) Isolation and partial characterization of SAA-an amyloid-related protein from human serum. J. Immunol. 116, 1415–1418.
8. Häggqvist, B., Näslund, J., Sletten, K., Westermark, G.T., Mucchiano, G., Tjernberg, L.O., Nordstedt, C., Engström, U., Westermark, P. (1999) Medin: an integral fragment of aortic smooth muscle cell-produced lactadherin forms the most common human amyloid. Proc Natl Acad Sci USA. 96, 8669–8674.
9. Kim, K., Keller, T.C. 3rd (2002) Smitin, a novel smooth muscle titin-like protein, interacts with myosin filaments *in vivo* and *in vitro*. J. Cell Biol. 156, 101–111.
10. Labeit, S., Lahmers, S., Burkart, C., Fong, C., McNabb, M., Witt, S., Witt, C., Labeit, D., Granzier, H. (2006) Expression of distinct classes of titin isoforms in striated and smooth muscles by alternative splicing, and their conserved interaction with filamins. Mol. Biol. 362, 664–681.
11. Hill, S.E., Robinson, J., Matthews, G., Muschol, M. (2009) Amyloid protofibrils of lysozyme nucleate and grow via oligomer fusion. Biophys. J. 96, 3781–3790. doi: 10.1016/j.bpj.2009.01.044.

PROTECTIVE EFFECTS OF ANTITHROMBOTIC DNA APTAMERS IN CASE OF RHABDOMYOLYSIS

I.I. Zamorskii1, V.A. Spiridonova2

[1]*Bukovinian State Medical University, Teatralnaya Square, 2, Chernovtsy, 58002, Ukraine*

[2]*Belozersky Institute of Physicochemical Biology, Moscow State University, Leninskie Gory, 1, Bldg. 40, Moscow, 119991, Russia*

Aptamers are small single-stranded molecules of DNA/RNA, sized in 30–60 nucleotides with high affinity and specificity to a selected target, which are

functional analogs of monoclonal antibodies by their specificity and affinity. Single-stranded aptameric molecules of nucleic acids have highly ranked tertiary structure that allows them to form stable and specific complexes with different targets, including thrombin. These substances are obtained by the methods of combinatorial chemistry of nucleic acids SELEX (Systematic Evolution of Ligands by Exponential enrichment) [1]. Antithrombotic DNA aptamers is a new class of direct thrombin inhibitors, of a key protein for the clotting process.

Rhabdomyolysis is a quick destruction of the skeletal muscles which is quite common as a result of their compression and crushing in case of a severe injury, e.g. in a crush syndrome as well as under the action of non-traumatic factors, in particular drugs, alcohol, myotropic poisons, microbial toxins, excessive exercise, cramps, hyperthermia, thrombosis, metabolic or electrolyte disorders, endocrine and autoimmune diseases [2]. As a result of myolysis, myocytes release myoglobin, which leads to acute kidney injury (AKI) caused by peroxidation of macromolecules, vasoconstriction, inflammation and apoptosis in the renal tissue as well as renal tubular obstruction by myoglobin cylinders and urothrombosis [3]. The body experiences disseminated intravascular coagulation (DIC) in this case. [2].

To prevent and treat AKI, a number of means is used, aimed at processes of oxidative stress (antioxidants and ferric ions chelators), inflammation and vasoconstriction (anti-inflammatory drugs and inhibitors of vasoconstrictors) [3]. However, according to current recommendations for the treatment of this life-threatening condition, insufficient attention is paid to the prevention of thrombosis both at a system level (DIC) and to urothrombosis at the level of the renal tubules. This is why, the purpose of this study was to identify the impact of the original antithrombotic DNA aptamers on the course of experimental rhabdomyolytic AKI. Until now, these molecules have been only studied as thrombin inhibitors *in vitro*.

Rhabdomyolytic AKI was simulated in mature male mongrel white rats by intramuscular injection of 50% glycerol solution at a dose of 10 ml / kg. DNA aptamers (TVA15, TVA31 and RE31) were administered intraperitoneally at a dose of 0.5 mg/kg daily for 3 days until the disease was simulated. The renal function was evaluated under conditions of water load (5% of body weight) in terms of urine output, glomerular filtration rate, proteinuria, creatinine concentration in plasma and urine excretion of ammonia and titrated acids in the urine. General protective effects of antithrombotic DNA aptamers were also evaluated for the survival of animals with this AKI model. Statistical analysis of the results was performed using Statistica 10.0 using Student's *t*-criteria (for normal data distribution), Mann-Whitney *U*-test (with non-normal distribution) and the angular transformation by Fisher (animal survival analysis). The critical level of probability was adopted at $p \leq 0.05$.

Animals with AKI experienced oliguria development after 12 and 24 hours of the study. Introduction of different DNA aptamers showed nephroprotective effects of the studied compounds. Thus, when aptamer TVA31was administered, creatinine in blood plasma, protein and values of titrated acids in the urine re-

mained at the level of control, changing compared to the data obtained in simulated disease by 24.4%, 22.3% and by 2,8 times respectively (180%, p <0.05). At the same time under the influence of TVA31 aptamer in the rats with simulated pathology the urine output increased by1.5 times (p <0.05) compared to those animals, in which AKI was simulated without aptamers. In this case the glomerular filtration rate increased significantly as well.

The survival rate of the animals in the group with simulated pathology within 7 days was 85.7%, and after the application of all studied DNA aptamers — 100% (p <0.05).

Thus, DNA aptamers with antithrombotic activity show neuroprotective effects of rhabdomyolysis-induced AKI, increasing the urine output, glomerular filtration rate and concentration of titrated acids in the urine, reducing the degree of proteinuria, and improving the 7-day animal survival which allows to recommend these compounds for further clinical trials.

This work was supported by a grant RFBR N11-04-01530_a.

References

1. Panizo N., Rubio-Navarro A., Amaro-Villalobos J. M., Egido J., Moreno J. A. Molecular mechanisms and novel therapeutic approaches to rhabdomyolysis-induced acute kidney injury. Kidney Blood Press. Res. 2015. Vol. 40, N 5. P. 520–532. doi: 10.1159/000368528.
2. Spiridonova V. A. Molecular Recognition Elements: DNA/RNA-Aptamers to Proteins (review). Biochemistry (Moscow), Supplement Series B: Biomedical Chemistry. 2010. Vol. 4. P. 138–149.
3. Torres P. A., Helmstetter J. A., Kaye A. M., Kaye A. D. Rhabdomyolysis: pathogenesis, diagnosis, and treatment. Ochsner J. 2015. Vol. 15, N 1. P. 58-69.
4. Zamorskii I. I., Shchudrova T. S. Main mechanisms of rhabdomyolysis-caused kidney injury and their correction by organospecific peptides. Biophysics. 2014. Vol. 59, N 5. P. 834–836.

MELAPHEN AND GARMATRON, AFFECTING THE ACTIVITY OF COMPLEX OF THE MITOCHONDRIAL RESPIRATORY CHAIN, INCREASE THE RESISTANCE OF PEA SEEDLINGS TO THE WATER DEFICIT

I.V. Zhigacheva, E.B. Burlakova

Emanuel Institute of Biochemical Physics, Russian Academy of Sciences, Kosygina str., 4, Moscow, 119334 Russia

The development and, probability, survival of plant in any case are more dependent on availability of water than on any other environmental factors. Metabolism of plants survived even short-term strong drought could not be recovered [2]. The reason for this is a shift of antioxidant-prooxidant balance towards increasing the ROS generation is a result of the action of water deficiency. Under stress mitochondria and chloroplasts in plants [3] are the main source of ROS [4]. The

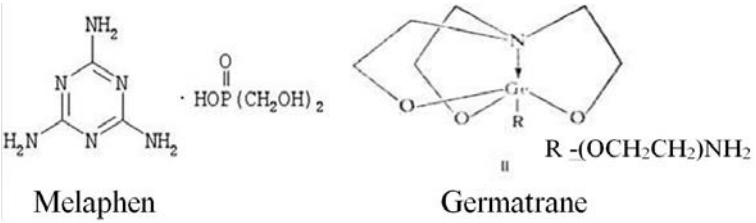

energy metabolism plays a significant role in adaptive response of the organism. Mitochondria play a key role in the energy, redox and metabolic processes in cell [5]. In this work we focus mainly on the mitochondria, as these organelles in plants and animals play a major role in the body's response to the action of stress factors. It can be assumed that the basic mechanism of action of preparations-adaptogens is the reduction of generation of ROS by these organelles. As known from the literature, regulators of plant growth and development improve their tolerance to biotic and abiotic stresses, to water deficiency in particular [6]. Such plant growth regulators are melaphen - a melamine salt of bis(oxymetyl)phosphonic acid and germatrane (1-(germatran-1-yl)-1-acetylamine):

The aim of this work is to study the effect of water deficit and the plant growth regulators – melaphen and germatrane on the functional state of 6-day pea seedling mitochondria.

Materials and Methods

Plant material. The study was carried out on mitochondria isolated from pea seedlings (*Pisum sativum.* L) cv. Alfa obtained in standard conditions and in the conditions of water deficit.

Pea seeds germination. The seeds from the control group were washed with soap solution and 0.01 % $KMnO_4$. Control seeds were then soaked in water, experimental seeds – in 10^{-5} M germatrane or in the $2 \cdot 10^{-12}$ M melaphen solution for 30 min. Thereafter, seeds were transferred on moistened filter paper in darkness. After 2 days, half of control (water deficit) (WD), germatrane (water deficit + germatrane) (WD + GER) treated seeds and melaphen (WD+MF) treated seeds were transferred on dry filter paper. After two days of water deficit treatment seeds were transferred on wet filter paper, where they were kept for next two days at 22°C. Another half of control plants were retained on wet filter paper, where they were kept for 6 days at 22°C. On the sixth day, mitochondria were isolated from seedling epicotyls.

Isolation of mitochondria from epicotyl 6-day-old seedlings was performed by differential centrifugation [7]. The isolation medium comprised: 0.4 M sucrose, 5 mM EDTA, and 20 mM KH_2PO_4 (pH 8.0), 10 mM KCl, 2 mM 1,4-Dithio-ditheiritol, and 0.1% fatty acids-free (FA-free) BSA. The first centrifugation is at 25000*g* for 5 min and the second – at 3000*g* for 3 min. Sedimentation of mitochondria was performed for 10 min at 11000*g*. The precipitate was resuspended in 2–3 ml of medium containing: 0.4 M sucrose, 20 mm KH_2PO_4 (pH 7.4), 0.1% BSA, (free from fatty acids), and again precipitated mitochondria at 11000*g* for 10 min.

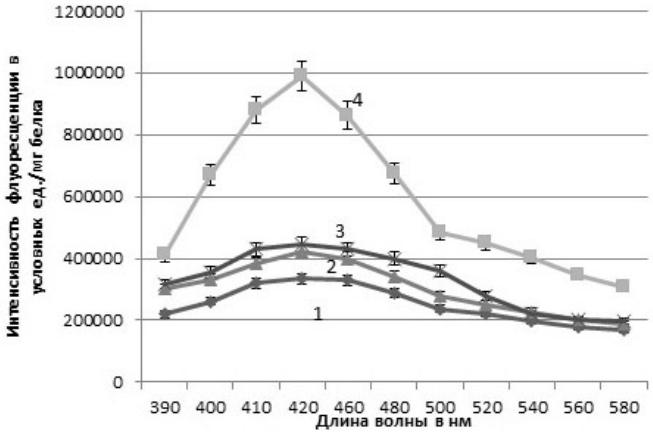

The fluorescence spectra of LPO products in the mitochondrial membranes of pea seedlings exposed to insufficient watering (WD) and in the mitochondrial membranes from pea seedlings treated by melaphen (WD+MF) or germatrane (WD+GER) and exposed to insufficient watering. 1 – Control; 2 – WD+MF ($2 \cdot 10^{-12}$ M melaphen); 3 – WD+GER; 4 – WD.

The respiration rate of mitochondria were recorded using a Clark type electrode on an LP-7 polarograph (Czechia). The incubation medium contained 0.4 M sucrose, 20 mM HEPES-Tris-buffer (pH 7.2), 5 mM KH_2PO_4, 4 mM $MgCl_2$, 0.1% BSA (28°C).

Lipid peroxidation (LPO) activity was assessed by fluorescent method [8]. Fluorescence was recorded using a spectrofluorometer FluoroMax Horiba Yvon, (Germany). The excitation wavelength was 360 nm, the emission wave length was 420–470 nm. The results were expressed in arbitrary units per mg protein.

Results and Discussion

Insufficient watering resulted in 3-fold increase in content of LPO products in pea seedling mitochondrial membranes (figure). The soaking of seeds in a $2 \cdot 10^{-12}$ M melaphen a $2 \cdot 10^{-12}$ M melaphen or 10^{-5} M germatrane resulted in a decrease of LPO products in the membranes of the pea seedling mitochondria. The fluorescence intensity of lipid peroxidation products decreased almost to the control level. It is probable that the LPO activation may lead to changes in the fatty acid (Fas) composition of mitochondrial membranes. Therefore, in the subsequent experiments we studied the effect of insufficient watering and PGRs on the fatty acid composition of the overall lipid fraction of mitochondrial membranes. Water deficit led to changes in the relative content of fatty acids (FAs) containing 18 and 20 carbon atoms. So the total content of C_{18} unsaturated FAs relative to the content of stearic acid was decreased from 16.61 ± 0.30 to 10.59 ± 0.20. Substantial changes occurred also in the relative content of fatty acids with 20 carbon atoms. The ratio (20:1ω7 + 20:1ω9 + 20:2ω6)/C20:0 in mitochondrial membrane lipids decreased from 3.65±0.03 to 1.20±0.16.

These changes may entail changing and lipid-protein interactions and, consequently, the activity of membrane-bound enzymes, in particular, enzymes of the mitochondrial respiratory chain. Indeed, insufficient watering resulted in decreasing the maximum oxidation rates of NAD-dependent substrates. Rates of oxidation of NAD-dependent substrates in the presence of FCCP (carbonyl cyanide-p-trifluoromethoxyphenylhydrazone) decreased from 78.0±5.7 to 50.9±4.3 ng mole O_2/mg protein x min and the efficiency of oxidative phosphorylation was also lower: the value of the respiratory control rate (RCR) reduced from 2.47±0.10 in control to 1.85±0.02. The soaking of seeds in a $2 \cdot 10^{-12}$ M melaphen has prevented by changes in the efficiency of oxidative phosphorylation and decreasing the oxidation rates of NAD-dependent substrates in the presence of FCCP caused by water deficiency. Treatment of pea seeds 10^{-5} M of germatrane partially prevented decreasing the oxidation rates of NAD-dependent substrates caused by water stress: the oxidation rates of NAD-dependent substrates under these conditions were 62.3±4.8 and the value of the respiratory control rate (RCR) was 2.0±0.15. Preventing by melaphene reducing maximum rates of NAD-dependent substrates oxidation by mitochondria seedlings, apparently, associated to the prevention of oxidation of unsaturated FAs with 18 and 20 carbon atoms. The weaker protective effect of germatrane in respect of the maximum velocity of oxidation of NAD-dependent substrates, apparently, associated with some decrease in the content of unsaturated FAs with 18 carbon atoms in the membranes of mitochondria of pea seedlings under conditions of water deficiency. Its protective effect is, evidently, accounted for by the prevention of oxidation of fatty acids having 20 carbon atoms under conditions of water deficiency.

Changes in physical and chemical properties of mitochondrial membranes resulting in changes in the energy metabolism have an influence on physiological indices, e.g., seedling growth. Water deficiency dramatically inhibited the growth processes. The treatment of pea seeds with melaphen and germatrane prevents the inhibition of root growth in these conditions. The length of epicotyls of seedlings in the processing of melaphen did not differ from the length of epicotyls of the control group, while under the processing germatrane epicotyl were 1.2 times lower than the control group epicotyls.

It can be assume that that maintaining a high level of unsaturated fatty acids, mainly linoleic acid, which is one of the basic fatty acids that enter into the composition of the cardiolipin, which ensures the effective functioning of the respiratory chain of mitochondria in connection with formation of super complexes of the respiration carriers. The maintenance of the high functional activity of mitochondria, which provide the metabolic processes by energy, especially important for sprouting seeds, which are in need of the energy resources.

References

1. Ribas-Carbo M., Tailor N.L., Giles L, Busquets S., Finnegan P.M., Day D.A. et al. Effects of Water Stress on Respiration in Soybean Leaves. Plant Physiol. 2005, 139, 466-473.
2. Boyer J.S. Plant Productivity and the Environment. Science.1982, 218, 443-448.

3. Halliwell B., Gutteridge, J. M. Free Radicals in Biology and Medicine, Oxford: Claredon Press, 1989, 215 p.
4. Tailor N.L., Day D.A., Millar A.H .Targets of stress-induced oxidative damage in plant mitochondria and their impact on cell carbon/nitrogen metabolism. J. Exp. Botany. 2003, 55 (394), 1-10.
5. Atkin O.K., Macherel D. The Crucial Role of Plant Mitochondria in Orchestrating Drought Tolerance. Ann. Bot. 2009, 103, 581-59.
6. Prusakova LD, Malevannaya NN, Belopukhov SL, Vakulenko VV. Plant growth regulators having antistress and immunoprotective properties. Agrokhimiya. 2005, 11: 76-86.Russ.
7. Popov V.N., Ruge E.K., Starkov A.A.. Effect of electron transport inhibitors on the formation of reactive oxygen species in the oxidation of succinate by pea mitochondria. Biochemistry. 2003. 68(7), 910-916
8. Fletcher B.I., Dillard C.D., Tappel A.L. Measurement of fluorescent lipid peroxidation products in biological systems and tissues// Anal. Biochem. 1973. 52. 1–9.

INDEX OF AUTHORS

C O N T E N T S

Materials of International Symposium

“Biological motility”

Научное издание

Издательство SYNCHROBOOK
142290, г. Пущино Московской обл.
E-mail: zeebvad@mail.ru

Отпечатано в типографии «Принт 71»
300028, г. Тула, ул. Смидович, 12б
http://print71.biz

Подписано в печать 22.04.2016
Печать цифровая Формат 60×84 /16
Усл. печ. л. 17,4 Заказ №307т
Тираж 140 экз.